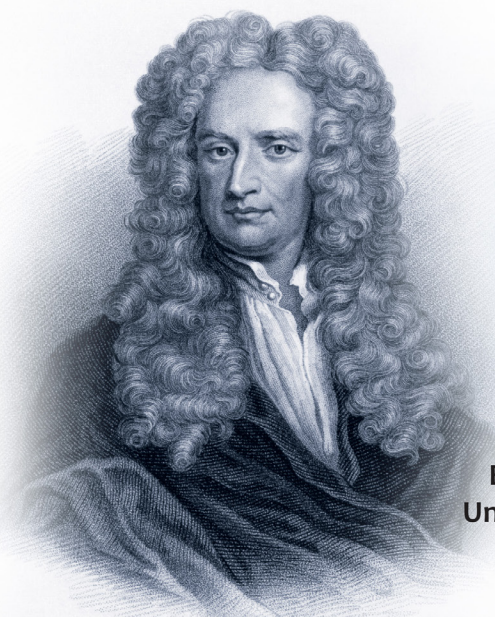




INTERNATIONAL CONFERENCE

**PROCESS  
MANAGEMENT AND  
SCIENTIFIC  
DEVELOPMENTS**



Birmingham  
United Kingdom



# **International Conference “Process Management and Scientific Developments”**

Birmingham, United Kingdom  
(Novotel Birmingham Centre, June 9, 2020)



Materials of the International Conference  
**"Process Management and Scientific Developments"**. Part 2  
(Birmingham, United Kingdom, June 9, 2020)

M67

ISBN 978-5-905695-40-7

These Conference Proceedings combine materials of the conference – research papers and thesis reports of scientific workers. They examines technical and sociological issues of research issues. Some articles deal with theoretical and methodological approaches and principles of research questions of personality professionalization.

Authors are responsible for the accuracy of cited publications, facts, figures, quotations, statistics, proper names and other information.

UDC 330

**ISBN 978-5-905695-79-7** ©Scientific publishing house Infinity, 2020  
© Group of authors, 2020

# CONTENTS

## MEDICAL SCIENCES

Efficacy of platelet rich plasma for treatment knee osteoarthritis Vasilchenko Nikita Vadimovich, Radish Ivan Ivanovich.....	8
Danini-Ashner test for boys aged 8-12 with year-round form of allergic rhinitis engaged in Greco-Roman wrestling Izvin Alexander Ivanovich, Prokopiev Nikolai Yakovlevich, Kolunin Yevgeny Timofeevich.....	14
Physiological - hygienic assessment of working conditions during the work on manual and mechanical averband Iskandarov Aziz Bakhromovich.....	22
Photodynamic therapy in the postoperative period in the treatment of panaritium and phlegmons of a hand Chepurnaya Julia Lvovna, Melkonyan Georgiy Gennadevich, Gulmuradova Nargis Tashpulatovna.....	29
The effect of experimental type 1 diabetes on the morphofunctional state of mast cells of the fallopian tubes of the offspring of female rats Drebit Veronika Vladimirovna, Bryukhin Gennady Vasilevich.....	39
Clinical and social aspects of functioning of epilepsy patients Tokareva Natalia Gennadievna.....	44
Combined neuroprotection in recovery treatment after ischemic stroke Badashkeev Mikhail Valeryevich, Shoboev Andrey Eduardovich.....	50
Mass training in the form of a master class for the early diagnosis of skin melanoma Neretin Evgeny Yuryevich, Kozlova Olga Anatolyevna.....	54
Features of the physical development of tuberculosis infected children in the Smolensk Oblast Krutikiva Nadezhda Yuryevna, Teschenkov Anton Viktorovich, Krikova Anna Vyacheslavovna.....	57
Enthesopathy: features of etiopathogenesis Krajnyukov Pavel Evgen'evich, Kokorin Viktor Viktorovich, Matveev Sergej Anatol'evich....	62
Incidence of infectious diseases related to occupational activities Smetanin Viktor Nikolaevich.....	77

## **BIOLOGICAL SCIENCES**

Environmental and physiological and hygienic aspects of the use of drinking water by schoolchildren of the city of Kaluga (Russia) Lykov Igor Nikolaevich, Arutyunova Elizaveta Romanovna.....	82
---	----

## **CHEMICAL SCIENCES**

Chemical transformations of n-alkanes under hydrodynamic cavitation action in water media Dudkin Denis Vladimirovich, Fedyaeva Irina Mikhailovna, Zhuravleva Lyudmila Anatolievna.....	88
Gossypol resin - in the future a valuable material for building bitumen without oil Jumaniyazov Makhsud, Jabbiyev Rasulbek.....	97
Technology for producing import substituting, export-oriented acid-resistant anticorrosive coatings Jumaniyazova Dilnoza, Jumaniyazov Makhsud.....	103

## **EARTH SCIENCES**

Quality of surface water in Eastern Donbass, Russia Gavrishin Anatoly Ivanovich.....	111
New control method "Microtriangulation network" Yeskaliyev Yertay Talgatovich.....	117

## **TECHNICAL SCIENCES**

Structural-basic technology of creating collective use systems. Methodological aspects of the creation Khalilov Abdurakhman Ismailovich.....	124
Deaf Sign Language Recognition Grif Mikhail Gennadievich, Prikhodko Alexey Leonidovich.....	133
New information about the use of shells with tangential developable middle surfaces Aleshina Olga Olegovna.....	140
Technological providing of surface layer performances of parts during the machining Sutyagin Aleksandr Nikolaevich.....	147
Plasticization of cold-rolled low-carbon steels by epilamization of the surface Doshchechkina Iryna Vasilievna, Lalazarova Nataliia Alekseevna.....	154

7.62 mm Yalquzag sniper rifle metrological research stages with coordinate metrology Isgandarzada Elchin Barat, Ahmadli Shukufa Vagif, Islamova Ulkar Rafiq, Aliyeva Lamiye Sulduz, Goycayeva Konul Akif.....	162
---	-----

**PHYSICS AND MATHEMATICS**

Analysis of the electric field of a plane lattice of sign-alternating axes Leonov Vladimir Semenovich.....	173
Dynamic Leonov interferometer for detecting the field of dark matter particles Leonov Vladimir Semenovich.....	183
On homomorphisms of some partial groupoids Arapina-Arapova Elena Sergeevna.....	193
Generalization of one theorem of Newman Bezverkhniy Vladimir Nikolaevich, Bezverkhniaia Natalia Borisovna.....	199

## EFFICACY OF PLATELET RICH PLASMA FOR TREATMENT OF KNEE OSTEOARTHRITIS

**Vasilchenko Nikita Vadimovich**

Clinical Resident

**Radish Ivan Ivanovich**

Department Head

Clinical Hospital № 1 of the Office of the President of the Russian Federation,  
Moscow, Russia

**Abstract.** The article presents the results of evaluating the effectiveness of treatment of patients with osteoarthritis of the knee joint of 1-3 degrees using platelet-rich plasma. According to the results of the study, it was found that the maximum decrease in indicators on the WOMAC and YOUR scales, in the form of relief of pain, reduction of stiffness and increase in range of motion, occurred in patients after 3 procedures of intraarticular injection of PRP.

**Keywords:** osteoarthritis, platelet-rich plasma, WOMAC and VAS scales.

### Introduction

Osteoarthritis (OA) of the knee joint is the main source of pain in the knee joint, and is detected in 35% of the population over 65 years of age [1]. In this case, the main non-surgical methods for treating OA of the knee joint are: taking non-steroidal anti-inflammatory drugs, reducing body weight, physiotherapy, as well as intra-articular injections of hyaluronic acid and corticosteroids. Intra-articular administration of platelet-rich autologous plasma is considered as one of the promising methods.

Biological therapies for osteoarthritis of the knee joint are becoming increasingly popular among patients and among healthcare providers [5]. Along with the popularity and frequency of use of biological methods of treatment, the number of publications in this area of therapy has increased. Perhaps this is due to a change in the concept of OA, shifting the main emphasis of etiology and pathophysiology towards inflammatory processes [3, 6, 8].

Platelet-rich plasma therapy is an autologous blood product with a high platelet concentration. Platelets have a high concentration of growth factors and cytokines, which have a stimulating effect on the regeneration of bone, cartilage and surrounding soft tissues. However, there are 4 categories of final PRP products: pure platelet rich plasma (P-PRP); plasma rich in white blood cells and platelets (L-PRP); pure platelet rich fibrin (P-PRF); white blood cell and platelet-rich fibrin (L-PRF). The main clinical benefit for treating knee OA is the use of pure platelet rich plasma (P-PRP), while the use of plasma rich in white blood cells and platelet (L-PRP) can potentiate inflammatory changes in OA [4]. The biological mechanisms of the interaction of platelet factors with various tissues of the body are quite complex and not yet sufficiently studied.

### **Purpose of the study**

Evaluate the effectiveness of treatment of patients with knee osteoarthritis of 1-3 degrees using platelet-rich plasma.

### **Materials and methods**

We examined 104 patients (of which 44 men and 60 women) aged 22-47 years, with a diagnosis of knee osteoarthritis of the 1-3 degree according to ICRC Cartilage MRI criteria, confirmed by MRI diagnosis.

Patients who had systemic blood diseases, oncological diseases (including a medical history), and the continuous use of anticoagulants were excluded from the study.

Platelet rich plasma (PRP) concentration of biologically active molecules of growth factors in plasma obtained from the patient's own blood is used in the treatment. Depending on the severity of osteoarthritis of the knee, patients were prescribed a course of intra-articular PRP injections from 1 to 3 with an interval of 7 days between injections. After the injection, patients were not allowed physical activity for 2-3 days, as well as taking non-steroidal anti-inflammatory drugs for 4 weeks.

The results were evaluated before the first injection, and also after a week of subsequent injections using the visual analogue VAS scale (with a rating from 0, complete absence of pain up to 10 points, intolerable pain) and the arthritis index scale of the Western Ontario and McMaster (WOM-AC) universities from 0 to 100 points as an indicator of pain, impaired function and stiffness [2, 9].

Statistical processing of the obtained data was performed using the computer program STATISTICA-12. When assessing the statistical significance of differences between groups, the non-parametric Mann-Whitney test was used, when comparing the indicators of one group at different stages of observation, the Wilcoxon test. The results of descriptive sta-

tistics are presented: the central characteristics of the distribution of the data of an indicator, that is, its measure of position: median (Me); statistical characteristics of the scatter of the trait data, that is, scattering measures: standard deviation (SD), standard error of the mean (SEM), interquartile range ( $Q_1-Q_3$ ). The critical level of reliability of the null statistical hypothesis was taken equal to 0.05.

### Results and discussion

An analysis of the data showed that before treatment on the WOMAC scale, the median was 58 points (interquartile range ( $Q_1-Q_3$ ) from 50 to 63 points) (Fig. 1). 7 days after the first intra-articular PRP injection, the median on the WOMAC scale was 38 points (interquartile range ( $Q_1-Q_3$ ) from 25 to 42 points).

One week after the second PRP injection, a WOMAC score was made, where the median was 23 points (interquartile range ( $Q_1-Q_3$ ) from 14 to 32 points). Moreover, the differences between intraarticular injection 1 and 2 were statistically significant ( $p < 0.0001$ ).

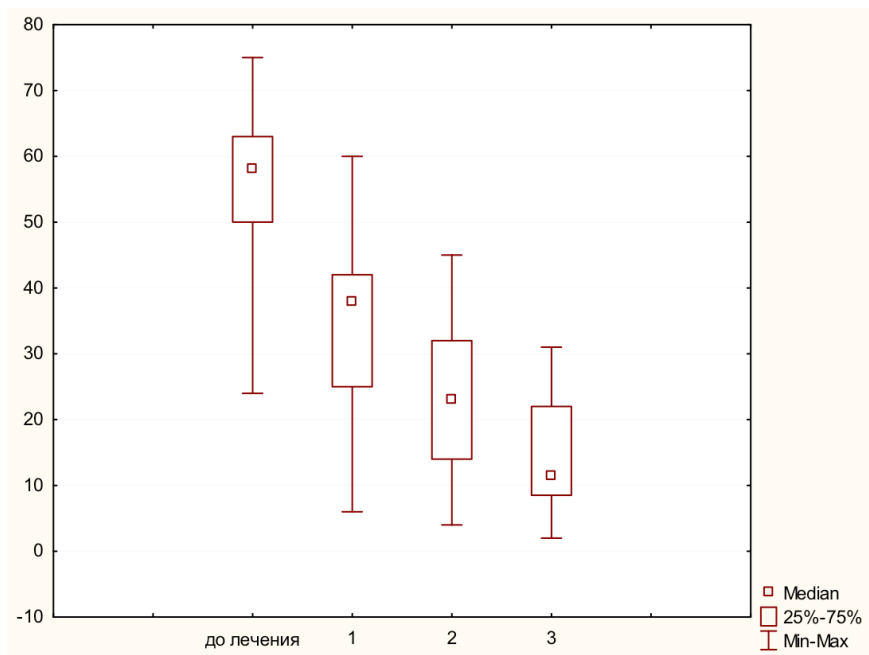


**Fig. WOMAC assessment (score) in patients treated with PRP**

In patients who required a PRP of 3 injections, the median was 11.5 points (interquartile range ( $Q_1-Q_3$ ) from 8.5 to 22 points). The differences between intraarticular injection 2 and 3 were statistically significant ( $p < 0.0001$ ).

As is known, to determine the number and frequency of injections, to obtain greater effectiveness of PRP therapy there are significant difficulties. So, some researchers came to the conclusion that precisely 2 PRP injections with an interval of 2 weeks are an effective treatment for OA of the knee joint [7, 10].

Thus, the use of PRP therapy can significantly improve the indicators of the functional state of the knee joint and the quality of life of patients.

Figure 2 shows the successful use of platelet-rich plasma for the treatment of OA of the knee, confirming an improvement in overall health assessment. So, against the background of the therapy, a week after the first procedure, a decrease in the median of the VAS scale was observed, which was 3 points (interquartile range ( $Q_1-Q_3$ ) from 3 to 4 points) ( $p < 0.0001$ ).

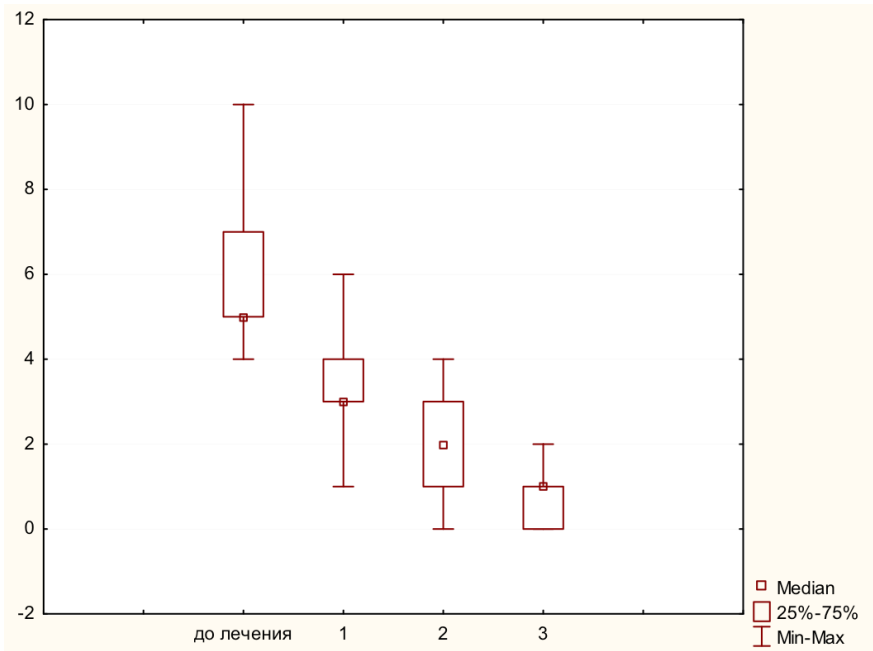


Fig. 2. VAS pain assessment (score) in patients with PRP therapy

One week after the second PRP injection, a VAS score was made, where the median was 2 points (interquartile range ( $Q_1-Q_3$ ) from 1 to 3 points). The differences between 1 and 2 by intraarticular injection of platelet-rich plasma were statistically significant ( $p < 0.0001$ ).

In patients who required a PRP of 3 injections, the median was 1 point (interquartile range ( $Q_1-Q_3$ ) from 0 to 1 point). The differences between 2 and 3 injections were statistically significant ( $p < 0.0001$ ).

The study of the correlation between the assessment of pain according to the WOMAC scale and pain according to the VAS scale against the background of the ongoing PRP therapy showed the following. The presence of a reliable direct correlation between the values of the WOMAC and VAS indicators was established: the Spearman rank correlation coefficient before treatment turned out to be 0.58 ( $p < 0.001$ ); 7 days after the first intra-articular injection, the PRP was 0.59 ( $p < 0.001$ ); after a week from the second it was 0.8 ( $p < 0.0001$ ), and after the third injection it was 0.81 ( $p < 0.0001$ ).

Thus, the maximum decrease in VAS, as well as a significant improvement in the clinical picture in the form of relief of pain, decreased stiffness and increased range of motion, occurred in patients after 3 procedures of intra-articular administration of PRP.

**Conclusions.** According to the results of the study, it was found that PRP therapy has great potential in reducing pain and improving function in patients with osteoarthritis of the knee joint. Despite the clinical effectiveness of PRP therapy, more standardized, multicenter controlled trials are needed to formulate protocols with clear indications of the number of injections and the interval between them.

In general, the proven clinical efficacy and high safety along with the simplicity of the method allows us to recommend it in the treatment of osteoarthritis of the knee joint, both in specialized departments of hospitals and in outpatient trauma and orthopedic practice.

## References

1. Altman R.D., Rosen J.E., Bloch D.A., Hatoum H.T. Safety and efficacy of retreatment with a bioengineered hyaluronate for painful osteoarthritis of the knee: results of the open-label extension study of the FLEXX. // *Trial Osteoarthr. Cartil.*, 19 (2011), pp. 1169-1175

2. Bellamy N., Buchanan W.W., Goldsmith C.H., Campbell J., Stitt L.W. Validation-study of WOMACdA health-status instrument for measuring clinically important patient relevant outcomes to antirheumatic drug-therapy in patients with osteo-arthritis of the hip or knee. // *J. Rheumatol.*, 15 (1988), pp. 1833-1840
3. Bize R., Johnson J.A., Plotnikoff R.C. Physical activity level and health-related quality of life in the general adult population: A systematic review. // *Prev. Med. (Baltim)*. 2007; 45:401–15. doi:10.1016/j.ypmed.2007.07.017.
4. Dohan Ehrenfest D.M., Rasmusson L., Albrektsson T. Classification of platelet concentrates: from pure platelet-rich plasma (P-PRP) to leucocyte- and platelet-rich fibrin (L-PRF). // *Trends Biotechnol.* 2009; 27:158–67. doi:10.1016/j.tibtech.2008.11.009.
5. Ehnert S., Glanemann M., Schmitt A., Vogt S., Shanny N., Nussler N.C., et al. The possible use of stem cells in regenerative medicine: dream or reality? // *Langenbeck's Arch Surg.* 2009;394:985–97. doi:10.1007/s00423-009-0546-0.
6. Filardo G., Di Matteo B., Di Martino A., Merli M.L., Cenacchi A., Fornasari P., et al. Platelet- Rich Plasma Intra-articular Knee Injections Show No Superiority Versus Viscosupplementation. // *Am J Sports Med.* 2015;43:1575–82. doi:10.1177/0363546515582027.
7. Kavadar G., Demircioglu D.T., Celik M.Y., Emre T.Y. Effectiveness of platelet-rich plasma in the treatment of moderate knee osteoarthritis: a randomized prospective study.// *J Phys Ther Sci* 2015;27:3863–7. doi:10.1589/jpts.27.3863.
8. Kuttapitiya A., Assi L., Laing K., Hing C., Mitchell P., Whitley G., et al. Microarray analysis of bone marrow lesions in osteoarthritis demonstrates upregulation of genes implicated in osteochondral turnover, neurogenesis and inflammation. // *Ann Rheum Dis* 2017;76:1764– 73. doi:10.1136/annrheumdis-2017-211396.
9. McConnell S., Kolopack P., Davis A.M. The Western Ontario and McMaster Universities osteoarthritis Index (WOMAC): a review of its utility and measurement properties *Arthritis Rheum.*, 45 (2001), pp. 453-461
10. Laudy A.B., Bakker E.W., Rekers M., Moen M.H. Efficacy of platelet-rich plasma injections in osteoarthritis of the knee: a systematic review and meta-analysis.// *Br J Sports Med*, 49 (10) (2015), pp. 657-672 pii: bjsports-2014-094036

**DANINI-ASHNER TEST FOR BOYS AGED 8-12 WITH YEAR-ROUND FORM OF ALLERGIC RHINITIS ENGAGED IN GRECO-ROMAN WRESTLING**

**Izvin Alexander Ivanovich**

Doctor of Medical Sciences, Full Professor  
Tyumen State Medical University

**Kolunin Yevgeny Timofeevich**

Candidate of Biological Sciences, Associate Professor  
University of Tyumen

**Prokopiev Nikolai Yakovlevich**

Doctor of Medical Sciences, Full Professor  
University of Tyumen

**Abstract.** The task is set by the Dagnini-Ashner test to assess the excitability of the parasympathetic department of the autonomic nervous system in boys of the second childhood of Tyumen, suffering from year-round allergic rhinitis of mild severity of clinical manifestations, during classes in Greco-Roman wrestling.

**Keywords:** allergic rhinitis, boys 8-12 years old, Dagnini-Ashner test, Greco-Roman wrestling.

**Relevance**

The beginning of the new millennium was marked by frightening predictions regarding the increase in the incidence of allergic rhinitis (AR), especially in children, leading to dire consequences [1, 2]. According to the forecasts of most researchers, the incidence of AR will steadily increase (according to some sources, up to 5% per year) and by 2020 may reach up to 50% of the child population [3]. Currently, the global average prevalence of AR is 30% [4]. So, in the USA, about 30 million people suffer from AR, in England AR is diagnosed in 16% of the population, in Denmark - 19%, in Germany - from 13 to 17%. Over the past decades, the prevalence of AR in children in Russia is up to 34% in different regions and is increasing from year to year [5, 6].

It should be noted that the incidence of AR in Russia varies from 13.3 to 38%, including seasonal AR from 13.7 to 24% [7]. Along with improved diagnostics, new AR treatment strategies are being developed [8, 9, 10, 11, 12, 13]. The ARIA expert working group, together with the World Health Organization, the World Organization of Family Doctors (Wonca) and the International Primary Care Respiratory Group (IPCRG), believe that AR is a chronic respiratory disease that plays a significant role in the development of bronchial asthma [14].

Symptoms of AR affect school attendance, and allergies are one of the main reasons for skipping school. So, in the USA, more than 2 million missed school days are associated with it [15, 16]. In children with insufficiently controlled AR, the ability to learn decreases, which affects their school activities [17]. Children with AR may be more irritable and more tired, be inattentive and have difficulty concentrating on the lesson [18, 19]. AR is a significant financial cost. So, the annual costs associated with the diagnosis and treatment of patients with AR in Europe are 1.5-2 billion euros, and indirect costs - 1.5-2 billion euros; in the United States, direct costs at the end of the 20th century amounted to 5.6 billion dollars [20].

The year-round and seasonal form of AR are distinguished [21, 22, 23]. Seasonal AR is associated with exposure to plant pollen allergens and manifests itself during certain periods of flowering of trees and grasses. Allergens can be pollen from trees (birch, hazel, oak, alder, elm, maple), grasses (timothy, fescue, bonfire, foxtail, bluegrass, rye) and weeds (quinoa, wormwood, ragweed), as well as mold fungi. Features of seasonal rhinitis is the frequency of exacerbations. Year-round AR is caused by allergens from house dust, ticks, cockroaches, rodents, and some types of mold fungi.

In the available literature, we did not find studies showing the effect of the Danyini-Ashner test to assess the excitability of the parasympathetic autonomic nervous system in boys of the second childhood period, suffering from AR of varying severity of clinical manifestations involved in Greco-Roman wrestling.

A test was proposed in 1908 independently by the Italian physician Giuseppe Dagnini (May 19, 1866 - October 19, 1928) and the Austrian physician Bernhard Aschner (January 27, 1883 - March 09, 1960) and currently bears their name [24, 25].

**Purpose of the study:** evaluate the excitability of the parasympathetic department of the autonomic nervous system in boys of the second childhood of Tyumen, suffering from year-round allergic rhinitis of mild severity of clinical manifestations during Greco-Roman wrestling.

### Material and methods

19 boys (the main group - MG) of the second childhood period (8-12 years old) involved in Greco-Roman wrestling, suffering from a year-round form of AR were examined. The control group (CG) consisted of 22 boys of the same age who did not have somatic diseases, also involved in Greco-Roman wrestling together with the boys of MG. Training sessions were held 4 times a week for 1.5 hours in the presence of a doctor. When selecting age groups, the "Scheme of age-related periodization of human ontogenesis" was used, adopted at the VII All-Union Conference on the problems of age-related morphology, physiology and biochemistry of the USSR Academy of Pedagogical Sciences (Moscow, 1965). All boys are indigenous and study in secondary schools of the city of Tyumen.

Given that among the boys involved in the gym there are children who suffer from the year-round form of AR, we tried to minimize the number of provoking factors of its manifestations. For this purpose, multiple wet cleaning was carried out not only of the gymnasium, but also of the wrestling mat, as well as utility rooms, regular airing of the hall, prevention of the appearance of ordinary clothes, street shoes, etc. in the hall.

The standard Danyini-Ashner test (eyes-heart reflex) consists in moderate pressure with the fingers of the hand for 20 seconds on the side sections of the eyeballs. In the classical test methodology, the calculation of the heart rate (HR, beats/min) is carried out 1 minute before the pressure and 1 minute after the pressure on the eyeballs.

We have modified the sample procedure, which consists in the fact that HR calculation was carried out within 15 minutes after the sample. HR was determined by palpation on the radial artery for the first and last 10 seconds of each minute, as well as using an electrocardiograph. In 6 (31.6%) boys with AR, an oculocompressor with a load of 300 g was used.

The studies corresponded to the ethical standards of the biomedical ethics committees developed in accordance with the Helsinki Declaration adopted by the BMA, Order of the Ministry of Health and Social Development of Russia №774n dated August 31, 2010 "On the Ethics Council", and Order of the Ministry of Health of the Russian Federation №226 dated 06.19.2003 "Rules clinical practice in the Russian Federation. " The principles of voluntariness, human rights and freedoms guaranteed by Art. 21 and 22 of the Constitution of the Russian Federation.

### Results and discussion

The eye-cardiac Dagnini-Ashner reflex is caused by afferent connections of the orbital branch of the trigeminal nerve and the vagus nerve of the parasympathetic nervous system [26], which form synoptic connec-

tions with the visceral motor nucleus of the vagus nerve of the reticular formation of the brain stem. Efferent pathways of the vagus nerve go from the cardiovascular center of the medulla oblongata to the heart, while increased stimulation of the cardiovascular center leads to suppression of the function of the sinus node [27].

The results of the study showed (Table 1) that one minute after the cessation of pressure on the eyeball, the normal type of eye-heart reflex, i.e. slowing of the pulse by 4-10 beats/min, occurred in 16 (88.9%) boys.

**Table 1. Types of responses of the cardiovascular system of boys of the second childhood MG and CG to the Danyini-Ashner test**

Types of reactions	Age, years				
	8	9	10	11	12
After one minute					
Normal – slowdown of HR of 4-10 beats/min. MG (n = 19)	2 (10,5%)	2 (10,5%)	5 (26,3%)	4 (21,1%)	4 (21,1%)
CG (n = 22)	3 (13,6%)	4 (18,2%)	8 (36,4%)	3 (13,6%)	4 (18,2%)
Sharply positive – slowdown of HR of over 10 beats/min. MG (n = 19)	1 (5,3%)	1 (5,3%)	–	–	–
CG (n = 22)	–	–	–	–	–
Negative – no HR change. MG (n = 19)	–	–	–	–	–
CG (n = 22)	–	–	–	–	–
After 15 min					
Normal – slowdown of HR of 4-10 beats/min. MG (n = 19)	1 (5,3%)	–	–	–	–
CG (n = 22)	–	–	–	–	–

A sharply positive reaction (vagotonic type of eye-cardiac reflex) was detected in two (10.6%) boys aged 8 and 9 years. Estimating the results of the test, we noted that eight and nine year old boys, firstly, when undergoing a medical examination at a physical-physical dispensary, were somatically healthy, not counting AR. Secondly, both are at the initial stage of training in Greco-Roman wrestling. We did not reveal a negative reaction of the cardiovascular system of the boys to the Danyini-Ashner test.

Examination of the Danyini-Ashner eye-heart reflex in boys of the second childhood period 15 minutes after pressure on the eyeballs showed that all had a normal type of reaction.

Based on the test results, we recommended that the trainer of boys with AR increase the duration of its introductory part to 15-20 minutes during training, using various gymnastic exercises aimed at preparing the body for intense muscle activity. In healthy children, the duration of "entry" into the main stage of training was 5-7 minutes.

Clinical observations during the year of the boys with AR, engaged in Greco-Roman wrestling, showed that regularly conducted dosed physical activity contributed to a significant reduction in the severity of the manifestations of rhinitis. After three months of training, 5 (26.3%) boys stopped rhinorrhea and nosebleeds, the severity of headaches, fatigue, decreased appetite, improved sleep, improved sleep. After 6 months from the start of training, 12 (63.2%) boys also noted the cessation of sore throat and coughing, discomfort in the abdomen and a decrease in irritability. After a year of playing sports, 18 (94.7%) boys noted the absence of AR symptoms that occurred before the Greco-Roman wrestling.

It is noteworthy that the duration of regular Greco-Roman wrestling exercises affects the severity of the clinical manifestations of AR. The lower the passport age, the weaker the allergization of the boys is less pronounced, and the influence of wrestling is more significant in terms of reducing the severity of the clinical manifestations of AR.

### **Conclusion**

1. In 89.4% of boys of the second childhood who are engaged in Greco-Roman wrestling and are sick with a year-round form of AR, immediately after the cessation of pressure on the eyeball, a positive (normal) type of Danyini-Ashner eye-heart reflex was revealed. The vagotonic type of eye-heart reflex is much less common (10.6%), and only in 8 and 9 year old boys. 15 minutes after pressure on the eyeballs in all boys, regardless of sports, there was a normal type of reaction.

2. AR is not an obstacle to sports, including Greco-Roman wrestling. In connection with AR, boys during training should increase the length of the introductory part to 15-20 minutes, while using various gymnastic exercises aimed at preparing the allergic body for intense muscle activity. In 18 (94.7%) boys, a year later, the absence of AR symptoms that occurred before the Greco-Roman wrestling was revealed.

The authors declare the absence of conflict of interest.

## References

1. Баранов И.И, Балаболкин А.А. Детская аллергология. М.: Геотар-Медиа, 2006. – 696 с. [Baranov I.I., Balabolkin A.A. Detskaya Allergologiya. M.: Geotar-Media, 2006. – 696 P. (in Russ.)].
2. Carr W., Bernstein J., Lieberman P., Meltzer E. A novel intranasal therapy of azelastine with fluticasone for the treatment of allergic rhinitis. //J.Allergy Clin Immunol, 2012;129:– 1282-1289.e10.
3. Зайцева О.В., Барденикова С.И. Аллергический ринит у детей. – М., 2015. – 98 с. [Zaitseva O.V., S.I.Bardenikova Allergic rhinitis in children. – M., 2015. - 98 P. (in Russ.)].
4. Cirillo I., Vizzaccaro A., Tosca M.A., M. Milanese M., Ciprandi G. Prevalence and treatment of allergic rhinitis in Italian conscripts. // AllergImmunol (Paris) 2003.35:204-207.
5. Хаитов Р.М., Ильина Н.И. Аллергология. Федеральные клинические рекомендации. М.: Фармарус Принт Медиа, 2014. – 126 с. [Khaitov R.M., Ilina N.I. Allergology. Federal clinical guidelines. M.: Farmarus Print Media, 2014. - 126 P. (in Russ.)].
6. Ревякина В.А., Виленчик Л.Л., Лукина О.Ф., Т.А. Филатова Т.А. Современные аспекты диагностики и лечения аллергического ринита. Российский аллергологический журнал, 2007. – №5. – С. 36-46. [Revyakina V.A., Vilenchik L.L., Lukina O.F., T.A. Filatova T.A. Modern aspects of diagnosis and treatment of allergic rhinitis. //Russian Journal of Allergy, 2007. - №5. - P. 36-46. (in Russ.)]
7. Тарабрина О.В., Сальникова И.Ю. Особенности иммунного статуса больных сезонным аллергическим ринитом. //Молодежный инновационный вестник, 2017. – Т. 6. № 1. – С. 118-121. [Tarabrina O.V., Salnikova I.Yu. Features of the immune status of patients with seasonal allergic rhinitis. //Youth Innovation Bulletin, 2017. – V. 6. № 1. – P. 118-121 (in Russ.)].
8. Крюков А.И., Туровский А.Б., Бондарева Т.П., Семкина О.В. Принципы лечения аллергического ринита // Медицинский совет. 2013. № 7. С. 42-47 [Kryukov A.I., Turovsky A.B., Bondareva T.P., Semkina O.V. The principles of treatment of allergic rhinitis // Medical Council. 2013. № 7. P. 42-47 ]
9. Носуля Е.В., Ким И.А. Современные стратегии лечения аллергического ринита //Вестник оториноларингологии. 2016. Т. 81. № 2. С. 74-76. [Nosulya E.V., Kim I.A. Modern treatment strategies for allergic rhinitis // Bulletin of otorhinolaryngology. 2016. V. 81. № 2. P. 74-76]

10. Носуля Е.В. Медикаментозный ринит //Вестник оториноларингологии. 2017. Т. 82. № 3. С. 84-90. [Nosulya E.V. Medical rhinitis // Bulletin of otorhinolaryngology. 2017. V. 82. № 3. P. 84-90.]

11. Овчинников А.Ю., Носуля Е.В., Рязанцев С.В. Аллергический ринит: новое решение старой проблемы //Эффективная фармакотерапия. 2016. № 20. С. 36-42. [Ovchinnikov A.Yu., Nosulya E.V., Ryazantsev S.V. Allergic rhinitis: new solution to an old problem // Effective pharmacotherapy. 2016. № 20. P. 36-42.]

12. Серебрякова И.Ю., Ким И.А., Носуля Е.В., Коробкин А.С. Вазомоторный ринит: новые диагностические подходы //Российская ринология. 2018. Т. 26. № 4. С. 40-44. [Serebryakova I.Yu., Kim I.A., Nosulya E.V., Korobkin A.S. Vasomotor rhinitis: new diagnostic approaches // Russian rhinology. 2018. V. 26. № 4. P. 40-44.]

13. Соболев А.В., Козлова Я.И., Пятакова А.В., Аак О.В., Клишко Н.Н. Аллергический ринит. Выбор рационального лечения //Российский аллергологический журнал. 2017. Т. 14. № 2. С. 71-75. [Sobolev A.V., Kozlova Y.I., Pyatakova A.V., Aak O.V., Klimko N.N. Allergic rhinitis. The choice of rational treatment // Russian Allergological Journal. 2017. V. 14. № 2. P. 71-75.]

14. Bousquet J., Khaltaev N., Cruz A.A. «Allergic Rhinitis and its Impact on Asthma (ARIA) 2008 update (in collaboration with the World Health Organization, GA2LEN and AllerGen. //Allergy: European Journal of Allergy and Clinical Immunology, 2008. – Vol. 63. –no. sup. 86. – P. 8-160.

15. Bender B.G., Fisher T.J. Differential impacts of allergic rhinitis and allergy medications on childhood learning. //Pediatr Asthma Allergy Immunol, 1998. – Vol. 12. – P. 1-13.

16. Kay G.G. The effects of antihistamines on cognition and performance //J. Allergy Clin. Immunol, 2000. – V. 105. – P. 622-627.

17. Vignola A. M. Humbert M., Bousquet J. Efficacy and tolerability of anti-immunoglobulin E therapy with omalizumab in patients with concomitant allergic asthma and persistent allergic rhinitis: SOLAR. // Allergy, 2004. – V. 59. – P. 709-717.

18. Richards W. Preventing behavior problems in asthma and allergies // Clin. Pediatr., 1994. – V. 33. – P. 617-624.

19. Schenkel E.J., Skoner D.P., Bronsky E.A. Absence of growth retardation in children with perennial allergic rhinitis after one year of treatment with mometasonefuroate aqueous nasal spray. Pediatrics, 2000. – V. 105. – P. 22.

20. Ross R. N. The costs of allergic rhinitis. //Am. J. Managed. Care, 1996. – V. 2. – P. 285-290.

21. Камашева Г.Р., Надеева Р.А., Амиров Н.Б. Сезонный аллергический ринит: современные возможности терапии. //Вестник современной клинической медицины, 2015. – Т. 8. № 6. – С. 44-48. [Kamasheva G.R., Nadeyeva R.A., Amirov N.B. Seasonal allergic rhinitis: current treatment options. Bulletin of modern clinical medicine, 2015. –V. 8. № 6. –P. 44-48. (in Russ.)].

22. Юдина С.М., Тарабрина О.В., Иванова И.А.,. Макеева И.Ю. Особенности местных и системных механизмов аллергического воспаления при сезонном аллергическом рините. //Курский научно-практический вестник. Человек и его здоровье, 2018. – № 2. – С. 38-43. [Yudina S.M., Tarabrina O.V., Ivanova I.A.,. Makeeval. Yu. Features of local and systemic mechanisms of allergic inflammation in seasonal allergic rhinitis. //Kursk scientific and practical messenger. The man and his health, 2018. – № 2. – P. 38-43.[in Russ)].

23. Янаева Х.А., Мачарадзе Д.Ш., Авилов К.К. Сезонный аллергический ринит: локальные особенности. //Лечащий врач, 2018. – № 3. – С. 73. [Yanaeva Kh.A., Macharadze D.Sh., Avilov K.K. Seasonal allergic rhinitis: local features. The attending physician, 2018. –№ 3. – P. 73. in Rus)].

24. Aschner B. Uber einenbishernochnichtbeschriebenen Reflex, vom Auge auf Kreislauf und Atmung. Verschwinden des Radialispulsesbei Druck auf das Auge. //Wiener klinische Wochenschrift, 1908; 21: 1529-1530.

25. Dagnini G. Interno ad unreflecsoprovocato in alcuniemplegicocolo stimolodellacorne e cola pressionesulbulbooculare. //Bull. Sci. Med, 1908. 8: 380.

26. Lang S., Lanigan D., M. van der Wall. Trigemino-cardiac reflexes: maxillary and mandibular variants of the oculocardiac reflex. Can J Anaesth, 1991. 38 (6): P. 757-760. DOI:10.1007/BF03008454. PMID1914059.

27. Paton J., Boscan P., Pickering A., Nalivaiko E. The yin and yang of cardiac autonomic control: vago-sympathetic interactions revisited. //Brain Res Brain Res Rev, 2005. 49 (3): 555-565. DOI:10.1016/j.brainresrev.2005.02.005. PMID16269319.

**PHYSIOLOGICAL - HYGIENIC ASSESSMENT OF WORKING  
CONDITIONS DURING THE WORK ON MANUAL AND  
MECHANICAL AVERBAND**

**Iskandarov Aziz Bakhromovich**

Doctor of Philosophy in Medical Sciences, Senior Research Officer  
Scientific-Research Institute of Sanitary, Hygiene and Occupational Diseases of  
the Ministry of Health of the Republic of Uzbekistan

**Abstract.** The working conditions of workers employed in the production operations of averbands in the silk-weaving industry, carried out both manually and on machine tools, do not comply with hygiene regulations. An analysis of the dynamics of the indicators of the functional state of their body showed that from the beginning to the end of the working day, physiological reactions are noted, indicating a pronounced industrial fatigue, more pronounced with manual averband.

**Keywords:** silk weaving, averband, working conditions, functional state of the organism, fatigue, prevention.

Among the fabrics made from natural silk, a special place is occupied by avlar atlases - fabrics of a national assortment that are in high demand, especially among the population of Central Asia. The technology for the production of avlar atlases is peculiar; it is based on special dyeing of the warp and weft before weaving them into fabric. The yarns of the base are subjected to special preparation: skeins of silk yarns of the required perimeter (libits) are stretched on the averband machine, averband workers use special wooden sticks with special coloring clay to apply the ornament of the future drawing, designed by artists, to the libids; areas of libits that should not be stained are tightly tied with cotton threads.

Until recently, manual averband was used at all enterprises of the silk-weaving industry of Uzbekistan. Averband workers worked sitting on the floor with legs crossed, bent at the knees. Manual tightening of the base was carried out by performing small circular movements of the hands and wrist joint with simultaneous muscle effort of 4.5-15.7 N at a high pace (1210±2.6 movements per hour). Workload of the main work reached 75.9% of the time budget.

Under these conditions, a pronounced local tension of the muscles of the hands and shoulder girdle with a static load of the working posture was noted, and requirements were imposed on the function of the visual analyzer.

To date, a mechanical averband has been designed and implemented at "Atlas" JSC, which has made it possible to increase labor productivity. Under these conditions, the process of manual winding of the libits is excluded, the need to perform small movements is eliminated, the working position is changed. Work is performed while standing. However, the static load on the shoulder girdle increased, while holding the winding thread it reaches 78.4 N.

**Purpose of the study** was an assessment of the hygienic and physiological effectiveness of the new averband machines with the development of recommendations for improving working conditions, rationalizing work and rest.

**Research methods.** Working conditions were studied by traditional methods using an aspirator, psychrometer, anemometer, sound level meter, light meter in accordance with the requirements of the Sanitary Rules, Norms and Hygienic Standards of the Republic of Uzbekistan № 0294-11 [1], 0325-16 [2], 0141-03 [3], 0324-16 [4], building norms and rules 2.01.05-96 [7], as well as the methodology "Methodology for assessing working conditions and certification of jobs according to working conditions" [6].

The physiological reactions of the working organism were studied in the following order: before starting work, the initial and background characteristics of the indicators of the functional state of various body systems were recorded, and at the end of the shift, physiological reactions developing during the working day were recorded. All measurements were made directly at the workplace.

To assess changes in the central nervous system, the speed of the visual - motor reaction (VMR) was determined using a chronoreflexometer apparatus. The functional state of the visual analyzer was evaluated by the critical frequency of light flicker on the apparatus KCHSM-80. The attention function was studied using adjustment tables with a regulated text. The functional state of the cardiovascular system was studied by hemodynamic parameters: the pulse rate was calculated by the palpation method on the radial artery, and the level of blood pressure was measured using the Korotkov sound method. Using the calculation methods, the systolic volume and cardiac output (SV and CO) were determined using the Stara formula. According to the Hickem formula, the average dynamic pressure and pe-

ripheral resistance in the capillaries were calculated [5]. The state of the neuromuscular system was studied by physiological tremor and muscle endurance.

The studies were conducted at the Atlas Margelan Production Association, which is a modern production facility whose workshops are located in airtight buildings and are equipped with new technological and sanitary equipment.

The working conditions and the state of physiological reactions of workers – averband workers employed both on manual and mechanical averband – were studied. 22 practically healthy volunteers aged 24 to 45 years with a work experience of 2-14 years were examined.

**Research results.** It was established that the microclimate of industrial premises in different seasons of the year can be described as heating. Air temperature ranged from 22 to 35 °C, humidity - from 55 to 75%, with an air velocity of 0.3–0.7 m/s. During the shift, the distribution of the supply air was uneven, as a result of which, in the areas located near the air conditioners, the temperature was 22-24 °C, and in the center of the workshop it reached 35 °C. Illumination at workplaces ranged from 220 to 400 lux. In the mechanical averband workshop, intense broadband noise was generated by the averband machines, which in the frequency range 125–1000 Hz exceeded permissible values by 2–6 dB.

A comparative study of the physiological reactions of those working on manual and mechanical averband showed the most informative data characterizing the functional state of the neuromuscular apparatus (muscle endurance, physiological tremor), as well as the attention function of workers (table 1).

When using a manual averband, the muscular endurance to a static load of  $\frac{3}{4}$  maximum was clearly reduced by more than 35%. When working on a mechanical averband, this decrease is less pronounced. Both the absolute number of touches and their growth from the beginning to the end of the work when measuring physiological tremor were significantly different. The critical frequency indicators of light flicker and the duration of the proofreading test in the compared groups were statistically significantly different.

**Table 1. Indicators of the functional state of the body of workers on manual and mechanical averbands**

Indicators of physiological reactions	Before work	In the middle of the working day	Upon completion of work	Difference (before work and at the end of work)	Reliability
	M±m	M±m	M±m	2-4	p< <sub>3-4</sub>
1	2	3	4	5	6
<b>MANUAL AVERBAND</b>					
Heart rate in minutes	70,1±1,2	70,5±1,4	75,7±1,9	+5,6	0,05
Blood pressure, mmHg					
maximum	119,9±1,8	118,2±1,7	112,5±2,0	-7,2	-
minimum	71,2±2,7	74,1±0,5	75,2±2,0	+4,0	-
pulse	48,7±2,8	44,1±1,9	37,3±2,3	-11,4	0,001
dynamic average	87,4±1,3	88,8±2,2	87,6±3,1	-0,8	-
Systolic heart volume, ml	60,6±3,4	56,6±2,8	52,0±3,2	-8,6	0,01
Cardiac output, ml	4248,0±42,6	3993,8±36,1	3936,4±	-311,6	0,01
Peripheral resistance in capillaries, din	1645,5±23,7	1778,3±21,8	1779,8±26,1	+134,3	0,05
Simple visual motor reaction time, sigma	28,0±0,3	35,7±2,2	38,1±0,5	+10,1	0,001
Duration of the corrective test, sec.	91,5±2,8	93,3±0,3	94,1±2,3	+2,6	-
Critical fusion frequency of light flickers, Hz	35,6±0,2	33,3±0,9	29,4±0,5	-6,2	0,001
Physiological tremor, number of touches	15,2±0,2	14,3±0,9	14,0±0,6	-1,2	-
Muscular endurance, sec.	80,0±0,6	62±0,4	52,0±0,9	-27,4	0,001
<b>MECHANICAL AVERBAND</b>					
Heart rate in minutes	67,1±1,7	67,9±1,4	71,8±1,7	+4,7	0,05

## Process Management and Scientific Developments

Blood pressure, mmHg					
maximum	115,4±1,4	116,2±1,5	120,8±1,5	+5,4	0,01
minimum	79,9±1,3	72,2±1,5	73,5±1,3	-6,7	0,01
pulse	35,5±2,3	44,0±2,1	47,3±2,6	+11,8	0,01
dynamic average	91,7±2,5	86,8±2,4	89,2±3,1	-2,5	-
Systolic heart volume, ml	48,0±1,9	57,5±2,1	58,5±2,4	+10,5	0,001
Cardiac output, ml	3274,4±23,4	3904,2±24,3	4200,3±26,3	-929,9	0,01
Peripheral resistance in capillaries, din	2239,8±28,4	1778,1±23,1	1698,5±21,3	-541,3	0,01
Simple visual motor reaction time, sigma	29,9±0,5	28,2±0,5	32,5±0,4	+2,6	0,001
Duration of the corrective test, sec.	90,0±0,4	92,0±0,8	100,0±0,5	+10,0	0,001
Critical fusion frequency of light flickers, Hz	35,8±0,3	32,4±0,5	32,1±0,5	-3,7	0,001
Physiological tremor, number of touches	21,6±0,2	21,8±0,4	29,5±0,5	+7,9	0,001
Muscular endurance, sec.	81,0±0,8	69,0±0,5	65,0±0,4	-16,0	0,001

The materials obtained indicate that a working posture sitting on the floor, a large number of small movements with a small amount of muscle effort are more tiring than working on a machine, although in the latter case the amount of muscle effort has increased. However, work on both manual and mechanical averband causes certain changes in the physiological state of the working organism. On the part of the cardiovascular system, when working on a manual averband in the dynamics of the working day, there is a significant increase in pulse rate, an increase in minimum blood pressure, a decrease in pulse blood pressure, systolic and cardiac output, an increase in peripheral resistance in the capillaries, which indicates tension of the functional state of the cardiovascular system [8]. When working on a mechanical averband, the dynamics of the indicators of the cardiovascular system are more favorable: a certain increase in pulse rate, an increase in the maximum and decrease in the minimum blood pressure, systolic cardiac volume and cardiac output increase, and peripheral resistance in the capillaries decreases.

On the part of the central nervous system, when working on both manual and mechanical averband, the dynamics of work shows an increase in the time of simple visual-motor reaction in manual averband workers by 26.6% of the background working level, and when working on a mechanical averband by 8.6 %, the task execution time for the proofreading test increases, the indicator of the critical frequency of light flickers decreases, which indicates the development of inhibitory processes and indicates industrial fatigue

Thus, the working conditions of workers employed in the averband production operation in the silk-weaving industry, performed both manually and on machine tools, do not comply with hygiene regulations. An analysis of the dynamics of the indicators of the functional state of their body showed that from the beginning to the end of the working day, physiological reactions are noted, indicating a pronounced industrial fatigue, more pronounced with manual averband.

To improve working conditions and reduce the fatigue of labor processes, physiological and hygienic recommendations have been developed for improving working conditions at silk-weaving enterprises in Uzbekistan. A number of measures were introduced at Atlas Margilan Production Association: the operation of the ventilation system was adjusted, which ensured a 12-fold air exchange, maintaining the temperature at 24-28 °C, relative humidity 55-60%. Illumination at workplaces was brought up to 500 lux. Individual protective anti-noise devices have been introduced, for employees of a mechanical averband, industrial gymnastics are being conducted in the second half of the working day. As a result, the physiological responses of averband workers stabilized, efficiency and labor productivity increased by 3.9%. Proposals are being implemented to streamline jobs, improve the ergonomic parameters of mechanical averband machines and other preventive measures to improve working conditions in silk weaving.

### **Conclusions**

1. Working on a manual averband with a working pose sitting on the floor, with a large number of small movements with a small amount of muscular effort is more tiring than working on a mechanical averband machine.
2. To improve working conditions and reduce the fatigue of labor processes when working on a mechanical averband, it is necessary to introduce physiological and hygienic recommendations for improving working conditions.

### References

1. Iskandarov T.I., Ibragimova G.Z., Iskandarova G.T., Feofanov V.N., Shamansurova H.Sh., Tazieva L.D. Sanitary rules, norms and hygienic standards of the Republic of Uzbekistan № 0294-11 "Maximum permissible concentrations (MPC) of harmful substances in the air of the working area". - Tashkent, 2004. -53 P.
2. Iskandarov T.I., Magay M.P., Tashpulatova G.A., Iskandarova G.T., Adylov U.K. Sanitary rules, norms and hygienic standards of the Republic of Uzbekistan № 0325-16 "Sanitary norms of permissible noise levels at workplaces".- Tashkent, 2001. -17 P.
3. Iskandarov T.I., Ibragimova G.Z., Shamansurova H.Sh., Slavinskaya N.V., Iskandarova M.S., Demidenko N.M., Iskandarova G.T., Parsegova L.G., Feofanov V. N. Sanitary rules, norms and hygienic standards of the Republic of Uzbekistan № 0141-03 "Hygienic classification of working conditions by indicators of harmfulness and danger of factors of the working environment, severity and intensity of the labor process". - Tashkent, 2004. -53 P.
4. Iskandarov T.I., Slavinskaya N.V. Sanitary rules, norms and hygienic standards of the Republic of Uzbekistan № 0324-16 "Sanitary and hygienic standards of the microclimate of industrial premises. - Tashkent, 2016. -10 P.
5. Likhmitskaya I.I. Assessment of the state of functional systems in determining the ability to work. – Leningrad, 1962, 237P.
6. Nichkasov V.M., Iskandarov T.I., Ibragimova G.Z., Slavinskaya N.V., Iskandarova G.T. "Methodology for assessing working conditions and certification of workplaces for working conditions." - Tashkent, 1996. -21 P.
7. Building Norms and Rules 2.01.05-98 "Natural and Artificial Lighting". - Tashkent, 1998. -48 P.
8. Umidova Z.I., Glezer G.A., Yanbaeva H.I., King G.P. Essays on the cardiology of a hot climat. – Tashkent, 1975. 394 P.

**PHOTODYNAMIC THERAPY IN THE POSTOPERATIVE PERIOD IN  
THE TREATMENT OF PANARITIUM AND PHLEGMONS  
OF A HAND**

**Chepurnaya Julia Lvovna**

Surgeon

City Clinical Hospital №4, Moscow, Russia

**Melkonyan Georgiy Gennadevich**

Doctor of Medical Sciences, Full Professor, Head Physician, Surgeon

City Clinical Hospital №4, Moscow, Russia

Russian Medical Academy of Continuous Professional Education,

Moscow, Russia

**Gulmuradova Nargis Tashpulatovna**

Doctor of Medical Sciences

City Clinical Hospital №4, Moscow, Russia

O.K. Skobelkin State Scientific Center of Laser Medicine under FBMA,

Moscow, Russia

**Abstract.** For many years, the treatment of purulent diseases of the hand has not lost its relevance. Despite the progress in modern medicine, this pathology retains its prevalence and, most importantly, is often found in patients of working age, which determines the socio-economic importance of the search for new approaches to the treatment of purulent diseases of this localization. On the basis of the department of purulent surgery of the SBHI CCH №4, two groups of patients were studied and treated: patients with purulent diseases of the hand with open postoperative wounds using traditional treatment methods (antibacterial therapy, immobilization, dressings with antiseptic solutions and ointments, wound enzymes) and with the use of photodynamic therapy (PDT) in the postoperative period.

The article describes the methodology for conducting a PDT session in patients with purulent diseases of the hand. The effectiveness of treatment in the studied groups was assessed: a comparison of the timing of inpatient healing in groups, an analysis of the dynamics of the course of the wound process. When comparing the results of the two groups, the acceleration of healing of postoperative wounds in patients for whom PDT was used was 1.8 times faster: the early appearance of granulations and the antibacte-

rial effect of this procedure were noted, which significantly improves the treatment outcome for this pathology. This makes the use of PDT relevant and appropriate in the complex treatment of purulent diseases of the hand.

**Keywords:** photodynamic therapy, purulent diseases of the hand, drainage-washing system, photosensitizer, necrectomy.

### Introduction

The problem of treating panaritium and phlegmon of the hand remains complex and relevant, despite the successes of modern medical science. Of all the primary patients visiting a surgeon with purulent diseases, patients with panaritium and phlegmon of the hand make up from 15% to 31% [1], while from 50% to 85.5% of them are patients of working age. It is noted that men are sick more often than women [2]. Economic losses associated with temporary disability caused by purulent diseases of the fingers and hand are many times greater than those with purulent processes of a different localization.

In particular, according to the literature, 17-60% of patients with bone panaritium amputation of phalanges is performed. It is also reported that up to 48% of minor hand injuries are complicated by suppurative process, which leads microtrauma to one of the leading factors in the development of severe purulent process on the fingers and hand [1-3].

Very often, pain with purulent-inflammatory pathology of the hand is permanent, which dramatically affects the quality of life of patients. Due to impaired function of the hand and the characteristics of the pathological process, purulent diseases of the hand dramatically reduce the effectiveness and quality of professional activity [2-4].

In the surgical treatment of purulent pathology of fingers and hands, the method of choice is the method whose main principles are optimal access, adequate necrectomy, and completion of surgery by installing a drainage-washing system (DWS) in the wound with primary suturing of the skin.

However, with extensive wounds of the hand, often there is no possibility for a full closure of the wound defect, which requires open wound management. In addition, there are a number of medical contraindications to the application of DWS and wound healing under primary sutures (bite and crush wounds, etc. [1-7]).

Open wound management of the wrist leads to an increase in the number of hospital days. At the same time, the risk of joining a secondary infection increases, there is a need for frequent dressings, which in the absence of sutures are very painful. Thus, it becomes necessary to search for newer and more effective methods of treating wounds in the early postoperative period [8].

One of the promising methods for treating purulent wounds of various localizations is photodynamic therapy (PDT), which is widely used throughout the world for the treatment of purulent diseases [9-10].

Photodynamic therapy is a method of treating cancer, some skin diseases (psoriasis, ichthyosis, pustular diseases, etc.) or infectious diseases, inflammatory diseases of the mucous membranes (including chronic periodontitis) based on the use of photosensitive substances, photosensitizers (PS), and laser radiation with a specific wavelength [11-14].

In the scientific literature there is practically no information on the use of PDT in the treatment of purulent diseases of the hand.

The purpose of this study was to compare the efficacy in the treatment of patients with purulent diseases of the hand with the open management of postoperative wounds using photodynamic therapy and using traditional treatment methods.

### **Materials and methods**

An analysis of the treatment of 86 patients with purulent diseases of the fingers and hand, admitted to the purulent surgery department of the SBHI CCH № 4 for the period from December 2017 to December 2019, was performed among them men - 60 (69.7%) people. The age of patients ranged from 19 to 64 years, 78 (90.7%) belonged to persons of working age. Deep forms of panaritium occurred in 51 (59.3%) patients, hand phlegmon in 31 (36.0%), hand phlegmon with a transition to the forearm in 4 (4.7%). In 90% of patients, damage to the right hand prevailed. Among patients with concomitant pathology, patients with type II diabetes mellitus predominated - 10 (20%), with diseases of the cardiovascular system - 8 (16%), with multidrug addiction - 3 (6%), with systemic lupus erythematosus - 1 patient. According to the causative factor: non-production injuries predominated - in 45% of patients, bitten wounds - in 30%, industrial injuries - in 10%, post-injection injuries - in 5%, unclear genesis - in 10%.

Patients, depending on the method of treatment, were divided into 2 groups. When comparing the control and the main groups by age and sex, forms of the disease, the duration of the disease before admission to the hospital, it can be stated that they are comparable in their characteristics: the main group included 43 patients who underwent PDT after opening the purulent foci, the control group also amounted to 43 patients, in the treatment of which was performed according to the traditional method.

Prior to the study, all patients underwent a standard examination, including assessment of clinical and laboratory data, radiography of the damaged hand, and ultrasound examination of the soft tissues of the hand. According to indications, vaccination against tetanus was carried out (ad-

ministration of tetanus toxoid and tetanus toxoid serum according to the scheme), as well as bacteriological and histological examination of wound components at various periods of treatment.

At the first stage, patients of both groups underwent surgical treatment. A purulent lesion was opened, necrectomy, and drainage under local conduction anesthesia corresponding to the level of infection.

Patients in the control group were subsequently given standard combined treatment, including antibacterial therapy, analgesics, daily dressings with antiseptics, physiotherapeutic treatment (UHF, UV, magnetotherapy).

And patients of the main group in the postoperative period underwent PDT. A photo-irradiation session was performed as early as possible: on the second (less often on the third) day after opening the purulent focus on the background of open wound management. The number of sessions ranged from 1 to 2, depending on the area of damage to the hand and the dynamics of wound cleansing.

The PDT session consisted of the following steps. A bandage was applied to the wound with the gel form PS of the "Chloderm" chlorin series (Declaration of Conformity of 04/19/17, GOST 31695-2012, LLC "Chloderm", Russia) with an exposure of 20-30 minutes (based on 1 ml of gel for 3-5 cm<sup>2</sup> of the treated surface). Over a given period of time, pathologically altered cells accumulated PS. Next, the wound was washed with saline to remove PS residues. PS activation was performed by light exposure to the wound surface with laser radiation of the "Atkus-2" apparatus ("Atkus" LLC, RF) with an output power of 1 to 2 W and a wavelength of 660±0.03 nm, energy density of 20 to 25 J/cm<sup>2</sup> (Fig. 1). The irradiation time for external light supply using light guides with a polished end was determined by the formula [15,16]:  $T (s) = D (J/cm^2) / P_s (W/cm^2)$ , where  $T$  – exposure time,  $D$  – required light dose (energy density),  $P_s$  – power density.

The energy density brought to the wound should be on average 30-40 J/cm<sup>2</sup>: at an energy density of less than 30 J/cm<sup>2</sup>, a weak effect was observed, complete destruction of the wound microflora did not occur, and at an energy density of more than 40 J/cm<sup>2</sup>, healthy wound tissue was necrotized. Therefore, the power density of the light emitted by the semiconductor laser was chosen in the range of 0.1-1 W/cm<sup>2</sup>, and the exposure time to the wound was varied from 30 to 400 s, depending on the area of the wound. The power density was chosen depending on the size of the light spot.

Under the influence of PDT, the toxic effect of bacterial products was reduced, phagocytosis was activated, wound cleansing, reduction of microcirculatory disorders, intensification of previously repressed successive

reparative processes were noted: macrophage reaction, collagen synthesis, scarring and epithelization (maturing granulation tissue with vertical vessels appeared on day 6-7) fibroblasts and severe fibrillogenesis). To assess the bacterial landscape of the wound, the wound contents were inoculated before and after the PDT session. A histological examination of tissues of the wound edges was also performed on days 2, 3, and 6 after a PDT session (to assess the dynamics of inflammation, determine the timing of the onset of granulation tissue).

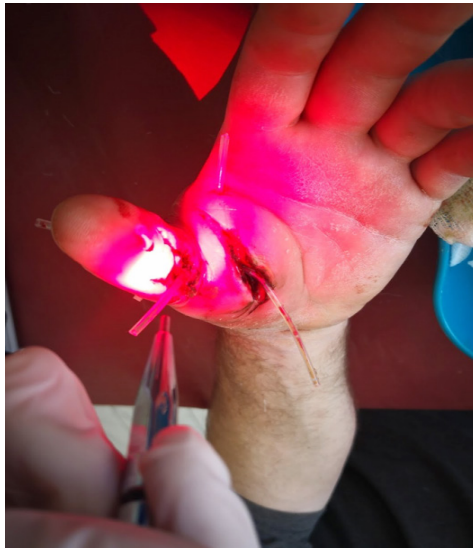


**Fig. 1. Laser exposure of the photosensitizer**

We evaluated the elimination of the photosensitizing drug using laser fluorimetry using the "Spectrum-Cluster" apparatus developed on the basis of a spectrometer ("Cluster" LLC, Russia,  $\lambda = 400-700$  nm). Optical spectrometers are apparatuses consisting of a grating polychromator with a multichannel photodetector and exciting laser sources (in an amount from one to three). The spectral range of the device is 400-1000nm. The spectral resolution of a spectrometer with a fiber optic probe is less than 3 nm, the spatial resolution when scanning the probe along the wound surface is about 1 mm. In this study, we evaluated the dynamics of absorption, distribution, and elimination of PS in a postoperative wound. At each PDT session, fluorescence intensity was measured in arbitrary units of tissue at several stages:

- on an unchanged area of the skin;
- in the wound before applying the drug;
- 20-30 s after application (to assess the fluorescence of the drug before its absorption by tissues);
- then every 5 min during the exposure period of the drug in the wound
- 10-15 minutes. A more frequent measurement led to a violation of the silent regime of the drug exposure and a decrease in the PS efficiency at the irradiation stage. At this stage, fluorescence dynamics was evaluated. In addition, at this stage, the peak of maximum fluorescence activity was estimated, after which a session of exposure to the wound with a laser device should be performed, otherwise, after this moment, the elimination of PS by the patient's body began, resulting in a decrease in the concentration of the drug in the wound, this, and the effectiveness of the procedure itself.
- during the "Atkus-2" laser session, fluorescence was measured to evaluate the total PS burnout in the wound.

Thus, the fluorescence measurement made it possible to confirm the optimal exposure time of PS in the wound, to evaluate the photoactivity of the drug, and also to establish the exact term for the end of the PS reaction in the wound - to confirm the complete photo-absorption of the drug.

Statistical processing of the data obtained from our own observations was carried out using the Microsoft Office 2017 application package (Word, Excel), by the method of variation statistics using Student's criteria. A comparison was made of the average values, including determination of the measurement error and the significance of differences in the timing of inpatient treatment, the timing of wound healing between the study groups. Differences were evaluated as significant at  $p < 0.05$ .

### Results

Assessment of fluorescence was carried out in conventional units. The fluorescence intensity of the patient's healthy skin was 0.4-0.5 conventional units, depending on the phototype. When comparing the fluorescence intensity in the wound after PS application, an increase in intensity was observed during 15 minutes of exposure in the wound: 20 s after application, the fluorescence intensity was  $0.6 \pm 0.05$  conventional units, after 5 minutes -  $5.9 \pm 0.07$ , after 10 min -  $8.3 \pm 0.07$ , at the 15th minute the fluorescence intensity was  $15.4 \pm 0.1$ . Next, laser irradiation was performed during the calculated irradiation time, after which the fluorescence intensity was again measured, which after the end of the PDT session fell to the initial values -  $0.7 \pm 0.03$ .

The terms of inpatient treatment of patients with purulent wounds of the hand depended on the genesis of the wound, the depth of the lesion and the duration of hospitalization from the moment of injury. On average, in the traditional treatment group, the duration of inpatient treatment was  $12.5 \pm 0.8$  days, complete wound healing was observed on  $17 \pm 0.8$  days. In 30% of patients of this group, repeated necrectomy and sanitation of a purulent necrotic lesion were required. In patients who underwent PDT in the postoperative period, the duration of inpatient treatment was  $6.88 \pm 0.7$  days ( $p=0.03$ ), complete wound healing was noted on 11.5 days.

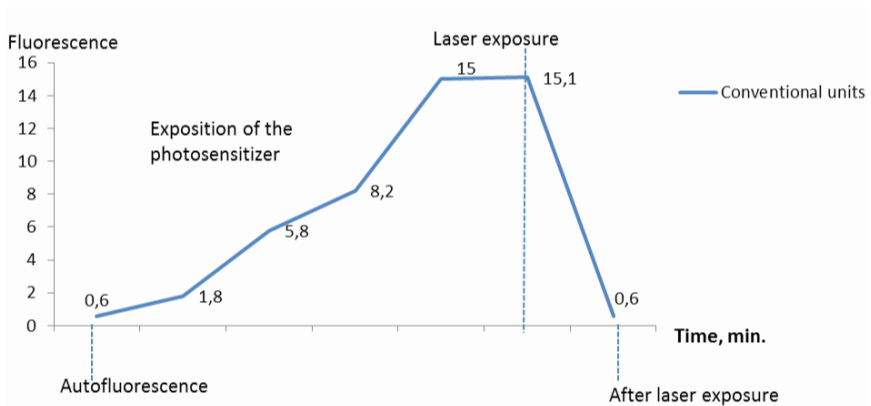


**Fig. 2. Time Dependence of Fluorescence Intensity**

During bacterial culture of the wound discharge prior to surgical treatment of wounds, most often - in 29 patients (67.4%) - *Staphylococcus aureus* was found, epidermal staphylococcus in 7 (16.3%). Anaerobic non-clostridial infection was observed in three cases.

According to the clinical picture and histological examination data on the 2nd, 3rd day after PDT, the wound was cleaned of purulent-necrotic masses, granulation tissue appeared.

On the first day after the PDT session, a histological examination showed a decrease in inflammatory phenomena (Fig. 3a), on the second day fresh granulations were visualized in the wound, purulent discharge was not detected (Fig. 3b), which is also confirmed by the results of inoculation of contents from the wound.

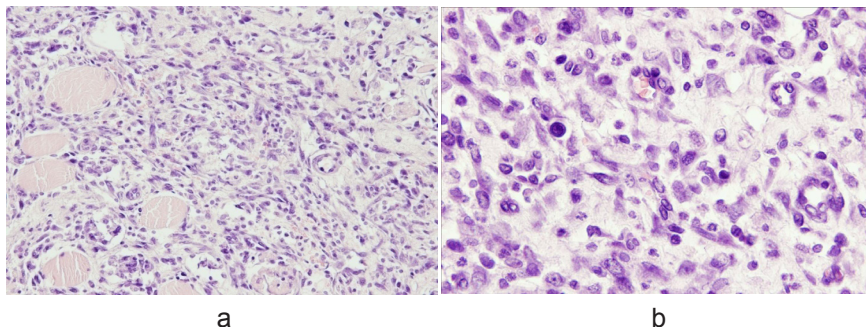


**Fig. 3. Biopsy of tissue taken from the edge of the wound of patient K. (stained with hematoxylin and eosin):**

a – before the PDT session: fragments of necrotic altered muscle fibers and fibrinous-leukocyte layer; edema, plethora of vessels of the deep sections of the wound, islets of forming granulation tissue (increase x120);

b – on the second day after the PDT session: macrophages and individual non-oriented fibroblasts near vascular elements (zoom x200)

Bacteriological studies revealed the antimicrobial effect of PDT: in the seedlings taken after completion of PDT, there was no growth of microorganisms detected in the initial bacteriological studies.

Amputation of phalanges, repeated necrectomy after PDT was not required. All patients after PDT showed a significant reduction in pain. The advantages of using this technique in the treatment of purulent wounds of the hand can also include the absence of additional destructive tissue lesions in the wound, the possibility of exposure to deeply located tissues and an analgesic effect. During PDT there was practically no bleeding during dressings.

There were no allergic reactions to PS. During the PDT session, pain was absent. During the PDT session and after it hyperthermia, no local inflammatory reaction was noted.

### **Conclusion**

The methodology developed by us for the use of PDT in the complex treatment of purulent diseases of the hand with open wound management has a positive effect on the course of the wound process, accelerates wound cleansing and significantly reduces the healing time of wounds (up to 1.4 times), and, consequently, reduces the duration of inpatient treatment (in 1.7 times) and the achievement of good functional results, which is of great socio-economic importance, leads to an improvement in the immediate and long-term results of treatment of this severe pathology.

## References

1. A.S. Lyubsky, M.S. Alekseev, A.A. Lyubsky, T.A. Gadzhikerimov, A.E. Brovkin. Errors and complications in the provision of medical care to patients with purulent-inflammatory diseases of the fingers and hands // Attending physician, 2000, № 21, P. 25-27.
2. Daigeler A. Differential diagnosis of "sterile" phlegmonous hand infections // A.Daigeler, M. Lehnhardt, M. Helwing et al. // Chirurg. - 2006
3. Goldstein -Ellie J. National hospital survey of anaerobic culture and susceptibility methods: III // J. Ellie-Goldstein, D.M. Citron, P.J. Goldman, R.J. Goldman Anaerobe. - 2008. V.14. - №2. - P. 68-72
4. Reichert B. Hand infections resulting from underestimation of minimal injuries/ B. Reichert, P. Oeynhausens-Petsch, P. Mailander // Handchir Mikrochir Plast Chir. - 2007
5. Stranadko E.F. The main stages of the development of photodynamic therapy in Russia // Photodynamic therapy and photodiagnostics, 2015., №1 P.3-10.
6. Stranadko E.F. et al. Photodynamic therapy for purulent diseases of the soft tissues // - Surgery, №9, 2000.
7. Pletnev S.D. Lasers in clinical medicine. // Guide for doctors. Ed. S.D. Pletnev. M. Medicine, 1996, 432 P.
8. E.A. Lukyanets Search for new photosensitizers for photodynamic therapy / Photodynamic therapy and photodiagnostics, 2013.
9. Machneva T.V. Doc. Diss. Photodynamic mechanism of therapeutic action of laser and LED radiation, Moscow, 2015.
10. Luz, A. F., Pucelik, B., Pereira, M. M., Dąbrowski, J. M. & Arnaut, L. G. Translating phototherapeutic indices from in vitro to in vivo photodynamic therapy with bacteriochlorins.// Lasers in surgery and medicine 50, 451–459 (2018)..
11. Malwina Karwicka, Barbara Pucelik, Michał Gonet, Martyna Elas Janusz M. Dąbrowski. Effects of photodynamic therapy with redaporfin on tumor oxygenation and blood flow in a lung cancer mouse model
12. Maksimova N.V. Tikhonov V.E. Evaluation of the effectiveness of photodynamic antibiotic therapy in the complex treatment of chronic antibiotic therapy in the complex treatment of chronic generalized periodontitis in patients requiring orthodontic treatment. // In the world of scientific discoveries, 2016; 11(83). P. 99
13. Dougherty T.J. Haematoporphyrin as a photosensitiser of tumours. //Photochem Photobiol 1983; 38: 377-379.

14. Tolstykh P.I., Klebanov G.I., Shekhter A.B. et al. Antioxidants and laser radiation in the treatment of wounds and trophic ulcers. M: Publishing House "Eco" 2006; 238.

15. Geynits A. V. Laser therapy in cosmetology and dermatology — Moscow; Tver: Triad, 2010 — 400 P. 54.

16. Geynits A.V., Sorokaty A.E., Yagudaev D.M., Trukhmanov R.S. Modern view of the mechanism of photodynamic therapy. // Photosensitizers and their bioavailability. Urology 2006; 5: 94-98.

**THE EFFECT OF EXPERIMENTAL TYPE 1 DIABETES ON  
THE MORPHOFUNCTIONAL STATE OF MAST CELLS OF THE  
FALLOPIAN TUBES OF THE OFFSPRING OF FEMALE RATS**

**Drebit Veronika Vladimirovna**

Applicant

Chelyabinsk State University, Chelyabinsk, Russia.

**Bryukhin Gennady Vasilevich**

Doctor of Medical Sciences, Head of Department

South-Ural State Medical University

**Abstract.** The article discusses the structural and functional state of mast cells of the fallopian tubes in sexually mature offspring of female rats with experimental type 1 diabetes mellitus. Given that mast cells secrete mediators responsible for the regulation of tissue homeostasis, the authors conducted a study in which the quantitative and subpopulation composition of mast cells was analyzed according to the degree of their granular saturation and degranulation, indices of granular saturation and degranulation were also calculated.

**Keywords:** type 1 diabetes, fallopian tubes, mast cells and their subpopulation composition.

**Introduction**

At present, diabetes mellitus takes the 1st place in prevalence among endocrine diseases and is considered “a threat to national security” [1]. It has been established that type 1 diabetes mellitus has a negative effect on the formation and functioning of the reproductive system [5]. At the same time, it is known that mast cells, thanks to the secretion of biologically active substances, take an active part in the implementation of homeostatic type protective reactions [6]. There are numerous studies that indicate a change in the content of mast cells, their secretory activity in the reproductive system, which indicates their participation in the paracrine regulation of the functioning processes of structural elements and confirm the opinion of mast cells as cells of a diffuse endocrine system that actively support tissue homeostasis of the reproductive system [4]. An analysis of the literature shows that the role of type 1 diabetes mellitus in the morphofunctional

formation of the reproductive system of offspring is not well understood. In connection with the foregoing, the goal of this study was to analyze the effect of experimental type 1 diabetes mellitus on the structural and functional state of mast cells of the fallopian tubes in the offspring of female rats.

### **Materials and research methods**

The studies were conducted on sexually mature offspring of white laboratory rats of the "Wistar" strain. To achieve this goal, experimental animals were divided into 2 groups. The first group consisted of 10 animals from intact mothers (control group). The second group included 10 animals of sexually mature offspring from mothers with experimental type 1 diabetes mellitus (experimental group).

To model type 1 diabetes mellitus, a conventional technique was employed using streptozotocin [2], which was administered intraperitoneally to animals 3 times with an interval of 7 days (2.5 mg per 100 g of body weight in the first and third weeks and 2 mg in the second week) per 100 g). Under the influence of streptozotocin, laboratory animals developed diabetes mellitus, as evidenced by the constant elevated values of glucose in the peripheral blood, which persisted for at least 3 months. For mating, 1 week after the last administration of streptozotocin, female rats were transplanted to intact males.

Work with experimental animals was carried out in accordance with the "European Convention for the Protection of Vertebrate Animals" (Strasbourg, March 18, 1986), used in the experiment for other scientific purposes.

The object of the study was the fallopian tubes of sexually mature (70-day) offspring of female rats with experimental type 1 diabetes mellitus. During the study, histological, histochemical and statistical research methods were used. The fallopian tubes were fixed in 10% neutral formalin. The preparations were made according to the generally accepted scheme. To detect mast cells, serial histological sections of the fallopian tubes were stained with 0.1% toluidine blue solution. To assess the morphofunctional state of mast cells, we calculated their number and analyzed the subpopulation composition of cells according to the degree of their granular saturation and degranulation, using the generally accepted method of D.P. Lindner et al., Followed by the calculation of indices of granular saturation and mast cell degranulation [7].

Statistical processing of the results was carried out using the PAST program (v.3.13). During statistical processing of data using the method of variation statistics, the arithmetic mean and its error were determined. To identify differences in the compared indicators, the nonparametric Mann -

Whitney test was used. In this case, results were taken into account where the significance level ( $p$ ) of the detected differences was less than or equal to 0.05 (95%).

**Research results and discussion**

The data obtained allow us to state that in diabetes mellitus there is a significant decrease in the content of mast cells in the wall of the fallopian tubes. It was found that in experimental animals the number of mast cells was reduced and amounted to  $89 \pm 2,627$  per 1 rat, while the quantitative composition of mast cells in intact animals was  $119 \pm 2,345$ . When studying the subpopulation composition of mast cells of the fallopian tubes of the experimental and control group of animals according to the degree of granular saturation, we obtained the following data (table № 1). We found that experimental type 1 diabetes mellitus causes a significant increase in the proportion of very dark cells by 19.31%, a decrease in dark cells by 9.7%, light cells by 6.19%, and very bright by 3.42%. Due to the fact that very dark cells predominate in experimental rat pups, it can be assumed that the excretory function of mast cells fades, and heparin cannot exhibit its antioxidant and antidiabetic properties [3,6]. When the subpopulation composition of mast cells changes, the index of granular saturation in experimental animals increases, which is equal to  $4.24 \pm 0.458$ , whereas in intact animals this indicator is  $2.48 \pm 0.299$ .

**Table 1**  
**Subpopulation composition of mast cells in the fallopian tubes of intact and experimental animals according to the degree of granular saturation (%)**

Groups	Cell types			
	Very dark cell (M±m)	Dark cell (M±m)	light cell (M±m)	Very light cell (M±m)
Control	12,82±1,572	58,46±2,113	17,43±1,907	11,29±1,116
Test	32,13±2,311*	48,76±1,804*	11,24±1,406*	7,87±0,664*

\* – the results are statistically significant ( $p < 0.05$ ) compared with the control

We noted that in experimental type 1 diabetes mellitus, the proportion of non-degranulating in experimental rat pups increases by 34.26% and in cells with a weak degree of degranulation by 12.42%. At the same time, there is a decrease in the proportion of moderately degranulating cells by 21.23% and cells with strong degranulation by 25.45% (table № 2). A change in the subpopulation composition of cells by the degree of degran-

ulation leads to a decrease in the mast cell degranulation index in experimental animals. So, if in intact animals the degranulation index turned out to be  $2.94 \pm 0.277$ , then in experimental rats the studied parameter was only  $1.89 \pm 0.153$ , which indicates a violation of the excretory activity of mast cells.

**Table 2**  
**Subpopulation composition of mast cells**  
**of the fallopian tubes according to the degree of degranulation (%)**

Groups	Cell types			
	N/d/cell (M±m)	W/d/cell (M±m)	M/d/cell (M±m)	H/d/cell (M±m)
Control	8,21±1,197	19,49±1,665	42,56±1,599	29,74±1,914
Test	42,47±1,571*	31,91±1,875*	21,33±2,071*	4,29±0,972*

\* – the results are statistically significant ( $p < 0.05$ ) compared with the control

- Note. N/d/cell– non-degranulating mast cell;
- W/d/cell– weakly degranulating mast cell;
- M/d/cell– moderately degranulating mast cell;
- H/d/cell– highly degranulating mast cell.

In general, the results suggest that mothers with experimental type 1 diabetes can have offspring with compromised reproductive health, which is self-convincing evidence of a decrease in the content and inhibition of the secretory function of mast cells of the fallopian tubes.

**Conclusion**

Thus, it can be concluded that the progeny of female rats with experimental type 1 diabetes mellitus experience changes in the content of mast cells, as well as their subpopulation composition according to the degree of granular saturation, which is manifested in an increase in the proportion of very dark cells, and the subpopulation composition according to the degree of degranulation, which is observed in an increase in the number of non-degranulating mast cells and cells with weak degranulation, compared with the control. These data are confirmed by a significant increase in the index of granular saturation of mast cells in experimental animals, which indicates an increase in their secretory activity, as well as a decrease in the degranulation index, which may indicate an inhibition of their excretory ability. The results also suggest a certain role for mast cells in the pathogenesis of disorders of the morphofunctional state of the female reproductive system in the offspring of mothers with experimental type 1 diabetes.

## References

1. Volynkina, A.P. Diabetes mellitus - a dangerous challenge to the world community [Text] / A.P. Volynkina, I.P. Gorshkov, V.I. Manannikova // Sci.-med. Bulletin of the Central Black Earth Region. – 2016. – № 63. P. 166-171. ; The Russian Federation. President (2000-2020; V.V. Putin). Decree of December 31, 2015 № 683 “On the National Security Strategy of the Russian Federation” [Text]: CIRF. – 2015. – 480 P.].
2. Zakiryanov A.R., Plahotniy M.A., Onishchenko N.A., Volodina A.V., Klimenko E.D., Kobozeva L.P., Michunskaya A.B., Pozdnyakov O.M. Diabetic complications in rats with long periods of modeling of type 1 diabetes mellitus. Pathological physiology and experimental therapy. 2007
3. Kondashevskaya M.V. The role of heparin in immune, inflammatory and reparative processes / M.V. Kondashevskaya // Clinical and experimental morphology. – 2012. – № 5. – P. 62-69
4. Lindner D.P., Kogan E.M. Mast cells as regulators of tissue homeostasis and their place in the series of biological regulators // Archive pathology. M., 1976, V. 48, № 8, P. 19-24.
5. Misharina, E.V. In vitro fertilization as a method of treating infertility in women with type 1 diabetes [Text] / E.V. Misharina, A.V. Tiselko, M.I. Yarmolinskaya, I.Yu. Kogan, E.I. Abashova, N.V. Borovik // Diabetes mellitus. – 2018. – № 5. – P. 425-430
6. Yaglova N.V., Yaglov V.V. Biology of mast cell secretion / N.V. Yaglova, V.V. Yaglov // Clinical and experimental morphology. – 2012. – № 5. – P.4-9
7. Lindner DP, Poberiy IA, Rozkin MYa, Morfometricheskii analiz populyatsii tuchnykh kletok. Arkh. patologii; 1980.42(6):60-64].

## CLINICAL AND SOCIAL ASPECTS OF FUNCTIONING OF EPILEPSY PATIENTS<sup>1</sup>

**Tokareva Natalia Gennadievna**

Candidate of Medical Sciences, Associate Professor

Medical Institute

National Research Mordovia State University N.P. Ogarev

**Annotation.** The analysis of clinical and sociological patterns of mental disorders in the personality structure of patients with epilepsy is carried out. During the study, such disease indicators as the type of attack and the duration of the disease were taken into account: simple and complex partial seizures, seizures with secondary generalization predominated, the duration of the disease was up to 30 years. The diagnosis was checked in the examined patients on the basis of the results of clinical, neurological, psychopathological, pathopsychological, neuropsychological, electroencephalographic examination and computed tomography of the brain. The study of clinical and psychological characteristics in patients with epilepsy was carried out using the following methods: clinical observation method, psychodiagnostic methods: “Methods for assessing mental activation, interest, emotional tone, tension and comfort”, method “Level of social frustration”. In patients with epilepsy, reliable multidimensional clinical and sociological characteristics of mental activity were revealed. The considered characteristics are of interest to doctors, clinical psychologists and other specialists who provide medical, rehabilitation, psychoprophylactic care to patients with epilepsy.

**Keywords:** epilepsy, clinical aspects, social aspects.

Epilepsy is one of the most common neuropsychiatric diseases. A large number of scientific works are devoted to diagnosis [1,2,3], social functioning [4,5], treatment and rehabilitation of patients with epilepsy [6,7].

**The purpose of this work** was to study the clinical and social aspects in patients with epilepsy.

**Material and methods of research.** The study included 317 patients, aged from 18 to 65 years, with various forms of epilepsy, in the structure of the disease which was dominated by simple, complex partial seizures,

---

<sup>1</sup>This work was supported by the RFBR (grant No. 20-013-00529).

disease duration of more than 30 years. The verification of the diagnosis in the examined patients was carried out on the basis of the results of clinical and neurological, psychopathological, pathopsychological, electroencephalographic examination and data of computed tomography of the brain. The study of mental disorders conducted using the following methods: clinical observation method, psychodiagnostic methods: "Methodology for assessing mental activation, interest, emotional tone, tension and comfort", method "Level of social frustration". Statistical data processing was carried out using the program Statistica 10.0.

The influence of the environment on a person has an important role in the functioning of the individual. The identity of a sick person is influenced by parents, close relatives, colleagues, friends, etc. It is important that the patient, on the one hand, understand his area of responsibility, but at the same time feel support, understanding. Self-confidence is a fundamental factor in success. It is difficult to be successful if people around say about your helplessness and failure. The patient is directly or indirectly affected by his immediate environment. The qualities that determine the personality of a particular person are formed under the influence of relations with people around them, under the influence of processes taking place in society.

The environment of a person is not only people, these are books, films, social networks. A person is born at a certain point in the world, in a country and a family with a certain culture, lifestyle, foundations and rules. To become a person, a person must learn from social experience and, on the other hand, contribute to society. At the same time, it reveals and manifests precisely the qualities inherent in nature by nature and formed by society through education. In the process of human development, his spiritual, mental and physical characteristics change from quantitative transformations to qualitative changes. In his youth, a person is still very dependent on his home circle of friends, on relatives and friends, but gradually outside influence is added to him. There are friends, acquaintances, teachers and mentors. Particularly strong influence is exerted by people whom one would like to be like. In this case, the so-called imitation mechanism works, the desired manners and behavior.

In process of spiritual growth, as a result of the influence of the disease, a sick person undergoes reappraisal of values. The patient can no longer communicate with his past friends. Its vibrational level rises, and ways with many people begin to diverge.

Man is a social being who cannot live alone and cannot stand the role of an outcast. To avoid this role, people often try to get lost in their environ-

ment, to become like everyone else. For example, if a person's environment, his close friends live an active life, play sports, a person can't ignore sports for a long time, sooner or later he will be drawn into a sports life, because one way or another the sports theme and the theme of an active lifestyle will be one of the most relevant and energetically powerful. A person will either have to take an active part in the life of friends, sharing their interests, thoughts with them, or change his environment.

The social environment plays an important role in the birth of personality. Everyone lives in society, so he needs to learn how to interact with him. To be implemented here, a person will need to develop communication skills. They can be easily achieved through frequent direct communication with people around him. In childhood, this can be communication with parents, later with teachers and friends. This factor in the development of the human personality can also be improved in adulthood. For example, a person can review his social circle and use the observation method to understand how he affects him and whether he is developing.

The social factor consists of the influence of society on a person. This may be the political situation in the country where the individual lives, or his religious preferences, the influence of the media and social norms and orders. Each person tries to create an environment around him that would in every way contribute to his development and self-improvement. At the same time, he should not feel constrained and restless. After all, everyone understands that it is much easier to develop in an environment where all other people also strive to improve and improve their lives.

Each person in his life has his own environment, which affects the formation of his personality. When a person has a positive environment, it supports him, motivates and brings joy to life. But if it is negative, then even successful people who find themselves in a bad environment become worse than they were. The human environment not only affects the personality, but also shapes it. If a person is goal-oriented, then it is much more natural and easier to achieve goals set in an environment of the same kind as to start walking towards a goal, convincing people around him that he is capable of something. And such people, in turn, can easily sow the seed of doubt in his abilities. Even failure will be perceived differently.

The influence of the environment in which a person is located occurs in such a way as not to stand out from it and be on a par with everyone. When someone begins to do something that is not the norm for the environment, it starts to bother him. Each word can affect a person and change his attitude to something. This is how consciousness and worldview are formed. Of course, not every opinion reverses the idea of the world.

Without a doubt, the environment affects the person, but how strong this influence will depend on the inner core of the person. At a young age, it is difficult to resist the environment, and then it becomes the task of adults - through their own examples, beliefs and just talking, to show what is good and what is bad. But adults always have the right to choose what to do their life, what to set goals for themselves and what kind of people to surround themselves with. Each word is interpreted by a person and passes through a series of internal mental filters, as in the production of a product in a factory, and as a result, after going through a great mental processing, an opinion is formed. Often people from the environment think that their advice helps, but in fact, on the contrary, they only prevent other people from achieving their goals. This is due to the lack of competence and own experience of consultants in those topics on which they give advice.

As a person develops and acquires life experience, the vast majority of people sooner or later create a family and children. Here, too, the environment has a direct impact.

Society forms social standards and stereotypes of behavior, so as not to stand aside, a person must learn these rules. First, it acquires general characteristics of the behavior of the social group in which it is located. Over time, individual character traits are developed that allow to realize the makings and abilities inherent in his genotype.

Modern society is a certain cultural sphere, falling into which the individual is attacked by opinions and assessments. There are many people who seek to impose their interests and their attitude to something. Of course, you need to be able to withstand this and, as mentioned above, build an internal system.

The influence of the environment on human life is great. As it turned out, half of the components of success are the environment. When a person can clearly and clearly determine his goals, desires, he will understand which path will bring him success. On the way to his goal, he will meet people who will influence him: someone will teach something, teach a lesson, someone will protect, support, inspire or try to stop his development. Each of the people he meets will play a role in his life.

To study the clinical and sociological characteristics in patients with epilepsy, the following methods were used: "Methodology for assessing mental activation, interest, emotional tone, tension and comfort", methodology "Level of social frustration." "Methodology for assessing mental activation, interest, emotional tone, tension and comfort" is intended to determine the characteristics of a person's mental state by indicators of mental activation, interest, emotional tone, tension and comfort. According to the results,

the severity of each of the mental states was determined - high, medium and low. Mental activation: high degree - 5.8% of patients, medium degree - 60% of patients, low degree - 34.2% of patients; interest: high degree - 11.5% of patients, medium degree - 42.8% of patients, low degree - 45.7% of patients; emotional tone: high degree - 22.8% of patients, medium degree - 54.4% of patients, low degree - 22.8% of patients; tension: high degree - 31.4% of patients, medium degree - 57.2% of patients, low degree - 11.4% of patients; comfort: high degree - 22.8% of patients, medium degree - 45.8% of patients, low degree - 31.4% of patients.

The methodology "Level of social frustration" was developed on the basis of preliminary expert selection and ranking of those areas of the system of social relations that appear to be most significant for any person in the context of its interaction with micro- and macro-social environment. According to the results of this methodology, the level of social frustration in the examined patients with epilepsy was determined - a low level was detected in 11.7% patients, a moderate level of social frustration was found in 52.8% of patients, and a high level of social frustration was found in 35.3% of patients.

The study shows: the importance of a comprehensive clinical, social and psychological study of epilepsy; the need to evaluate the totality of clinical and socio-psychological indicators and their multidirectional results, which makes it possible to more accurately build the treatment and rehabilitation process.

Thus, a disease such as epilepsy has a significant impact on the formation and manifestations of manifestations of psychopathological symptoms, options for the social functioning of patients, which is important to consider when conducting treatment and rehabilitation measures. The rehabilitation of patients with epilepsy in the near future will become a holistic system that will strive to achieve a common goal - to restore or maintain their biological and social status.

## References

1. Leaffer EB, Hesdorffer DC, Begley C. Psychosocial sociodemographic associates of felt stigma in epilepsy. *Epilepsy Behav.* 2014, 37, 104-9.
2. Leaffer E.B., Hesdorffer D.C., Begley C. Psychosocial sociodemographic associates of felt stigma in epilepsy. *Epilepsy Behav.* 2014, 37, 104-109.

3. Tokareva N.G. Changes in the psyche and the social functioning of patients with epilepsy: auto-ref. dis. on the competition scholarly step. Cand. honey. Sciences. Moscow Research Institute of Psychiatry: Moscow, Russia, 1998, 16.

4. Zheleznova E.V., Tokareva N.G. Clinical and psychological characteristics of the functioning disorders in epilepsy. Russian Psychiatric Journal, 2017, 3, 27-32.

5. Tokareva N.G., Zheleznova E.V. Clinical and psychological assessment of the attention of patients with epilepsy. J. scientific Articles Health and education in the XXI century. 2016, 18 (1), 28-30.

6. Inozemtseva V.S., Tokareva N.G. Indicators of social functioning of patients with epilepsy (according to the data of the epileptic center of Mor-dovia). Social and clinical psychiatry. 1998, 8(3). 86-88.

7. Mula M. The interictal dysphoric disorder of epilepsy: Legend or reality? Epilepsy & Behavior. 2016, vol. 58, 7–10.

## COMBINED NEUROPROTECTION IN RECOVERY TREATMENT AFTER ISCHEMIC STROKE

### **Badashkeev Mikhail Valeryevich**

Candidate of Pedagogical Sciences, Psychologist  
Regional State Health Budget Institution  
Bokhansky district hospital

### **Shoboev Andrey Eduardovich**

Neurologist  
Regional State Health Budget Institution  
Bokhansky district hospital

**Summary.** This article discusses ways to improve the effectiveness of combined neuroprotection in the recovery of cognitive functions in stroke patients. We place the combined pharmacotherapy "Citicoline" in complex application with the preparation "Cortexin" at the centre of the recovery of cognitive functions. A clinical study of 75 patients with the duration of the disease from the development of ischemic stroke for more than 1 year was carried out. The Montreal Scale was used to objectify the assessment of cognitive deficits. The statistical analysis of the obtained data shows an increase in the effectiveness of combined cyticoline neuroprotection in combination with cortexin in the recovery of cognitive functions in the rehabilitation period of ischemic stroke.

**Keywords:** stroke, combined neuroprotection, cyticoline, cortexin

In the modern period in Russian reality, cerebrovascular diseases are one of the most pressing problems of modern neurology, given the high prevalence of this pathology in the population. According to many scientists researchers, the most problematic field is disorders of cognitive functions of the brain. Scientific studies of A.N Boyko, I.V. Damulin confirm that cognitive deficiency after a stroke reaches about 40 to 70% of cases [4, 7].

Modern clinical studies in recent years have shown a steady increase in patients of 30-40 years of age, which subsequently leads to disability, 84% of patients have pronounced cognitive disorders after a stroke, which is our global medical and social problem. In the basis of our combined pharmacotherapy and psychotherapy we first of all see a systemic approach in the restoration of memory, attention, mental, intellectual activity, as well as social and psychological adaptation and working capacity [3].

In modern medical science, the most famous, common drugs with neuroprotective properties, positively affecting the recovery of postinsult cognitive disorders: cerebrolysin, cortexin, actovegin, cyticoline, cholinalphocerate. However, in many scientific sources the highest efficiency according to meth analysis is noted in cyticoline [10]. Cyticolin has a non-protective effect in acute and chronic cerebral ischemia. Cyticoline is known to improve the synthesis of phosphatidylcholine in ischemic tissue, resulting in stabilization of cell membranes. In addition, the synthesis of proteins, nucleic acids, acetylcholine and other neurotransmitters is restored in the injured neurons of the brain [8].

Particular attention is paid to the properties of low molecular weight neuropeptides that penetrate the blood-brain barrier and have multilateral effects on the central nervous system. One of the neuropeptide neuroprotectors is the domestic preparation cortexin containing a complex of low molecular weight peptides (weighing 1 to 10 kDa). The mechanism of action is due to the activation of neuropeptide brain neurotrophic factors; Stabilising the balance of braking and excitatory amino acids, serotonin, dopamine; GAMK-ergichesky influence; Reduced level of brain convulsive readiness. [5,9].

In most cases the drugs have been tested as monotherapy, relatively recently much interest has emerged in a combined approach in the recovery of neurological functions after stroke.

The combination of cyticoline with a drug of natural origin (neuropeptide "Cortexin") can be used in patients with vascular cognitive disorders in the rehabilitation period after ischemic stroke, both of which have a wide spectrum of pharmacological action [2].

Comparative study of pharmacotherapeutic effectiveness of drugs "Cyticolin" and "Cortexin" in patients with ischemic stroke in rehabilitation period, comparable by sex, age, duration of disease, was carried out. The study included patients with moderate cognitive disorders who had a duration of more than 1 year since the development of the stroke.

Patients with pronounced motor (hemiplegia) or speech (aphasia) disorders caused by stroke are excluded from the group. To study the effectiveness and portability of drugs ("Cyticolin" and "Cortexin"), patients who have undergone psychological diagnosis were selected, as well as informed in detail about the tactics and strategies of the process of recovery of cognitive functions (ICD data - 10. I67.2, I67.8). In strict compliance with the criteria, 55 patients who entered the neurological department No. 3 of the N.A. Semashko RCB in the period 2017-2018 were examined and treated. The method of blind randomization divided the patients into 2

groups. The first group - 28 patients who received basic therapy in combination with the preparation "Cortexin" 20 mg/m. The second group - 27 patients who were treated with basic therapy, combination therapy with preparations "Cortexin" 20 mg v/m and "Cyticolin" at a dose of 1000 mg v/a cap per day [1].

The diagnosis and evaluation of the patient's cognition functions included the study of language functions, short-term and working memory, attention, abstract thinking. The Montreal Cognitive Assessment Scale (MoCA) was used for this purpose. Non-parametric methods were used to determine differences between groups: U-test Mann-Whitney for two independent samples and Wilcoxon signed-rank test for two dependent samples. The differences between the compared groups were considered statistically significant at  $p < 0.05$ . Statistical analysis is performed in the package STATISTICA 20.0.

In the analysis of the assessment of intellectual impairment evaluated by the Montreal Scale of Cognitive Functions on the day of arrival, no reliable differences between the groups were identified. The duration of hospital treatment was 12 days.

Age list of patients: 30-39 years - 1.8%, 40 - 49 years - 12.7%, 50-59 years - 38.18%, 60 years are also more senior - 47.2%.

Clinical studies conducted in Group 1, patients who were treated with cortexin in combination, showed that the average results of the MoCA scale, although statistically significant after treatment, remained below the standard of 26 points (Wilcoxon Z-criterion = 2.73;  $p < 0,006$

In the second group, the averages reached the norm (Wilcoxon Z-criterion = 4.54;  $p < 0,00001$ ).

The results of differences in the distribution of scales between groups of patients with different combinations of therapeutic preparations demonstrate that the recovery rates of cognitive impairment after treatment with cyticolin and cortexin are statistically significantly higher than in treatment with cortexin alone (U-criterion = 194.5;  $p\text{-level} = 0.01$ ).

Thus, our clinical study fully confirms the efficacy of Citicolin and Cortexin combination therapy compared to Cortexin monotherapy (U-criterion = 194.5;  $P\text{-level} = 0.01$ ) in the recovery of cognitive functions in the rehabilitation period of ischemic stroke. The findings suggest the effectiveness of the complex therapy of these drugs, which may be recommended for introduction into clinical practice of the treatment of cognitive impairment in patients in the rehabilitation period.

## References

1. Badashkeev, M.V. Multidisciplinary approach in the treatment of cognitive dysfunctions following stroke [Text]: article / M.V. Badashkeev, A.E. Shoboev // European Sciences review. Premier Publishing s.r.o. - Vienna, Austria, 2020 - No. 1-2 - Page 23-26.
2. Badashkeev, M.V. Efficiency of neuroprotectors in treating ischemic stroke [Text] article / M.V. Badashkeev, A.E. Shoboev // XII Materials of the international scientific and practical conference "Open innovation" /hl. edition G. Gulyaev. - Penza.: Prod. MTsNS "Science and Education", - 2020. - Page 107-109.
3. Batysheva T.T., Boyko A.N., Skorometz A.A. et al. Neuroprotection in the therapy of chronic cerebral circulation failure. Vestn. Grew. Voen-medical. Akad., 2007, № 1 (17). - S. 11-18.
4. Boyko A.N., Batysheva T.T., Bagir L.V. et al. Experience of outpatient application of the preparation cerebro in ischemic stroke in early recovery period. Journal neuropath and psychiatrist 2007; 107 (10): 34 - 40.
5. Homazkov O.A. Cortixin: molecular mechanisms and targets of neuroprotective activity. Journal of Neurology and Psychiatry. 2015; 8: 99–104.
6. Granstrom O.K. et al. Cortixin: neuroprotection at molecular level/ Neuroimmunology, 2010 - T.8, - № 1-2.-c.34-40.
7. Damulin I.V. Differential Diagnosis and Dementia Therapy. Consilium medicum 2003;5(12):721—6.
8. Pyramads M.A., Sergei D.V., Crotenkova M.V. Application of Ceraxon in acute period of hemispheric ischemic stroke: clinical and CT - perfusion assessment. Annals of Clinical and Experimental Neurology. 2012; 6(3): 31–35.
9. Yahno N.N. Cognitive Disorders in Neurological Practice./ Neurological Journal, 2006, Vol. 11, Ex. 1, p. 4-12.
10. Saver J.L. Cyticolin: new information about a promising drug that performs neuroprotection and neuroreparation. Mezhdunarodn neurologic magazine 2010;1(31):108-17.

## MASS TRAINING IN THE FORM OF A MASTER CLASS FOR THE EARLY DIAGNOSIS OF SKIN MELANOMA

### **Neretin Evgeny Yuryevich**

Candidate of Medical Sciences, Associate Professor  
Medical University «Reaviz», Samara, Russia  
Oncologist of the highest category  
Samara Regional Clinical Oncology Center

### **Kozlova Olga Anatolyevna**

Head of the Department of Medical Prevention, doctor  
Samara Regional Clinical Oncology Center

**Annotation.** The current problem is considered in the article - early diagnosis of skin melanoma, unsatisfactory results of early diagnosis can be solved, among other things, by training primary contact specialists - oncologists, dermatologists, and surgeons. The authors conducted training in a master class format according to the authors patented methodology of specialists, which led to an improvement in the sensitivity, specificity, and accuracy of diagnosis of skin melanoma. The training was conducted in 3 cities - Samara, Moscow, Chelyabinsk. It is concluded that the use of training methods for specialists in the master class format can significantly improve the diagnosis of skin melanoma and reduce the unjustified number of biopsies.

**Keywords:** Skin melanoma, training in the early diagnosis of skin melanoma, an author's methodology for teaching the diagnosis of skin melanoma, early diagnosis of skin melanoma

### **Introduction**

The early diagnosis of skin melanoma is one of the most important problems in oncology (Holmes GA, Vasantachart J M et al., 2018; Dinnes J, Deeks JJ, Chuchu N, 2018). It should be noted that the accuracy of diagnosis by doctors of primary contact is low. So, according to the data of Anisimov V.V., only in 37% of cases, skin melanoma can be placed at the initial appointment in the consultative department (Anisimov V.V., 2001). Many authors note an unacceptably high proportion of stage 3-4 (ne-

glect) in case of skin melanoma, which amounted to 21.3% (2014 - 22.1%) (A.D. Kaprin, V.V. Starinsky et al., 2016). At the same time, the necessary knowledge about the signs of MK among the population without special education is available only from 5 to 9.9% (Halteh P, Scher R, et al., 2017). Self-examination by an untrained specialist, according to a number of authors, the sensitivity is from 25% to 93% depending on the stage of the tumor process, while the specificity is usually higher (83% - 97%). Attempts have been made to increase the skills for diagnosing melanoma through various training programs have proven effective (Czajkowska Z, Hall NC, 2017; Robinson JK, GaberR, et al., 2014; McWhirterJE, et al., 2013), and therefore this technique can be used as a simple and cheap screening (Hamidi R, et al., 2010). Although many authors note that the diagnosis of "melanoma of the skin" can be made already at the initial examination of a patient by a doctor of almost any specialty (Fink C, Haenssle HA., 2017).

### **Purpose of the study**

To evaluate training opportunities for diagnosing skin melanoma of specialists of various levels in the training format - a master class. Tasks - to evaluate the sensitivity, specificity and accuracy of diagnosis of skin melanoma before and after training.

### **Material and research methods**

In the format of the master class, mass training was carried out according to the author's method (certificate No. 2018613017) using the author's database (patent for the invention No. 2018620399) and remotes in various centers of the Russian Federation. At the input stage, a test was presented, according to which, basing on the results of the voting, initial indicators were evaluated - sensitivity and specificity, general accuracy of the diagnosis of respondents of doctors of various specialties. Then, clinical cases were analyzed with an audience presenting photographs of clinical data, medical history, digital dermatoscopy with and without immersion. The diagnosis was confirmed by histological examination. Clinically and dermatoscopically indicated characteristic symptoms that help to make the correct diagnosis in each case. After conducting a clinical analysis of cases, the audience was presented with exit control, according to the results of which the effectiveness of training was calculated. Criteria - sensitivity, specificity and accuracy of diagnosis. In the learning process, a developed author database was used.

### **Research results**

Table 1 presents the average values of the diagnostic parameters for all students according to the results of input and output testing.

**Table 1. The dynamics of diagnostic parameters in the study group, the average diagnosis of skin melanoma**

General characteristics of the group	Doctors oncologists and dermatologists (n = 138)		
	sensitivity	specificity	accuracy
Input diagnostic parameters	95,17%	73,99%	84,58%
Diagnostic output parameters	97,58%	87,37%	92,48%

As can be seen from the data presented, after training, the diagnostic parameters of the group significantly increased. So, if before the master class the sensitivity of determining skin melanoma was 95.17%, and the specificity was 73.99%. After the lecture, the sensitivity of the group was 97.58%, and the specificity was 87.37%. In absolute numbers, the data are presented in table 2.

**Table 2.  
An increase in the number of all correct answers after training in a master class format.**

City	melanoma	benign skin neoplasms
Samara, 2016	82	319
Moscow, 2017	30	253
Chelyabinsk, 2018	47	269

As can be seen from the data presented, the greatest increase was achieved in the specificity of the diagnosis of skin melanoma.

**Discussion of the data**

In practical terms, the constant use of this technique can mean: fewer unnecessary biopsies of pigmented skin neoplasms suspicious of melanoma in patients, including in cosmetically significant parts of the body, fewer days of fear in anticipation of a histological conclusion, fewer referrals to specialized specialists, possible saving material and technical resources of healthcare facilities. At the same time, the obvious drawback of this method is the lack of an individual approach to students (all tests and training take place in a large group), the brevity of the training program.

**Findings**

1. After training, the number of unjustified biopsies, especially in cosmetically significant areas of the body, may decrease.
2. The use of specialist training methods in a master class format can significantly improve the diagnosis of skin melanoma.
3. In a short time, you can increase the diagnostic parameters of a large number of specialists.

**FEATURES OF THE PHYSICAL DEVELOPMENT  
OF TUBERCULOSIS INFECTED CHILDREN  
IN THE SMOLENSK OBLAST**

**Krutikiva Nadezhda Yuryevna**

Doctor of Medical Sciences, Associate Professor  
Smolensk State Medical University  
ORCID: 0000-0003-0900-078X

**Teschenkov Anton Viktorovich**

Rheumatologist  
Pirogov Russian National Research Medical University

**Krikova Anna Vyacheslavovna**

Doctor of Pharmaceutical Sciences, Associate Professor, Head of Department  
Smolensk State Medical University  
ORCID: 0000-0002-5288-0447

**Abstract.** Introduction: The state of the child's physical development (height, weight and body mass index) is an important predictor for assessing the risk of developing local forms of tuberculosis (TB) in tuberculosis children.

Purpose: assess the weight, height and BMI in children with latent tuberculosis infection and without it at certain age periods.

Materials and methods: the study included 200 children aged 5-15 years, 131 children were in the VI dispensary group - the main group, 69 conditionally healthy children of 2 health groups - control group. The z-score (StandardDeviationScore - SDS) of growth, weight, BMI were calculated using the WHO AnthroPlus program, and the interpretation of the results was carried out according to WHO recommendations.

Results: Growth rates among tuberculosis patients, which belong to the group of low values: z-score  $< -2$  SD, were observed in 2.3% (95% DI: 0.7-6.5%), in the control group, such indicators were not registered. At the same time, the relative number of girls with lower than average growth rates was statistically significantly different from the control group. Among boys, growth indicators in the main group differed statistically significantly from the control group. When analyzing the results of measuring body mass indicators in the studied groups, it was found that the indicators in

the main group were reduced. So, among tuberculosis patients, who belong to the group of values "below average": z-score  $-1$  SD - ( $-2$  SD), were observed in 28.24% (95% DI: 21.24–36.49%), in the control group, such indicators were not found. Moreover, differences in this category of values are statistically significant, since they do not overlap with DI, since in the second group 95% of DI is 0-5.2%. Significant differences are also determined in the category where the values exceed the average body weight parameters for a given age (z-score  $> +1$  SD - ( $+2$  SD)). In the main group, the number of children with a range of BMI estimates below the average: z-score  $-1$  SD - ( $-2$  SD), in the main group was 9.1% (95% DI: 5.3-15, 3%), for the control group such indicators were not registered 0%. Disharmonious physical development was observed in 34 children of the main group (25.9%; 95% DI: 19.2–34.1%), which significantly differs from the control group (8.7%; 95% DI: 4.05-17, 7%).

Conclusion: Significant changes in length and body weight, regardless of age and gender in the main group were revealed. The predominance of disharmonious and sharply disharmonious development is most pronounced in patients in the prepubertal period. The delay of growth crosses was established by the main anthropometric indicators. Inadequate physical development is closely interconnected with the normal psycho-emotional state of the child, directly affect the outcome of tuberculosis infection, as well as the development of concomitant pathology.

**Keywords:** children, age, physical development, latent tuberculosis infection.

### SUBSTANTIATION OF RESEARCH

One of the indicators in children with a reactive response to external factors is growth. The negative impact can be due to both exogenous and endogenous causes. This nature of the response is due to the fact that it is in childhood that the growth rate acquires the maximum value. Low body mass index (BMI) is an important predictor for assessing the risk of developing localized forms of tuberculosis (TB) in tuberculosis children. It was found that TB occurred three times more often in patients with a BMI below 10% or more of body weight corresponding to the required standards for age and gender.

**PURPOSE OF THE STUDY:** evaluate weight, height and BMI in children with latent tuberculosis infection and without it at certain age periods.

**METHODS:** the study included children aged 5-15 years who were registered in the clinic in connection with latent tuberculosis infection, consisting in the VI dispensary group. A total of 200 children were included in the study, of which 131 were infected with *Mycobacterium tuberculosis*, the

remaining conditionally healthy children with the second group of health. This work was carried out on the bases of RSBIHC Smolenskaya Oblast Children's Clinical Hospital, RSBIHC Smolensk Tuberculosis Clinical Dispensary Children's Department, RSBIHC Children's Tuberculosis Sanatorium "Priselye". A transverse (simultaneous) study was carried out. Criteria for inclusion in the control group: patients uninfected with Mycobacterium tuberculosis, patients aged 5-15 years, patients of 1-2 health groups. Criterion for inclusion in the main group: patients infected with mycobacterium tuberculosis, patients of the age group 5-15 years old, children do not receive vitamin-mineral preparations, children did not have oncological diseases, thyroid and parathyroid diseases, hereditary and musculoskeletal diseases, chronic diseases of kidney, gastroenterological diseases accompanied by malabsorption syndrome.

Body weight was determined using TVES VMEN-200-50/100-DZ electronic floor scales with an accuracy of up to 50 g. Body growth was measured using a vertical medical height meter MSK-233 with an accuracy of 0.5 cm. Z-score values (StandardDeviationScore - SDS) growth, mass, BMI were calculated according to the WHO AnthroPlus program, and the interpretation of the results was carried out according to WHO recommendations. The study period - August - August 2018-19.

### RESULTS

When comparing the study groups, it was found that growth rates in the main group were reduced. Thus, growth rates among tubified patients, which belong to the group of low values: z-score  $< -2$  SD, were observed in 2.3% (95% DI: 0.7-6.5%), in the control group, such indicators were not recorded. At the same time, differences in this category of values are not statistically significant, since 95% DI overlap, since in the second group 95% DI is 0–5.2%. Significant differences are determined among the remaining categories. In the range of average values, the relative number of patients of the first group is lower than 29.7% (95% DI: 22.5–38.1%) versus 59.4% in the control group (95% DI: 47.64–70.21%). In addition, 95% of the DI relative frequencies do not overlap in terms of values below average (z-score  $-1$  SD -  $(-2$  SD)) and above average (z-score  $> +1$  SD -  $(+2$  SD)).

When comparing growth rates depending on gender, it was revealed that in the main group, the number of girls with indicators that belong to the "above average" and "high development" (z-score =  $+1$  SD) groups was statistically significantly different from the control group. The percentage of girls with average growth between the groups did not differ 15.27% (95% DI: 10.11-22.4%) in the main group and 28.9% (95% DI: 19.62-40.5%). At the same time, the relative number of girls with lower than average growth

rates was statistically significantly different from the control group.

Among boys, growth indicators in the main group differed statistically significantly from the control group, except for the range of average DI values overlapped: in the main group - 14.5% (95% DI: 9.49-21, 54%), and in the control group - 30, 43% (95% DI: 20.8–42.1%).

When analyzing the results of measuring body mass indicators in the studied groups, it was found that the indicators in the main group were reduced. So, among tuberculosis patients, who belong to the group of values “below average”: z-score -1 SD - (-2 SD), were observed in 28.24% (95% DI: 21.24–36.49%), in the control group, such indicators were not found. Moreover, differences in this category of values are statistically significant since they do not overlap with DI, since in the second group 95% of DI is 0-5.2%. In the range of average values, the relative number of patients of the first group does not differ from the control - 71.7% (95% DI: 63.51-78.76%) versus 84.1% in the control group (95% DI: 73.6-90,8%). Significant differences are also determined in the category where the values exceed the average body weight parameters for a given age (z-score > +1 SD - (+2 SD)).

In the range of average values, the relative number of patients of the first group does not differ from the control - 71.7% (95% DI: 63.51-78.76%) versus 84.1% in the control group (95% DI: 73.6-90,8%). Significant differences are also determined in the category where the values exceed the average body weight parameters for a given age (z-score > +1 SD - (+2 SD)).

According to the analysis of calculated BMI values in the main and control groups, the absence of statistically significant differences between the groups was determined: for all groups of values, 95% DI overlapped

The results of the assessment of body mass indices showed that the relative number of children of the main group and the control group, which are not statistically significantly different, are in different categories.

At the same time, the addition of an extra variable, which grouped the data according to gender, revealed differences among boys in the studied groups. So, in the main group, the number of children whose BMI assessment range falls into the category “below average”: z-score -1 SD - (-2 SD), in the main group was 9.1% (95% DI: 5.3— 15.3%), for the control group such indicators were not registered 0%.

In order to identify the possible disharmony of physical development, a comparison of signal deviations in growth and body weight was performed. Disharmonious physical development was observed in 34 children of the main group (25.9%; 95% DI: 19.2–34.1%), which significantly differs from the control group (8.7%; 95% DI: 4.05-17, 7%). An analysis of the age data of this subgroup of children showed that the greatest number of sub-

jects with disharmonious development occurs at the age of 11–13 years (61.7%; 95% DI: 45.1–76.1%). It should be emphasized that the distribution of children depending on gender in each age period, for the subgroup under consideration, did not significantly differ. In the period of 5-7 years, the number of girls with disharmonious development was 20.5%; 95% DI: 10.35-36.8%, boys 14.7%; 95% DI: 6.45-30.13%). For the age range of 11–13 years, the female subjects were 35.2%; 95% DI: 21.49-52.09% versus male 26.4%; 95% DI: 14.6-43.1%.

### CONCLUSION

In tubified children and adolescents, a decrease in length and body weight is determined. Disharmonious and sharply disharmonious development options prevail. Growth crosses are late in terms of basic anthropometric indicators. In children of prepubertal age, physical development is below average and low in 23% of cases, among which the disharmonious type is 40% of cases. Inadequate physical development is closely related to the normal psycho-emotional state of the child and directly affects the outcome of tuberculosis infection, the ability to overcome the disease and the exit of a full-fledged personality into adulthood, despite tuberculosis.

### References

1. Аксенова В.А., Барышникова Л.А., Севостьянова Т.А., Клевно Н.И. Туберкулез у детей в России и задачи фтизиатрической и общей педиатрической службы по профилактике и раннему выявлению заболевания // Туберкулез и болезни легких. – 2014. – №3. – С.40-46.[Aksenova V.A., Baryshnikova L.A., Sevostyanova T.A., Klevno N.I. Childhood tuberculosis in Russia, goals of the tb service and general pediatric service for tb prevention and early detection. Tuberculosis and Lung Diseases. 2014;(3):40-46. (InRuss.)] <https://doi.org/10.21292/2075-1230-2014-0-3-64-73>
2. Lönnroth K. A consistent log-linear relationship between tuberculosis incidence and body mass index // International Journal of Epidemiology. 2010. 1 (39). P. 149-155.
3. Zhang H. [H AP.]. Association of Body Mass Index with the Tuberculosis Infection: A Population-based Study among 17796 Adults in Rural China //Scientific Reports. 2017. (7).
4. Cegielski J.P., Arab L., Cornoni-Huntley J. Nutritional risk factors for tuberculosis among adults in the United States // American Journal of Epidemiology. 2012. 5 (176). P. 409-422.
5. Ilavská S. [H ap.]. Association between the human immune response and body mass index // Human Immunology. 2012. N5 (73). P. 480—485.

## ENTHESOPATHY: FEATURES OF ETIOPATHOGENESIS.

### **Krajnyukov Pavel Evgen'evich**

Central Military Clinical Hospital. P.V. Mandryka  
Professor, Peoples Friendship University of Russia (RUDN University)  
ORCID 0000-0002-2531-5960

### **Kokorin Victor Viktorovich**

Candidate of Medical Sciences  
Central Military Clinical Hospital. P.V. Mandryka  
National Medical and Surgical Center named after N.I. Pirogov  
ORCID 0000-0002-9470-0491

### **Matveev Sergej Anatol'evich**

Full Professor, National Medical and Surgical Center named after N.I. Pirogov  
ORCID 0000-0003-0237-608x

**Abstract.** Summary data of contemporary literature focuses on enthesopathies. The article describes the issues of etiology, pathogenesis, clinic and diagnosis. The area of enthesis becomes a “weak link” in the apparatus of the periarticular tissues, where under excessive load micro- and macroscopic lesions occur, which subsequently lead to inflammation. Inflammation of the enthesis enhances the degeneration of adjacent tissues of the tendons, ligaments, cartilage, bone. The causes of enthesopathy are congenital bone abnormalities, osteochondrosis leading to radicular syndrome (compression of the spinal nerves), microtrauma of ligaments and tendons, metabolic disorders (for example, with osteoporosis and gout), severe prolonged physical activity, various endocrine and infectious diseases, and also autoimmune and inflammatory joint damage. The question of the etiopathogenesis of the disease remains open, as a result of which there is no pathogenetically substantiated treatment. Despite the variety of medical devices and physiotherapeutic procedures, the treatment results remain unsatisfactory, there is a high percentage of relapses and a chronic process. Inflammatory and degenerative-dystrophic damage to the enthesis is attracting increasing attention, as it represents one of the peculiar groups of diseases of the bone-ligament-tendon complex and makes a significant contribution to the clinical picture and pathology.

**Keywords:** enthesis, bone-ligament-tendon complex, non-calcified fibrocartilage, etiopathogenesis

### **Introduction**

Enthesopathy - one of the forms of paraarticular inflammation that occurs at the site of attachment of the tendon, fascia and capsule of the joint to the periosteum (entheseo complex). The term "enthesopathy" was introduced by La Cava in 1959 to describe the process observed in entheses after mechanical trauma [1]. Despite the fact that the adjective "enthetic" comes from the ancient Greek word "enthetikos", which means "introduced into the body from the outside," in the XIX century the adjective was increasingly used to refer to diseases that were "implanted into the body from the external environment." Currently, the term is used to refer to focal abnormalities occurring at the site of attachment of tendons, ligaments, fascia, muscle or articular capsule to the periosteum.

The joints remain the most mobile area of the locomotor apparatus, which adequately explains their frequent traumatization, leading to various severity of inflammatory changes. With the entry of plasma components and leukocytes into the joint cavity, the rapid release of intracellular lysosomal enzymes, a synovial cell response occurs. Normally, synovial fluid is represented by synovial integument cells - synoviocytes (34.2 - 37.8%), histiocytes (8.9 - 12.5%), lymphocytes (37.4 - 42.6%), monocytes (1.8 - 3.2%), neutrophils (1.2 - 2.0%) and unclassified cells (8.3 - 10.1%). A significant part of integumentary synovial cells is active monocytic phagocytes capable of capturing infectious or any other antigenic material (including autoantigen) [2].

If a person has joint problems, such as arthrosis or arthritis of various forms, then, as a rule, in more than half of cases this has a connection with the entheses and the development of enthesopathy, this pathology makes up one fourth of all diseases of tendons and ligaments, it is considered quite common among degenerative inflammatory diseases of the musculoskeletal system of the body, is one of the most difficult to treat today and is found in 60-85% of the adult population [3, 4, 5, 6].

The causes of damage, the mechanism of development and the course of the inflammatory process in the entheso complex are studied very intensively, there are studies in the available literature on the issues of diagnosis, treatment and rehabilitation, as well as histological, cytological, autoimmune and other changes occurring in the complex in different phases of its physiological and pathophysiological functioning, however, a clear answer still does not exist, and the opinions of the authors on some issues radically differ.

### **Purpose of the study**

Examine the etiological and pathogenetic features of enthesopathies, analyze and systematize the data obtained.

### **Material and methods**

The work used a systematic review of literature in the public domain, and our own research materials.

### **Results and discussion**

*Anatomical features.* Consider the structure of the enthesis on the example of the Achilles tendon. We emphasize the bone-ligament-tendon complex (BLTC), which has a trapezoidal shape, with the apex facing up. The distal part of the tendon spreads along the tubercle of the calcaneus, while increasing the area of the tendon does not lead to an increase in the number of its fibers. A feature is the absence of fatty layer of tendon-bone transitions. BLTC includes: tendon-fibro-osteo-cartilaginous part (TFOC); periosteal-fibro-cartilaginous part (PFC); tendon-fibro-cartilaginous part (TFC); capsule part (C) and fatty “clutch””, all these parts are combined into a complex and function as a single organ (Fig. 1).

A feature of the anatomical structure of the enthesis is inelasticity and high mechanical strength under relatively unfavorable conditions of local blood circulation. Entheses are deprived of their own vessels, tissue nutrition is provided by adjacent arteries, providing blood supply to the bone and tendon.

The elasticity and strength of the enthesis is ensured by the alignment of the acting forces, while maintaining the rigidity of the connection. A physiological change in the position and shape of collagen fibers does not lead to a concentration of force in the area of connection of the bone and soft tissues, and the stress is exponentially distributed to the proximal tendon, which reduces the risk of rupture in such a biomechanically vulnerable area as enthesis [7].

*Etiopathogenesis.* The reasons for the development of pathology of periarticular tissues may include: acute or chronic trauma, mechanical overload, often repeated stereotypical movements in the joint. Secondary pathology of periarticular tissues occurs against various diseases, such as diseases of the musculoskeletal system (orthopedic developmental abnormalities, arthrosis, arthritis, spondylitis, syndrome of dysplasia of the connective tissue, joint hypermobility), endocrine-metabolic disorders (diabetes mellitus, disorders of fatty, calcium metabolism, hypothyroidism, hypovitaminosis), neurotrophic disorders, vascular disorders, hyperimmune reactions, etc. [8, 9].

There are two types of enthesopathies: primary inflammatory and primary degenerative. Primary inflammatory enthesopathies develop with the spread of inflammation from adjacent joints with arthritis [10]. The primary degenerative process occurs as a result of repeated minor injuries with

constant overload or is the result of a single major tissue damage in the area of enthesitis. The cause of the overload can be both high physical activity and a violation of the biomechanics of movements in diseases of the musculoskeletal system [11, 12].

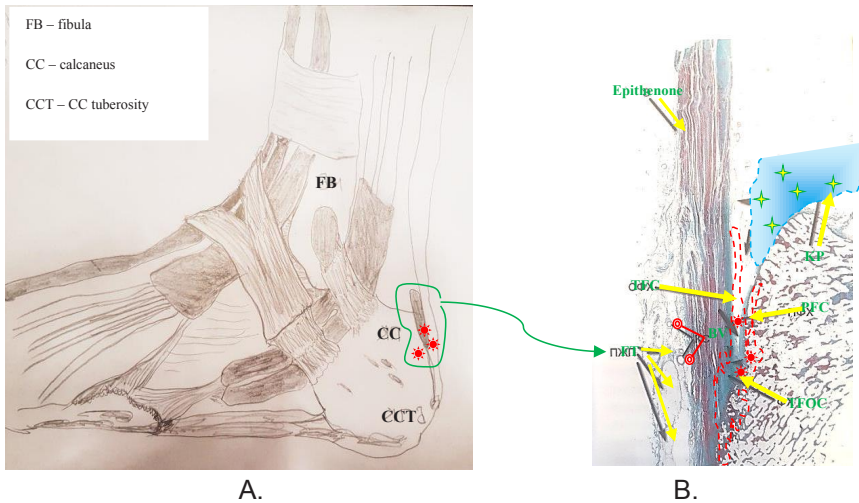


**Fig. 1. A. The lateral-dorsal section of the ankle joint; B. BLTC (KP - Kager Fat Pad; BV - blood vessels; FT - fatty tissue).**

The pathogenesis of enthesopathy is based on a degenerative inflammatory process. With a load in the area of enthesitis, the zone of the most intense tension is formed. Due to its high mechanical strength, most fibers remain intact. Moreover, in the areas where the collagen bundles are connected to the bone tissue (with fibrous enthesitis) or the transformation of collagen fibers into fibrous cartilage (with fibro-cartilage connection), single microfractures are formed. A single microdamage is asymptomatic and goes unnoticed. With repeated microtraumatization, the number of breaks gradually increases. In the tendon tissue, zones of fatty degeneration appear. All this negatively affects the strength of enthesitis, increases the likelihood of subsequent damage and contributes to the development of inflammation. With a primary inflammatory lesion, the reverse mechanism is observed. Inflammatory phenomena create favorable conditions for the appearance of microcracks, the tendon tissue is scarred and undergoes fatty degeneration, enthesitis degeneration sites are formed [13; 14; 15; 16].

Currently, various theories of the emergence and development of human enthesopathy are being considered - mechanical, autoimmune, genetic, synovial-complex. Consider some of the most significant, in our opinion, of them.

**1. Mechanical theory.** Inflammation caused by a mechanical factor partially damages the non-calcified fibro-cartilaginous part of enthesitis, which in turn leads to the activation of mainly macrophages of the innate immune system. In addition to activating the innate immune system, a factor that damages the fibro-cartilaginous part of enthesitis, regardless of its nature (mechanical, infectious, or stress-related), can cause an inflammatory response, including the activation of Toll-like receptors (TLR), belonging to the group of cellular receptors with one transmembrane fragment, which recognize the conserved structures of microorganisms and activate the cellular immune response of recognition receptors of the conserved structures of microorganisms, the characteristic structures of microbes, such as bacterial or viral DNA, RNA, and dendritic cells, are identified. According to this hypothesis, TLRs are activated as a result of the deposition of auxiliary molecules originating from intestinal bacteria at the site of damage to the fibro-cartilaginous part of enthesitis. Macrophages M1 (pro-inflammatory phenotype) activated by damage to enthesitis begin to secrete pro-inflammatory cytokines (TNF- $\alpha$ , IL-18, 12 and 23), prostaglandins (PGE2), nitric oxide, various growth factors and neuropeptides. This is followed by apoptosis, the release of pain mediators and matrix metalloproteinases, which decompose collagen and proteoglycans. Subsequently, under normal conditions, that is, with typical mechanical damage to enthesitis, sequential secretion of immunosuppressive cytokines IL-10 and IL-13 is observed, which signal macrophages M2 (immunomodulatory and tissue remodeling phenotype) to switch the phenotype from M1 to M2, stop inflammation, reduce TLR reactivity and inhibit the production of pro-inflammatory cytokines (Fig. 2).

The intestinal mucosa is a key site of IL-23 production, however, *Chlamydia trachomatis* can also serve as a source of IL-23 production. The pro-inflammatory cytokine IL-23 induces, acting on an isolated population of CD3 + CD4-CD8-enteral resident lymphocytes, which leads to an increased concentration of TNF and IL-6 in enthesitis. Thus, it can be concluded that IL-23 is a key pro-inflammatory cytokine in the structure of enthesitis when exposed to a mechanical factor.

The TNF- $\alpha$  cytokine produced by macrophages M1 stimulates synovial fibroblast-like synoviocytes, as a result of which inflammation progresses.

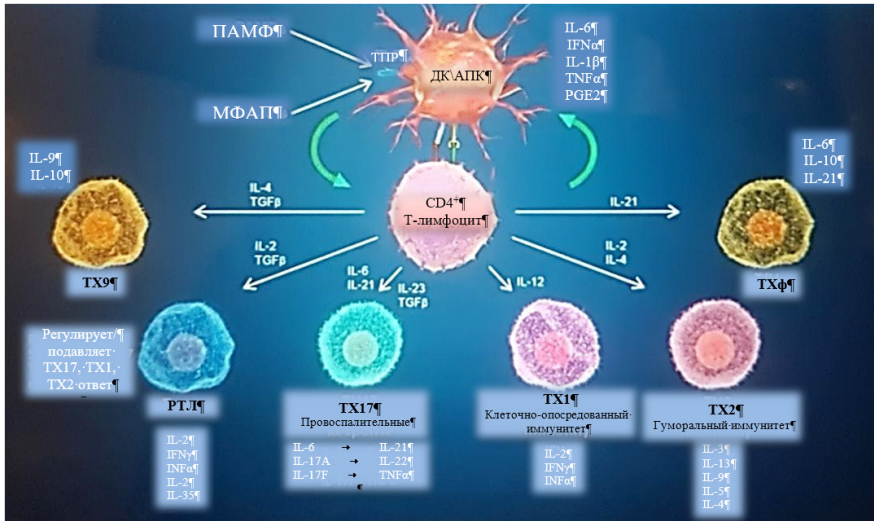


**Fig. 2. Scheme for triggering a cascade of inflammatory processes in response to TLR cell activation. Pathogen-associated molecular fragment of the molecule (PAMF); damage-associated molecular fragment (DAMF); dendritic cell (DC); antigen presenting cell (APC); regulatory T-lymphocyte (RTL); T-helper (TH); follicular TX (THF)**

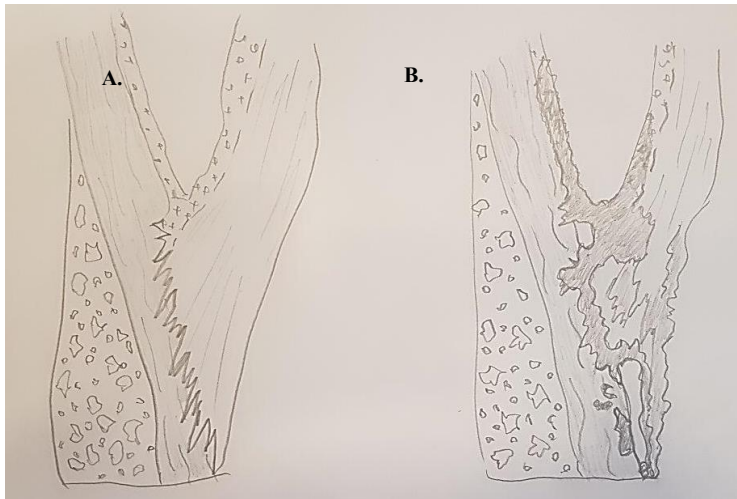


**Fig. 3. A. Physiological attachment of BLTC. B. Damaged BLTC, vascularization, impaired fiber structure, fibrosis.**

Patients with clinical signs of enthesopathy have increased vascularization and cell infiltration in the non-calcified fibrocartilaginous (FC) part of enthesitis (Fig. 3).

### ***II. Synovial-enteral-complex theory***

Benjamin and McGonagle (2009) observed the relationship between enthesitis and the adjacent synovial membrane of the bursa or adipose tissue and coined the term “synovioentesis complex” (SEC) [17; eighteen]. They drew attention to inflammation of the surrounding tissues of enthesitis as a major factor in the etiopathogenesis of enthesopathy [19].

According to SEC theory, partial damage to enthesitis can activate the mechanisms of innate immunity and stimulate the rapid development of bursitis. The authors give a similar explanation of their theory of “functional enthesitis,” according to which a conflict of a tendon moving in close proximity to a bone that acts like a pulley (for example, tibialis posterior tendon and medial malleolus) can cause tenosynovitis. Benjamin and McGonagle have also demonstrated the pro-inflammatory possibility of adipose tissue in tendons and surrounding enthesitis tissues. Adipose tissue exhibits endocrine or paracrine activity and releases growth factors and pro-inflammatory cytokines. It is vascularized and innervated, and can be a source of pain and play a role in the inflammatory response [19; 20]. The blood vessels that appear in the tendons during inflammatory-reparative processes can be from adipose tissue adjacent directly to the tendon (patella ligament, quadriceps tendon), from parathenone (Achilles tendon), from loose connective tissue in the tendon and from the mesentery tendons (eg, tendon sheath and Achilles tendon), from the bone marrow [17]. Vascular invasion contributes to the absence of periosteum in enthesitis, which allows bone marrow stem cells to gain direct access to the soft tissues of enthesitis and facilitates its recovery. With fibro-cartilaginous enthesitis, FC degeneration creates favorable conditions for vascularization of bone marrow capillaries [17; 18; 19]. Damaged as a result of chronic inflammation of the tendon and ligament, they are restored due to the proliferation of blood vessels that occur within the boundaries of enthesitis. The patient may show clinical symptoms of enthesopathy, but a visual examination cannot determine the order of events: was the inflammation of the adipose tissue near enthesitis caused by microdamage, which is, for example, enthesophyte, or regardless of whether the primary inflammatory process in the adipose tissue (or in the bursa), and whether there is an enthesophyte (a mineralized scar) that has no causal connection with the pathology of the tissues surrounding enthesitis [21].

### ***III. Autoimmune theory.***

Aggrecan - is a large proteoglycan, which is one of the constituent components of the fibro-cartilaginous structure, and can be a potential autoantigen. In an experiment, aggrecan introduced into mice caused peripheral arthritis and spondylitis [22]. The content of aggrecan and binding protein increases with tendon contraction, while type I collagen is replaced by type II collagen. In patients with rheumatism, these autoimmune response molecules have been identified as autoantigens. However, not all authors agree that the fibro-cartilaginous structure is the place where the development of enthesopathy begins. This is due to the fact that joint damage has a different etiology [19, 22].

### ***IV. Genetic theory.***

In recent years, intensive studies have been carried out on the sequence of genes encoding numerous proteoglycans and glycoproteins, which play a key role in the development, structure and function of the tendons and ligaments that make up enthesitis. They not only allowed to learn more about the etiopathogenesis of various diseases or pathological foci, but also to develop pathogenetically substantiated therapy of these diseases, including the affected problem of enthesopathy [23, 24]. It is known that the presence of chromosome 9q33 is correlated with Achilles tendon break causes. In the absence of fibromodulin, tendon fibers undergo reduction: the diameter changes, the shape is blurred, the location is disturbed, and the number of tenocyte cells and the number of endotendon are reduced. Studies in mice showed the development of ectopic calcification in the Achilles tendon in the absence of biglycan and fibromodulin. The absence of proteoglycan 4 led to the development of calcifications (calcified scars) in tendons and tendon membranes [25, 26].

**Diagnostics** of enthesopathy is a very difficult task, a lack of understanding of the etiopathogenesis of the disease and the choice of the necessary treatment tactics determines today the need for a wide diagnostic spectrum of the patient's examination [27, 28].

Acute or chronic damage to BLTC is most often associated with prolonged physical activity, repetitive exercises, activities or operations of a professional nature, affecting, as a rule, the area of the joint and adjacent tissues. Usually, the enthesopathic clinic is represented by the commonplace Celsus-Galen inflammatory pentad [9]. Physical and clinical research has low sensitivity, the incidence of enthesopathies does not exceed 20% [29, 30]. However, some distinguishing features of enthesopathy can be formulated:

the mismatch between active and passive movements (active are limited, with a normal volume of passive); pain intensifies exclusively in a certain position of performing movements and is absent when the vector and direction of these movements change; puffiness, pastiness are slightly expressed and are exclusively local in nature; the superficial arrangement of the topical structures of enthesitis makes it possible to determine local pain points during palpation.

*In a general clinical blood test*, a systemic analysis noted a shift in the formula to the left, the appearance of monocytes, medium and wide cytoplasmic lymphocytes. In the absence of an anamnesis and obvious clinical signs of the presence of a viral disease, the accumulation of lymphocytes in the microscopy of exudative fluid and their increase in the systemic circulation indicates their possible relationship.

*X-ray signs* of enthesopathy in the initial phase of the development of the disease are not explicitly expressed, are characterized by indirect manifestations in the form of compaction (lightening) of periental tissues. In the future, with a long course and chronicity of the process, signs of soft tissue compaction are revealed, a periosteal reaction is manifested, calcifications are detected.

*Ultrasound* is a sensitive and non-invasive test method for assessing the presence of enthesopathy. Ultrasonic signs include a decrease in echogenicity, a violation of the tendon structure, its thickening, calcifications at the attachment site, enthesophytes and bone erosion. The use of dopplerography in the energy doppler mode allows you to detect abnormal vascularization of the attachment site both in soft tissues and in the adjacent bone [31].

Ultrasound signs of BLTC enthesopathy: disturbance of the normal fibrillar echostructure - thickening of the tibial-fibular ligament, inflammatory edema - accumulation of fluid around the tendon of the fibular muscle, in the cavity of the tibial-fibular joint, signs of arterial blood flow in the thickness of the synovial membrane and its proliferation, linear hyperemia talus-fibular ligament.

*Magnetic resonance imaging (MRI)* can be performed using a high (from 1 to 3 T) or low (up to 1 T) field [32] and allows you to establish the inflammatory and destructive nature of the lesions of the tendon-ligamentous apparatus and its fixation sites. For the purpose of MRI of the diagnosis of lesions of the enthesocomplex, the following multiprojection modes are used - T1W, T2W, STIR, as well as a mode with signal suppression from adipose tissue (STIR) [33].

The MRI picture of the damaged enthesocomplex is characterized by the following structural changes: thickening, snapping, the appearance of

areas of reduced and increased density, microfractures (defects) of the fibers; in the paraarticular region, portions of local osteitis and an erosive defect in the bone plate are visualized.

The normal tendon in MR images has a uniformly low signal intensity in all sequences. When examining MR images for enthesopathy, the following should be evaluated: thickness and signal intensity of tendons and ligaments; periental (the area surrounding the LTC complex) soft tissue; adjacent bone marrow to detect edema (sequences with fat suppression); erosion of the adjacent bone (cortical defects of the bones and irregularities of the contours) and enthesophytes (lengthening of the contents of the bone marrow are iso-intensive to the medullary bone) - T1-VI sequence; additional findings in neighboring structures (articular or bursal fluid) [32, 34].

*Cytological research method* -microscopic results of exudative fluid give an idea of the cellular composition and nature of inflammation - an increase in white blood cells corresponds to the signs of a bacterial presence, in other cases we can talk about an autoimmune origin.

*Histological examination* of enthesitis can be considered as the gold standard of diagnosis, but it is rarely carried out due to ethical and legal difficulties [29].

A correctly established diagnosis, as a rule, makes it possible to carry out etiopathogenetic treatment. However, we are faced with various situations that do not allow this to be done - there is no well-defined standard scheme for diagnosing and treating enthesopathy, the circle of specialists who should deal with this problem is not outlined, there is no clarity in understanding the pathogenesis of the ongoing process.

### **Discussion.**

Enthesopathy is one of the forms of paraarticular tissue damage that has been little studied to date, it can be characterized as a degenerative-dystrophic inflammatory process that occurs at the sites of attachment of tendons, ligaments, joint capsules and fascia to the bone, in the presence of common clinical, radiological, ultrasound, magnetic resonance and other characteristic signs and the absence in the blood plasma of rheumatoid and similar factors [35, 36].

It should be recognized that the etiopathogenesis of the occurrence of enthesopathies is still not entirely clear. Considering the many theories of the occurrence of enthesopathy, we come to the conclusion that both septic and aseptic inflammation can underlie. Infectious lesion of enthesitis often remains undiagnosed, often mistaken for a degenerative pathology of the disease. The role of the infectious agent in the development of en-

thesopathy is very significant, as a provoking factor can be a very extensive human microbiome (usually the intestines, foci of chronic infections of the oropharynx, teeth, kidneys, etc.), and in some cases there is a latent infection (Fig. 9).

- Borrelia
- Yersinia
- Chlamydia
- Campylobacter jejuni
- Salmonella
- Streptococcus
- Parvovirus B19
- etc.



**Fig. 9. The most common representatives of latent infections (in descending order).**

A secondary factor in the damage of enthesitis when exposed to an infectious agent is the launch of immunopathological processes associated with the development of a hyperimmune response. So *Chlamydia* and *Yersinia*, can serve as a source of IL-23 production and are able to initiate a cytotoxic T-cell response. The pro-inflammatory cytokine IL-23, acting on an isolated population of CD3 + CD4-CD8-enteral resident lymphocytes, leads to an increased concentration of TNF and IL-6 in enthesitis, and an increase in phagocytosis and destruction mechanisms.

Identifying enthesitis involvement remains an important task for the surgeon because initial acute edema, inflammatory infiltration, and micro-damage of the cartilage can go into chronic intra-cartilage ossification and late-stage bone erosion.

Analyzing the data of modern literature that are in the public domain, we have to admit that enthesopathies remain difficult for the diagnosis and treatment of the form of damage to the periarticular tissues of the LTC complex. Despite the wide variety of technical equipment available today, multidirectional drug support, modern methods and techniques of diag-

nosis, treatment and rehabilitation, the results of treatment leave much to be desired. There is a high percentage of relapses and chronicity of the process. It can be assumed that further study of enthesopathy will allow us to approach understanding of etiopathogenesis, pathomorphology and significantly improve the diagnosis and, as a result, treatment of the patient.

## References

1. Amy SK, Maripat C, Michael H. New Insights Into Pathogenesis, Diagnostic Modalities, and Treatment. *Enthesits*. 2016; 68(2):312-322.
2. Сигидин Я.А., Лукина М. Биологическая терапия в ревматологии // *Практическая медицина*. – 2015. – С.304. [Sigidin YA, Lukina M. Biologicheskaya terapiya v revmatologii. *Prakticheskaya meditsina*. 2015:304. (In Russ).]
3. Балабанова Р.М. Энтезиты: диагностика и лечение // *Русский медицинский журнал*. - 2012. - №11 - С.538. [Balabanova RM. Enthesitis: diagnosis and treatment. *Russkiy meditsinskiy zhurnal*. 2012; 11:538. (In Russ).]
4. Жигало А.В. Современный подход к классификации контрактуры Дюпюитрена // *Вопросы реконструктивной и пластической хирургии*. – 2018. - Т.21 - №2(65) - С.50-61. [Zhigalo AV. A modern approach to the classification of Dupuytren's contracture. *Voprosy rekonstruktivnoy i plasticheskoy khirurgii*. 2018; Vol.21(2):50-61. (In Russ).]
5. Dennis MG, Kay-Geert AH, Ai LT. Differentiation between osteoarthritis and psoriatic arthritis: implications for pathogenesis and treatment in the biologic therapy era. *Rheumatology*. 2015; Vol. 54(1):29–38.
6. Juneja SC, Veillette C. Defects in Tendon, Ligament, and Entesis in Response to Genetic Alterations in Key Proteoglycans and Glycoproteins: A Review. *Arthritis*. 2013; 154812:doi. 10.1155/2013/154812.
7. Грицук А.А., Середя А.П. Ахиллово сухожилие // М.:РАЕН. – 2010. – С.313. [Gritsuk AA, Sereda AP. *Akhillovo sukhzhiliye*. M.: RAEN. 2010; 313. (In Russ).]
8. Wang X, Xie L, Crane J, et al. Aberrant TGF- $\beta$  activation in bone tendon insertion induces enthesopathy - like disease. *Journal of Clinical Investigation*. 2018; Vol.128(2):846-860.
9. Хитров Н.А. Параартикулярные ткани: варианты поражения и их лечение // *Русский медицинский журнал*. – 2017. – №3 – С.177-184. [Khitrov NA. *Paraartikulyarnyye tkani: varianty porazheniya i ikh lecheniye*. *Russkiy meditsinskiy zhurnal*. 2017; 3:177-187. (In Russ).]

10. Wes C. Enthesopathy – A personal perspective on its manifestations, implications and treatment. *Australas J Ultrasound Med.* 2010; 13(4):19-23.

11. Gleb S, Itzhak R. Enthesis as a target organ in rheumatic diseases: an expanding frontier. *Clinical Rheumatology.* 2017; 36(10):2163–2165.

12. Wilkinson HA. Injection therapy for enthesopathies causing axial spine pain and the "failed back syndrome": a single blinded, randomized and cross-over study. *Pain Physician.* 2005; 8(2):167-73.

13. Орёл А.М. Механизмы повреждения enthesitis у больных анкилозирующим спондилитом // Мануальная терапия. – 2013. – №2(50) – С.34-40. [Orel AM. Mechanisms of damage to entheses in patients with ankylosing spondylitis. *Manual therapy.* 2013; 2(50):34-40. (In Russ).]

14. Juneja SC, Veillette C. Defects in Tendon, Ligament, and Enthesis in Response to Genetic Alterations in Key Proteoglycans and Glycoproteins: A Review. *Arthritis.* 2013; 154812:doi. 10.1155/2013/154812.

15. Бельский А.Г. Энтезопатии при серонегативных спондилоартритах // *Consilium medicum.* – 2006. – Т.8 – №2 – С.11-14. [Belen'kiy AG. Entezopatii pri seronegativnykh spondiloartritakh. *Consilium medicum.* 2006; 8(2):11-14. (In Russ).]

16. Dennis MG, Kay-Geert AH, Ai LT. Differentiation between osteoarthritis and psoriatic arthritis: implications for pathogenesis and treatment in the biologic therapy era. *Rheumatology.* 2015; Vol. 54(1):29–38.

17. Benjamin M, McGonagle D. The enthesis organ concept and its relevance to the spondyloarthropathies. *Adv Exp Med Biol.* 2009; 57–70.

18. Benjamin M, McGonagle D. The anatomical basis for disease localisation in seronegative spondyloarthropathy at entheses and related sites. *J Anat.* 2001; 199:503-526.

19. Benjamin M, Toumi H, Ralphs JR, et al. Where tendons and ligaments meet bone: attachment sites ("enthuses") in relation to exercise and/or mechanical load. *J Anat.* 2006; 208:471–490.

20. Sudoł-Szopińska I, Kontny E, Zaniewicz-Kaniewska K, et al. Role of inflammatory factors and adipose tissue in pathogenesis of rheumatoid arthritis and osteoarthritis. Part I: Rheumatoid adipose tissue. *J Ultrason.* 2013; 13:192–201.

21. Sudoł-Szopińska I, Zaniewicz-Kaniewska K, Kwiatkowska B. Spectrum of ultrasound pathologies of Achilles tendon, plantar aponeurosis and flexor digiti brevis entheses in patients with clinically suspected enthesitis. *Pol J Radiol.* 2014.

22. François RJ, Braun J, Khan MA. Entheses and enthesitis: a histopathologic review and relevance to spondyloarthritis. *Curr Opin Rheumatol.* 2001; 13:255–264.

23. Hébert HL, Ali FR, Bowes J, et al. Genetic susceptibility to psoriasis and psoriatic arthritis: implications for therapy. *Br J Dermatol.* 2012; 166:474–482.

24. O'Rielly DD, Rahman P. Advances in the genetics of spondyloarthritis and clinical implications. *Curr Rheumatol Rep.* 2013; 15:347.

25. Goldring SR. Osteoimmunology and bone homeostasis: relevance to spondyloarthritis. *Curr Rheumatol Rep.* 2013; 15:342.

26. Sudoł-Szopińska I, Kwiatkowska B, Maśliński W. Enthesopathies and enthesitis. Part 1. Etiopathogenesis. *J Ultrason.* 2015; 15(60):72-84.

27. Каратеев А.Е., Каратеев Д.Е., Орлова Е.С., и др. «Малая» ревматология: несистемная ревматическая патология околоуставных мягких тканей верхней конечности. Часть 1 // Современная ревматология. – 2015. – 9(2) – Р.4-15. [Karateyev AY, Karateyev DY, Orlova YS, et al. «Malaya» revmatologiya: nesistemnaya revmaticheskaya patologiya okolosustavnykh myagkikh tkaney verkhney konechnosti. Chast' 1. Sovremennaya revmatologiya. 2015; 9(2):4-15. (In Russ).]

28. Arend CF. Role of sonography and magnetic resonance imaging in detecting deltoideal acromiointerosseous ligamentopathy: an early finding in the diagnosis of spondyloarthritis and an under-recognized cause of posterior shoulder pain. *Journal of ultrasound in medicine.* 2014; 33(4):557-61.

29. Гайнуллина Г.Р., Кириллова Э.Р., Абдулганиева Д.И. Энтезопатии при воспалительных заболеваниях кишечника // Практическая медицина. – 2019. – Т.17 – №6-1 – С.6-10. [Gaynullina GR, Kirillova ER, Abdulganiyeva DI. Entezopatii pri vospalitel'nykh zabolevaniyakh kishhechnika. *Prakticheskaya meditsina.* 2019; 17:6-10. (In Russ).]

30. Хитров Н.А. Локальная инъекционная терапия поражения параартикулярных тканей // Хирургия. Журнал им. Н.И. Пирогова. – 2017. – № 11- С.44-50. [Hitrov NA. Local injection therapy of periarticular tissue lesions. *Khirurgiya. Zhurnal im. N.I. Pirogova.* 2017; 11:44-50. (In Russ).]

31. Аджигайтканова С.К. Диагностика и лечение отдельных форм ревматических заболеваний с позиции доказательной медицины // Учебно-методическое пособие. – 2013. – С. 6-23. [Adzhigaytkanova SK. Diagnostika i lecheniye otdel'nykh form revmaticheskikh zabolevaniy s pozitsii dokazatel'noy meditsiny. *Uchebno-metodicheskoye posobiye.* 2013; 6-23. (In Russ).]

32. Зубков М.А., Андрейченко А.Е., Кретов Е.И., и др. МР-томография в сверхвысоком поле: новые задачи и новые возможности. – 2018. [Zubkov MA, Andreychenko AE, Kretov EI, et al. MR-tomografiya v sverkhvysokom pole: novyye zadachi i novyye vozmozhnosti. 2018. (In Russ).]

33. Сиротко О.В. Вопросы инструментальной диагностики реактивного артрита // Вестник ВГМУ. – 2016. – Т.15 – №4 – С.33-39. [Sirotko OV. Voprosy instrumental'noy diagnostiki reaktivnogo artrita. Vestnik VGMU. 2016; 15(4):33-39. (In Russ).]

34. Iris E, Matthias B, Dennis GM, et al. MRI of enthesitis of the appendicular skeleton in spondyloarthritis. Ann Rheum Dis. 2007; 66:1553-1559.

35. Кирсанов В.А., Бордуков Г.Г., Половинко В.В. Анализ эффективности плазмотерапии при лечении энтезопатий верхней конечности. – 2019. – P.116-119. [Kirsanov VA, Bordukov GG, Polovinko VV. Analysis of the effectiveness of plasma therapy in the treatment of enthesopathies of the upper limb. 2019; 116-119. (In Russ).]

36. Кириллова Э.Р., Лапшина С.А., Мясоутова Л.И., и др. Подходы к объективизации поражения периартикулярных тканей // Ревматология. Нефрология. Травматология. – 2008. – №25. – С.11-14. [Kirillova ER, Lapshina SA, Myasoutova LI, et al. Approaches to Objectification of Periarticular Tissue Damage. Revmatologiya. Nefrologiya. Travmatologiya. 2008; 25:11-14. (In Russ).]

## INCIDENCE OF INFECTIOUS DISEASES RELATED TO OCCUPATIONAL ACTIVITIES AMONG MEDICAL WORKERS

**Smetanin Viktor Nikolaevich**

Candidate of Medical Sciences, Associate Professor  
Ryazan State Medical University

**Abstract.** The questions of studying the role of the biological factor in the formation of professional and professionally determined morbidity of workers of medical and preventive organizations are considered. Statistical data of nosocomial infection of medical personnel are analyzed, conclusions are made about the leading risk factors and the main preventive measures.

**Keywords:** nosocomial infections, biological factor, occupational and occupationally caused morbidity, medical personnel.

One of the components of the HCAI problem is the incidence of medical personnel. Among the many professional factors that medical staff encounters in the process, communication with infectious patients occupies a special place. Medical workers, as well as hospital patients, are involved in the epidemic process. According to many authors, occupational morbidity among medical workers exceeds that in many leading industries [1].

Medical workers are a contingent of high risk of infection with infectious diseases caused by both opportunistic and pathogenic microorganisms. Diseases of workers of medical organizations arising as a result of their professional activities are an important practical public health problem. The health issues of medical workers are among the priority due to their enormous socio-economic importance [2].

Infection of health workers is facilitated by:

- uniqueness of the environmental conditions of the medical institution;
- presence of a large number of sources of infection among medical personnel (carriers, patients);
- aggravation of the epidemiological situation among the population in the country: an increase in the incidence of HIV infection, syphilis, tuberculosis, viral hepatitis B, C, etc.;

## Process Management and Scientific Developments

---

- growing shaft of aggression of invasive interventions (diagnostic and therapeutic procedures), during which not only patients, but also medical staff can become infected;

- widespread use of antibiotics and cytostatics that change the bioecosis of the mucous membranes and skin of the medical staff, open the "entrance gate" for fungi and other microorganisms;

- acceleration of the rate of evolution of microorganisms – pathogens of HCAI;

specifics of the hospital department: the departments of least risk can be considered cardiological resuscitation, neurological, neurosurgical, traumatological - the smallest percentage of detection of microorganisms from patients;

- length of service in the hospital: the greatest risk is in the first two years of medical staff, it is 10%, then there is a reduction in risk: 3-8 years of service - 4%; 9-11 years old - 3%; over 15 years - 0.3%;

- compliance with hygiene standards: the incidence of medical personnel in departments that do not comply with the standards is 2 times higher than the same indicator in the departments that comply with the standards.

Infection of medical personnel occurs as a result of the implementation of both natural transmission mechanisms and the artifact, artificial transmission mechanism created by medicine. The artifactual transmission mechanism is associated with invasive diagnostic and therapeutic procedures. The risk of infection through the blood is especially great. In contact with blood, more than 30 infections can be transmitted, the most significant are viral hepatitis B and C, HIV infection.

In recent years, in Russia there has been a significant risk of infection of medical staff, especially in tuberculosis dispensaries. Among occupational diseases of medical workers in our country, respiratory tuberculosis occupies the first rank [4].

The medical staff, especially young people, in children's hospitals have been infected with rubella, chicken pox. The shift in the incidence of measles by older age groups poses a real danger of infection of medical personnel not only in children's, but also in adult departments.

A high prevalence of respiratory infections by medical personnel was also found, among which Legionella, influenza, and coronaviruses were detected. Medical workers were the first to encounter a beginning wave of influenza and other acute respiratory viral infections, have closer contacts with patients throughout the entire period of epidemic trouble, which explains the increase in the incidence of these infections.

The literature describes cases of nosocomial outbreaks associated with herpes viruses. Viruses are able to be transmitted by airborne droplets, contact household and other ways, survive on environmental objects, therefore wearing gowns and masks does not always protect against infection [6].

Among medical workers, there are diseases of salmonellosis, dysentery with nosocomial infection. Outbreaks of acute gastroenteritis of rotavirus etiology among patients and medical personnel are described. Outbreaks may be associated with common transmission factors: contamination of drinking water in the event of a malfunction in the water supply system; infection of medical personnel during manipulations (patient care).

Cases of professional infection by doctors with typhus, pneumocystosis, helicobacteriosis, rubella, and malaria have been reported. Fatalized generalized meningococcal infection has been reported by the dentist.

In 2011, a nosocomial outbreak of Crimean hemorrhagic fever was described in the infectious diseases department of the Central District Hospital of the Rostov Oblast (8 medical workers fell ill) [3].

Medical personnel are exposed to the risk of infection not only by infections caused by pathogens, but by conditionally pathogenic microorganisms that circulate in the hospital. Infectious processes caused by CPM are devoid of specificity: caused by the same pathogen, occur in different organs, and vice versa, different types of microorganisms can cause inflammation of the same organ or tissue. Conditionally pathogenic microorganisms cause respiratory infections (pharyngitis, laryngitis, bronchitis, tonsillitis, pneumonia); urinary tract (cystitis, pyelonephritis); diseases of the gastrointestinal tract; skin and subcutaneous tissue and others.

The risk of occupational exposure threatens endoscopic medical personnel. The risk of infection depends on experience and intensity of work.

In the departments of purulent surgery, 63% of the medical staff develop various forms of purulent-inflammatory infections during the year.

The problem of mycoses is becoming more and more significant. In the hematological departments of St. Petersburg, for example, candidiasis of the oral cavity and esophagus was detected in 6% of medical personnel.

HCAI risk groups among medical workers are people who have a chronic pathology (somatic or infectious), a reduced immune response, age over 45-50 years. Constant communication with infectious patients in the process of work causes a change in the immune status and reactivity of the body of medical workers. According to I. A. Khrapunova, 40% of physicians show signs of secondary immunodeficiency [5].

### *Control measures and prevention:*

#### a) organizational and administrative:

- compliance with the rules for the admission of personnel to work;
- preliminary and periodic medical examinations;
- examination of medical personnel for epidemiological indications;
- organization of a medical examination of medical personnel;
- treatment of all identified infectious diseases, both professional and non-professional;
- according to indications - immunological examination of medical staff and correction of immune status;
- organization of immunization of medical personnel;
- development of a standard case of occupational disease;
- development and implementation of instructions for medical procedures, safety measures during their implementation;
- development of personal protective measures;
- training of medical personnel.

#### b) hygienic:

- architectural and planning decisions;
- effective ventilation system;
- rational labor regime;
- providing a balanced diet;
- providing workwear and personal protective equipment;
- introduction of modern safe medical technologies;
- compliance with hygiene standards when working with occupational hazards;
- compliance with the rules for the disposal of medical waste.

Conscious attitude and compliance by the medical staff with the requirements of the anti-epidemic regime will prevent occupational morbidity of employees, which will significantly reduce the risk of HCAI diseases and maintain the health of staff and patients.

## References

1. Badleeva M.V. The role of medical personnel in the prevention of nosocomial infections / M.V. Badleeva A.G. Markhaev, I.P. Ubeeva // Bulletin of the VSNS SB RAMS. – 2010. – № 2. – P. 124-128.
2. Biological factor of working conditions in medical institutions and its impact on the health status of medical workers / L.P. Zueva [et al.] // Occupational medicine and prom. ecology. – 1998. – № 5. – P. 37-41.

3. Kovaleva E.P. Protection of medical personnel from nosocomial infection / E.P. Kovaleva, I.A. Khrapunova, N.A. Semina // *Epidemiology and vaccination*. – 2003. – № 6. – P. 9-13.
4. Satsuk A.V. Features of the epidemiology and prevention of tuberculosis among employees of medical institutions: dis. ... cand. med. sciences / A.V. Satsuk. – M., 2010. – 201 P.
5. Khrapunova I. A. Sanitary and epidemiological surveillance of nosocomial infections of medical personnel: dis. ... doc. med. sciences / I. A. Khrapunova. – M., 2004. – 222 P.
6. Khrapunova I.A. HIV risk for mid-level healthcare workers. Measures for the prevention of occupational infection / I.A. Khrapunova // *Sterilization and hospital infections*. – 2008. – № 2. – P. 46-49.

**ENVIRONMENTAL AND PHYSIOLOGICAL AND HYGIENIC  
ASPECTS OF THE USE OF DRINKING WATER BY  
SCHOOLCHILDREN OF THE CITY OF KALUGA (RUSSIA)**

**Lykov Igor Nikolaevich**

Doctor of Biological Sciences, Full Professor,  
Scientific Director of the Institute of Natural Kaluga State University  
named after K.E. Tsiolkovsky, Kaluga, Russia

**Arutyunova Elizaveta Romanovna**

9th grade student of the  
Municipal budgetary educational institution "Gymnasium No. 24"  
Kaluga, Russia

**Abstract.** This study examined the preference of children for drinking various types of drinks and estimated the amount of fluid consumed by schoolchildren during the day. It was found that most students drink any type of water, and one in five of the children surveyed prefers sweet soda. In the course of the questionnaire, children were informed about the importance of water for the human body and animals, about the role of water in the life of the planet. Associative perceptions associated with the word water were clarified. For most students, the word "water" is associated with the seas and oceans. Students receive most of the information about water during class. The study involved 300 schoolchildren aged 7 to 17 years.

**Keywords:** schoolchildren, water, drinks, preferences, awareness

**Introduction**

Water is an indispensable component of all living organisms. The amount of water contained in the body of an adult is 65-70% of its mass, including up to 31% in the bones and up to 83% in the lungs [1]. The human body cannot store water, so every day we constantly lose water with exhaled air, with perspiration and with physiological secretions. Ensuring timely replenishment of the lost fluid is of great importance for the optimal functioning of the body. Every system in the body, from cells and tissues to vital organs, requires water to function. Water transports nutrients to all the cells of our body and oxygen to our brain. Water allows the body to absorb and ingest minerals, vitamins, amino acids, glucose and other substances. Water flushes toxins and waste from cells, helps regulate body temperature.

Drinking water activates the metabolism. For example, drinking 500 ml of water increases the metabolic rate by 30% within 30–40 minutes [2]. It was found that even mild dehydration leads to a general disturbance in mood, reduces cognitive and motor skills, affects memory and sensitivity to pain [3, 4, 5]. The brain works better with enough water.

The daily requirement of the human body for water under normal conditions is about 2.2 liters. The amount a person needs depends on age, body size, health status, activity level, as well as weather (temperature and humidity level). A person replenishes his water balance with both drinking water and other liquids, vegetables and fruits. But the best sources are drinking water and milk.

The drinking regimen of children is formed in early childhood based on family and collective childhood preferences. Moreover, children are poorly informed about the importance of water in human life and living organisms. These questions are addressed in this study.

### **Research method**

The main method used in the study was a questionnaire. The main questions during the survey were:

- type of water consumed: tap, bottled, sweet carbonated drinks and tea, any, milk;
- amount of fluid drunk during the day;
- where students get information about the role of water in life on the planet;
- what schoolchildren associate with the word “water”;
- feel tired during the day or get tired only in the evening, note fatigue and decreased working capacity by the middle of the day.

300 students participated in the survey. The age of respondents was from 7 to 17 years. Gender of respondents: 150 - female, 150 - male. Student performance is average.

### **Research results**

The results of the schoolchildren’s response about the type of water they consume are shown in Figure 1. The diagram shows that 30% of students drink any type of water. One in five of the children surveyed prefers sweet soda.

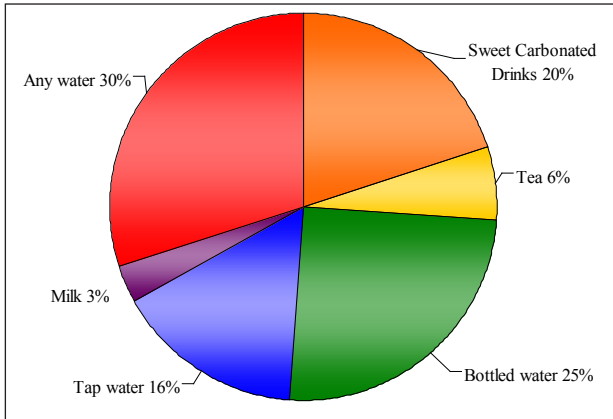


**Fig. 1.** The responses of students about the type of water they consume

Most children (168 people) drink 2.5 liters of water daily, on average, 132 people drink 2 liters of water daily (Fig. 2).

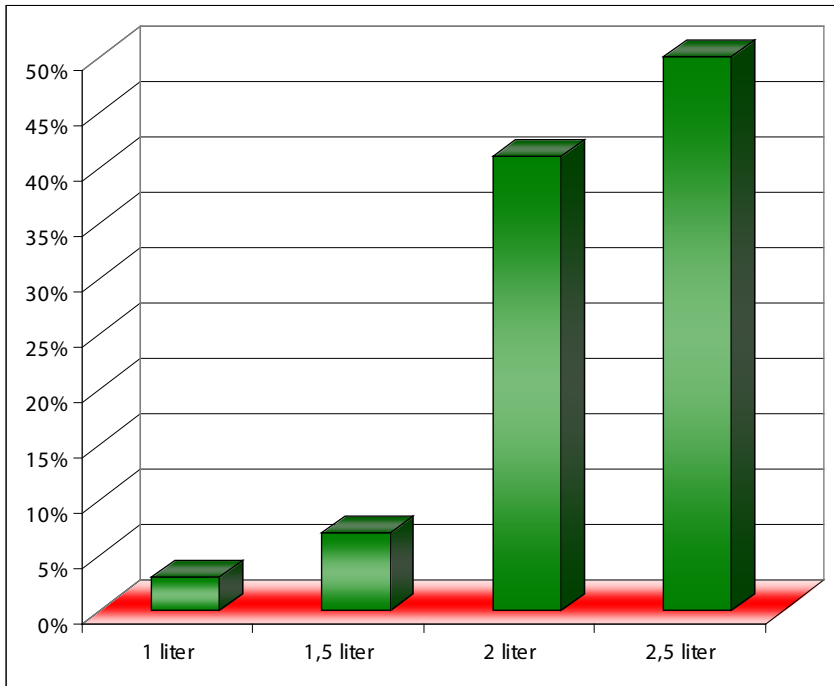


**Fig. 2.** The amount of fluid consumed by schoolchildren during the day.

Most of the students surveyed learned about the importance of water for humans and animals, about the role of water in the life of the planet during lessons (48% of respondents). The remaining students received information from books and during conversations with adults (Fig. 3).

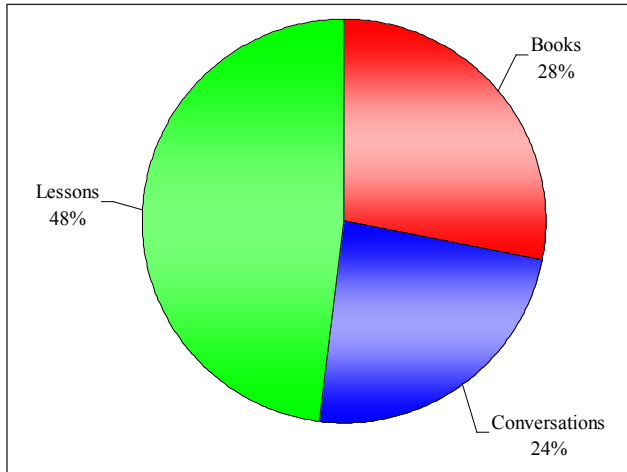


**Fig. 3. Where do students get information about the meaning of water**

When asked what the word “water” is associated with, respondents answered: seas and oceans, you can wash your hands, drink tea, wash dishes and swim (Fig. 4). For most students, the word “water” is associated with the seas and oceans (37% of respondents).

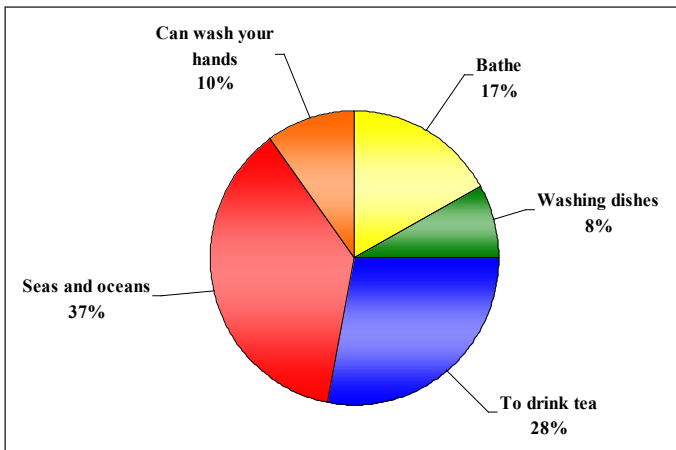


**Fig. 4. What is associated with the word "water" among students**

Most students note fatigue and decreased performance by evening (97%) and only 3% get tired in the middle of the day (Fig. 5).

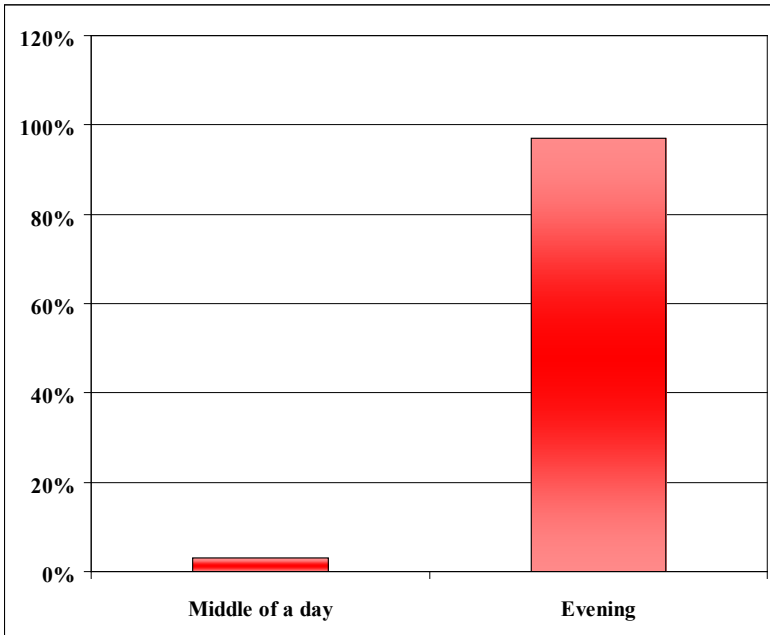


**Fig. 5. The results of responses of students about the onset of fatigue.**

**Conclusions**

1. Most schoolchildren follow family preferences when drinking water. Moreover, most children drink any water or sugary sodas and tea. Purified and bottled water is consumed by 25% of schoolchildren, and tap water - only 16%.

2. Most children (56%) consume up to 2.5 liters of fluid per day.

3. Schoolchildren receive basic information about the importance of water in human life and living organisms in lessons (48%). They get the rest of the information from books (28%) from conversations with adults (24%).

4. The word water in schoolchildren is associated with the sea (37%), tea (28%), swimming (17%).

5. The overwhelming majority of schoolchildren show fatigue by evening (97%), and only 3% - in the middle of the day.

## References

1. Lykov I.N., Shestakova G.A. Microorganisms: Biology and Ecology. - Kaluga. Publishing House "SerNa". 2014. 451 P.
2. M. Boschmann, J. Steiniger, U. Hille, J. Tank et al. Water-induced Thermogenesis // *J. Clin. Endocrinol. Metab.* 2003 V. 88(12). P. 6015-6019. doi: 10.1210/jc.2003-030780).
3. Armstrong L.E., Ganio M.S., Casa D.J. et al. Mild dehydration affects mood in healthy young women // *J. Nutr.* 2012. V. 142(2). P. 382–388.
4. Watson P., Whale A., Mears S.A. et al. Mild hypohydration increases the frequency of driver errors during a prolonged, monotonous driving task // *Physiol. Behav.* 2015. V. 147. P. 313–318. doi: 10.1016/j.physbeh.2015.04.028.
5. Ogino Y., Kakeda T., Nakamura K., Saito S. Dehydration enhances pain-evoked activation in the human brain compared with rehydration // *Anesth. Analg.* 2014. V. 118(6). P. 1317–1225.
6. Lykov I.N., Shestakova G.A. Man-made systems and environmental risk. – M.: IMPC "Globus", 2005. – 262 P.
7. Lykov I.N., Shestakova G.A. Environmental toxicology. Kaluga. Publishing House "SerNa", 2013, 256 P.

## CHEMICAL TRANSFORMATIONS OF N-ALKANES UNDER HYDRODYNAMIC CAVITATION ACTION IN WATER MEDIA

### **Dudkin Denis Vladimirovich**

Candidate of Chemical Sciences, Associate Professor  
Surgut State University

### **Fedyaeva Irina Mikhailovna**

Leading Manager  
High technology Park, Khanty-Mansyisk

### **Zhuravleva Lyudmila Anatolievna**

Candidate of Chemical Sciences, Associate Professor  
Surgut State University

**Abstract.** On the example of n-decane, chemical transformations of alkanes of normal structure in an aqueous and water-acidic medium under hydrodynamic cavitation action were studied. Based on the data of gas chromatography and gas chromatography with mass spectral detection, it is established that the main products of the reactions are n-alkanes with a higher and lower molecular weight, in comparison with n-decane, cycloalkanes, benzene and its alkyl derivatives, condensed polycyclic compounds. Based on the chemical composition of the reaction products, it is shown that the main reactions are dehydrocyclization, accompanied by the formation of benzene and its alkyl derivatives, alkylation of the resulting aromatic compounds and their subsequent dehydrocyclization, accompanied by the formation of naphthalene and its alkyl derivatives. The acidic reaction of the medium suppresses the flow of free-radical condensation transformations of n-alkane, strengthens the processes of heterolytic destruction of n-alkanes, contributing to the intensive formation of aliphatic limit hydrocarbons with a lower molecular weight.

**Keywords:** mechanochemistry, alkanes, cavitation, destruction, condensation, isomerization.

### INTRODUCTION

The steady growth of global consumption of motor fuels, along with a high level of capital expenditures of oil refineries, actualizes research in the field of mechanical destruction of oil and its components [1-7]. It is established that the mechanochemical effect on hydrocarbons initiates processes of condensation and destruction [3-7]. The chemical transfor-

mation is free-radical in nature. Ultrasonic action due to the effect of cavitation in water media allows generating free radical states and water ions [8] in quantities sufficient for the mechanochemical initiation of transformations of oil hydrocarbons already in the liquid state. Since alkanes are the main component of commercial oil, the purpose of this study was to study the general regularity of the chemical transformation of n-alkanes under hydrodynamic cavitation treatment of hydrocarbons in an aqueous emulsion.

### EXPERIMENTAL PART

Water was introduced into the system as a diluting medium, as well as as a primary source of free radicals and ions, and to suppress condensation processes.

Under the action of cavitation, the molecular bonds of water were subjected to homolysis with the formation of free radicals that initiate the process of dissociation of alkanes. In order to shift the balance in the direction of destruction, mechanochemical treatment was carried out under conditions of continuous distillation, similar to distillation with water vapor. The research was carried out on the model compound - n-decan.

An emulsion of water and n-decane prepared from components taken in a ratio of 9 : 1 (by volume), was placed in a cavitator of the design of Petrakov A.D. and treated with ultrasound for 10 min. The total volume of the processed mixture was 2 liters.

An experiment was also performed with the acidification of an aqueous emulsion with glacial acetic acid taken in a volume of 1.14 ml, similar to the experiment described in [5].

The content of hydrocarbons in the obtained samples was studied using a PerkinElmer gas chromatograph Clarus 500 with a flame ionization detector and a capillary column 30 m long, with an internal diameter of 0.32 mm and a fixed phase "Elite - 1" (film thickness 0.25 microns). Conditions for chromatography: programming the temperature of the column thermostat from 40°C, thermostating for 5 minutes, then heating at a speed of 5°C/min to 310°C and hold the final temperature-10 min. The carrier gas is nitrogen. The temperature of the injector (sample input node) is 220°C, the detector is 300°C. The data collection and processing program is TotalChrom. Identification of n-alkane peaks was carried out by the relative retention times and yield sequence on the chromatogram relative to the standard of n-dodecane and isoprenoids: pristan and phytane. The mass fraction of paraffin is determined by the external standard method based on calibration charts. The peak area was calculated in relation to the sum of the areas of all peaks on the chromatogram of the full ion current.

Other hydrocarbons were determined using a gas chromatograph with mass detection on a Clarus 500/Turbomass-Gold device equipped with a 30 m × 0.25 mm × 0.25 mm capillary column with a MS-5 methylphenyl-silicon elastomer.

Conditions for chromatography of other hydrocarbons: programming the temperature of the column thermostat from 40°C, thermostating for 5 minutes, heating up to 310°C at a speed of 5 deg / min, holding the final temperature – 20 min. The carrier gas is helium. The temperature of the injector is 220°C, the electron source is 190°C, and the transfer line is 300°C. Registration of mass spectra at an electron energy of 70 eV, mass scanning range 41-450 m/z, spectrum scanning time 0.2 s, delay between scanning 0.05 s. The internal calibration standard acenaften-D10 in chloroform in the amount of 0.912 micrograms was introduced into each analyzed sample.

Identification of organic compounds by GC–MS was performed by processing the spectra for relative retention times and by reconstructing the chromatogram of the total ion current from characteristic ions.

After the peak detecting of the identified component, its mass spectrum and all characteristic fragment ions were determined and the original chromatogram was reconstructed. The mass spectra of the components were compared with the NIST 98 mass spectrum catalog. If the mass spectra matched by more than 90%, the substance was considered as identified. If the match was less than 90%, the most likely group of organic compounds was determined, which included the substance under study.

**Table 1-Main characteristic ions used for identification of hydrocarbons**

Characteristic ions, m/z	The name of the hydrocarbon	Characteristic ions, m/z	The name of the hydrocarbon
55, 69, 83	cycloalkane	155, 156	dimethylnaphthalene
91, 92	n-alkylbenzenes	178	phenanthrene
105, 106	methylalkylbenzene	191, 192	methylphenanthrene
128	naphthalene	202	pyrene, fluoranthene
141, 142	methylnaphthalene	228	chrysene, benzanthracene

Then the peak area was calculated in relation to the sum of the areas of all peaks on the chromatogram of the full ion current.

**RESULTS AND DISCUSSION**

The obtained products of mechanochemical reactions were studied by the method of GC and GC-MS (tables 2 and 3).

**Table 2 - Content of n-alkanes in decane subjected to mechanochemical action according to gas-liquid chromatography**

N-alkanes	Content, % mass.		N-alkanes	Content, % mass.	
	without CH <sub>3</sub> COOH	with CH <sub>3</sub> COOH		without CH <sub>3</sub> COOH	with CH <sub>3</sub> COOH
C5	0.0004	-	C20	0.0002	0.0038
C6	-	-	C21	0.0002	-
C7	0.0467	0.2268	C22	0.0002	0.0031
C8	-	-	C23	0.0001	0.0027
C9	0.2394	0.2088	C24	0.0002	0.0029
C10	97.2034	94.9543	C25	0.0001	0.0093
C11	0.1473	0.0222	C26	0.0002	0.0039
C12	0.0354	0.0107	C27	0.0001	0.0034
C13	0.0150	0.0051	C28	0.0002	-
C14	0.0146	0.0031	C29	0.0093	0.0028
C15	0.0023	-	C30	0.0081	0.0017
C16	0.0014	-	C31	0.0047	-
C17	0.0010	0.0050	C32	0.0041	-
Pristan	0.0006	-	C33	-	-
C18	0.0006	-	C34	-	-
Phytan	0.0004	-	Total	0.5332	0.5094
C19	0.0004	-			

**Table 3 - Content of the main classes of hydrocarbons in the Decan after ultrasonic exposure in an aqueous medium according to gas-liquid chromatography with a mass detector**

Main classes of hydrocarbons	Mass content, %	
	without CH <sub>3</sub> COOH	with CH <sub>3</sub> COOH
Monocyclic hydrocarbons	1.58521	0.17125
Aromatic hydrocarbon	1.31561	0.16651
Dicyclic hydrocarbons	0.00602	0.00195
Polycyclic hydrocarbons	0.00137	-
Cycloalkane	0.00042	0.01039

**Chemical transformations of hydrocarbons in the conditions of homolysis of bonds (without acetic acid)**

Analyzing the presented data, it should be noted that both destructive and condensation processes occur. Alkanes with higher and lower molecular weight, aromatic hydrocarbons are formed. The directions of the main transformations of n-decane can be described in the following diagram (Fig. 1):

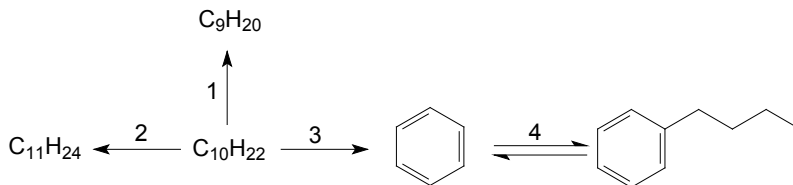


**Figure 1 - Diagram of the main transformations of the n-decane**

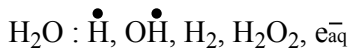
These reactions are free-radical in nature and are described by three kinetic stages: initiation, chain growth, and chain breakage.

Initiation is associated with the occurrence of free-radical states caused by homolysis of C-C-decane bonds and reactions of the water environment.

There are two hypotheses about the products of primary splitting of water molecules in the ultrasonic field. According to the hypothesis of Anbar and Gaisinsky, the scheme of this process can be presented in the following form:



and according to the hypothesis of Margulis and Maltsev:



Formed radicals and molecules capable of interacting with hydrocarbon molecules can both enhance and reduce the flow of condensation and destructive processes in the system [8].

Consider successively all the patterns of conversion of hydrocarbons flowing in aqueous medium under the effect of cavitation treatment. The radicals obtained in the process of splitting water transfer the free valence to the decane molecules, being at the interface of the phases. Since the reactor can be considered as an ideal mixing reactor, the process of free valence transfer at the interface of the phase contact should be considered the main one.

As a result of ultrasonic exposure, individual decane molecules undergo homolytic rupture of the C-C bond to form free radicals. It is assumed that the break of the hydrocarbon chain is possible, both in the middle of the molecule, at the weakest C-C bonds, and at the end of the carbon chain (Fig. 2):

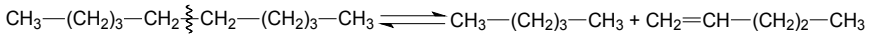
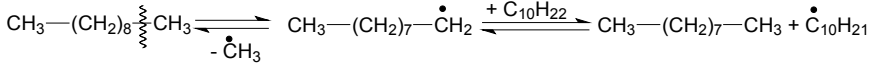


**Figure 2 - Main directions of destruction of the n-decane molecule**

The formed radicals are able to recombine with neighboring decane molecules, forming alkanes with a lower molecular weight and new radicals. Thus, the first direction of transformation shown in Figure 1 is realized.

Chemical transformations in direction 2 (Fig. 1), leading to the formation of undecane and, to a lesser extent, higher homologues, are realized by recombination of the radical on the reactor wall or in the reaction volume [9] (Fig. 3):

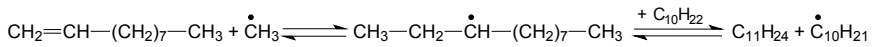
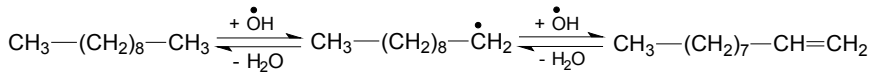
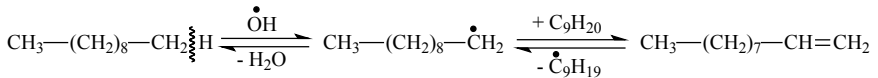


**Figure 3 - Scheme of formation of n-alkanes with a higher molecular weight under the action of peroxide radicals formed as a result of hemolysis of water molecules**

The simplest radicals, having increased reactivity due to the content of unpaired electrons, tend to stabilize and are double bonded to the olefin molecule to form n-alkane (Fig. 3). The flow of reactions in the direction 3 leads to the formation of benzene and its alkyl-substituted derivatives.

The production of benzene and butylbenzene occurs as a result of cyclization of the formed unsaturated radicals. The reaction is preceded by isomerization of primary radicals into more stable secondary ones, which occurs as a result of migration of the hydrogen atom inside the molecule from position 1 to position 5 through a cyclic transition state. This transformation leads to cyclization of the alkene (Fig. 4):

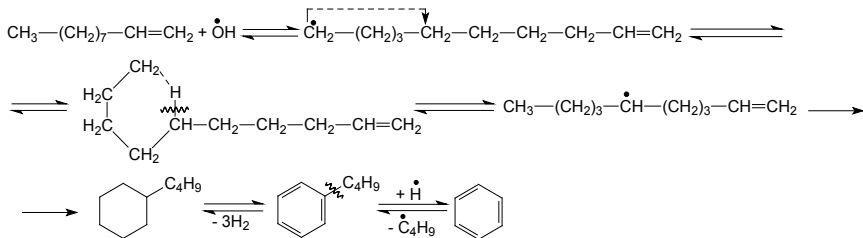
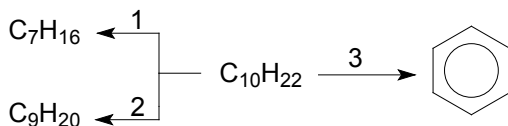


**Figure 4 - Scheme of formation of cycloalkanes and arenes**

Dehydrogenation and dealkylation of the alkylbenzene side chain results in unsubstituted benzene (Fig. 4).

**Chemical transformations of oil n-alkanes under ultrasonic influence of water-acidic media**

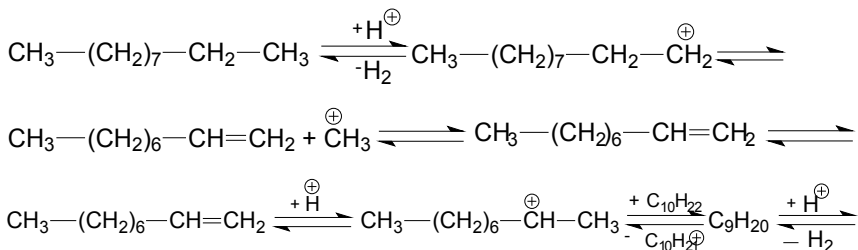
Destructive processes are noticeably enhanced in the conditions of acid catalysis (tables 2, 3). Most clearly, based on the obtained experimental data, the process can be described by the scheme of the main directions of transformation of n-decane (Fig. 5).



**Figure 5 - Diagram of basic transformations of n-decane in acidic media under hydrodynamic receipt action**

Alkanes undergo two main transformations during ultrasonic exposure: degradation (Fig. 6) and dehydrocyclization (Fig. 7)..

The C-C bond degradation (direction 1-2, Fig. 5) is due to the heterolytic bond break occurring according to Table 2 at the end of the alkane molecule (Fig. 6):



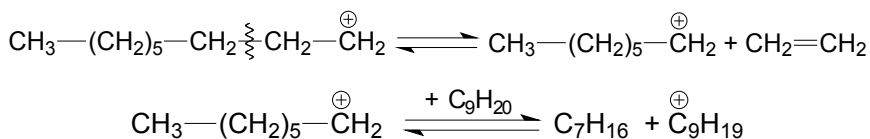


**Figure 6 - Scheme of heterolytic destruction of n-alkane during hydrodynamic cavitation treatment of aqueous media in the presence of acid**

Dehydrocyclization (direction 3, Fig. 5) is caused by successive heterolytic cyclization of the alkane molecule, its dehydrogenation with the formation of aromatic hydrocarbons and the subsequent breaking of the  $\beta$ -C-C-bond of the alkyl fragment of the benzene ring, which is capable of further separation of the alkyl radical from the benzene ring (Fig. 7):

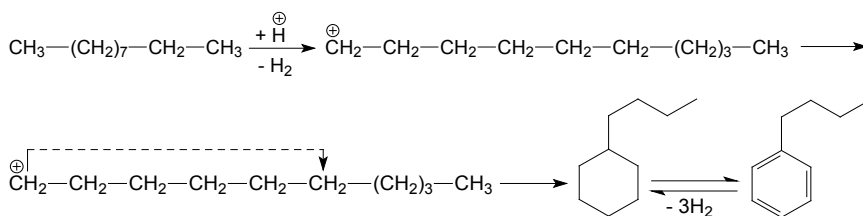


**Figure 7 - Scheme of heterolytic dehydrocyclization of n-alkane under hydrodynamic influence of water-acidic media**

## CONCLUSION

Ionic and free radical mechanisms of mechanodestruction of n-alkanes are equally characterized by a qualitatively common set of products of mechanochemical transformation of normal hydrocarbons in the water environment under hydrodynamic cavitation action. Quantitative differences in the reaction products indicate a deeper course of reactions of dehydrocyclization and alkylation of the formed aromatic hydrocarbons with the formation of condensed poly-nuclear aromatic compounds in an acidic environment.

Hydrodynamic cavitation action of water media under neutral pH conditions contributes to the intensive flow of dehydrocyclization processes of n-alkanes, with the formation of cyclohexane, mono- and dionuclear arenes and their derivatives.

The acidic reaction of the medium suppresses the flow of free-radical condensation transformations of n-alkane, strengthens the processes of heterolytic destruction of n-alkanes, contributing to the intensive formation of aliphatic limit hydrocarbons with a lower molecular weight.

### References

1. Davaatseren B., Golovko A. K. Improving the Quality of Straight-Run Gasoline Fractions of High-Paraffin Mongolian Oils [Povysheniye kachestva pryamogonnykh benzinovykh fraktsiy vysokoparafinystrykh mongol'skikh neftey]. *Khimiya v interesakh ustoychivogo razvitiya* [Chemistry for Sustainable Development], 2007, vol.15, no. 4. pp.473-479.
2. Dneprovsky K.S., Golovko A.K., Lomovsky O.I., Vosmerikov A.V. The Study of Mechanochemical Treatment Effect on the Composition of Gasoline Oil Fraction. *Petroleum and Coal*, 1999, vol. 41, no. 3-4, pp. 166-168.
3. Dudkin D. V., Kul'kov M. G., Shestakova Ye. N., Yakubenok A. A., Novikov A. A. Processing of Oil Residues under Mechanical and Chemical Influence [Pererabotka neftyanykh ostatkov v usloviyakh mekhanokhimi-cheskogo vozdeystviya]. *Khimiya i tekhnologiya topliv i masel* [Chemistry and Technology of Fuels and Oils], 2012, no. 4, pp. 34-37.
4. Dudkin D. V., Kul'kov M. G., Shestakova Ye. N., Yakubenok A. A., Novikov A. A. Transformations of Petroleum Hydrocarbons under Mechanochemical Influence [Prevrashcheniya uglevodorodov nefi pri mekhanokhimi-cheskom vozdeystvii]. *Khimiya i tekhnologiya topliv i masel*. [Chemistry and technology of fuels and oils]. 2012. no 2 (570). pp. 39-42.
5. Dudkin D. V., Yakubenok A. A., Novikov A. A., Kul'kov M. G., Korzhov Yu. V. Changes in the Chemical Composition of Heavy Oil Residues under Hydrodynamic Cavitation [Izmeneniye khimicheskogo sostava tyazhelykh neftyanykh ostatkov pri gidrodinamicheskom kavitatsionnom vozdeystvii]. *Tekhnologii nefi i gaza* [Oil and gas technologies]. 2013. no. 5 (88). pp. 3-7.
6. Dudkin D. V., Kul'kov M. G., Yakubenok A. A., Novikov A. A. The Transformation of Petroleum Hydrocarbons on Aluminum Oxide in Terms of Tribochemical Effects [Prevrashcheniye uglevodorodov nefi na okside alyuminiya v usloviyakh tribokhimi-cheskogo vozdeystviya]. *Tekhnologii nefi i gaza* [Oil and gas technologies]. 2014. no. 2 (91). pp. 39-45.
7. Torkhovskiy V. N., Vorob'yev S. I., Antonyuk S. N., Yegorova Ye. V., Ivanov S. V., Kravchenko V. V., Gorodskiy S. N. The Use of Multi-cycle Cavitation for the Intensification of Processing of Oil Raw Materials [Ispol'zovaniye mnogotsiklovoy kavitatsii dlya intensivatsii pererabotki nefyanogo syr'ya]. *Tekhnologii nefi i gaza* [Oil and Gas Technologies], 2015, no. 2 (97), pp. 9-17.
8. Margulis M. A. *Osnovy zvukokhimmii* [Fundamentals of Sound Chemistry]. Moscow, Higher School Publ., 1984. 272 p.
9. Bogomolov A. I., Gayle A. A., Gromova V. V. et al. *Khimiya nefi i gaza* [Oil and Gas Chemistry]. Saint-Petersburg, Chemistry Publ., 1995. 448 p.

UDC 661.66.658.567:620.197

**GOSSYPOL RESIN - IN THE FUTURE A VALUABLE MATERIAL  
FOR BUILDING BITUMEN WITHOUT OIL**

**Jumaniyazov Makhsud**

Doctor of Technical Sciences, Full Professor,  
Urgench State University, Republic of Uzbekistan

**Jabbiyev Rasulbek**

undergraduate  
Urgench State University, Republic of Uzbekistan

**Abstract.** This work presents the results of many years of research on the production of bitumen-polymer materials based on gossypol resin, intended for waterproofing various building structures, isolating underground steel pipelines in order to protect them from aggressive environments, as well as for roofing and asphalt concrete coatings.

**Keywords.** Oil depletion, bitumen composition, gossypol, softening point, alternative method, unconventional raw materials.

**Introduction**

Oil bitumens – are one of the many-toned oil products, and at the same time one of the scarce ones. The share of oil bitumen in the total volume of commodity products of world oil refining is 3-4%. The total demand for bitumen today is estimated at 102 million tons per year, while 85% of the bitumen demand is in the road industry. The bitumen produced by its physical and mechanical properties and technical indicators does not meet the requirements that are necessary for modern construction. They are too fragile, have low adhesion properties and are not resistant to aging. Obviously, this is due to the fact that bitumen was not considered a target product for a long time, and due attention was not paid to improving the technology of its production, as a result of which the quality of bitumen and its volumes do not correspond to the modern market. At the same time, the demand for it by a number of industries is increasing every year. The total demand for bitumen in Uzbekistan is satisfied by 50%. On the other hand, according to the annual report of the BP Statistical Review of

World Energy, by the beginning of this year, the total volume of explored oil in the world amounted to 1.7 trillion barrels, which is enough at the current level of consumption for 53 years [1].

*However, the problems of oil depletion, as well as the acute shortage of oil bitumen in the national economy, make it expedient to develop and use unconventional raw materials for the production of bitumen.*

**The purpose of this study** was to develop a new, competitive bitumen composition based on gossypol resin and a method for producing it with improved physical, mechanical and technological parameters, with high adhesive, anticorrosive properties, with resistance to aging, wide temperature range of ductility, increased heat and frost resistance.

### **Materials and methods**

The main objects in conducting theoretical and applied research in this article were calcium oxide, urotropine, urea and gossypol resin - waste of oil industry. To achieve the goal of the study, a modern laboratory base of the Urgench State University was used. Various modern physicochemical research methods were used.

### **Results and discussion**

When fats and oils are treated with alkali solutions during chemical refining, salts, soaps, which are insoluble in neutral fat, are formed, aqueous solutions of which are easily separated from fat due to their high density. Such a soap mass is called soap stock. Cotton stocks of the Urgench oil and fat factory (Uzbekistan) contain 40.5-62.2% of total fat, 17.4-22.0% of neutral fat, 3.7-6.1% of non-fat substances, 10.0-30.7% of moisture. The average molecular weight of 276.

Soapstock is lightened by the decomposition of fats, followed by distillation of the resulting crude fatty acids. Fatty acid distillation is carried out at temperatures of 220-230 °C. As a result of these processes, at the same time as part of the fatty acids is distilled off, a gossypol resin is formed in the cube, containing from 40 to 50% of the products of condensation, polymerization, and gossypol interaction products.

Despite the seemingly obvious benefit, if we involve in the production of bituminous materials huge reserves of secondary raw materials - gossypol-containing waste, unfortunately, the main issue has not yet been resolved - their immediate or planned disposal. However, gossypol resin as a large-capacity waste of the oil and fat industry, containing a significant amount of fatty acids, along with other products of condensation and polymerization, could serve as a raw material for valuable, severely deficient products for various purposes with very high economic and social effects.

Our scientific studies have proved that the structural features and properties of the resulting waste gossypol resin show a very diverse and rich chemical nature, upon closer examination of which the possibility of obtaining valuable materials becomes quite obvious. At the same time, analysis of literary sources shows that the use of gossypol resin in the development of oil-free bitumen technology is one of the most effective and efficient directions.

In this work, gossypol resin was used, resulting from the distillation of fatty acids at a temperature of 220-230 °C, containing from 40 to 50% of condensation, polymerization and gossypol reaction products. In the composition of gossypol resin, 12% of nitrogen-containing compounds, 36% of the products of the conversion of gossypol, which retained naphthol hydroxyls and 52% of fatty and hydroxy fatty acids in the form of lactones, were found. Gossypol resin is composed of polyphenol, fatty acids, hydrocarbons, nitrogen and phosphorus compounds, as well as gossypol conversion products. The presence of naphthalene core compounds in the composition also makes the products of the modification of the gossypol resin thermo-, chemo- and radiation-resistant, and the phenolic, hydroxyl, carboxyl and aldehyde groups - reactive with high complexing properties. However, gossypol resin is fundamentally different in composition from traditional oil tars, therefore, obtaining a substitute for oil bitumen based on gossypol resin has its own specific feature and requires the search for certain conditions using non-traditional modifier additives.

Obtaining a high-quality substitute for petroleum bitumen based on gossypol resin has its own specific feature and requires the search for certain conditions, as well as the use of non-traditional additives of modifiers, plasticizers and builders. Long-term experimental research yielded positive results. To obtain the specified grades of bitumen, a thermally oxidized gossypol resin was used as a binder - waste from oil and fat plants, rubber crumb (plasticizer) - waste from worn tires (CRU). According to the proposed composition, VAT residue of monoethanolamine purification (VRM), urotropine and urea were used as the active modifier. Quicklime was used as the builder, in the following ratio of components, wt.%: Thermally oxidized gossypol resin - 88.0 ÷ 90.0; CRU - 4.0 ÷ 5.0; VRM -3.5 ÷ 4.0; urea - 0.45 ÷ 0.50; quicklime - 0.5 ÷ 1.0; urotropin - 0.04 ÷ 0.05.

For thermal oxidation of the resin, air was used. It was oxidized at a temperature of 250-260 °C, for 120 min, with constant stirring, the plasticizer — rubber crumb — wastes of worn tires (up to 1 mm in size) were loaded, and the extract was allowed to stand for 30 min to swell, the crumb destruction in a gossypolic medium, then vat was gradually added the

precipitate of monoethanolamine purification, after its uniform distribution throughout the volume, was added - building quicklime and mixed until the gas evolution ended, then, when the mass was cooled with atmospheric oxygen to 135 °C, the rest of the modifier, namely urea and urotropine, was added to let the mass sit until gas evolution was completed.

The addition of urea and urotropine to the composition makes gossypol resin modification products thermo-, chemo-, and corrosion-resistant. In many respects, it can successfully replace expensive oil bitumen, the deficit of which is felt every year. In this case, the introduction of urotropine and urea, which exhibits complexing properties in the proposed composition, makes it possible to streamline and strengthen the structure of polycondensed molecules. As a result of this interaction of all the constituent ingredients, the product obtained from this composition acquires the properties necessary for building bitumen: reducing the depth of penetration of the needle, water saturation, increasing the temperature of softening and flash, which leads to the achievement of the task - increase fire safety, water resistance, corrosion resistance and hardness of the cover [1].

Thus, the physicochemical characteristics of bitumen compositions based on gossypol resin are increased - the temperature range of plasticity is expanded, frost resistance is increased, resistance to cyclic deformations at low temperatures, and their service life is increased.

If we take into account that the main function of bitumen in a mixture of asphalt concrete is to bind the components into a single unit, while maintaining the desired elasticity, plasticity and strength, the pavement constructed using the bitumen developed by us over time under the influence of air oxygen, sunlight and under the influence of many different factors after evaporation, low-boiling fractions, high-molecular compounds have the best required characteristics and are densely compacted. As a result of this, the road surface becomes mechanically strong and heat resistant.

Building bitumen based on gossypol resin is used in the construction of road coatings, for insulation of metal structures and for roofing. They completely replace the oil bitumen of the brands BND 60/90, BNI 70/130, BNK 90/10. Tested and approved by MAC "Autoyul" of the Republic of Uzbekistan. Bitumen-polymer composition meets the requirements of technical specifications TU 64-22518677-01: 2001 and is produced according to the technological instructions approved in the established manner. Depending on the purpose of the bitumen, the following grades are produced: UBC, IBC, RBC, where:

- UBC - universal bitumen-polymer composition designed for waterproofing building structures and for preparing asphalt concrete coatings;

- IBC - insulating bitumen-polymer composition is intended for waterproofing underground and insulation of surface steel pipelines;
- RBC - roofing bitumen-polymer composition is intended for roofing.

The results of physical and mechanical properties of bitumen based on gossypol resin are given in the table.

**Table**  
**Physico-mechanical properties of obtained bitumens**  
**based on gossypol resin**

1. Needle penetration depth, at 25 °C, 0.1mm UBC IBC RBC	60-90 22-41 6-22
2. The softening temperature on the ring and the ball, °C, not lower than UBC IBC RBC	47 69 91
3. Tensility at 25 °C, cm, not lower than UBC IBC RBC	54 3.2 1,1
4. Flash point, °C, not lower than UBC IBC RBC	315 315 315
5. Solubility in benzene or chloroform,%, not less than	99,5
6. Mass fraction of water	Traces
7. Water absorption in 24 h,%, no more than	0,1

For the novelty of the development, 2 patents of the Republic of Uzbekistan were obtained, and there is also an international certificate of compliance with ISO 9001:2015. The production enterprise "Khorezm anticorr invest" has organized mass production of the above bitumen [2,3].

The proposed bitumens in appearance and physico-mechanical parameters does not differ from oil bitumen, they have the appropriate sanitary and hygienic conclusions and toxicological passports. Tested and agreed at the Republican Center for certification and standardization in construction.

The developers guarantee, if subject to the application technology, the high efficiency of bitumen for the insulation of building structures, foundations, pipes, metal structures, power transmission towers, petrochemical facilities, water pipes, gas pipelines from aggressive environments, as well as the preparation of asphalt for repair and restoration and roofing.

### References

1. Evdokimova, N. G. Development of scientific and technological foundations for the production of modern bitumen materials as oil disperse systems: diss. ... doc. tech. sciences : 05.17.07 / Evdokimova Natalya Georgievna. - M., 2015. - 417 P.
2. Zhumaniyazov M.Zh. Chemistry and technology of anticorrosive materials based on industrial waste Abstr. diss. ... doc. tech. sciences. – Tashkent. 2005. – 40 P.
3. Patent № IDP 2002 0108 RUz. Composition for obtaining building bitumen / Zhumaniyazov M.Zh., Yuldashev N.Kh. Dyussebekov B. / Bull. 26.03.2003. Publ.17.01.2005.
4. Patent No. IAP 04550 RU. Bitumen-polymer composition based on gossypol resin / Zhumaniyazov M.Zh., Marakhimov A.R., Kurambaev Sh.R. / Bull. 15.02.2010. Publ.04.07.12.

UDC 620. 193.41: 667.632.4

**TECHNOLOGY FOR PRODUCING IMPORT SUBSTITUTING,  
EXPORT-ORIENTED ACID-RESISTANT ANTICORROSIVE  
COATINGS**

**Jumaniyazova Dilnoza**

Doctor of Philosophy (PhD) in Technical Sciences, Lecturer,  
Urgench State University, Republic of Uzbekistan

**Jumaniyazov Makhsud**

Doctor of Technical Sciences, Full Professor,  
Urgench State University, Republic of Uzbekistan

**Abstract.** This paper presents the results of research on the development of technology for acid-resistant anticorrosive coatings. Technical conditions have been created for obtaining anticorrosive agents, registered with Uzstandard agency, an international certificate of conformity ISO 9001 for a new type of product has been obtained.

**Keywords:** acid-resistant coatings, corrosion, damage, rusting, corrosion protection, technological scheme, technical regulations

**Introduction**

In the world, metals are considered the main, most important structural material in the development of any industry, and at present there are no economic areas without its application. The problem of protecting metals from corrosion appeared in the early times of human use of metals. Every country on a global scale suffers very large losses in economic terms due to rusting of metals and serious economic losses due to corrosion of structures. In this regard, the prevention of failure of various buildings, structures, equipment due to damage by aggressive media is of particular importance.

Today in the world, scientific research is being conducted on the production of corrosion protection products for metal structures and equipment, the production of anticorrosion agents in various environments, ensuring their comprehensive action as much as possible and reducing costs, scientific justification is needed in the following areas: to determine

the physicochemical properties of raw materials used in the manufacture of anti-corrosion agents; conduct research work for the production of acid-resistant and anti-corrosion agents; to develop a basic technological scheme of their production and make its description; to improve the stages of obtaining anti-corrosion agents, the development of technological regulations for production [1].

**The purpose of this study** was to develop a technology for producing import-substituting, export-oriented and highly effective acid-resistant anticorrosive coatings based on waste oil and grease industry - gossypol resin and local resources and putting it into practice.

### Methods

In this work, we used chemical and modern physicochemical methods of analysis: X-ray phase, IR spectroscopic, differential thermal methods of analysis.

### Results and its discussion

To create anti-corrosion coatings that meet international standards for performance, to develop new generations of coatings with low cost, the easily available industrial waste - gossypol resin - was chosen as the main raw material. Qualitative indicators of the selected gossypol resins for the study are given in table 1 [2].

**Table 1**  
**Qualitative indicators of gossypol selected for research**

Name of indicators	Characteristic and norm	
	First grade	Second grade
<b>Appearance and color</b>	<b>homogeneous mass from dark brown to black</b>	
Acid number, mgKOH/g	71-100	50-70
Solubility in acetone, %, not less	80	70
Mass amount of ash, % not less than	1,0	1,2
The amount of moisture and volatile substances, %	4,0	4,0
Melting temperature, °C	70	70
Flash point temperature, °C	250	250
Ignition temperature, °C	285	285

In order to increase the diversity of acid-resistant coatings, increase the drying rate and enhance adhesion, as well as provide rust modification, CaO, zinc oxide, phosphoric acid, and an acid corrosion inhibitor, urotropin ( $(\text{CH}_2)_6\text{N}_4$ ), were introduced into the composition of gossypol resin.

Chemical and electrochemical methods were used to test the corrosion resistance of the obtained samples based on the results of numerous studies in order to determine the optimal ratios of the components in the composition. The data obtained are proved by chemical methods. The corrosion rate is estimated as surface mass loss per unit time ( $\text{g}/\text{m}^2 \times \text{h} \cdot 10^{-3}$ ). The test results are shown in table 2.

**Table 2**  
**Test results for steel samples in a 20%  $\text{H}_2\text{SO}_4$  solution treated with a gossypol resin based anti-corrosion coating**

Samples	GR:CaO: ZnO:H <sub>3</sub> PO <sub>4</sub> : (CH <sub>2</sub> ) <sub>6</sub> N <sub>4</sub> , mass.%,	The difference in sample mass, g (day)		Corrosion rate, g/m <sup>2</sup> , 10 <sup>-3</sup> (day)			The degree of protection, % (day)				Appearance of the sample after 90 days
		7	28	90	7	28	90	7	28	90	
0	Without coatings	0,0105	0,0567	0,0696	44,4	56,16	22,08	-	-	-	severe corrosion
Gossypol resin: CaO: ZnO: H <sub>3</sub> PO <sub>4</sub> : (CH <sub>2</sub> ) <sub>6</sub> N <sub>4</sub>											
1	91:2:0:2:4:5:0,5	0,0014	0,0067	0,0742	5,91	7,13	4,48	86,4	88,2	89,6	little corrosion
2	90:2:2:5:5:0,5	0,0010	0,0089	0,0013	4,03	9,22	4,35	90,6	94,3	90,1	traces of corrosion
3	89:2:2:6:1	0,0001	0,0005	0,0009	0,41	0,46	0,29	99,0	99,2	98,2	Clear
4	88:2:2,0:6:5:1,5	0,0007	0,0008	0,0014	3,47	5,27	1,64	98,2	98,1	97,2	traces of corrosion
5	87:2:2,0:5:5:1,5	0,0014	0,0019	0,0025	5,1	7,35	3,19	97,2	96,5	95,5	little corrosion

The change in the anticorrosive properties of coatings over time is determined according to the requirement of GOST 6992 visually on an eight-point scale. Coating a - stainless and b - rusted to 1 mm in samples of steel St 3 were tested in distilled water, 3% NaCl solution, 20% solutions of  $\text{H}_2\text{SO}_4$ ,  $\text{HNO}_3$ , HCl. Five types of coatings were prepared. The content of the amount of urotropin in them was in the range from 0.5 to 1.0%, respectively, tests have been conducted. The influence of the atmosphere on the stability of coatings was measured in urban conditions of Urgench (the Aral Sea region) of moderate aggressiveness for 2 years. The optimal samples of the acid-resistant anticorrosion coatings we created were evaluated in the range of 1-2 points, their resistance to the effects of the atmosphere, water, 3% NaCl and 20%  $\text{H}_2\text{SO}_4$ ,  $\text{HNO}_3$  and HCl was completely proved and were approved. The conformity of all coatings to the standard requirements for the test time is determined. Based on the foregoing, it can be

concluded that anticorrosion coatings synthesized on the basis of thermally oxidized gossypol resin and local resources, unlike analogues, have specific properties. It has been fully proven that they form on the surface of carbon steels a thin, stable, chelate-type shell tightly glued to the metal base and are very stable in acidic media.

The physicomachanical properties of the film were checked on plates made of sheet steel grade 08KP and 8KS according to GOST 16523-78, size 150x70x1.0 mm. Coatings were applied to plates, both uncoated, with corrosion products on the surface, and stripped, by brush or by dipping, until a layer thickness of at least 60-80 microns was reached. Rust was obtained artificially by holding the plates in a 3% sodium chloride solution for 3 days at room temperature. Drying of the coatings was carried out at room temperature (22-25°C) for 24 hours. Before testing, the dried samples were kept at room temperature for 2.5-3 hours. When preparing anti-corrosion coatings, the most optimal solvent was nefras 130/210 (TU ANP 3-8-94) or white alcohol C4 155/200 (GOST 3134-78).

The conditional viscosity of the coatings was determined using a VZP-4 viscometer at 20 °C. The film thickness of the anticorrosion coating was measured with a magnetic thickness meter ITP-1. The thickness of the coatings is determined on an ITP-1 magnetic device. The strength of the coatings for bending is determined according to GOST 6806. The impact strength of coatings was determined according to the requirements of GOST 4765. The measurement was carried out on a U-1A device. The adhesion of the applied coatings was determined on the basis of the requirements of GOST 15140. The determination was carried out on a 4-point scale. If one part flies out of 100 parts - 1 point, two parts fly off - 2 points, etc. The resistance of the protective properties of the coatings was determined by soaking them in distilled water to water, a 3% NaCl solution to salt, and acid resistance in 20% solutions of various acids, respectively, for 14 days. The weathering resistance of the coatings was tested on samples located on the roofs of the "Khorezm anticorr invest" in Urgench for 2 years. The penetration depth of the needle in the compositions was determined on a penetrometer according to GOST 11501. In this case, the temperature of the test substance, the load and the duration of immersion are recorded. The usual load is 100 g, the duration of immersion of the needle in the substance is 5 seconds, and the temperature of the substance at the time of the test was +25 °C. The depth of penetration of the needle is expressed in degrees, determined by the disk of the penetrometer, where each degree of the disk corresponds to lowering the needle by 0.1 mm.

To determine the corrosion rate in various environments, the method of measuring polarization resistances was used. The softening temperature of the coatings was determined by the ring and ball method according to GOST 11506. The generalized results of the physicochemical parameters of acid-resistant coatings based on gossypol resin, calcium oxide, zinc oxide, phosphoric acid and hexamethylenetetraamine are given in Table 3. Based on the tabular data, it can be concluded that all indicators of the physicochemical properties of the coatings meet the requirements of GOST [3].

**Table 3**  
**Physico-mechanical properties of coatings based on gossypol resin**

№	Name of indicators	Norm of indicators
1	Colour	from dark brown to black
2	Appearance	Resinous
3	Smell	Specific
4	Flash point temperature °C	315
5	Strength with metal upon application (adhesion), MPa, not less than	4,0
6	Impact strength, n·m, not less than	1,9
7	Bending strength, mm, not more than	7,0
8	Temperature range during application, °C	4-45
9	The rate of hydrogen ions, (pH)	5,6-6,1
10	Crystallization temperature, °C	- 40
11	Consumption, g/m <sup>2</sup> , no more than	100,0
12	Water absorption, %, no more than	0,1
13	Drying time, hours, no more than	12-14
14	Protective ability, days, not less than	1000,0
15	Full formation of the protective layer, days	4-5

These coatings are superior to foreign analogues in their quick drying, resistance to impact, elasticity, resistance to bending, a high degree of adhesion, the ability to apply any decorative varnishes and a high degree of acid resistance.

Based on the above data, we can conclude that the created acid-resistant coatings based on gossypol resin and technogenic resources meet all the parameters of world standards. The results of their tests in various industrial facilities have fully proved the reliability of the above results, about which the relevant acts are drawn up. In order to determine the optimal solvents for dissolving acid-resistant coatings, studies were carried out with nefras, white alcohol, gas condensate and kerosene. Studies have

shown that when dissolving acid-resistant coatings in solvents (kerosene, gas condensate, white spirit and nefras) at a ratio of 1: 3, a homogeneous acid-resistant mass with a glossy texture is preserved in all solvents, preserving all physicochemical properties. Further studies drew attention to an even greater increase in the resistance of coatings to high temperatures and the acid resistance of chromates. In studies, an increase in the inhibitory properties of chromates was observed, starting from  $1.6 \cdot 10^{-3}$  mol/l (when using potassium dichromate, a solution with a concentration of 2-3 g/l is taken). The created compositions were tested in acidic media in three concentrations at a temperature of 50-150 °C.

Tests show that the addition of  $10^{-4}$ - $10^{-3}$  mol/l potassium dichromate ensures reliable protection in heat exchange devices and high temperatures. It is noteworthy that with a sufficient number of bichromate ions, the anticorrosive protective force increases with increasing temperature and the possibility of using chromate compositions as acid-resistant coatings at high temperatures is created. As a result of research, the production of heat-resistant coatings was achieved. Test + was carried out for 24 hours, the data obtained is given in table.4.

**Table 4**  
**Test results of acid-resistant coatings when exposed to various acids and high temperatures**

Acids	Concentration	Temperature °C	Ratio of components							The difference in mass of the plate g	Corrosion rate	Degree of protection, %							
			GR	CaO	ZnO	H <sub>3</sub> PO <sub>4</sub>	(CH <sub>2</sub> ) <sub>6</sub> N <sub>4</sub>	K <sub>2</sub> Cr <sub>2</sub> O <sub>7</sub>											
H <sub>2</sub> SO <sub>4</sub>	20	50	88,0	2,0	2,0	6,0	1,0	1,0	0,0067	0,72	72,2								
			87,5									2,0	2,0	6,0	1,0	1,5	0,0032	0,53	85,5
			87,0																
	40	100	87,0	2,0	2,0	6,0	1,0	2,0	0,00770,00320,0006	0,23	93,0								
			86,5									2,5	3,0	0,22	93,6				
			86,0													3,0	0,17	94,1	
60	150	86,0	2,0	2,0	6,0	1,0	3,0	0,00780,00330,0005	0,24	93,1									
		85,5									3,5	0,19	93,7						
		85,0												4,0	0,15	95,5			
HNO <sub>3</sub>	40	25	2,0	2,0	6,0	1,0	3,0	0,0032	0,22	93,6									
		30									3,5	0,0006	0,17	94,1					
HCl	20	25	2,0	2,0	6,0	1,0	3,0	0,0039	0,63	81,5									
		30									3,5	0,0045	0,33	90,1					

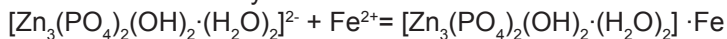
From the results of numerous studies conducted, the optimal ratios of compositions stable at high temperatures (100-150 °C) in aggressive chemical environments and reliably protecting steels were determined.

The next stages of the study were devoted to enhancing the acid resistance of coatings at high temperatures. According to the results of numerous studies, it was determined that the inhibitory strength of the mixture of chromates and ZnSO<sub>4</sub> gave a greater effect than the sum of individual compounds at maximum concentrations, and the complete cessation of corrosion of St3 steels under the influence of a mixture of 20 mg/l of chromate and 60 mg/l of sulfate in the range pH = 1.5-3.0.

Due to its low toxicity and low cost, zinc phosphates are widely used in the synthesis of anticorrosive substances. Its anti-corrosion mechanism is justified by the formation of the following complex compounds under the influence of water and other aggressive substances:



These are the bases of the complex type acid at the anode sites with Fe<sup>2+</sup> and Fe<sup>3+</sup> ions form very stable corrosion inhibitors:0



The formed stable complex salt has a sufficient inhibitory property, in addition, this shell sharply counteracts the osmotic absorption of water and other aggressive substances. Another feature of the inhibitor is the stability of the coating during prolonged use of the material. It is based on high adhesive ability [4].

Based on the laboratory studies and tests performed on the laboratory model unit, a process flow diagram for the production of acid-resistant anticorrosive coatings from gossypol resin was developed and the material balance was calculated.

The main scientific and practical results are as follows:

A comparative study of the physicochemical properties of gossypol resin - the waste of oil plants in the country and local resources by modern methods, i.e. As a result of studying the processes of dehydration and thermal oxidation of gossypol resin from various sources, the optimal parameters of these processes were determined: the dehydration time for the release of 94.1-96.6% of water and the heating temperature of 170-240 °C. In order to increase acid-resistant properties, drying speed and adhesion, as well as modification, CaO, zinc oxide, orthophosphoric acid and an acid corrosion inhibitor - hexamethylenetetramine (CH<sub>2</sub>)<sub>6</sub>N<sub>4</sub> were introduced into the composition of gossypol resin, their optimal ratio is equal to GR:Ca O:ZnO:H<sub>3</sub>PO<sub>4</sub>:(CH<sub>2</sub>)<sub>6</sub>N<sub>4</sub>=89:2:2:6:1 and due to the absence of changes on the surface of the test samples even after 90 days, the production of these types of coatings on an industrial scale is recommended.

The difference between the created anti-corrosion coatings and imported analogues was determined to be due to faster drying, shock resistance, elasticity, bending resistance, high adhesion and the ability to apply any decorative varnish and high acid resistance. Technical conditions have been created for the production of anticorrosive agents, registered with Uzstandard, an international certificate of conformity ISO 9001 for a new type of product has been obtained.

### References

1. Akbarov Kh.I., Alibekov R.S., Dyussebekov B.D., Tillaev R.S. The electrochemical behavior of an aqueous dispersion of gossypol resin // Uzb. chem. journal. – 1999. – № 5-6. – P.26-28
2. Alibekov R.S., Dyussebekov B.D., Khodzhaev O.F. Modification of rust with anti-corrosion coatings based on gossypol resin // Uzb. chem. journal. – 2001. – № 5 –P.18-20.
3. Zhumaniyazov M.Zh., Kurambaev Sh.K, Zhumaniyazova D.M. Synthesis of new modified forms of hydrolysis lignin and their application // "High Technologies and Prospects for the Integration of Education, Science and Production" Proceedings of the International Scientific and Technical Conference, Tashkent-2006, P.205-207.
4. Zhumaniyazova D.M., Zakirov B.S., Zhumaniyazov M.Zh. Studies of the synthesis of competitive anticorrosion coatings on gossypol resin and phosphoric acid // Uzbek chemical journal – Tashkent, 2018. - №3. - P.10-15.

## QUALITY OF SURFACE WATERS IN ESTERN DONBASS, RUSSIA

### Gavrishin Anatoly Ivanovich

Dr.of Sciences, Professor

South-Russian State Polytechnic University

(Novocherkassk Polytechnic Institute) named after M.I. Platov. SRSPU(NPI),  
Russia.

The purpose of the research is to assess the role of mine water in the management of surface water pollution in the Eastern Donbass. The leading drivers of environmental transformation in the region are the coal mining and coal processing industries. Under the influence of these factors, many negative consequences and, above all, intensive pollution of surface water are formed. To solve the problem, standard methods of mathematical statistics and the original method of assessing water quality by the total pollution indicator are used. Mn, Fe, Se, Be, as well as  $SO_4$ , M, Na, Mg. contribute the largest share of surface water pollution. Mine waters play a leading role in the pollution of surface water in the region studied. The high efficiency of the original method of assessing water quality by the total pollution indicator is shown. The level of pollution of mine and surface waters demonstrates the need to implement environmental rehabilitation measures and improve treatment technologies.

**Keywords:** mine, surface water, chemical composition, pollution indicator, Eastern Donbass

### Introduction

In the Eastern Donbass, the coal mining and coal-processing industries have a significant impact on the environment, causing serious damage to public health and environmental potential in the region. These factors form man-made cracking of rocks, deformation of buildings and structures, silting of watercourses, salinization of soils, and mass elimination of mines intensified the processes of subsidence of the earth's surface, flooding of areas, formation of powerful flows of pollution of air, water and geological environments, the release of "dead air" and other negative phenomena [1-3, 10]. Such negative effects are typical for many coal basins in the world [1, 4, 6, 8, 9]. To achieve this goal, more than 2,000 analyses of the chemical composition of mine and surface waters were used, standard methods of mathematical statistics and the original method of assessing water quality by the total pollution indicator were used.

### Methodology

The original method of calculating the concentration ratio and the total pollution indicator is used to assess surface water pollution [2, 3]. The categories of water and environmental pollution (table 1) are used. The i-component concentration ratio is calculated according to the following formula:

$$K_{ic} = C_i / C_{mac}$$

where the component's Ci-concentration, Cmac, is the maximum permissible or background concentration of the component.

The degree of water and environmental pollution by n components is estimated by the total pollution indicator:

$$Z_c = \sum_i K_{ic} - (n-1).$$

The categories of water pollution and the environment are listed in Table 1.

**Table 1**  
**Water and environmental pollution categories**

Total pollution indicator	Water and environmental pollution categories
<2	Norm
≥2 - 16	Risk
≥16 - 128	Crisis
≥128 - 1024	Disaster
≥1024	The Great Disaster

The total pollution indicator makes it possible to assess the quality of the chemical composition of any type of water (atmospheric, surface, underground, man-made) relative to any regulatory indicators.

In this paper, the MAC rules are set for the following documents: for the United States: "U.S. Environmental Protection Agency (U.S.EPA); for the EU - EU directive "On the quality of drinking water intended for human consumption" 98/83/EU; for WHO - "1992. Drinking Water Quality Control Guide"; for Russia – in documents [5, 7].

### Research results

Mine water is the main source of surface water pollution in the Eastern Donbass. The composition of this water is sulphate magnesium-sodium water (table 2), in which the concentration of SO<sub>4</sub> reaches 12, and mineralization 17.5 g/l. On average, the mineralization of mine water is five times and higher than the mineralization of clean surface water, and for surface water this ratio is three times. For all limited components in mine waters there is an excess of MAC for drinking water (table.2).

**Table 2**  
**The average composition of mine and surface water (mg/l and %-mole)**

Type of water	pH	HCO <sub>3</sub>	SO <sub>4</sub>	Cl	Ca	Mg	Na	Fe	M
Mine water	6,95	591	2837 +	347 +	293	267 +	966 +	33.7	5301 +
		12	76	12	17	28	55		
Surface water	7,95	428	1773 +	212	267	146 +	575 +	0.45	3401 +
		14	74	12	26	24	50		
Clear surface water	7,98	303	304	200	153	85	50	0.04	1095
		30	37	33	46	42	12		

Note. Here and in all tables the sign "+" means exceeding the concentrations of components on MAC for water of drinking and cultural use [5], M – mineralization

Special studies have shown that mine water is classified as a "disaster" by drinking water pollution standards. The highest polluting indicators are Fe and Mn, where the concentration rate exceeds hundreds of times. In addition, heavy pollution is observed in Al, Li, Be, Ni, and macro components for SO<sub>4</sub>, Na, Mg and M. Regarding the requirements for fisheries water, the total figure is 1013, which is very close to the category of "disaster".

Tables 3 and 4 provide parameters for the distribution of macro-component concentrations and trace elements of surface water chemistry. The distributions of all components are highly volatile. So<sub>4</sub> concentration reaches 4, Na - 1.6, mineralization - 6.8g/L; Fe - 5.65, Mn - 7.72 mg/l, etc.

**Table 3**  
**Distribution of macro components in surface waters (mg/l)**

Component	The average	Median	Minimum	Maximum	Standard
pH	7,95	7,99	7,00	8,73	0,31
HCO <sub>3</sub>	428	406	98	793	142
SO <sub>4</sub>	1773 +	1585	17	4007 +	815
Cl	212	157	50	917 +	146
Ca	267	276	80	621	88
Mg	146 +	146	6	353 +	76
Na	575 +	343	25	1574 +	313
M	3401 +	2948	1104	6772 +	1324

**Table 4**  
**Distribution of trace elements in surface waters (mg/l)**

Element	The average	Median	Minimum	Maximum	Standard
Al	0,34 +	0,11	0,02	11,60 +	1,18
Be	0,0008 +	0,0007	0,0001	0,0037 +	0,0006
Fe	0,45 +	0,21	0,04	5,65 +	0,68
Cd	0,0005	0,0001	0,0001	0,0065 +	0,0010
K	13,0	7,5	0,3	67,0 +	14,3
Co	0,002	0,001	0,001	0,039	0,005
Li	0,16 +	0,08	0,02	0,65 +	0,15
Cu	0,003	0,002	0,001	0,009	0,002
Mn	0,61 +	0,27	0,01	7,72 +	1,00
Ni	0,009	0,001	0,001	0,482 +	0,051
Pb	0,0010	0,0010	0,0010	0,0013	0,0001
Se	0,019 +	0,009	0,005	0,070 +	0,017
Sr	3,92	3,75	0,37	8,76 +	2,15
Cr	0,0018	0,0010	0,0010	0,0060	0,0014
Zn	0,014	0,006	0,005	0,335	0,034

Table 5 provides an assessment of the quality of the surface waters of the Eastern Donbass. According to WHO and Russian regulations, the region's surface waters are classified as "risk" and, according to US and EU regulations, as a "crisis." According to the requirements for fisheries, pollution is classified as a "crisis".

**Table 5**  
**Assessment of surface water quality**

Компонент Component	X	Ki MAC USA	Ki MAC EU	Ki MAC WHO	Ki MAC RF Drinking	Ki MAC RF Fisheries
pH	7.2	0	0	0	0	0
SO <sub>4</sub>	1773	7.0	7.0	7.0	3.5	17.73
Cl	212	0.85	0.85	0.85	0.6	0.7
Na	575	H	H	2.8	2.8	4.8
Mg	146	H	2.9	H	2.9	3.65
M	3001	6.0	2.0	3.0	3.0	3.0
Al	0.34	1.7	1.7	1.7	1.7	8.5
Be	0.0008	0.2	H		4.0	4.0
Fe	0.45	1.5	2.2	1.5	1.5	4.5
Cd	0.0005	0.1	0.1	0.17	0.5	0.1
K	13.0	H	1.2	H	0.4	0.26
Co	0.002	H	H	H	0.02	0.2

Li	0.16	H	H	H	5.3	5.3
Cu	0.003	0.002	0.0015	0.003	0.003	1.0
Mn	0.61	12.2	12.2	1.2	6.1	61
Ni	0.009	H	H	0.45	0.45	0.9
Pb	0.001	0.07	0.1	0.1	0.1	0.17
Se	0.019	0.38	1.9	1.9	1.9	9.5
Sr	3.92	H	H	1.3	0.44	1.55
Cr	0.0018	0.02	0.04	0.04	0.04	0.04
Zn	0.014	0.003	0.003	0.005	0.014	1.4
Z <sub>c</sub>		17	19	8	10	109

Note. M - water mineralization, H - lack of information about MAC.

### **Conclusion**

A detailed analysis of the quality of the chemical composition and pollution of mine and surface waters in the Eastern Donbass has been carried out. The high efficiency of the original method of assessing water quality by the total pollution indicator, which allows to estimate the degree of pollution of different types of water for any number of components, is shown. Mine water contains very high concentrations of many components, much higher than MAC. The highest concentrations are observed by Fe and Mn, for which the excesses of MAC are hundreds, and in some cases thousands of times. Typically, the excess of MAC is ten times detected for Al, Li, Be, Ni, Se, Cu and zn. From macro components, significant pollution is manifested by concentrations of SO<sub>4</sub>, Na, Mg and M. Mn, Fe, Se, Be, as well as SO<sub>4</sub>, M, Na, Mg.

Comparison of the list of components of pollution of mine and ground-water strongly demonstrates that mine water plays a leading role in the management of surface water quality. The very high level of pollution of mine and surface waters indicates the urgent need to perform monitoring observations, to carry out measures to rehabilitate the environment in the region and to improve treatment technologies, primarily to reduce fe and Mn concentrations.

### **References**

1. Bazhin V. Yu., Beloglazov I. I., Feshchenko R. Yu. Deep conversion and metal content of Russian coals // Eurasian Mining. 2016. No. 2. P. 28-36.
2. Gavrishin A.I. Mine Waters of the Eastern Donbass and Their Effect on the Chemistry of Groundwater and Surface Water in the Region // Water

Resources. 2018. Vol. 45. No. 5. P. 785-794.

3. Gavrishin A.I. Assessment of the quality of the chemical composition of surface waters in the Eastern Donbass / *Geoecology*. 2019. No 4. P. 61-67. DOI: 10.31857/S0869-78092019461-67.

4. Giulio D.C., Jackson R.B. Impact to Underground Sources of Drinking Water and Domestic Wells from Production Well Stimulation and Completion Practices in the Pavilion, Wyoming, Field // *Environmental Science and Technology*. 2016. Vol. 50 (8). P. 4524-4536.

5. GN 2.1.5.1315-03. Maximum allowable concentrations (MAC) of chemicals in water-drinking and cultural and domestic water use // Hygiene standards. The Ministry of Health of the Russian Federation. Resolution 78. M. 2003. 152 P.

6. Griazev M.V., Kachurin N.M., Stas G.V. Pyllegas emissions from the surface of the rock dumps of the liquidated coal basin mines / *Sustainable development of mountain areas*. 2018. T. 10. N 4(38). P. 500-509.

7. MAC of Water Objects of Fisheries Value // Hygiene standards. Order of Rosryboloolo from January 18, No.20. 2010. 5 P.

8. Neidell, Matthew; Gross, Tal; Graff Zivin, Joshua; Chang, Tom Y. The Effect of Pollution on Worker Productivity: Evidence from Call Center Workers in China // *American Economic Journal: Applied Economics*. 2019, vol. 11 (1), pp. 151-172.

9. Pfunt H., Houben G., Himmelsbach, T . Numerical modeling of fracking fluid migration through fault zones and fractures in the North German Basin // *Hydrogeology Journal*. 2016, vol. 24 (60), P. 1343-1358.

10. Zakrutkin V. E., Sklyarenko G. Y. The influence of coal mining on groundwater pollution (Eastern Donbass) // *International multidisciplinary Scientific GeoConference Surveying Geology and Mining Ecology Management, SGEM 15<sup>th</sup>*. 2015. P. 927-932.

## NEW CONTROL METHOD “MICROTRIANGULATION NETWORK”

**Yeskaliyev Yertay Talgatovich**

master student

East Kazakhstan State Technical University after Daulet Serikbayev,  
Republic of Kazakhstan

**Abstract.** In this scientific article shows potential of created microtriangulation network, results what we have got if we will use this method of surveying. All works has done in Oil&Gas project in Kazakhstan. Beside new method article has all process detail explanation about coordinate systems, its calculation, determination and transformation. After all, article shows rconclusions of searching and checking new method in construction.

**Key words:** microtriangulation, survey control works, geodetic system, verification, new method of survey works, field survey methodology.

### Introduction

The availability of accurate and reliable information relating to the position and uncertainty of the site survey control marks is critical to the integrity of the Project. The purpose of this report is to introduce innovations in higher geodesy by creating new microtriangulation network and thereafter use it for survey control works. In addition, as the Survey Control Network itself defines the accuracy of all survey work carried out on the project, it is imperative the survey control used placement matches the design coordinate system used throughout the design and fabrication of all next works. This report outlines the existing the methodology used to verify the survey control network, the results and parameters must be following to as coordinate delta listings, the procedure for performing surveys on the subject site and the recommendations and conclusions.

### Synopsis

Provided the proposed new localised site grid contains survey control points that are homogeneous, accurate and reliable with respect to position and uncertainty and:

- the above-mentioned factors mentioned in the "Implications of Coordinate Shift" are of no significance or are negligible;
- the positioning relative to the site datum 122 or any other datum is of no significance, then the revised coordinate values with applied scale factor should be adopted.

### Survey Control Network Verification

GNSS equipment and observation techniques employed have a direct impact on the accuracy and uncertainty of the survey results. Discussions with the project surveyor revealed the original supplied control (second order control) was performed by GNSS observations connected to only one 1st order control point. This is far from ideal and not the standard practice of utilising surround control. Further, static observations session length at each of the second order control marks was apparently in the order of 1 to 1.5 minutes. The standard practice for GNSS control surveys to the accuracy required on the project is a session length of one (1) hour plus five (5) minutes per one (1) km baseline length. The project surveyor has informed me that the stated accuracy of these control points is in the order of 20mm at best (Report required for confirmation).

Quality of Control Network is beyond the scope of this verification survey to audit the quality of the originally supplied survey control network as it is dependent upon the following components:

- The Network Design;
- The survey practices adopted to older will;
- The equipment and instrumentation used;
- The reduction techniques employed.

These components are usually proven by the results of a successful, minimally constrained least squares network adjustment computed on the ellipsoid associated with the datum on which the observations were acquired.

Survey Control verification surveys have been performed with precision total stations utilizing methods appropriate to achieving the standards specified.

The quality of the control survey were qualified in terms of uncertainty in three ways:

1. Survey Uncertainty. The uncertainty of the horizontal and vertical coordinates of the survey control marks relative to the survey in which it was observed. This verification process is independent from the influence of any imprecision or inaccuracy in the underlying datum realisation.

2. Positional Uncertainty. The uncertainty of the horizontal and vertical coordinates of the survey control marks with respect to the defined datum. This represents the combined uncertainty of the existing datum realisation and the new control survey.

3. Relative Uncertainty. The uncertainty between the horizontal and vertical coordinates of any two survey control marks within the survey control network.

**Field Survey Methodology**

Lack of inter-visibility and line of sight between survey control marks within the supplied survey control network restricted the use of direct observation verification. Instead, a separate network of interconnecting control stations with sufficient redundancies was set up to connect the relevant survey control marks. This process involved large degrees of freedom and eliminated traditional traverse errors providing a solution that:

- Had no instrument plumbing errors (everything is measured from the perspective of the instrument axis);
- Minimised orientation errors;
- Provided the opportunity to set the Instrument closer to the survey control mark (increased accuracy), as free stations are not reliant upon pre-existing ground control to setup over;
- Provided substantial redundancy leading to sub millimetre residuals;
- Enabled easy and fast future identification survey control verification.

Survey instrument setup coordinates for each station within the interconnecting network were established through a minimum of six (6) to ten (10) pre-established control points. Refer "Table 3 – Existed Control Points". A least squares multiple iteration bundle fit was then applied to the network and further transformations applied to set the coordinate system.

This control method is very similar to the triangulation technique. Refer "Table 4 - Triangulation classes and categories". However, none of existing classes does not fit the parameters.

**Table 3 – Triangulation classes and categories**

<b>Class, category</b>	<b>Angle root-mean-square error, min</b>	<b>Fractional error of basis</b>	<b>Length of triangle side, km</b>
I class	0,7	1: 400000	>20
II class	1,0	1: 300000	7 - 20
III class	1,5	1: 200000	5 - 8
IV class	2,0	1: 200000	2 - 5
1 category	5,0	1: 50000	0,5 - 5
2 category	10,0	1: 20000	0,25 - 3

Micro triangulation network is a chain of triangles with sides not less than 200 m and not more than 1000 m, laid between two sides or points of triangulation.

The triangles that define the analytic network should be close to equilateral. Angles at the defined points must be at least 30° and not more than 150°. All angles in the theodolite triangles shall be measured with an accuracy of not less than 30", the residual angles in triangles shall not exceed 1'. The relative error of the farthest side should not exceed 1/2000.

**Table 4: Existed control points**

Supplied				Verification				Difference		
Point ID	Easting	Northing	Elevaton	Point ID	Easting	Northing	Elevaton	ΔE	ΔN	ΔELE
C13	2924.994	2922.679	103.47	C13	2924.994	2922.679	103.470	0.000	0.000	0.000
C30	2919.187	2911.501	104.663	C30	2919.187	2911.501	104.663	0.000	0.000	0.000
C31	2915.49	2911.683	105.153	C31	2915.489	2911.684	105.153	0.001	-0.001	0.000
C32	2913.218	2911.499	105.079	C32	2913.217	2911.500	105.079	0.001	-0.001	0.000
C33	2913.961	2911.781	106.536	C33	2913.960	2911.782	106.536	0.001	-0.001	0.000
C34	2917.113	2911.781	106.521	C34	2917.113	2911.782	106.522	0.000	-0.001	-0.001
C35	2913.21	2922.293	104.686	C35	2913.210	2922.295	104.686	0.000	-0.002	0.000
C36	2919.106	2922.292	104.888	C36	2919.106	2922.293	104.889	0.000	-0.001	-0.001
C37	2918.209	2922.01	106.663	C37	2918.210	2922.011	106.663	-0.001	-0.001	0.000
C38	2915.69	2922.012	106.64	C38	2915.691	2922.013	106.640	-0.001	-0.001	0.000
C41	2931.318	2911.534	104.869	C41	2931.317	2911.534	104.869	0.001	0.000	0.000
C46	2919.201	2922.288	107.953	C46	2919.202	2922.290	107.953	-0.001	-0.002	0.000
C47	2925.184	2922.297	107.915	C47	2925.184	2922.297	107.915	0.000	0.000	0.000
C48	2931.203	2922.293	107.902	C48	2931.202	2922.292	107.901	0.001	0.001	0.001
C49	2922.723	2922.012	107.061	C49	2922.724	2922.013	107.062	-0.001	-0.001	-0.001
C50	2913.206	2911.509	107.501	C50	2913.205	2911.510	107.501	0.001	-0.001	0.000
C51	2919.205	2911.514	107.872	C51	2919.204	2911.515	107.872	0.001	-0.001	0.000
C52	2925.203	2911.516	107.929	C52	2925.203	2911.516	107.929	0.000	0.000	0.000

The new type of microtriangulation with the following parameters:

1. The use of auxiliary control points for triangulation;
2. Using at least 12 control points;
3. Distance is not more than 80 m;
4. Full accounting of atmospheric parameters (temperature, atmospheric pressure, humidity)
5. From each setup observe as many visible existing control points as possible;
6. Minimum 6 existing control points must be observed;
7. Minimum 6 connecting points between current station and the next station must be observed;
8. All new Control points need to be observed minimum 2 times from separate setups;

9. All control points need to be observed 2 faces LF/ RF;
10. All benchmarks in the vicinity should be observed to verify the vertical component;
11. Ideally a minimum of benchmarks should be observed;
12. All benchmarks should be observed to a traverse prism accurately setup over the control point;
13. All control points should be observed from as may setups as possible.

Compliance with these parameters ensures maximum accuracy in the initial data up to microns. Also identified those strong points:

- which were affected by external physical factors and exceeded the permissible residual or destroyed, were subsequently excluded from the catalogue;
- which had incorrect initial data in the directory of strong points, were subsequently changes to correct data.

**Results**

**Table 5 – Results of verification**

Benchmark ID	Supplied Local Control		Verification Survey Local Control		Comparison	
	Easting	Northing	Easting	Northing	Easting	Northing
KV1	2630.658	3193.177	2630.656	3193.174	-0.002	-0.003
KV2	2440.048	3069.360	2440.050	3069.361	0.002	0.001
KV3	2440.075	2888.601	2440.076	2888.603	0.001	0.002
KV4	2550.611	2813.670	2550.614	2813.675	0.003	0.006
KV5	2707.369	2813.673	2707.370	2813.675	0.001	0.002
KV7	3153.547	2454.590	3153.538	2454.611	-0.009	-0.021
KV9	3277.315	2340.259	3277.299	2340.273	-0.016	-0.014
NM4	3040.725	3238.008	3040.720	3238.003	0.005	-0.005
NM5	2849.264	3069.284	2849.265	3069.283	0.001	-0.001
NM6	3087.560	2918.929	3087.561	2918.928	0.001	-0.001
NM7	3155.101	2696.211	3155.101	2696.219	0.000	0.008
NM8	3491.691	2811.346	3491.686	2811.348	0.005	0.002

**Conclusion**

All Local coordinate values listed in the "Catalogue for Coordinates and Elevations of Monuments in site" that are not highlighted in yellow are suitable for use on the site for further survey control identification and module installation works. However, prior to implementation and issuance of any "new localised" survey control coordinates, it is recommended that:

## Process Management and Scientific Developments

---

- Any impact associated with datum and/or survey monument coordinate shifts is considered;
- Reference is made referring actual position of R. L. on the survey monument;
- Transformation parameters are provided to allow conversion between UTM 39 grid and 3GP plant grid and;
- Coordinates are supplied in both UTM-39 and 3GP Plant Grid.

The survey control coordinates that are highlighted in yellow, namely KV7, KV9 and NM7 will need to be rechecked, re-coordinated and re-verified for position prior to release and issuance.

Compliance with parameters ensures maximum accuracy in the initial data up to microns. Also identified those strong points:

- which were affected by external physical factors and exceeded the permissible residual or destroyed, were subsequently excluded from the catalogue;
- which had incorrect initial data in the directory of strong points, were subsequently changes to correct data.

In the end, new microtriangulation method of control gives the most accuracy coordinate data. Precise quality of measurement is the most important in all survey works and appears the valuation of surveyor qualification.

## References

1. Iouri Volodine Statistical Error Model of Active Triangulation Method for CAI// Moscow State Technical University n.a. N. E. Bauman – Moscow, Russia, 2003
2. Krakiwsky E. J., Wells D. E. Coordinate Systems in Geodesy// University of Brunswick – Fredericton, Canada, 1971
3. Mefod'eva M. A., Ixanova G. R., Fakhrutdinova A. V. Geodesy// Federal University of Kazan', 2014
4. Szafranek K., Schillak S. Introduction to joint analysis of SLR and GNSS data// Military University of Technology, Warsaw, 2012
5. Tsoulis D. Geodetic use of global digital terrain and crustal databases in gravity and field modeling// Journal of Geodetic Science №3(1), 2013, p. 1-6
6. Malkov A. G. High-precision Geodetic works// Siberian State Geodetic Academy, Novosibirsk, 2013

7. Gorbunova V. A. Engineering Geodesy//Kuzbass State Technical University n. a. Gorbachev, Kemerovo, 2012
8. Medvedskaya T. M. Geodetic observation of Deformations of Oil Industry Objects// Interexpo GEO-Sibir'-2017. XIII International scientific conference "Geodesy, geoinformation, cartography, mine surveying", Novosibirsk: 2017. Book 1 – p. 109-113
9. Tafesse W., Gobena T. Surveying// Haramaya University, Haramaya, 2005
10. Seeber G. Satellite Geodesy//New York, 2003

## STRUCTURAL-BASIC TECHNOLOGY OF CREATING COLLECTIVE USE SYSTEMS. METHODOLOGICAL ASPECTS OF THE CREATION

**Khalilov Abdurakhman Ismailovich**

Doctor of Technical Sciences, Full Professor  
Dagestan State University

**Abstract.** The paper discusses the methodology for creating interactive systems of collective use of parallel action with elements of artificial intelligence, based on such concepts as a structurally basic approach to creating and researching systems of shared use, parallelization of information and computing processes, multiplicativeness, parametricity and sociability of databases, presentation and the use of knowledge, modeling, adaptive dialogue systems, etc.

**Keywords:** system, structure, parallelism, collective use system, database, knowledge base, artificial intelligence, interactivity, multiplicativeness, parametricity, sociability, dialogue system, modeling.

### Introduction

The intensive development of the processes of creating the information society leads to the creation of universal collective use systems (CUS), adaptable to various subject areas and invariant to operating systems and other system-wide and tool software. This increases the relevance of the problem of the optimal organization of the computing process, providing a flexible and dynamic discipline of service. Obviously, such a CUS has a number of specific properties [1]. A wide class of applications requires CUS flexibility and high adaptability. It should ensure interactivity not only between users and the system, but also between elements of the system, i.e. it must possess the property of sociability.

For CUS, the problem of organizing the computing process, dynamically maintaining the optimal mode of functioning of the computing complex as a whole, taking into account many parameters, is very relevant, that is, CUS should be parametric.

The composition of users assumes the presence of people of very different computer literacy. The system should serve them all at a high level, provide them with the opportunity to invest their intelligence in the product they create, use their knowledge, skills, experience, i.e. CUS must be intelligent.

In other words, the problem of the collective use of software, technical and information resources requires the development of a methodology and technology for creating interactive collective use systems of parallel action (ICUSPA) with elements of artificial intelligence that have the properties of parametricity, sociability and intelligence.

This paper discusses the methodology for creating ICUSPA and its main components. A significant place in it is occupied by the principles of structuring and the concept of databases, in connection with which it is called "Structural-Basic Technology" (SBT).

### Structuring of CUS

Since CUS is a complex system, methods for studying complex systems are applied to it [2]. According to SBT, CUS can be represented as

$$\mathcal{G} = \langle \mathfrak{S}, \mathcal{C}, \mathfrak{M} \rangle,$$

where  $\mathfrak{S}$  – system interface with the external environment;  $\mathcal{C}$  – system management;  $\mathfrak{M}$ – subject area model.

The set  $\mathfrak{S}$  contains means for converting input-output messages to the internal representation and vice versa, providing syntactic invariance of the set of system states (and, therefore,  $\mathcal{C}$  and  $\mathfrak{M}$ ) with respect to the sets of input and output messages.

In dialog systems, the components  $\mathfrak{S}$  can be represented as

$$\mathfrak{S} = \bigcup_{i=0}^N L_i,$$

where  $N$  – number of user categories;  $L_0$  – system administrator language  $L_i$  ( $i=1,2, \dots, N$ ) – language of the  $i$  category user.

The component  $\mathcal{C}$  is represented by the triple  $\mathcal{C} = \langle L, S, M \rangle$ , where  $L$  – language (means) of interaction with the control component;  $S$  - resident program of the control component,  $M$  – control component model.

Component  $\mathfrak{M}$  includes a database  $\mathcal{D}$ , a database of relations  $\mathfrak{R}$  between elements  $\mathcal{D}$  and a database of algorithms (laws, rules)  $\mathfrak{A}$  interactions of elements of a database of relations  $\mathfrak{R}$  and, possibly, a database  $\mathcal{D}$ , i.e.  $\mathfrak{M} = \langle \mathcal{D}, \mathfrak{R}, \mathfrak{A} \rangle$ . Database  $\mathcal{D}$  may consist of the database of the object  $\mathcal{D}_o$  and the database of the environment  $\mathcal{D}_c$ .

This conceptual decomposition is applicable to each component of the system at each level of the hierarchy.

The blockiness, modularity, structuredness and structural homogeneity of the system modules at all levels of the hierarchy determine the standard and recursive nature of control processes, which corresponds to the natural structures of complex objects.

This approach also helps minimize (unify) many CUS tools while maximizing the number of subject areas (adaptability of the first to the second) in the system and the invariance of the first with respect to many operating environments in which the software tools operate over many subject areas. Along with this, the problem of the optimal organization of the information-computing process, which provides a flexible and dynamic discipline of service, is being updated.

In SBT, tree structures are considered as the basis using appropriate research methods. To represent network structures, both methods for converting them to tree structures are provided, as well as methods and means for representing and processing hierarchical networks using, if necessary, advanced relational models and special operations on them (naming and dereferencing operations).

CUS as a whole and a number of its elements, tools (software, databases, dialog schemes) are partially ordered hierarchical structures. As a toolkit for their analysis, initial structuring and transformation (dynamic restructuring), the sequential deepening method [3] (SDM) is used, which, due to its versatility and simplicity, makes it possible to isolate, structure, simplify and unify control processes.

### Sequential deepening method

Let  $\mathfrak{A} = \{A_{i_1, i_2, \dots, i_n}\}$  – be a partially ordered set of hierarchical structure ( $k - 1, 2, \dots, n$  – the level of the hierarchy;  $i_k$  – element serial number at the  $k$  - th hierarchy level). On a set  $\mathfrak{A}$  a certain relation of order  $\delta$  is defined from the set  $\Delta$  of relations admissible on this set.

Denote by  $S(A_{i_1, i_2, \dots, i_n})$  the component set of the element  $A_{i_1, i_2, \dots, i_n}$ , and  $f(i_1, i_2, \dots, i_n)$  - the number of elements in this set (for the highest level  $f()=m$ , for the terminal element –1). Let the set  $\mathfrak{A}$  be analyzed for the truth of some predicat  $p_i \in P = \{p_i\}$ . In each case, the predicate  $p_0$  chooses  $p_i$ , the truth of which is checked. If the predicate  $p_i$  is true, some procedure  $p_i$  is true, some procedure  $q_i$  from the set of procedures  $Q = \{q_i\}$  is performed, where  $q_0$  - is the control procedure for choosing  $q_i$  ( $j = 1, 2, \dots, k$ ), corresponding to  $p_i$ .

The SDM mechanism is determined by such a recursive algorithm scheme:

for  $\{A_{i_1} | i_1 = 1, 2, \dots, m\}$  execute  $P'$ ;

for  $i_1$  from 1s with step 1 to  $m$  execute:

if  $f(i_1) > 1$ , for  $\{A_{i_1, i_2} \mid i_2 = 1, 2, \dots, f(i_1)\}$  execute  $P'$ ;

.....

$n$ ) for  $i_1$  from 1s with step 1 to  $m$  execute: if  $f(i_1) > 1$ , for  $i_2$  from 1s with step 1 to  $f(i_1)$  execute:

..... execute:

if  $f(i_1, i_2, \dots, i_{n-1}) > 1$ , for  $\{A_{i_1, i_2, \dots, i_n} \mid i_n = 1, 2, \dots, f(i_{n-1})\}$  execute  $P'$ .

$P' = \eta: \varphi(p_o) \rightarrow \psi(q_o), \varphi(p_o) = p_i, \psi(q_o) = q_j; i = 1, 2, \dots, m; j = 1, 2, \dots, k.$

CUS as a whole and a number of its elements, tools (software, databases, dialog schemes) are partially ordered hierarchical structures. SDM is used as a tool for their analysis and transformation, which, thanks to its versatility and simplicity, makes it possible to isolate, structure, simplify and unify control processes.

Each specific application of SDM is associated with the determination of a relation of order  $d$ , procedure  $q$  and conditions for its application  $p$  (in the general case, these elements can be sets).

Plurality conditions  $P$  may also contain conditions for limiting the recess.

**Information structures and means of their organization**

CUS uses the concept of a virtual integrated database (VDB) [4], which allows to describe hierarchical relations. The latter allows us to consider complex hierarchical structures within the framework of an extended relational data model (RMD), in which either a simple domain or a relation can correspond to an attribute. The operations of the RMD link algebra take place in the extended RMD with some reservations.

For set-theoretic intersection, union, and addition operations, the compatibility condition for circuits is required. The product, projection, and division of relations are distinguished in that, in addition to data elements  $r_i$ ,  $D_i$  domains are allowed in relations; or relationships  $R_i^{j_i}$ , where  $j_i$  - the rank of the relationship (the depth of the relationship). The operations of  $\theta$ -connection and  $\theta$ -restriction take place only in the case of simple domains.

To manipulate compound domains, operations of naming (increasing the rank of the ratio by one) and dereferencing (decreasing the rank by one) are intended.

The latter can be performed until the rank of the relation is equal to zero. In this case, the relation turns into attribute  $A_i$ .

The concept of data multibase (DMB) is defined in relation to the advanced RMD. It is based on the concept of procedural independence, which is defined in relation to single data, its sets, domains, composite domains, tuples, attributes and relationships.

After that, DMB is determined using its scheme and a set of functional dependency structures  $\mathfrak{R}'(\mathcal{L}')$ ,  $\{(\mathfrak{R}'(\mathcal{L}_j), \mathfrak{F}_{\mathfrak{R}'_j})\}$ ,

where  $\mathfrak{R}' = \{\mathfrak{R}_1, \mathfrak{R}_2, \dots, \mathfrak{R}_k\}$ ;  $\mathcal{L}' = \{\mathcal{L}_1, \mathcal{L}_2, \dots, \mathcal{L}_k\}$ ,

$$\mathfrak{R}_1 = \{R_1, R_2, \dots, R_{i_1}\},$$

.....

$$\mathfrak{R}_k = \{R_{i_k+1}, R_{i_k+2}, \dots, R_m\},$$

$$\mathfrak{R}_p \langle \mathfrak{R} \rangle \mathfrak{R}_q; \quad p, q = 1, 2, \dots, k;$$

$$\mathcal{L}_j = \{\mathcal{L}_{l_{R_l}}\}, \quad j=1, 2, \dots, k; \quad l = \{i_{j+1}, \dots, i_j\}.$$

In DMB, functional dependencies can only occur within each of the sets  $\mathfrak{R}_j$ .

This definition of DMB is sufficiently general for other databases and multisets to be presented as its special cases.

Operations such as intersection, union, addition, multiplication, coordination, projection, division,  $\theta$ -connection,  $\theta$ - restriction, defined for RMD, occur in the DMB if the operands and their results do not go beyond the scope of the DMB (or multiset) and under the conditions specified above, which determine the feasibility of operations in the extended RMD. Naming and dereferencing operations, like the previous ones, take place within the framework of one DMB element.

Special operations on DMB are  $\mu$ -decomposition and  $u$ -union operations. The first is intended to convert the database to DMB, the second - to combine several (or all) DMB elements into a single DMB element (or database). The operations of  $\mu$ - decomposition and  $u$ -union can be applied to any data sets that make up the base, i.e. to domain, tuples and relationships. The relation to which the  $\mu$ -decomposition operation is applicable is called multi-relation. Then the database, in which there is at least one multi-relation, can be called DMB. These operations contribute to the implementation of the most important feature of the CUS database - multiplicativity.

CUS implies, on the one hand, the use of databases focused on solving various classes of problems, and on the other hand, their independence from applications and the ability to use the information concentrated in them by many application programs or users. Since the application program or user query language is oriented to a specific DBMS, to exclude the replication of programs (queries) by the number of databases, it is necessary to ensure the exchange of information between them, i.e. their sociability. One of the ways to ensure database interoperability is the introduction of a virtual layer and advanced RMD.

The communicability of the database is also due to the need to provide a mechanism for responding to a top-level request, when the required information is placed in the database at the lower levels of the system hierarchy, which is associated with the exchange of control information at the language level (delegation of the request along the database chain and delivery of the response to the point of the original request). This allows calling CUS interactive, considering dialogue as a special case of such systems.

The flexibility and responsiveness of the database is significantly due to its parametricity. Database parameters can be: the physical amount of memory  $V$ , the response time to requests (responsiveness)  $T$ , the number of elements of DMB  $N$ , the operating mode  $R$ , etc.

In the parametric system of each function of data management or manipulation, which determines the degree of system responsiveness, many algorithms must be compared. In the control graph, the node that implements such a function represents many equifunctional algorithms. Each task in such a column corresponds to a certain chain (path) with many implementation options (due to multi-nodes). The function of the control system is to choose the option of a given fixed path that most closely matches the given value of the responsiveness parameter.

The implementation of the parameters  $V$  and  $T$  substantially determines the type of data model. The performance of the same function in different models can vary significantly in time.

The parameterization mechanism is also used in the construction of dialogue schemes using frames.

The performance of a DMB depends on the structures of the data presented in it. One of the effectively multiplicable structures is a multilayer structure adequate to a wide range of tasks. The reorganization of the multilayer structure is carried out by the generalized operations of joining and splitting, the implementation of which in this case is also greatly simplified.

### Constructing dialogue systems (DS)

The effectiveness of a DS depends not so much on the appropriate technical or software tools for dialogue as on the content of knowledge exchanged between a person and a computer, and the degree to which the language means of the system correspond to the characteristics of the object displayed in its model and the user. These considerations were not the last in the formation of the SBT of the creation of CUS [5].

Highlighting  $\mathfrak{S}$ ,  $\mathfrak{C}$  and  $\mathfrak{M}$ , as well as  $\mathfrak{D}$  and  $\mathfrak{R}$  represents the most important feature of SBT. This is one of the most significant points that determine the orientation of DS to various classes of objects and users, on the one hand, and to the representation of knowledge in the system, on the other. The latter provides, in turn, the adaptability and extensibility of DS due to the unified methods of accumulation and presentation of knowledge from various subject areas. This is achieved through the creation of an integrated model from a set of domain models, served by a single monitor, universal in functions and implementation methods. Such an integrated model consists of two components:  $M_D$  – integrated data model (DB) and  $M_S$  – a set of computational schemes that make up the set of oriented weighted graphs (possibly with multinodes representing equifunctional modules). The nodes of the graph correspond to transitions to subgraphs of a lower level or moments of user interaction with a computer. Frames are used to store information about the graph in the database.

Analysis of the DS structure allows us to conclude that it is possible to implement the functions of the control component  $\mathfrak{C}$  and the means of organizing components  $\mathfrak{M}$  and  $\mathfrak{S}$  in the form of a fairly universal software complex in which three levels of hierarchy can be distinguished: system processes, functional processes, functional program modules.

This module controls the course of the dialogue process in accordance with the structure of a specific dialogue scheme. For each application, a dialogue diagram is compiled that is implemented under the control of a dialogue monitor (DM). As a toolkit, a special set of DS developer programs is used. To create a scheme, its descriptor is set with general information about the dialogue scheme and its parameters (unique name of the scheme, numbers of the initial and final states, sizes of the general area of the scheme parameters, comment text) and state descriptors containing information about the actions performed in this state. The following types of states are possible: control U, information I, information control C, format F, computational V, macrostate M.

### **Submission of knowledge in CUS [1]**

One of the requirements for developed CUS is the availability of means for presenting knowledge in two aspects - the knowledge base as part of the subject area model and as an intelligent interface between the user and the system.

The decomposition of the subject area model mentioned above, which includes, along with the database, a base of relations between data elements and the rules for changing these relations, creates the basis for representing knowledge in CUS as a set of rules. The instant situation containing the current data about the object is replaced by a second-level model in which knowledge about the object is presented, i.e. the relationship between data and the situation, the patterns of change in time and space. It is also necessary to have rules for manipulating them, procedures for using these structures, bearing in mind that rational behavior is peculiar only to a system of information processing elements.

The elements of knowledge, interconnected, form a network. This is a prerequisite for using semantic networks or frame technology to represent knowledge of the apparatus. Frames are the most appropriate mechanisms for presenting knowledge because they can describe not only static objects or situations, but also their changes in time, various actions. Due to the variety of visual means of frames, a number of program synthesis elements can be assigned to the system itself, using the knowledge gained from matching frames with specific objects. This increases the intelligence of the system.

Representation of the dialogue scheme in the form of a system of frame-states along with the representation of knowledge in the structure of the domain model provides ample opportunities for creating hierarchical, distributed according to the scheme, knowledge base in CUS. The addition of their language means of logical inference determines the possibility of constructing various artificial intelligence systems, in particular expert systems.

The SBT for creating CUS also provides appropriate methods and tools for their modeling, interactive multi-data processing and other components [6-7].

### **Referecnes**

1. Khalilov, A.I., Kalantarov, G.A. Technological aspects of creating a shared computing environment with elements of artificial intelligence // *Resp. mix. sci.-tech. coll.* – Kharkov.: Publishing House "Basis", 1990. – Issue 45. – P. 35-42.

2. Khalilov, A.I. On the structural-base model of a parallel-action system // Scientific. journal "Problems of programming." Materials of the 2nd international SPC by program. Kiev, May 23-26 2000. – Kiev: ISS NASU, 2000. - № 1-2, Spec. Issue – P. 122-128.

3. Khalilov, A.I. The method of successive deepening and some of its applications // Coll. "Theory and practice of system programming". - Kiev: RIO IK AN UkrSSR. – 1976. – P. 180-191.

4. Khalilov, A.I. Some issues of database organization in complex automated control systems // J. "Cybernetics". – 1981. - № 3. – P. 40-45.

5. Khalilov, A.I., Shilkin, A.I. About one approach to designing interactive systems for collective use // Automated systems for scientific research of collective use: Coll. sci. work.– M, 1984.– P. 38–44.

6. Khalilov, A.I. About one application of structural-base technology // Materials fifth region. NPK "Computer technologies in science, economics and education. CT-SEE2004". Makhachkala, November 23-25, 2004 – Makhachkala: CPI DGU, 2004. – P. 70-73.

7. Khalilov, A.I. Problems of dynamic parallelization of computations // J. "Cybernetics and systems analysis." – Kiev, publishing house "Scientific thought". - 1997. - № 2. – P. 11-19.

## DEAF SIGN LANGUAGE RECOGNITION<sup>1</sup>

### **Grif Mikhail Gennadievich**

Doctor of Technical Sciences, Full Professor  
Novosibirsk State Technical University, Novosibirsk, Russia

### **Prikhodko Alexey Leonidovich**

Junior Researcher  
Novosibirsk State Technical University, Novosibirsk, Russia

**Abstract.** Communication between hearing people and the deaf through computer sign language systems is a significant problem in any country. In the article, we suggest an original approach to recognize the Russian sign language, based on the notation system for describing any sign language (The Hamburg Sign Language Notation System). Detecting two of gesture components – the shape of the hand and its location – results in building corresponding neural networks. A training dataset for deep learning was created to provide a successful training process of neural networks (the Dataset). An alternative approach based on biologically-inspired neural networks and the prospects of its developing was also considered.

**Keywords:** sign language; gesture recognition; artificial neural network.

### **Introduction**

The 70 million deaf people worldwide who use sign languages (SLs) as their primary language of communication are represented by the World Federation of the Deaf (WFD). According to the 2010 All-Russian Census, the number of signers of the Russian sign language in the Russian Federation is about 120.5 thousand people, but according to other estimates this number is several times larger. Need to develop systems for machine translation of sign languages (From hearing to deaf and vice versa) consists of both insufficient number of sign language interpreters and not always desirable mediation (Medicine, personal relations, etc.) in the communication of deaf and hearing citizens.

---

<sup>1</sup>The reported study was funded by RFBR and DST according to the research project No. 19-57-45006.

An example of a sign language translation system available in the world can be mentioned: HandTalks (Brazil), ProDeaf (Brazil), ViSiCAST (Europe), The American Sign Language Avatar Project at DePaul University (USA) и Surdophon (Russia) [1].

Deaf gestures are characterized by the following components on which the meaning of the gesture depends: palm configuration, palm orientation, gesture location, nature of movement and non-manual component [2, 3].

### **Methods and Related Work**

Overall, there are several criteria for measuring the efficiency of gesture recognition systems: scalability, reliability, real-time performance and user independence [4]. Application of the deep learning techniques that currently show their effectiveness in general visual recognition remains problematic for SLs, due to limited availability of labeled datasets. Compared to speaking languages they are scarce, and for some national sign languages are virtually non-existent<sup>2</sup>. One of the directions of our work involves creation of SL dataset for Russian language, for which we already collected 927 video image files with static one-handed signs (Fig. 1). After converting the video files to JSON using OpenPose library and analyzing 21 points of the right hand's skeletal model (Fig. 2), we obtained the points' selection confidence of 0.61. This accuracy confidence so far remains insufficient to recognize one-handed static gestures, so we are considering other approaches, as described in the current paper.

Accurate recognition of SL is also challenging due to high dynamism, overlaps, etc., so traditional NNs, including the ones based on deep learning methods, have problems accounting for all the possible movement vectors. Hence, lately the recognition based on biosimilar neural networks [5] is gaining increased interest. In the visual cortex of the brain, the motion analysis begins already in the primary visual cortex. In particular, complex cells, acting as the basis for pooling neurons, have detection of elementary movements as the main function. Further, the movement is analyzed sequentially in zones V3 (dynamic form) and V5 (perception of movement). Ultimately, a general motion map is constructed within the visual field.

In [6] they relied on Leap Motion controller for recognizing the signs, and used hand's skeletal model, neural networks and machine learning methods. On average, accuracy of 90% was achieved for the handshake. The histograms approach for detection and localization of the hand is considered a classic [7]. To detect the object, the histograms based on the criterion of color or brightness uniformity are constructed, while for the object localization the histograms are based on the number of bright dots in the image.

---

<sup>2</sup>See a review and comparison of SL datasets at e.g. [https://facundoq.github.io/unlp/sign\\_language\\_datasets/index.html](https://facundoq.github.io/unlp/sign_language_datasets/index.html)

The algorithm for the sign localization proposed in [8] works stably in low lighting, both of the environment (background) and the user's workplace, and allows identification of two-handed gestures (Fig. 3). The transformation of the image into grayscale on the early stages of the localization allows to increase the speed of the processing. Another way for speeding up is to decrease the size of the processed frames.

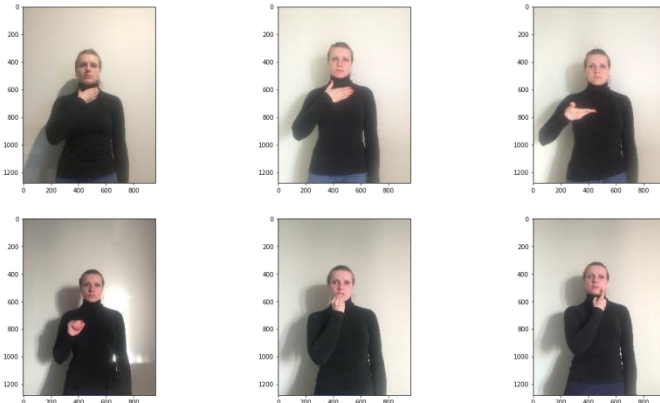


**Fig. 1. Extract from the dataset with one-handed signs we are developing for the Russian SL.**

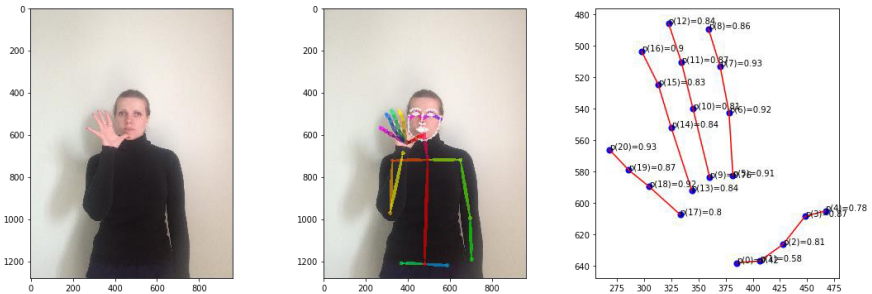


**Fig. 2. The OpenPose detection procedure for assessing the probability (confidence) of choosing 21 points of the skeletal model of finger joints.**

The experiments have shown that for stable localization the image of 256\*256 pixels is enough. The employment of the double removal – of the background and the final frame, the use of the fast localization method for the region of interest on the histograms allows applying the proposed algorithm on both desktop and mobile devices.

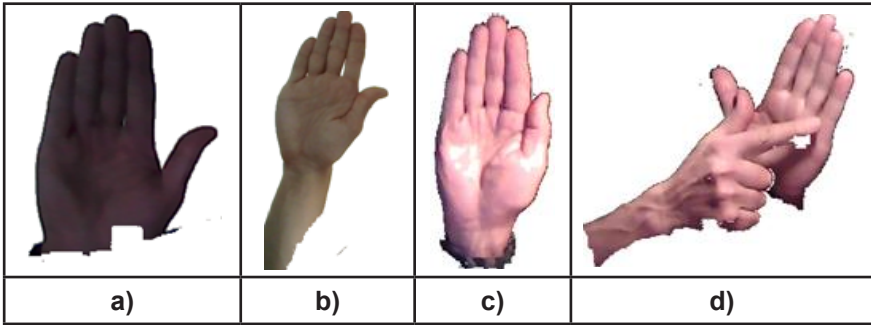


**Fig. 3. Localized images with low lighting (a) and medium lighting (b) of the work area, with low lighting of the background (c) and localization of the two-handed sign showing the number 7 (d).**

**Recognition of palm configuration based on Leap Motion controller**

Our palm recognition method is based on the Hamburg Sign Language Notation System [9].

The handshape recognition is performed in the following steps:

1. Hand tracking using the Leap SDK.
2. Transformation of the hand joints' coordinates into angles.
3. Recognition of the particular handshape.
4. Transcribing to the HamNoSys.

Based on Leap Motion technology [10], 21 joints for the hand and 12 joints for the hand are distinguished (Fig. 4.).

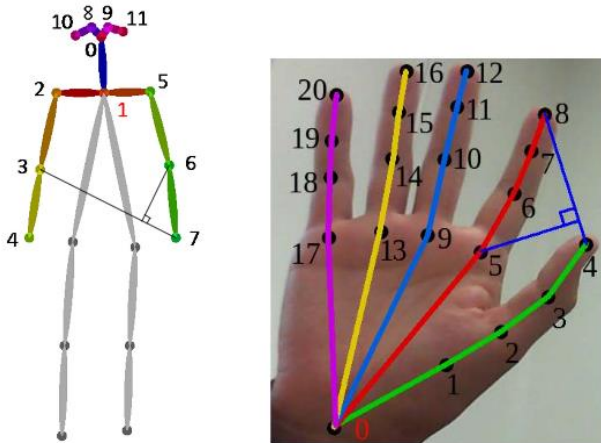


**Fig. 4. The joints' points used in the recognition.**

The experimental validation was done with two groups of 10 subjects each – adults and children. In the first group, consisting of 5 males and 5 females, the age ranged from 21 to 37 (average 28). In the second group, there were 5 boys and 5 girls, aged from 6 to 9 (average 8).

The subjects were presented with 19 handshapes drawn on sheets of paper. They could train the signing for up to 30 minutes before the actual experiment, in which they showed the prescribed handshapes sequentially. The time for identifying each of the handshapes was 1 second, and the software would show the presumably recognized handshape. The software operator was recording the correctness or failure in the recognition. Each subject had 3 trials for each of the 19 configurations. The recognition accuracy was calculated as the ratio between the number of correct recognitions to the total number of trials. The accuracy for the adult group in the experiment was 98.9%, while for the children group it was only 76.4%.

We believe the difference in the accuracy was due to lower clarity and higher variability in handshape signing in children.

### **Recognition of the Sign Location Based on OpenPose Library**

In our work, to recognize the location of the gesture, we used the OpenPose library, which is intended for 2D-determination of key points of a person's arm and body in real time.

The coordinates of the key points of the hand are separated from the original image, which are then translated into notations HamNoSys. As a result, we have a component of the location of the gesture (Fig. 5).

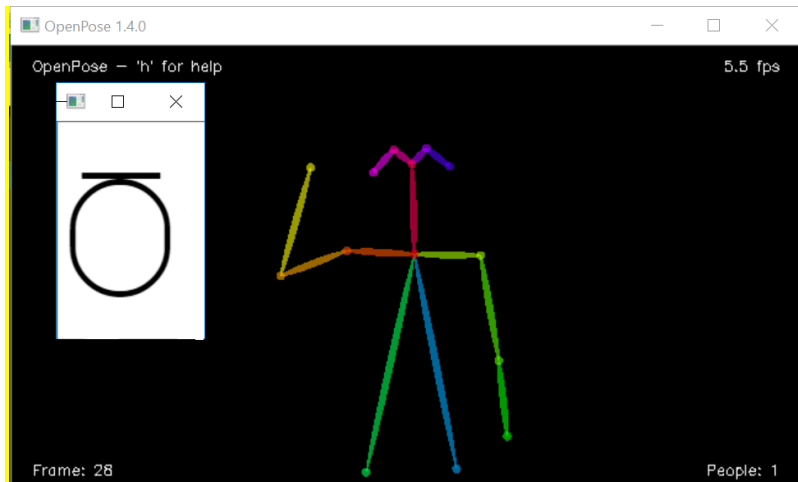


**Fig. 5. Recognition of the sign located at the face level.**

We further performed experimental validation of the sign location recognition. There were 5 possible locations: at the face level, left shoulder, right shoulder, chest, and stomach. There were 8 subjects (4 males, 4 females), with the age ranging from 21 to 34 (average 26). The subjects were presented with the 5 possible sign locations drawn on the sheets of paper, and they had up 10 minutes for the training. After that, they would make the signs in the specified locations, and each sign was fixed for 1 second. The software output the presumable location, and the operator would record the correctness or failure of the recognition. The number of trials for each subject and each of the 5 locations was 3. The accuracy in the experiment, calculated as the ratio between the number of correct recognitions to the total number of trials, amounted to 88%.

### Conclusions

In this paper, we suggested an approach to recognition of the sign language, based on combining the notation system for sign languages (HamNoSys) and the deep machine learning. The example of recognizing the two of gesture components was presented. Neural networks were built to recognize the shape of the hand by the Leap SDK, and the location of the gesture was detected by the OpenPose library and a 2D camera. A special training dataset was formed for the successful training of neural networks by the techniques of deep learning. An experimental verification of the quality of the hand shape recognition showed the probability of correct recognition at 98.9% for the adults and a little less accuracy (76.4%) for children. Recognizing the location of the gesture provided the 88% accuracy. An alternative approach based on the biologically-inspired neural networks and the prospects of designing this kind of networks was also considered.

### References

1. Grif M.G., Prihodko A.L. Approach to the Sign language gesture recognition framework based on HamNoSys analysis //Actual problems of electronic instrument engineering (APEIE–2018) : proc. [progr. and abstr.], Russia, Novosibirsk, 2–6 October 2018. – Novosibirsk, 2018. – V. 1, part 4. - P. 426–429. - ISBN 978-5-7782-3615-8. - DOI:1109/APEIE.2018.8545086.
2. Kendon A. Current Issues in the Study of Gesture. The Biological Foundation of Gestures: Motor and Semiotic Aspects. Lawrence Erlbaum Associate, 1986, pp. 23-47.

3. Al-khazraji S. et al. Modeling the speed and timing of American Sign Language to generate realistic animations //In Proc. 20th International ACM SIGACCESS Conference on Computers and Accessibility, 2018, pp. 259-270.
4. Rautaray S.S., Agrawal A. Vision based hand gesture recognition for human computer interaction: a survey. *Artificial Intelligence Review*, 2015, 43 (1), pp. 1–54.
5. Kugaevskikh, A.V, Sogreshilin, A.A. Analyzing the Efficiency of Segment Boundary Detection Using Neural Networks. *Optoelectronics, Instrumentation and Data Processing*, 2019, 55(4), pp. 414-422.
6. Du Y., Liu S., Feng L., Chen M., & Wu J. Hand Gesture Recognition with Leap Motion. arXiv preprint arXiv:1711.04293, 2017.
7. McKenna S., Gong S. Gesture Recognition for Visually Mediated Interaction using Probabilistic Event Trajectories //Proc. of BMVC'98, Southampton (England), 1998, pp. 498-508.
8. Grif M.G., Lukoyanychev A.V. Gesture localization in the test mode in the integral system of sign language training. *Journal of Physics: Conference Series*, 2019, 1333, Art. 032023.
9. Hanke, T. HamNoSys – representing sign language data in language resources and language processing contexts //In Workshop Proceedings Representation and processing of sign languages (LREC), Paris: ELRA, 2004, pp. 1-6.
10. Simon T. et al. Hand Key-point Detection in Single Images Using Multiview Boot-strapping //Proc. IEEE Conf on Computer Vision and Pattern Recognition, 2017, pp. 4645-4653.

## NEW INFORMATION ABOUT THE USE OF SHELLS WITH TANGENTIAL DEVELOPABLE MIDDLE SURFACES

**Olga O. Aleshina**

Civil Engineering Ph.D student

Peoples' Friendship University of Russia (RUDN University)

Today, shells with developable middle surfaces are widely used in architecture, civil, industrial and road construction, mechanical engineering and instrument making, aircraft construction, rocket and ship building, textile industry, and sculptural compositions. Due to the ability to be developed on a plane by all points of the surface without folds and breaks, while keeping the length of curves and the angles between any curves belonging to the surface unchanged, developable surfaces are used for approximating complex surfaces, thereby contributing to their even greater use in all areas of human activity. The study of torse shells at the Peoples' Friendship University of Russia (RUDN University) has been conducted since 1963. The scientists of the RUDN University have obtained great results in the field of setting developable surfaces with analytical equations, in the section of moment and membrane (momentless) calculation theories, methods of design of surface developments, replacing complex surfaces with developable surfaces, and parabolic bending of torsos.

**Keywords:** developable surface, equal slope shell, torse, architecture, sculpture, aircraft, shipbuilding, textile industry, agricultural engineering

### Introduction

The design of large-span spatial structures in modern architecture and construction has become possible due to the appearance of thin-walled shells in combination with the rational use of materials and the advent of numerical methods for calculating strength. Having various advantages, certain forms of shells are also used in many areas of industry and production.

Most technical products and elements are described and modeled by analytical surfaces. To simplify the manufacturing process of such products, these surfaces are approximated by the simplest surfaces, in particular torse shells, which can be developed on a plane without folds and

breaks. Numerous methods of designing developable structures and products allow you to give them the necessary shape with the specified engineering requirements [1].

When cutting thin-walled developable products, previously, the methods of descriptive geometry were mainly used. Now modern computer programs are used. The monograph [1] provides seven analytical methods of design of surface developments.

### **Application of developable surfaces and shells**

Today, the problems of applying the obtained theoretical results in architectural, construction, machine-building practice and in other branches of human activity are widely discussed. The most interesting suggestions for the use of developable surfaces are contained in [2-5].

In the aviation industry, due to the simplicity of formation, shells in the form of developable surfaces are used when specifying complex surfaces of segments of the outer skin of aircraft. The most commonly used method is to construct developable surfaces by moving a straight line along two original guide curves. Free bending is one of the most effective ways to shape the skin panels. This technology is used as an independent process for bending panels, and for editing workpieces.

In shipbuilding, torse shells are used in the design of hull contours. Developable surfaces are of particular interest to builders of boats and yachts made of plywood, since the effort required to form the torse shells is less than in the manufacture of surfaces of double curvature.

In agricultural engineering, the developable surface in the form of an open helicoidal shell is widely used as devices for transporting bulk, straw and semi-liquid cargo (Fig. 1).



**Figure 1. Application of developable surfaces in agricultural engineering**

Degenerate developable surfaces (cones, cylinders) are widely used in the design and manufacture of various pipelines for the oil and gas and chemical industries, for cotton processing and cotton gin enterprises. The developable surface in the form of an open helicoid is found in drilling machines, in screw conveyors intended for transporting grain, flour, feed and other bulk products in technological lines at grain processing and feed mills.

Developable surfaces are used in a wide range of industries, including the textile industry in the production of clothing and footwear [5]. The use of developable surfaces for cutting clothing is considered in many works, including [6]. Also, in the fashion industry, geometric methods for design developments of undevelopable surfaces using a torse shell are proposed for designing clothing products.



**Figure 2. Walt Disney Concert Hall), Anaheim, United States**

In modern architecture, the use of developable surfaces is demonstrated in a number of developed projects and implemented structures. There are proposals for the use of torse shells for covering the building of repair and mechanical workshops, for overlapping an arbitrary quadrangular plan with parabolic arches at the ends as guide curves, or for a shell with the ends in the form of two inclined flat parabolas [1]. The most famous architects of our time are Frank Owen Gehry (Fig. 2), Hans Hollein, Santiago Calatrava and Zaha Hadid used the developable shape when creating their projects. The article [4] describes examples of using developable surfaces in modern architecture. In [7], the influence of surface shape on the creation of unique structures is studied, and examples of the use of

developable surfaces are given. The project of the awning of developable surface shape is proposed in [8].

Design of spatial structures in the form of torse shells in architecture and construction is simplified in some cases due to the possibility, for example, to use rolled or flat reinforcement mesh for reinforcement of reinforced concrete shells, and to perform formwork in the same way as for planar elements of structures made of straight or sheet elements that can be made directly on the site of construction of a building. However, no real reinforced concrete structures in the form of developable surfaces have been found in the technical literature [9].

### Geometric research of developable surfaces

The study of the geometry of developable surfaces begins in 1805 after the publication of the book by G. Monge "Application of analysis to geometry". In total, there are 10 ways to design developable surfaces [1] and all of them are based on the positions put forward by G. Monge.

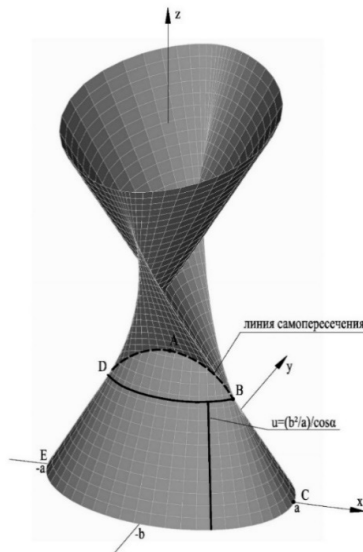


**Figure 3. Developable surface of the equal slope with a guide ellipse at the base**

The most recent work devoted to the study of the geometry of a particular case of a developable surface, namely the equal slope shell with

the director ellipse, is an article by O. O. Alyoshina [8], (Fig. 3). Interesting regularities have been established for the construction of this class of surfaces depending on the geometric parameters of the guide ellipse at the base and the angle of inclination  $\alpha$  of the rectilinear generators  $u$ . The law of setting a flat curve ( $D-A-B$ ) obtained at the self-intersection of rectilinear generators  $u$  is also defined. It is established that this flat curve is a hyperbola.

Information about earlier studies of developable surface geometry can be obtained from the monograph [1] and from the article [3].

### **Membrane (momentless) and moment theory of developable shell calculation**

The most complete information on this section is contained in [1, 3, 10]. The results obtained in these works were supplemented and analyzed in other works of researchers from the RUDN University [8, 11, 12, 13, 14].

In [15], we compare the results of calculating the torse shell of the equal slope with the director ellipse on the results obtained by the finite element method and the variational-difference method when the director ellipse is rigid fixed. The advantages and disadvantages of each method are identified. The use of the SCAD Office computer system based on the finite element method is more versatile than the variational-difference method for solving complex spatial structures. However, the results obtained in some nodes of the shell turned out to be more correct when solving the variational-difference method.

### **Conclusion**

The author sees great resources for the use of developable surfaces that have undeniable positive properties in architecture, construction, and engineering, and suggests that we look at the great potential for creating interesting and unusual forms of structures, buildings, and small architectural forms from developable surfaces and compositions of these surfaces. The class of developable surfaces is extensive, including cylindrical, conical, and torse shells. Currently, the technical literature describes 24 developable surfaces of general appearance and 10 developable surfaces of the equal slope [1]. The most complete information for understanding the nature of geometry, on the research of the stress-strain state and on the use of developable shells, the interested reader will find in the works from the literature list. It should be noted that among the torse products, the most popular is the open helicoid, which is devoted to many works, such as on geometry, for example, [1, 7, 11, 16], so and according to its calculation on durability [1, 13].

## References

1. Krivoshapko S N 2009 Geometry of Ruled Surfaces with Cuspidal Edge and Linear Theory of Analysis of Torse Shells: Monography (Moscow: Peoples' Friendship University of Russia Press) 357 p (in Russian)
2. Lawrence Snežana. Developable surfaces: their history and application. Nexus Network Journal, 2011, 13 (3): 701-714.
3. Sergey N. Krivoshapko, Iraida A. Mamieva, Andrey D. Razin. Tangential Developable Surfaces and Shells: New Results of Investigations// Journal of Mechanics of Continua and Mathematical Sciences. – March 2019. – Special Issue – 1. – Pp. 324-333 [DOI: <https://doi.org/10.26782/jmcms.2019.03.00031>].
4. Glaeser Georg, Gruber Franz. Developable surfaces in contemporary architecture. Journal of Mathematics and the Arts, Vol. 1, Issue 1, March 2007, pp. 59-71.
5. Chen Ming, Kai Tang. A fully geometric approach for developable cloth deformation simulation // The Visual Computer. 2010. Vol. 26 (6–8). Pp. 853–863.
6. Ito Miori, Imaoka Haruki. A method of predicting sewn shapes and a possibility of sewing by the theory of developable surfaces // Journal of the Japan Research Association for Textile End-Uses. 2007. Vol. 48. No 1. Pp. 42–51.
7. Mamieva I.A. (2019). Influence of the geometrical researches of ruled surfaces on design of unique structures. Structural Mechanics of Engineering Constructions and Buildings, 15(4), pp 299–307.
8. Aleshina O.O. 2019 Studies of geometry and calculation of torse shells of an equal slope Structural mechanics and analysis of constructions. № 3 pp 63-70.
9. Krivoshapko S.N. Perspectives and advantages of tangential developable surfaces in modeling machinebuilding and building designs. Vestnik grazhdanskikh inzhenerov – Bulletin of Civil Engineers, 2019, no. 1 (72), pp. 20–30.
10. Krivoshapko S N 2018 The application, geometrical and strength researches of torse shells: The review of works published after 2008 Structural Mechanics and Analysis of Constructions № 2 pp 19-25
11. Krivoshapko S. N. and Rynkovskaya Marina. Five types of ruled helical surfaces for helical conveyers, support anchors and screws// MATEC Web of Conferences. – 2017. – Vol. 95 (2016 the 3<sup>rd</sup> International Conference on Mechatronics and Mechanical Engineering (ICMME 2016)). - 5 p. (DOI: <http://dx.doi.org/10.1051/mateconf/20179506002> ).

12. Filipova J. (2016). Comparative analysis of the results of calculation of a thin shell in the form of carved surface of Monge with an application of membrane (momentless) theory and finite element method. *Structural Mechanics of Engineering Constructions and Buildings*, 3, pp 8-13.

13. Rynkovskaya M. (2017). Analysis of displacements in beam structures and shells with middle developable surfaces. *MATEC Web of Conferences "ICMAA 2017"*, 108, 16001: 4 p.

14. Krivoshapko S.N., Timoshin M.A. (2012). Static stability analysis of an elliptic shell of equal slope, two conical shells with the director ellipse and a torse with two ellipses placed in parallel planes. *V Int. Scientific and Practical Conference "Engineering System - 2012": Proc., Moscow: RUDN, April 16-18: 40-46.*

15. Ivanov V.N., Alyoshina O.O. (2019). Comparative analysis of the results of determining the parameters of the stress-strain state of equal slope shell. *Structural Mechanics of Engineering Constructions and Buildings*, 15(5), 373–382. <http://dx.doi.org/10.22363/1815-5235-2019-15-5-373-382>. (In Russ.)

16. Krivoshapko S.N. Geometry and strength of general helicoidal shells// *Applied Mechanics Reviews (USA)*. – Vol.52. – No 5. – May 1999. – P. 161-175.

## TECHNOLOGICAL PROVIDING OF SURFACE LAYER PERFORMANCES OF PARTS DURING THE MACHINING

**Sutyagin Aleksandr Nikolaevich**

Candidate of Technical Sciences, Associate Professor

Dean of the Faculty

P.A. Solovyov Rybinsk State Aviation Technical University

**Summary.** The article describes the problem of friction unit surface layer parts wear resistance assurance based on control of geometrical and physic mechanical properties to be formed the machining. Also paper presents operation of a newly-developed software providing visualization of topography of a machined surface on the basis of ISO 25000 standard and taking into account physical and mechanical properties of material, as well as changes in the surface during running-in.

**Keywords:** friction, wear, surface layer, performances, machining

### Introduction

Mechanical engineering and aviation industries use various technological methods to ensure predefined performances of surface quality of parts taking into consideration the required operating conditions, including heating temperature, operating loads, environment, duration of different processes. For example, surface roughness determines not only fatigue strength and durability, but it is interrelated with mechanical properties of various surface layers. To ensure the predefined surface quality parameters of an item and thus the performances of machine parts, finishing stages of machining include so-called optimal cutting modes that provide not only minimal wear rate of the cutting tool, but also maximum value of fatigue strength and wear resistance of the parts.

Machine components' wearing is characterized by destruction of contact surface layers. Physical, chemical and fatigue processes occur in these layers as a result of parts mating surfaces interaction. Wearing phenomena has accumulative character and grows out of repeated accumulation of damages, thus the wear resistance is rather sensitive to insignificant changes of materials properties.

The normal operation of a unit is characterized by the minimal wear rate of the material and the simultaneous forming of balanced roughness and rate of the mechanical hardening of a surface layer of machine components [1-5]. Duration of break-in period of interfaced machine components depends upon the difference between the initial quality parameters and optimal parameters of the surface layer.

Operation of metal cutting equipment under the optimal condition of machining ensure regular profile of surface pattern, thus allowing obtaining minimal values of wear intensity in mating machine parts [6]. Thus, setting certain technological conditions of machining ensure the best values of several performance characteristics of machine parts at the same time.

### Theoretical part

Since 2016, alongside existing standards GOST 25142-82, GOST 2789-73, new standards GOST R ISO 4287-2014 and GOST R ISO 25178-2-2014 have been introduced in Russia that define regulated three-dimensional parameters of surface roughness. Besides, the rough surface may be represented as a Fourier space including parameters that characterize the machining process and tool geometry [7].

Consider a square wave  $f(x)$  of length  $2L$ . In the range  $[0, 2L]$ , this can be described by an expression of the form (1)

$$f(x) = 2[H(x/L) - H(x/L - 1)] - 1, \quad (1)$$

where  $H(x)$  is the Heaviside function,  $x$  is the argument, and taking into account that the formation of the transverse roughness depends on the radius at the vertex  $r$  of the cutting tool, the angles in the plan  $\varphi$  and  $\varphi_1$ , the feed  $S$ , the cutting depth  $t$ , the cutting forces  $P_x$  and  $P_y$ , the cutting zone temperature  $\theta_p$ , for the function of transverse roughness for turning (2)

$$f_1(x) = F(t, P_x, P_y, r, \varphi, \varphi_1, \theta_p, S, x). \quad (2)$$

In addition to the transverse roughness, there is a longitudinal roughness measured in the direction of the cutting speed due to the oscillations of the technological system, as a consequence of the rigidity of the technological system  $j$ , as well as the cutting speed  $v$ , the front  $\gamma$  and the posterior  $\alpha$  angle of the cutting tool, cutting forces  $P_z$  and  $P_y$ , temperature in the cutting zone  $\theta_p$ . In addition, the longitudinal roughness can be influenced by errors associated with the wear and tear of equipment, for example, the spindle of the machine.

Longitudinal roughness can be represented by a pseudo-random number algorithm that is based on the Box-Muller transformation or described by the transition function to the general normal distribution after obtaining the standard normal random profile value, which allows the generation of a normal random variable to be completed.

In this case, for the longitudinal roughness function for turning (3)

$$f_2(y) = F(j, P_z, P_y, \gamma, \alpha, \theta_p, v, R, \sigma, z, y) \quad (3)$$

where  $z$  is the surface roughness value due to the action of random factors,  $\sigma$  is the intensity of the impact of random factors on the longitudinal roughness, or after the transformation,  $R$  is the radius of the workpiece.

By varying the parameters of these equations, one may describe the regularities in profile formation after lathe turning with sufficient accuracy and obtain its mathematical model. Such an approach served as a foundation for developing a software solution (Certificate of state registration of software no. 2017614676), allowing calculating the coordinates of the surface points of a part processed with lathe turning (Fig. 1), as well as plotting the spectrogram of the surface roughness (Fig. 2).

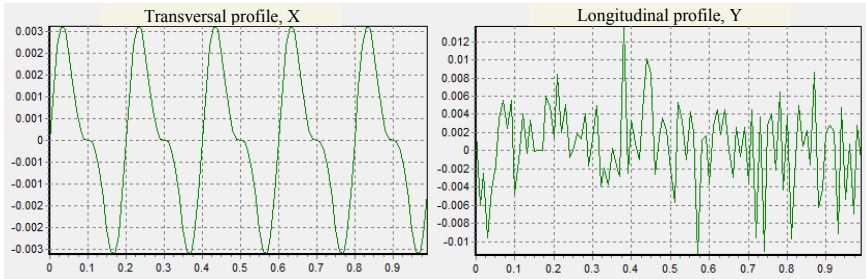


**Figure 1. An example of using the developed software**

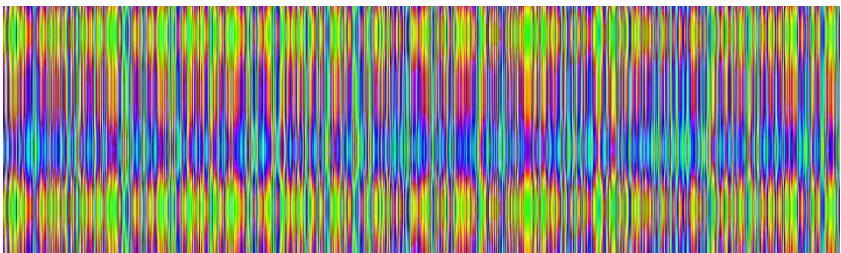


**Figure 2. An example of plotting the spectrogram of the surface roughness**

Basing on the proposed methodology of the mathematical description of the profile, 3D models of surface after lathe turning were created and their interaction (contact) was modeled with the help of a Finite Element Method-based system. The profiles were modeled for various processing modes:  $v = 41$  m/min,  $t = 0.5$  mm,  $S = 0.2$  mm/rev made of 20Cr13 according to GOST 5632-72 with a hardness of 330HV.

The testing was conducted at a rubbing velocity of 0.08 m/s and a normal load of 9.81 N. The design model is shown in Figure 3.

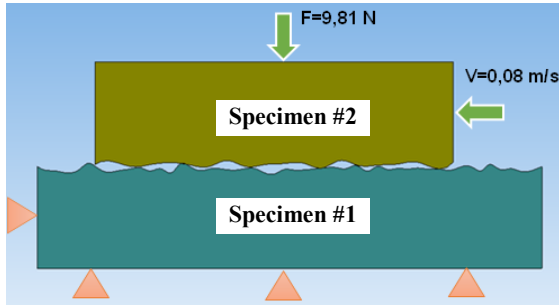


**Figure 3. A design model of contact interaction between the specimens for analysis with the Finite Element Method: F is a normal force, V is a rubbing speed, specimen 1 is still, specimen 2 is moving**

At the first stage of modeling, the contact interaction between two surface profiles, the number of contact areas was predicted and their locations as the profiles are closing. Then, a calculation was performed in accordance with the loading diagram shown in Figure 3, that resulted in obtaining the deformation distribution pattern when the profiles come into contact (Figure 4).

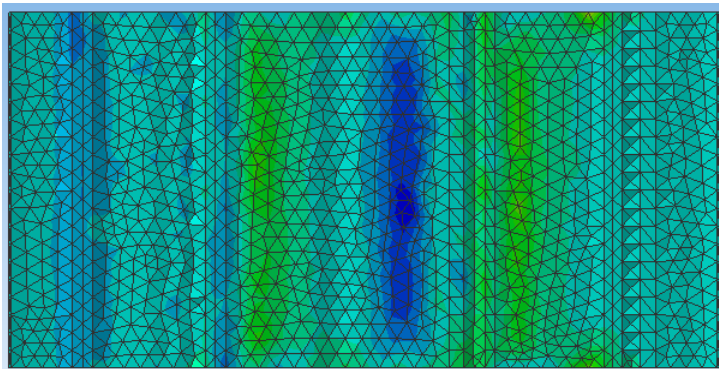


**Figure 4. Deformation distribution pattern after running-in of the specimen profiles**

### Experimental part

From analysis of Figure 4, one may conclude that after running-in, the contact interaction pattern became more uniform. The number of areas with a pinpoint contact reduced, while the number of areas with a larger contact area increased (flat contact areas).

The experiments were conducted in the laboratory of the Department of Aircraft Engines and General Engineering, P.A. Solovyov Rybinsk State Aviation Technical University with the help of a T-11 friction machine. In the figure, you can see picture of the second specimen after running-in, as well as the results of modeling the run-in surface with the equations 2 and 3.

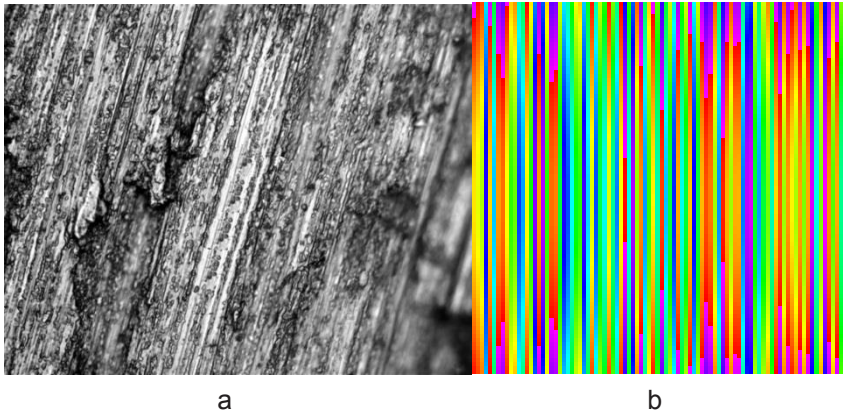


**Figure 5. Picture of the specimen surface after running-in (magnified x40) (a) and spectrogram of the run-in surface obtained with the equations 2 and 3 (b).**

Based on the foregoing, it is possible to present an algorithm for calculating the equilibrium 3D roughness in the following form (Figure 6).

As initial data the conditions of operation of parts in the friction unit, the physical and mechanical properties of the materials of the mating parts are taken into account. The calculation of the parameters of the equilibrium roughness can be performed using the dimensionless Kragelsky-Kombalov criterion. Based on the calculated value of the parameter of the equilibrium roughness and the geometry of the working surfaces of the parts, a choice is made of the processing method: turning, milling, grinding etc. Next, the longitudinal and transverse surface roughness functions are calculated from equations (2) and (3). Calculation of technological processing

conditions is performed on the basis of known design dependencies for selected methods of surface treatment of the workpiece. Depending on the method and processing modes, recommendations for choosing lubricant-cooling agent are offered.

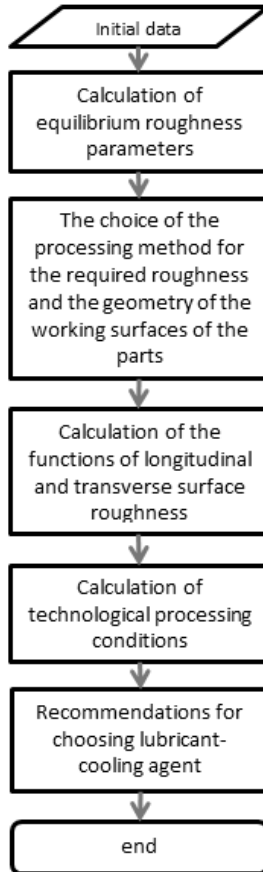


**Figure 6. Algorithm for calculating the equilibrium 3D roughness**

### Conclusion

Using the Finite Element Method has allowed finding the contact interaction area, the values of deformation and stresses in the contact zone, load distribution patterns along the surface, the value of contact closing and a number of other parameters.

The developed software solution allows calculating the longitudinal and transversal roughness of items produced with lathe turning according to GOST R ISO 4287-2014 and GOST R ISO 25178-2-2014, which are created on the basis of ISO 25000 international standard. It allows for fast import of data into any top-level CAD systems for subsequent plotting and analysis of a 3D rough surface.

The developed algorithm of treatment conditions calculation providing of machine components surface layer wear resistance allows technologist in the processing design stage to determine machining conditions providing forming of the balanced geometrical and physic mechanical properties of machine components surface layer permitting to reduce running-in time of machine components.

### References

1 A. G. Suslov, A. M. Dalsky: Nauchnye osnovy tehnologii mashinostroeniya (Scientific Basis of Mechanical Engineering), - Mashinostroyeniye, Moscow, 2002.

2 A. V. Chichinadze, E. D. Brown, N. A. Boucher: Osnovy tribologii (treniye, iznos, smazka) (Fundamentals of tribology (friction, wear and lubrication)), - Mashinostroyeniye, Moscow, 2001.

3 V. S. Kombarov: Ocenka tribotekhnicheskikh svoystv kontaktiruyushchih poverkhnostey (Evaluation of tribological properties of contacting surfaces), - Nauka, Moscow, 1983.

4 V. S. Kombarov: Ocenka tribotekhnicheskikh svoystv kontaktiruyushchih poverkhnostey (Evaluation of tribological properties of contacting surfaces), - Nauka, Moscow, 1983.

5 A. G. Suslov: Inzheneriya poverkhnosti detaley (Part surface engineering), Mashinostroyeniye, Moscow, 2008.

6 V. F. Bezvazychny: Method of Similarity in Engineering technology, - Moscow: Mashinostroyeniye, 2012.

7 A. N. Sutyagin: Developemtn of a 3D model of surface roughness for items produced with lathe turning. Reference. Engineering Journal with Supplements, 2017, 8 (245) 22-26.

## PLASTICIZATION OF COLD-ROLLED LOW-CARBON STEELS BY EPILAMIZATION OF THE SURFACE

**Doshchechkina Iryna Vasilievna**

Candidate of Technical Sciences, Associate Professor

**Lalazarova Nataliia Alekseevna**

Candidate of Technical Sciences, Associate Professor

Kharkiv National Automobile and Highway University

**Abstract.** The influence of surface epilamization on the deformation behavior of products and their mechanical properties has been studied. A significant increase in technological ductility and improvement of stampability of low-carbon thin-sheet cold-rolled steels due to a significant reduction in roughness and “healing” of surface defects has been proved. A significant advantage of epilamization is the increase of technological plasticity not due to the weakening of the sheet, but on the contrary, with an increase in the actual resistance to destruction.

**Key words:** cold-rolled steel, thin sheet, epilamization, surface roughness, strength, ductility, tensile, stamping, ability to stretch.

### Introduction

World production of sheet and strip is constantly growing, occupying more than 70% of total steel production, of which thin sheet and strip constitute a significant part. Further development of the main branches of mechanical engineering and construction, as well as production of household appliances show that consumption of this type of rolled iron will only increase and the range of areas of its application will obviously expand. This, in turn, stimulates the intensive introduction of new technologies in manufacturing products from more technological steels, which will improve their quality, ensure significant energy and resource-saving effect and reduce costs.

A significant part (up to 90%) of cold-rolled sheet metal is processed by cold stamping methods, which make possible to obtain a varied in forms and accurate in size products with significant savings in me

In the automotive industry, sheet metal stamping has become the most widespread both in the range of products and in their number. It is impossible to imagine the design of any car or lorry without this production process.

Modern automatic high-performance lines of cold stamping of products from cold-rolled steel sheet billets require high plasticity, deep and complex stretching due to the complexity of the geometric shape of the stamped parts. At the same time, increasing level of operational requirements implies the need to maintain the strength of steel after stamping. However, increasing the strength of the rolled product causes reduction in its technological ductility, and thus significantly impairs stamping [1]. In this regard, developing new methods of processing rolled steel, which combine these conflicting requirements and improve the properties of steel is topical.

### Status of issue

At the stage of sheet production, its technological plasticity depends on the chemical composition of steel and the mode of recrystallization annealing: the less carbon and impurity atoms in steel, and the lower the yield strength  $\sigma_{0.2}$  after annealing, the higher the plasticity [2]. Recrystallization annealing of cold-rolled steel completely removes hardening, the metal acquires an equilibrium structure, and its plasticity is restored. However, the attenuating treatment of cold-rolled steel takes time, requires special equipment, and significant power costs.

Recently, new steels (TRIP (transformation induced plasticity steels), DP (dual phase steels), etc.) of high strength with sufficient ductility and constant capability of stamping have been developed and are increasingly used, especially in the automotive industry [3]. To obtain modern high-strength (High-strength steels, HSS; Advanced-high-strength steel, AHSS) and high-quality steels a set of complex problems must be solved that are associated with determining and creating conditions for optimal chemical and phase composition, microstructure at each stage of a complex process (thermomechanical processing, controlled rolling, micro-alloying), which requires significant financial costs to improve and develop steel-making technologies. Such steels must certainly be used, for example, for the elements of the power frame of machines. The parts, that are not subject to significant loads and require deep and complex stretching during stamping, are made of mild steels of grades 08кп (analog of 1449-1HR, 1HR, 2HR, DC01, DD13) or 08ЮА (DC 04 / FeP 04 HR 1 HR 2), which is stabilized by aluminum.

Quite often in the practice of automotive industry there is insufficient stampability of sheet billets, which leads to significant economic losses, because there have not been any methods to improve the ability to stretch the finished sheet so far. This determines the relevance of finding new solutions to solve this important problem.

Based on theoretical and experimental research in the field of modern materials science, it is proved that the state of the surface layer of a deformed body is a functional independent subsystem and radically affects the level of its plastic flow and properties [4,5]. Guided by this, the paper investigates the effect of epilamination (EP) of the surface of steel sheet billets on their deformation behavior and the formation of properties. EP [6] is one of the modern types of nano-coatings, which are widely used to reduce friction and wear of contact surfaces, increase the stability of cutting tools and stamping equipment, protect metal surfaces from corrosion [7,8]. There is no information though concerning the impact of EP on the technological properties of steel and on the deformation behavior of steel products and their mechanical characteristics.

### Tasks and objectives

The aim of the work is to increase the technological plasticity while maintaining the strength of cold-rolled low-carbon sheet steel billets by surface EP.

The following tasks were set in the work: 1 – to investigate the effect of EP on the deformation behavior and properties of sheet steel in tension; 2 – to determine the effect of surface EP on the deformability of sheet billets that will be subject to cold stamping.

### Material and methods of research.

The experiments were performed on the sheet low-carbon cold-rolled steels 20 (rolled thickness 1.2 mm) and 08кп (thickness 0.5 mm). The surface of the sheet samples in the state of delivery was covered with a nanosized monomolecular film of epilam – fluorine surfactant (fluorine surfactant) – by immersion in the bath with epilam for 10 min at a temperature of 50 - 55 ° C. Roughness and surface profile were measured using a profilometer-profilograph with the analyzer sensor whose sensitivity allowed to estimate the topography of the surface from 0.005  $\mu\text{m}$ . Mechanical characteristics were determined during the tensile test of flat samples with a working part size of 80×12.5×1.2 mm. The ability to stretch was evaluated on the samples of size 50×50×0.5 mm according to the results of Eriksen tests.

### The main results of the research

Fig. 1 shows the curves “stress  $\sigma$  - deformation  $\varepsilon$ ” of steel 20 samples in the initial state and after EP. The values of the mechanical characteristics are given in Table 1.

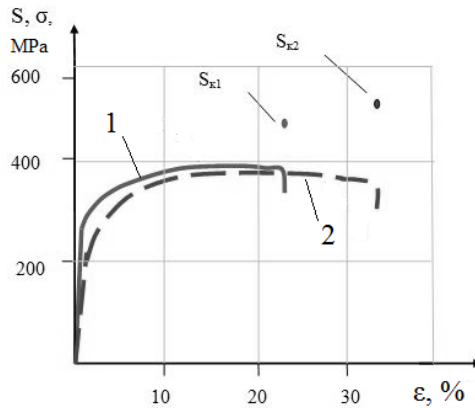


**Fig. 1. Dependence “stress  $\sigma$  - deformation  $\epsilon$ ” for steel 20 samples:  
1 - before EP; 2 - after EP**

The research results show that EP with a relatively slight decrease in strength characteristics ( $\sigma_B$ ,  $\sigma_{0.2}$  decrease by 4% and 9%, respectively) leads to a significant increase in plasticity: relative elongation by 44% and relative narrowing by 57%. At the same time, the actual fracture stress  $S_k$  due to extremely high plasticization increases by 12.5%. Thus, the true strength of the sheet billets after the surface EP is higher than that of the sheet in the state of delivery.

**Table 1– Mechanical characteristics of steel 20 samples before and after EP**

State	$\sigma_B$ , MPa	$\sigma_{0.2}$ , MPa	$S_k$ , MPa	$\delta$ , %	$\gamma$
Without EP	375	290	480	25	21
After EP	360	265	540	36	33

It should be noted that the hardness of the sheet remained unchanged (before EP HV5 = 130 - 133 MPa, after EP - 129 -132 MPa). This indicates that the change in properties after surface treatment by EP is not associated with the characteristics of the material, but with a change in the behavior of sheet samples during deformation, which clearly illustrate the tensile curves in Fig. 1.

As is known, the deformability of the product significantly depends on the roughness of its surface. In the initial state, the sheet had a high roughness –  $R_a = 1.6 \mu\text{m}$  (Fig. 2, a). EP significantly reduced the roughness to  $0.21 \mu\text{m}$ . Against the general smoothed background only insignificant separate buckles are registered (fig. 2, b).

Surface smoothness is also well illustrated by the study of surface scanning using an electron microscope (Fig. 3).

This striking change in the state of the surface is explained by the fact that the epilam has a low surface tension, due to which it flows into the smallest surface irregularities and “cures” surface defects (cavities, submicroscopic cracks, pores), which prolongs the stage of elastic-plastic deformation of metal.

Significant improvement of the surface condition and significant effect of plasticization of samples should affect the quality of stamping. To confirm this, a steel sheet made of steel 08кп and 0.5 mm thick after EP was tested for extrusion by the Eriksen method. The results are given in Table 2. It should be noted that after EP of steel 08кп the depth of the hole during extrusion even exceeds the requirements of the category Extremely Complicated Stretching (SCS) for steel 08YUA, which has less carbon and harmful impurities (especially oxygen).

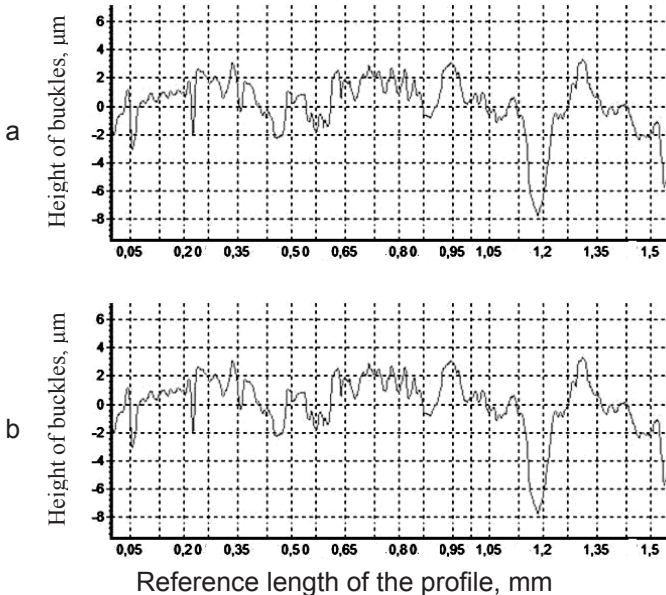
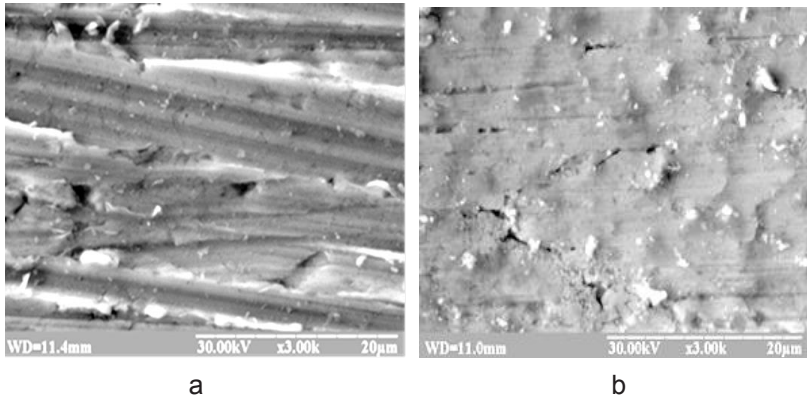


Fig. 2. Profilograms of steel 20 samples: a - initial state; b - after the EP



**Fig. 3. The surface of the samples of steel 20 after various treatments: a - grinding (initial state); b - EP**

**Table 2 - Test data for extrusion of steel sheet 08kp**

State	Hole depth, mm	Stretching category
Initial before the EP	9,05	Very Deep Stretching (VDS)
After the EP	11,85	Extremely Complicated Stretching (SCS)

This very significant improvement in the capability of steel for such a complex stretching will dramatically increase the efficiency of the process of its cold stamping – reduce the number of transitions, reduce the cost of stamping tools, increase the process productivity. At the same time, we should expect improvement of products quality, appreciable reduction of flaws and considerable economic effect. The recommended method of plasticization of cold-rolled thin-sheet low-carbon steel is protected by patents [9].

### Conclusion

1. When sample surfaces were tested for tensile, their EP significantly increased the plasticity characteristics (relative elongation by 44% and relative narrowing by 57%) without a significant decrease in strength indexes (temporary resistance  $\sigma_b$  and yield strength  $\sigma_{0,2}$  are reduced by 4% and 9% respectively). Moreover, the actual fracture stress  $S_k$  increases by 12%. Thus, the strength of the sheet billets after surface EP, despite the significant plasticization, is higher than that of the sheet in the state of delivery.

2. The main reason for the plasticization of sheet billets is healing surface defects, which continues the stage of elastic-plastic deformation and complicates the beginning of the formation of concentrated deformation, which causes destruction.

3. EP significantly improves the stamping of low-carbon sheet steels. The ability to stretch sheet from steel 08кп increases 1.3 times (from the group of Very Deep Stretching, regulated by GOST 9045-93, to values that exceed the requirements of Extremely Complicated Stretching for steel of better quality 08ЮА), which will significantly increase the efficiency of the stamping process and improve product quality.

4. A significant advantage of epilamination is the increase in the ability to stretch not at the expense of weakening the sheet, but on the contrary, with increasing the actual resistance to destruction

### References

1. Popov Y.A. Technology and automation of sheet stamping / Y.A. Popov, V.G. Kovalov, I.M. Shubin. – M.: Publishing house of N. Bauman Moscow Higher Technical University, 2000. – 480 P.

2. Guseva S.S. Continuous heat treatment of steel sheets / S.S. Guseva, V.D. Gurenko, U.D. Zvarkovskiy. - M.: Metallurgy, 1979. – 224 P.

3. Leyrikh I.V. Тенденция развития и применения листовых сталей в автомобилестроении / I.V. Leyrikh, A.N. Smirnov, K.Y. Pismarev // Donetsk National Technical University. Scientific Works. «Metallurgy». – 2007.– Release 9 (22). – P. 12–18.

4. Panin V.E. Effect of the surface layer in a deformable solid / V.E. Panin, A.V. Panin // Physical Mesomechanics. - 2005. - V. 8. - № 5. - P. 7-15.

5. Panin V. E. Multilevel wave model of a deformed solid in physical mesomechanics / Panin V. E., Grinyaev Yu. V., Panin A. V., Panin S. V. // Proceedings of the Sixth International Conference for Mesomechanics «Multiscaling in Applied Science and Emerging Technology. Fundamentals and Applications in Mesomechanics». – 2004. – P. 335 – 342.

6. Vakhidov A.S. Epilamination: an effective method for creating nanofilms / A.S. Vakhidov, L.A. Dobrovolsky // Nanomaterials and Nanoindustry. 2012. – № 4 (34). – P. 32 – 35.

7. Khripunov V.V. The performance of the tool, hardened by epilamination / V.V. Khripunov, T.V. Medvedovskikh, V.A. Makarova, Ye.Ya. Nikulin // Engineering Bulletin, 2000. – №5. – P. 62 – 64.

8. Movshovich A.Y. Increasing the wear resistance of the guiding elements of punch tools by method of epilamization / A.Y. Movshovich, Ye.S. Deryabkina, M.G. Ishchenko, M.Ye. Fedoseyeva // Material processing, 2012. – № 4 (33). – P. 232 – 236.

9. Patent for invention UA 114635 Ukraine, IPC C 21D 1/04. Method of surface treatment of the sheet from cold-rolled sheet steel for cold stamping / S.S. Dyachenko, I.V. Doshcheckkina et al. - u2014 10886 Bull. № 13, 2017. – 5 P.

## 7.62 MM YALQUZAG SNIPER RIFLE METROLOGICAL RESEARCH STAGES WITH COORDINATE METROLOGY

### **Isgandarzada Elchin Barat**

Doctor of Technical Sciences, Professor, Head of Department

### **Ahmadli Shukufa Vagif**

assistant

### **Islamova Ulkar Rafiq**

doctoral student

### **Aliyeva Lamiye Sulduz**

doctoral student

### **Goycayeva Konul Akif**

master

Azerbaijan Technical University, Baku, Azerbaijan

**Abstract.** The article provides a comparative analysis of the 7.62 mm Yalquzag sniper rifle, the first national weapon of our country to meet world NATO standards, its technical characteristics, its leading position in the world arms industry, and similar weapons of the world. At the same time, for higher-precision production of complex shaped parts of the 7.62 mm Yalquzag sniper rifle, the stages of their technological process measurement control on coordinate measuring machines (on the example of Hexagon Tigo SF 3D coordinate measuring machine) are given.

**Keywords:** sniper rifle, optical sight, geometric dimensions, shape errors, model, lighter frame

Yalquzag sniper rifle was created by Azerbaijani engineers. The information about this lightweight sniper rifle was released to the public in December 2012 by the Ministry of Defense Industry. The sniper rifle was presented to the President on December 17, 2012.

Yalquzag has a range of 1,000 meters, a capacity of 10 cartridges and a weight of 7.1 kg. The Yalquzag is a weapon that fully meets NATO standards. At present, all parts of the weapon are manufactured in local factories, ie "Yalquzag" is a 100% NATO sniper rifle produced in local factories.



**Figure 1. Sniper rifle Yalguzag**

The parts of Yalguzag are made of high-strength aluminum alloy. Based on the results of the tests, the weapon underwent certain changes, while maintaining the overall design and ballistic properties compared to the previous model.

According to experts, Yalguzag, which was created and developed with great care and precision, due to its tactical and technical features, which has been popular in its class for the last 10 years JNG-90 "Bora-12" (Turkey), "Truvelo CMS-7.62" (CAR), CDX Lite, CDX Tac (Canada), "Orsis T-5000" (Russia), Accuracy International AX308 (England), APR 308 (Switzerland) are among the weapons that can compete with sniper rifles [1-5].

Channels have been opened in the barrel of the weapon to provide additional rigidity, light weight and improve cooling. A new mounting bus is envisaged in the plane where the pipe is connected to the box. The open areas on the sides of this cover provide additional cooling function to the pipe during firing, which in turn increases the durability and service life of the pipe.

One of the important features of the weapon is the presence of "Picatinni" type spectacles in accordance with the MIL 1913 NATO standard to combine it with optics and various accessories. It is possible to add various accessories to the top and sides of the weapon through these performances prepared at the Ministry of Defense Industry.

In accordance with the research plan, in order to achieve higher accuracy in the processing of complex shaped parts of the 7.62 mm Yalguzag sniper rifle, we determined the following step-by-step algorithm for their measurement and control operations on coordinate measuring machines using coordinate metrology:

1. Selection of complex shaped details that require high accuracy during the processing process.
2. Full mastery, analysis, analysis and study of geometric configuration of complex high-precision details.
3. Thorough study of constructive documents, drawings of complex high-precision details, norms and requirements to them.
4. AutoCAD and Solidworks, etc. in modern engineering programs of high-precision details of complex shapes. Development of 2D and 3D drawings and models.
5. Development of PS DMIS CAD program to determine the required high-precision geometric dimensions and shape errors of complex shaped high-precision details on coordinate measuring machines.
6. Determination of required geometric dimensions and shape errors of high-precision details of complex shape on coordinate measuring machines.
7. Preparation of the report protocol, analysis of the obtained results and submission of expert suggestions.

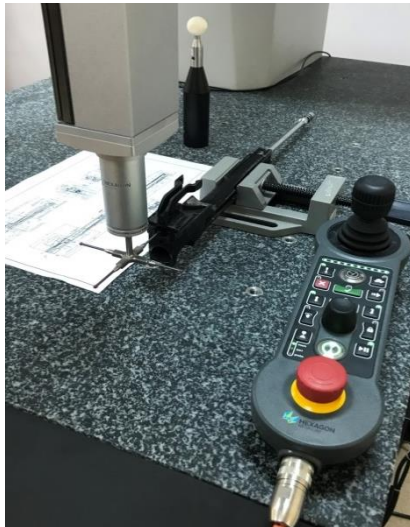


**Figure 2. Coordinate measurements of the lighter frame on a Hexagon Tigo SF machine**

The following experimental-research works were carried out in accordance with the above algorithm.

**Traditional metrological research of the lighter frame:** The lighter frame is the moving part of the automatic 7.62 mm Yalquzag sniper rifle.

The lighter frame is designed to move the lighter and transmitter and pull the cartridge out of the belt (Figure 3). At the back of the lighter frame, the extractor is mounted on a pole with a shaft. The lighter is designed to transfer the cartridge to the cartridge housing of the barrel, close the barrel channel, blow up the cartridge capsule and remove the shell from the cartridge housing. The lighter consists of a body, an extractor, a spring and an axis with an arrow and an axis of the extractor. The extractor and spring cartridge are used to remove the barrel from the cartridge housing and hold it in place until it touches the protrusion of the ejector in the barrel box. The return battle spring with the guide shaft is designed to return the lighter frame to the front position with the lighter and provide the energy needed to blow up the capsule of the striker cartridge.

To make a combination of lighter and lighter frame, one of the intricately shaped details of the 7.62 mm Yalquzag sniper rifle, the beaten pistachio is processed on a programmed machine immediately after the plating process, followed by heat treatment.

After heat treatment, a magnetic defectoscope detects internal defects (such as internal cracks). These types of defects usually occur when the pistachio is beaten and stratified. Once the internal defects of the lighter joint under investigation have been identified, if no cracks are found inside the part, the part is transferred to the chemical coating operation.

The choice of metrological research tools for any of the finishing operations of the lighter frame design of the 7.62 mm Yalquzag sniper rifle, of course, begins with the metrological study of the design.

In this section of the study, we must select metrological research (measurement) tools to monitor and verify the deviation of the  $\varnothing 14.6H9$  inner surface of the shell from the uniformity of the lighter along the central M axis after the final operation in the lighter frame combination of the 7.62 mm Yalquzag sniper rifle. The following provisions are taken as a basis for the selection of metrological research (measurement) means:

1. In order to guarantee the relative measurement error  $\delta_o$  given or calculated, the given relative error  $\delta\delta$  of the measuring instrument selected for metrological research must be less than  $25 \div 30\% \delta_o$ . That is,  $\delta_o = 0,7\delta_o$

2. The choice of research tool depends on the scale of production or the number of identical tools used in operation.

3. The measurement method determined based on the purpose of the control and study provides the requirements for the measurement tool to be grounded.

4. The following should be taken into account when selecting measuring, control and metrological research tools based on their metrological characteristics. If the technological process of the product under study is unstable, ie if any parameter we measure significantly deviates from the given field of application, then the scale of the selected tool should exceed the specified distribution range of the value of the measured parameter. When choosing a measuring instrument, it is important to know the scale of the measuring instrument as well as the length of the working area.

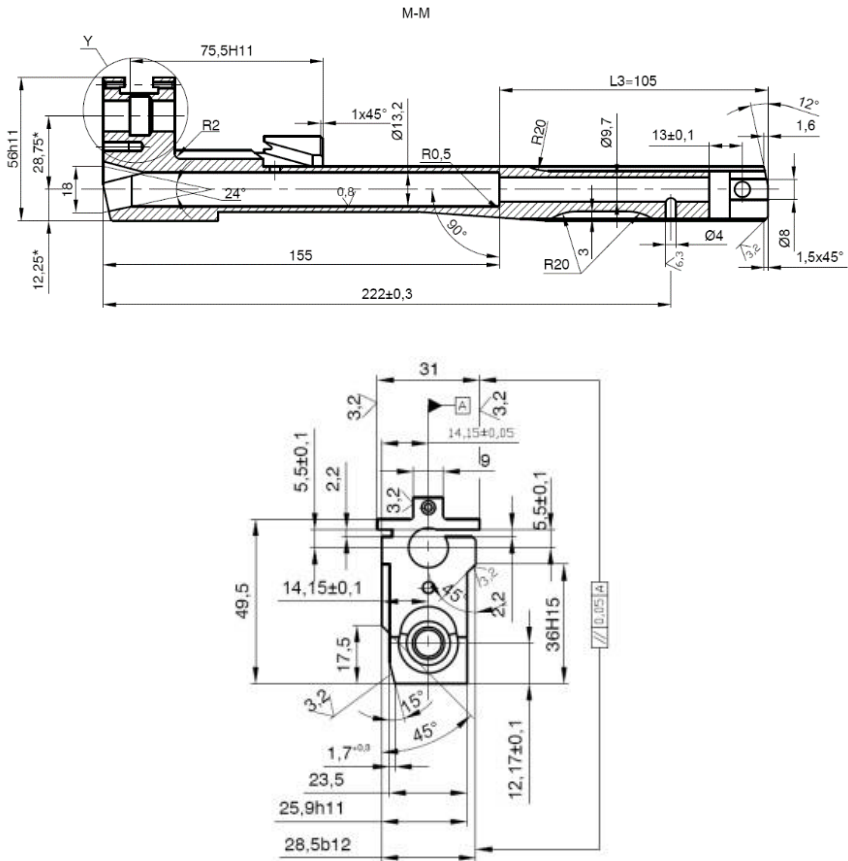


Figure 3. Drawing of the lighter frame of the 7.62 mm Yalqazag sniper rifle

The correct choice of measurement, control or metrological research tools for the part under study is one of the most important issues for the control operations on the part under study.

This in turn applies equally to each of the categories of technological five of control.

Bu isə öz növbəsində texnoloji nəzarətin beş kateqoriyasının hər birinə eyni dərəcədə aiddir. The categories of technological control are as follows:

- Complete control
- Selective control
- continuous control
- Period control
- Due control.

To control the deviation (error, deviation) of the surface of the lighter frame part  $\varnothing 14,6H9$  from the same axis on the surface M, we determine that the support from ST SEV 144-75 is  $T = 0.05 \text{ mm} = 50 \text{ m km}$ .

Half of the support will be  $T / 2 = 50/2 = 25 \text{ microns}$ .

The average value of the required accuracy is calculated as follows.

$$K'_{\text{davr}} = \frac{2,5 + 1,4}{2} = 1,95$$

The error of the measuring or control device we choose

$$\Delta_{ol} = \frac{T/2}{1,3 \cdot K_d} = \frac{25}{1,3 \cdot 1,95} = \frac{25}{2,535} = 9,86 \text{ mkm} \quad \text{will be.}$$

As a result of the calculations, we take 10.0 as the closest price to the price we determined. This value corresponds to the indicator with a distribution value of 0.01 mm. Therefore, we can use this measuring head (indicator) as a measuring tool that we need to monitor the part under study.

One of the main tasks of metrological research is the process of designing a control caliber for the joint surface of the part. Since the joint surface of the part under study is ( $\varnothing 14,6h9$ ), the control caliber for it is designed as a result of calculations shown in the following sequence.

1. First of all, the fit and support for smooth cylindrical parts and parts are determined from the standard tables.

2. Then the nominal values of the dimensions of the non-passing and passing sides of the working gauges are determined.

Calculate the value of the working dimensions for the gauge plug in the following sequence:

We choose the values of deviations  $es$  (mm) and lower  $ei$  (mm) from GOST25347-82:

$$ES = 43mkm = 0,043mm;$$

$$EI = 0mkm = 0mm.$$

We determine the values of the largest and smallest limits of the hole (slot):

$$D_{\max} = D + ES = 14,6 + 0,043 = 14,643mm;$$

$$D_{\min} = D + EI = 14,6 + 0 = 14,6mm.$$

We find in GOST 24853-81:

$$Z_1 = 8mkm = 0,008mm;$$

$$Y_1 = 0;$$

$$H_1 = 5mkm = 0,005mm;$$

$$H_p = 2mkm = 0,002mm.$$

We calculate the values of the working dimensions of the side of the caliber plug to be designed:

$$PP^{\max} = D_{\min} - Z_1 + \frac{H_1}{2} = 14,6 - 0,008 + \frac{0,005}{2} = 14,5945mm;$$

$$PP^{\min} = D_{\min} - Z_1 - \frac{H_1}{2} = 14,6 - 0,008 - \frac{0,005}{2} = 14,5895mm.$$

We also calculate the values of the working dimensions of the impenetrable side of the caliber plug we are going to design:

$$HE^{\max} = D_{\max} + \frac{H_1}{2} = 14,643 + \frac{0,005}{2} = 14,6455mm;$$

$$HE^{\min} = D_{\max} - \frac{H_1}{2} = 14,643 - \frac{0,005}{2} = 14,6405mm.$$

We determine the wear price for the side of the gauge plug:

$$PP^{yey} = D_{\max} + Y_1 = 14,5945 + 0 = 14,5945mm.$$

Calculate the values of the working dimensions of the side of the gauge plug:

$$N - PP^{\max} = D_{\min} - Z_1 - \frac{H_p}{2} = 14,6 - 0,008 - \frac{0,002}{2} = 14,593mm;$$

$$N - IP^{\min} = D_{\min} - Z_1 - \frac{H_p}{2} = 14,6 - 0,008 - \frac{0,002}{2} = 14,591mm.$$

We calculate the values of the working dimensions of the impenetrable side of the control caliber.

$$N - HE^{\max} = D_{\max} + \frac{H_p}{2} = 14,643 + \frac{0,002}{2} = 14,644mm;$$

$$N - HE^{\min} = D_{\max} - \frac{H_p}{2} = 14,643 - \frac{0,002}{2} = 14,642mm.$$

We calculate the value of the wear size of the control caliber;

$$N - IP^{vee} = D_{\max} + Y_1 + \frac{H_p}{2} = 14,643 + 0 - \frac{0,002}{2} = 14,642mm.$$

**Research of the lighter frame of the 7.62 mm Yalquzag sniper rifle with coordinate metrology.** The 7.62 mm Yalquzag sniper rifle, the object of our research, is an automatic mode combat weapon and is the most widespread firearm in the world (Figure 2). It has the ability to fire sequentially in both single and automatic mode. This weapon differs from others by its high reliability and simple maintenance.

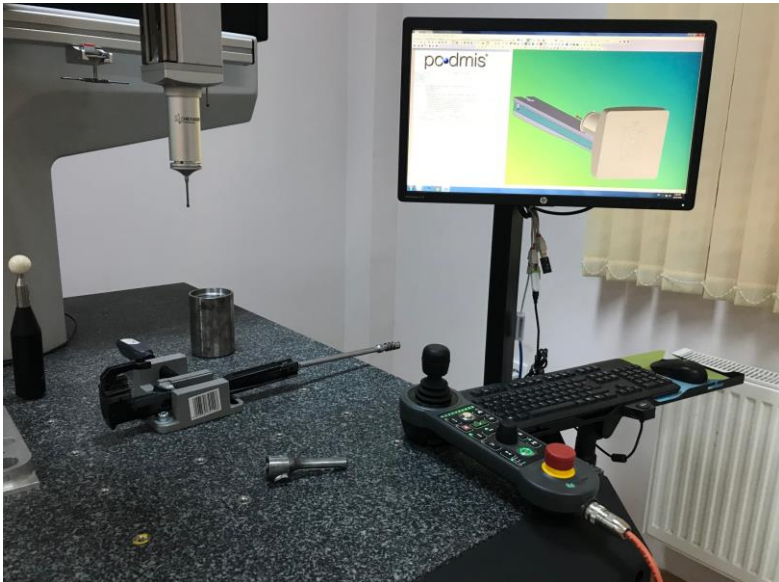


Figure 4. Lighter and lighter frame on a Hexagon Tigo SF machine performing coordinate measurements

podmis		PART NAME : lighter frame				07.02.2020	11:17
		REV NUMBER :	SER NUMBER :			STATS COUNT : 1	
#	MM	LOC1 - CIR2					
AX	NOMINAL	+TOL	-TOL	MEAS	DEV	OUTTOL	
X	19.038	0.001	0.100	19.040	0.002	0.001	
Y	76.155	0.100	0.001	76.156	0.001	0.000	
D	25.362	0.001	0.001	25.359	-0.002	0.001	
#	MM	LOC2 - CIR3					
AX	NOMINAL	+TOL	-TOL	MEAS	DEV	OUTTOL	
X	145.985	0.001	0.100	145.987	0.002	0.001	
Y	83.756	0.100	0.001	83.763	0.007	0.000	
D	18.830	0.001	0.001	18.833	0.003	0.002	
#	MM	LOC3 - CIR1					
AX	NOMINAL	+TOL	-TOL	MEAS	DEV	OUTTOL	
X	19.044	0.001	0.100	19.046	0.003	0.002	
Y	25.365	0.100	0.001	25.369	0.004	0.000	
D	25.375	0.001	0.001	25.372	-0.003	0.002	
←→	MM	DIST1 - CIR2 TO CIR3 (X-AXIS)					
AX	NOMINAL	+TOL	-TOL	MEAS	DEV	OUTTOL	
M	127.000	0.010	0.070	126.946	-0.054	0.000	

Figure 5. Measurement protocol obtained from measurements made on a Hexagon Tigo SF machine.

One of the important conditions for improving the quality of the 7.62 mm Yalquzag sniper rifle is to obtain accurate, accurate measurement information about the parameters, characteristics and properties of the lighter frame, which is one of its parts [6-9].

Model and detail of the 7.62 mm Yalquzag sniper rifle lighter and lighter frame were examined as follows in the Hexagon Tigo SF coordinate machine (Figure 4, 5).

As a result, a study of the lighter frame on the Hexagon Tigo SF showed that if the complex details of the 7.62 mm Yalquzag sniper rifle were tested and put into operation in a coordinate machine, high-precision results would be obtained and better weapons would be produced.

### **Results and suggestions.**

1. The concept of ensuring the unity of coordinate measurements by coordinate methods of geometric parameters of complex shaped surfaces has been developed theoretically and experimentally.
2. Algorithms and programs for coordinate measurements of geometric parameters of surface shape and roughness have been developed.
3. Mathematical models of the principles of analysis of error organizers of coordinate measurements obtained on the basis of scientific research allow to select the coordinate measurement system for accuracy, to carry out their verification methods, as well as to evaluate the accuracy of measurement results.

### **References**

1. <https://ordu.az/az/news/124412/azerbaycanin-nato-kalibrinde-ilk-silahi-yalquzag>
2. [https://az.wikipedia.org/wiki/Yalquzag\\_\(snayper\\_t%C3%BCf%C9%99ngi\)](https://az.wikipedia.org/wiki/Yalquzag_(snayper_t%C3%BCf%C9%99ngi))
3. Koch, A. W., Ruprecht, M. W., Toedter, O., Häusler, G. Optische Messtechnik an technischen Oberflächen. Expert-Verlag, 1998, 210 s.
4. V. G. Lisenko, Sh. V. Ahmadli, A. A. Lavrukhin Pecularity of metrology assurance coordinate measurements of geometrical parameters of the shaped surfaces. 27th international scientific symposium "Metrology and metrology assurance 2018" september 8-12, 2018, Sozopol, Bulgaria, p.173-176
5. В. Лысенко, Э. Искендерзаде, Ш. Ахмедли, К. Маликов, У. Исламова. Проверка и калибровка координатно измерительных машин с помощью высокоточной интерференционной измерительной системы. "Ölçmə və keyfiyyət: problemlər, perspektivlər" mövzusunda Beynəlxalq Elmi-texniki konfransın materialları, Bakı, 2018. səh. 31-33

6. Э. Б. Искендерзаде, В. Г. Лысенко. Метрологическое обеспечение измерений геометрических параметров эвольвентных зубчатых колес. Монография. – М.: АСМС, 2020. – 220 с.

7. Э. Б. Искендерзаде, В. Г. Лысенко. Научно-методические основы 3D-метрии шероховатости поверхности. Монография. – М.: АСМС, 2020. – 236 с.

8. E. B. Isgandarzada, V. Q. Lysenko, A. A. Lavrukhin, Sh. V. Ahmadli “Pecularity of metrology assurance coordinate measurements of geometrical parameters of the shaped surfaces” / Metrology and metrology assurance, 27th International Scientific Symposium, September 8-12, Sozopol – Bulgaria, 2017

9. В. Г. Лысенко, Д. Н. Черепов. Обеспечение единства трехкоординатных оптических измерений геометрических параметров поверхностей сложной формы. Всероссийская научно-техническая конференция «Метрологическое обеспечение современной военной техники» 17-19 июня 2003 г. г. Москва

## ANALYSIS OF THE ELECTRIC FIELD OF A PLANE LATTICE OF SIGN-ALTERNATING AXES

**Leonov Vladimir Semenovich**

Ph.D., Professor

International Academy of System Studies – IASS, Moscow

**Abstract.** The electric field of a plane lattice of sign-alternating axes can be represented by a complex potential. Separating the real and imaginary parts of the complex potential, we find the electric field strength function and its modulus. Analysis of the electric field of a plane lattice of sign-alternating axes shows us that this field is short-range. When moving away from the lattice, its electric field strength decreases very quickly. We see that at a distance equal to the lattice step  $1.0a$ , the field strength decreases by an order of magnitude, and at a distance of two steps  $2.0a$  from lattice its electric field can be neglected in practical calculations. Our analysis shows us that the electric field of the lattice of sign-alternating axes is a very inhomogeneous field and this is a short-range field at a distance of one step of the lattice. Sign-alternating fields are widely used in my fundamental theory of Superunification: sign-alternating superstrings, sign-alternating shells of nucleons and others [1-5].

**Keywords:** sign-alternating fields, short-range fields and forces, theory of Superunification, sign-alternating superstrings, bifilar winding, quantum engines, Universe.

**1. Calculation of the lattice field of sign-alternating axes.** Fig. 1 shows a plane lattice of sign-alternating electric axes. The signs of polarity of the electric charge of such axes are alternating when the plus (+) sign changes to a minus (-) sign on the adjacent axis. Such a plane lattice is accepted by us as infinite. The origin of the Y coordinate is the axis with a positive charge (+), and the X axis is lying in the plane of the lattice.

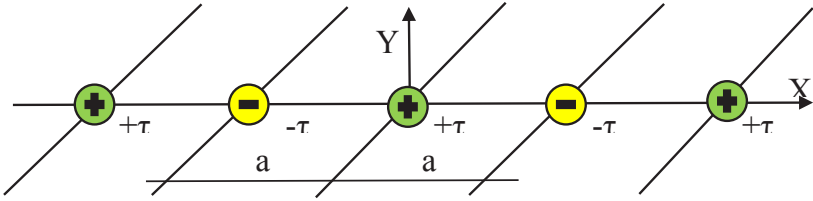


**Fig. 1. This is a plane lattice of sign-alternating electric axes.**

The electric potential  $U$  of sign-alternating electric axes of a similar bifilar winding (Fig. 4) is described by a function of a complex variable [1]:

$$U = \frac{\tau}{4\pi\epsilon_0\epsilon_1} i \text{Ln} \left( \text{tg} \frac{a}{\pi} z \right) \quad (1)$$

where  $\tau$  is the linear density of electric charges of the axis, C/m;

$\epsilon_0 = 8.85 \cdot 10^{-12}$  F/m is electric constant;

$\epsilon_1$  is the relative dielectric constant of the medium;

$a$  is the distance between the centers of the axes, m;

$z = x + iy$  is a complex number ( $i^2 = -1$ ).

We separate the real part of the complex potential (1) from its imaginary part and we obtain the function of the electric potential  $\varphi(x, y)$  in a rectangular coordinate system [5]:

$$\varphi = \frac{\tau}{4\pi\epsilon_0\epsilon_1} \ln \frac{\text{ch} \frac{\pi}{a} y + \cos \frac{\pi}{a} x}{\text{ch} \frac{\pi}{a} y - \cos \frac{\pi}{a} x} \quad (2)$$

Next, we find the function of the electric field intensity vector  $E$  as the gradient from the scalar field of the potential  $\varphi(x, y)$  of the lattice of sign-alternating electric axes [6]:

$$E = \text{grad} \varphi = \frac{\partial \varphi}{\partial x} \mathbf{i} + \frac{\partial \varphi}{\partial y} \mathbf{j} = \frac{\tau}{2\pi\epsilon_0\epsilon_1 a} \left( \frac{\text{ch} \frac{\pi}{a} y \cdot \sin \frac{\pi}{a} x}{\text{ch}^2 \frac{\pi}{a} y - \cos^2 \frac{\pi}{a} x} \mathbf{i} + \frac{\text{sh} \frac{\pi}{a} y \cdot \cos \frac{\pi}{a} x}{\text{ch}^2 \frac{\pi}{a} y - \cos^2 \frac{\pi}{a} x} \mathbf{j} \right) \quad (3)$$

where  $\mathbf{i}$  and  $\mathbf{j}$  are unit vectors in the  $x$  and  $y$  axes, respectively.

As we see from (2) and (3), the electric field of the lattice of alternating electric axes is represented by special functions [7, 8]. So that we can make a graphical representation of the electric field in equipotential and electric lines of force, we must write the equations for equipotentials and electric lines of force, provided that equipotential lines are always perpendicular to the electric lines of force. The line perpendicularity condition is satisfied by equation (1) and its solutions (2) and (3).

We assume that the electric potential of an axis with a small radius  $r_0$  has a maximum value  $\frac{1}{2} \varphi_{\max}$ . The potential difference along the axes (+) and (-) is equal to  $\frac{1}{2} \varphi_{\max} - (-\frac{1}{2} \varphi_{\max}) = \varphi_{\max}$ . By this we set the boundary conditions for solving our equations. Further, from (2) we find the linear density  $\tau$  of electric charges of the axis under the boundary conditions  $\frac{1}{2} \varphi_{\max}$ ,  $x = r_0$ ,  $y = 0$ :

$$\tau = \frac{2\pi\epsilon_0\epsilon_1\varphi_{\max}}{\ln \frac{1 + \cos \frac{\pi}{a} r_0}{1 - \cos \frac{\pi}{a} r_0}} \quad (4)$$

**2. Equations equipotential and electric field lines of the lattice of sign-alternating fields.** Next, we separate the variables with respect to  $y$  and  $x$  in equation (2) and obtain the equipotential equation in implicit form through hyperbolic functions:

$$\operatorname{ch} \frac{\pi}{a} y = \operatorname{cth} \frac{2\pi\epsilon_0\epsilon_1}{\tau} \cdot \cos \frac{\pi}{a} x l \quad (5)$$

After substituting (4) in (5) we obtain the equation of equipotentials of a lattice of sign-alternating electric axes:

$$y = \pm \frac{a}{\pi} \ln \left( k_1 \cos \frac{\pi}{a} x + \sqrt{k_1^2 \cos^2 \frac{\pi}{a} x - 1} \right) \quad (6)$$

where  $k_1$  is the equipotential coefficient which has its own formula:

$$k_1 = \left| \operatorname{cth} \left( \frac{\varphi}{\varphi_{\max}} \ln \frac{1 + \cos \frac{\pi}{a} r_0}{1 - \cos \frac{\pi}{a} r_0} \right) \right| \quad (7)$$

The lines of equipotentials intersect the X axis at the point  $x$  at  $y = 0$ :

$$x = \pm \frac{a}{\pi} \arccos \frac{1}{k_1} \quad (8)$$

Equations (6), (7) and (8) allow us to graphically represent the lattice field of sign-alternating electric axes in the form of equipotential surfaces having the potential  $\varphi/\varphi_{\max}$  expressed in relative units (Fig. 1).

To build a picture of the field in electric lines of force we use the stream function  $\Psi$  of intensity  $\mathbf{E}$  (3) which penetrates the lattice of alternating electric axes (Fig. 1) [7]:

$$\Psi = \frac{\tau}{2\pi\epsilon_0\epsilon_1} \operatorname{arctg} \frac{\operatorname{sh} \frac{\pi}{a} x}{\sin \frac{\pi}{a} x} \quad (9)$$

Next, we find the total flux  $\Phi$  of the electric field emerging from the charged axis using the Gauss theorem for surface  $S$  around an axis:

$$\Phi = \oint_S \mathbf{E} d\mathbf{S} = \frac{\tau}{\epsilon_0\epsilon_1} \quad (10)$$

From (10) we find:

$$\tau = \epsilon_0\epsilon_1\Phi \quad (11)$$

Substituting (11) in (9) we get:

$$\Psi = \frac{\Phi}{2\pi} \operatorname{arctg} \frac{\operatorname{sh} \frac{\pi}{a} x}{\sin \frac{\pi}{a} x} \quad (12)$$

From (12) we obtain the equation of the electric lines of force:

$$y = \pm \frac{a}{\pi} \ln \left( \operatorname{tg} 2\pi \frac{\Psi}{\Phi} \cdot \sin \frac{\pi}{a} x + \sqrt{\operatorname{tg}^2 2\pi \frac{\Psi}{\Phi} \cdot \sin^2 \frac{\pi}{a} x + 1} \right) \quad (13)$$

The total flux  $\Phi$  and its parts in the form of the ratio  $\Psi/\Phi$  are included in (13). The magnitude of the flux penetrating the first quadrant of the coordinate system between the  $X$  and  $Y$  axes is one quarter:  $\Psi/\Phi = 1/4$ . The beginning of the coordinate is the  $X$  axis, and we will do the counting direction of the flux counterclockwise. Then along the  $X$  axis at  $y = 0$  the flux is equal to zero  $\Psi = 0$ , and along the  $Y$  axis as  $y \rightarrow \infty$  the flux is equal to one quarter (12):

$$\Psi = \frac{\Phi}{2\pi} \arctg \infty = \frac{1}{4} \Phi \quad (14)$$

Equation (13) allows us to determine the coordinates of the electric lines of force for the relative flux  $\Psi/\Phi$  from 0 to  $\frac{1}{4}$  inside the first quadrant with any interval. Due to the symmetry of the field, we can always construct its complete picture for four quadrants of the coordinate system from the calculated data for the first quadrant.

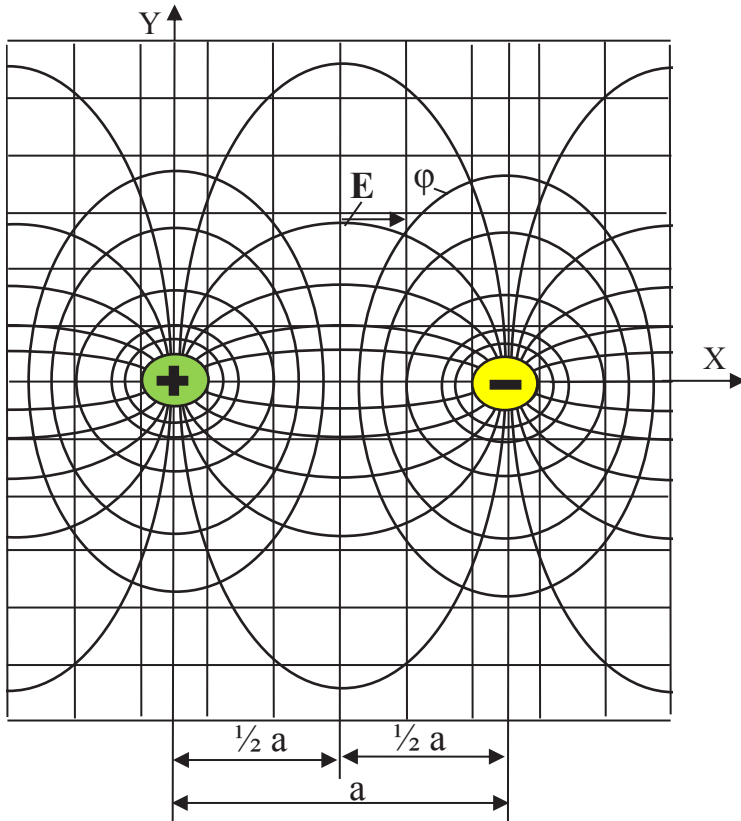


**Fig. 2.** The picture of the electric field of the lattice of sign-alternating electric axes is represented by the equipotentials  $\phi = \text{const}$  and electric lines of force E.

Based on equations (2), (3), (6) and (13), we constructed a graphic picture of the electric field of the lattice of sign-alternating electric axes in the form of equipotentials  $\varphi = \text{const}$  and electric lines of force  $\mathbf{E}$  (Fig. 2). Analysis of the electric field of the lattice of sign-alternating electric axes shows us that this field is very inhomogeneous and is mainly concentrated in the lattice itself at distances of no more than the step of the lattice  $a$ . This is a short-range electric field.

**3. Analysis of a short-range field of a lattice of sign-alternating fields.** Next, we find from (3) the modulus of the electric field strength  $E$  of sign-alternating electric axes:

$$E = \sqrt{\left(\frac{\partial E}{\partial x}\right)^2 + \left(\frac{\partial E}{\partial y}\right)^2} = \frac{\tau}{4\pi\epsilon_0\epsilon_1 a} \left( \text{ch}^2 \frac{\pi}{a} y - \cos^2 \frac{\pi}{a} x \right)^{-\frac{1}{2}} \quad (15)$$

On the Y axis at  $x = 0$ , the modulus of the electric field strength  $E_{1y}$  (15) will have the form:

$$E_{1y} = \frac{\tau}{2\pi\epsilon_0\epsilon_1 a \left(\text{sh} \frac{\pi}{a} y\right)}; \quad f_1 = \frac{1}{\text{sh} \frac{\pi}{a} y} \quad (16)$$

As we see from (16), the field strength  $E_{1y}$  changes according to the inverse hyperbolic sinus law ( $f_1$ , Fig 3), which is characterized by a very rapid decline when we move away from the lattice of sign-alternating electric axes.

On the Y axis at  $x = 0.5a$ , the modulus of the electric field strength  $E_{2y}$  (15) will have the form:

$$E_{2y} = \frac{\tau}{2\pi\epsilon_0\epsilon_1 a \left(\text{ch} \frac{\pi}{a} y\right)}; \quad f_2 = \frac{1}{\text{ch} \frac{\pi}{a} y} \quad (17)$$

As we see from (17), the field strength  $E_{2y}$  changes according to the inverse hyperbolic cosine law ( $f_2$ , Fig 3), which is characterized by a very rapid decline when we move away from the lattice of sign-alternating electric axes.

Figure 3 shows graphs of a rapid decrease in field strength when we move along the Y axis moving away from the lattice plane of sign-alternating axes (Fig. 1). We see that at a distance equal to the lattice step  $1.0a$ , the field strength decreases by an order of magnitude, and at a distance of two steps  $2.0a$  from lattice its electric field can be neglected in practical

calculations. Our analysis shows us that the electric field of the lattice of sign-alternating axes is a very inhomogeneous field and this is a short-range field at a distance of one step of the lattice.

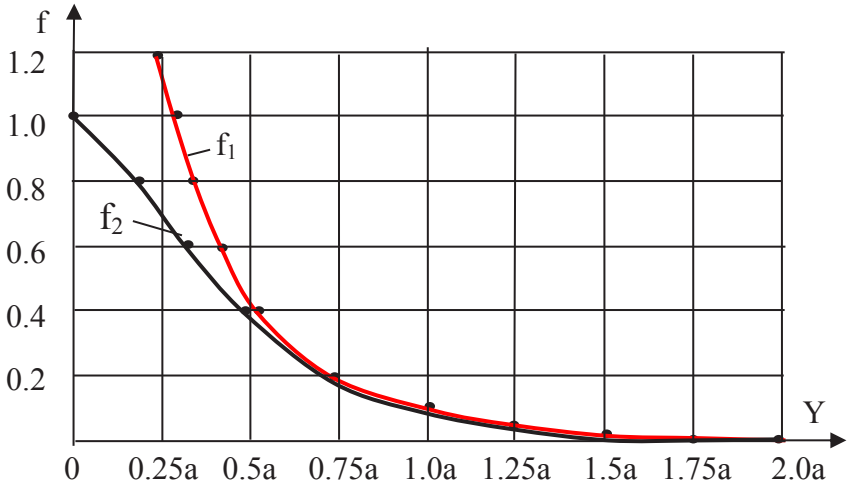


**Fig. 3.** We see a rapid decrease in the field strength  $E_{1y}$  (16) and  $E_{2y}$  (17) as a function of  $f_1$  (16) and  $f_2$  (17) when we move along the Y axis moving away from the lattice plane of sign-alternating axes (Fig. 1).

The electric force  $F_e$  acting on the electric charge  $q_e$  in a sign-alternating field (Fig. 1) is proportional to the field strength  $E$  (3), (15), (16), (17). These are short-range forces:

$$F_e = q_e E \tag{18}$$

**4. Practical application of sign-alternating fields in science and technology:**

**4.1. “Antigravity” dielectric separators of finely dispersed particles.** The separator includes: bifilar winding 1, drum 2, brush 3, hopper 4, fraction receiver 5, particles 6 (Fig. 4).

Bifilar winding was used by Nikola Tesla in electric devices. We wrapped the bifilar winding 1 on the drum 2 in two wires with insulation. Power winding 1 is AC, frequency 50... 3000 Hz, voltage 1... 10 kV. Bifilar winding has a unique property, it attracts both non-magnetic (dielectric and conductive) and magnetic materials. Earth gravity also manifests itself in a similar way. The force  $F_e$  attraction of the particles by the bifilar winding is due to their polarization  $p$ , where  $p$  is the electric dipole moment of the particle [9]:

$$F_e = p \cdot \text{grad}E \tag{19}$$

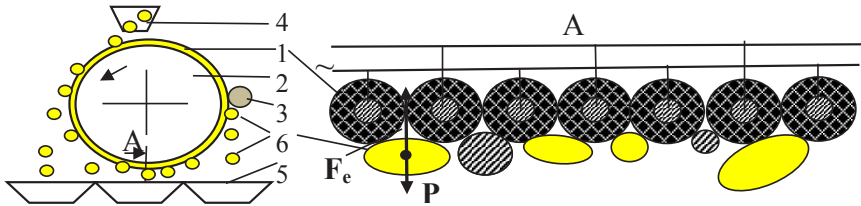


**Fig. 4. This is a scheme of an “antigravity” dielectric separator with a bifilar winding in section A (increase ).**

The separator works as follows [10]. Particles 6 (seeds, dust and crushed rock) from the hopper 4 are fed to the surface of the bifilar winding 1 which attracts them with force  $F_e$ . The drum 2 has a rotation and under the action of the force  $P$  of gravity, various particles are divided into fractions in the receiver 5. For this work, I was awarded the Russian Government Prize in Science and Technology in 1995.

The name “antigravity” separator is taken by me in quotation marks, since fully antigravity is created due to the combined influence of the gradients of electric (19) and magnetic fields as a gradient of electromagnetic energy  $\text{grad}W$ .

**4.2. The creation of artificial gravity and antigravity quantum engines.** My studies of the behavior of particles in the field of a bifilar winding allowed me to recognize the electromagnetic nature of quantum gravity. To create gravity force  $F$ , we must, like formula (19), create an energy gradient  $W$  which quantized space-time is filled with [11, 1]:

$$F = \text{grad}W \tag{20}$$

Formula (20) is the main one when describing the fundamental forces of nature: gravity, electromagnetism, nuclear and electroweak forces. From (20) it follows Newton's gravitation law and the momentum conservation law, which are special cases of the formula (20) by the enormous energy quantized space-time. In astrophysics, the energy  $W$  (20) is dark energy and it is able to move the galaxies with acceleration by force  $F$  (20). The Universe has tremendous elasticity and tension, which are set by sign-alternating superstrings.

**4.3. The Universe has sign-alternating superstrings.** Our Universe is pierced by electric and magnetic superstrings which are an endless chain of sign-alternating electric ( $\pm e$ ) and magnetic ( $\pm g$ ) charges-quarks. These are point charges. Fig. 5 shows a scheme for calculating the electric force  $F_e$  acting on elementary quark-charges ( $\pm e$ ) inside a superstring.

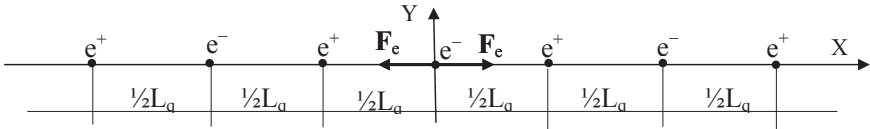


**Fig. 5. Calculation of the tensioning of sign-alternating electrical superstring.**

For  $a = \frac{1}{2}L_{q0} = 0.37 \cdot 10^{-25}$  m, we obtain the superstring tension force using the field superposition principle, where  $e = 1,6 \cdot 10^{-19}$  C is an elementary electric quark-charges [1, 12]:

$$F_{\dot{a}} = \frac{1_x}{4\pi\epsilon_i} \frac{e}{(0,5L_{q0})^2} \left( 1 - \frac{1}{2^2} + \frac{1}{3^2} - \frac{1}{4^2} + \dots \right) = \frac{1_x}{\pi\epsilon_o} \frac{e}{L_{q0}^2} \left( \frac{\pi^2}{12} \right) = \frac{\pi}{12\epsilon_o} \frac{e}{L_{q0}^2} 1_x = \pm 1.4 \cdot 10^{23} \text{ N} \quad (21)$$

The magnetic superstring has a similar tension force:  $F_g = \pm 1.4 \cdot 10^{23}$  N, confirming the colossal elasticity of quantized space-time (dark matter). For the first time I was able to calculate these forces based on the methodology for the analysis of sign-alternating fields.

**4.4. A nucleon has an alternating shell as the basis of nuclear forces.** The theory of Superunification has made significant adjustments to our understanding of the nature of nuclear forces. We left the quark structure of nucleons. But we replaced fractional quarks with entire quarks ( $\pm 1e$ ). In addition, we placed quarks in the sign-alternating nucleon shell. The nucleon shell can be compressed and by this action it itself forms the nucleon mass as a result of spherical deformation (Einstein's curvature) of quantized space-time (dark matter). But most importantly, we got the effect of the attraction of the alternating shells of nucleons to each other, regardless of the presence of an unbalanced charge on the nucleon (Fig. 6) [1, 13, 14].

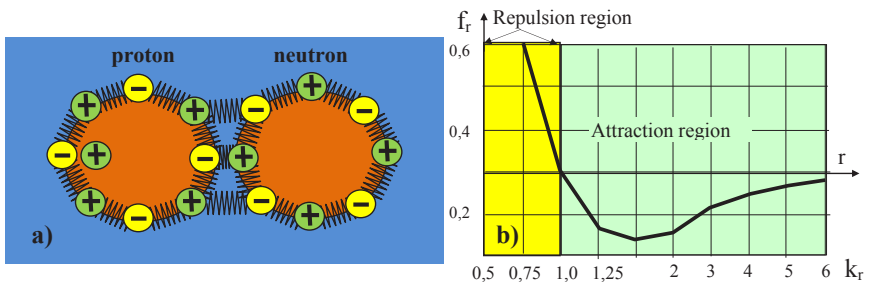


**Fig. 6. Variation of electrical forces of repulsion and attraction (b) in interaction of the sign-alternating nucleons shells (a) [1].**

The attraction of sign-alternating shells of nucleons implements the principle of short-range contact forces at distances  $r \sim 10^{-15}$  m. The nature of these short-range forces, as shown by the calculations (see the graph in Fig. 6b), fully corresponds to the nuclear forces between nucleons in the nuclei of atoms [1].

### References:

- [1] V. S. Leonov. Quantum Energetics. Volume 1. Theory of Superunification. Cambridge International Science Publishing, 2010, 745 pgs.
- [2] V.S. Leonov. Quantum Energetics: Theory of Superunification. Viva Books, India, 2011, 732 pages.
- [3] Download free. Leonov V. S. Quantum Energetics. Volume 1. Theory of Superunification, 2010. <http://leonov-leonovstheories.blogspot.com/2018/04/download-free-leonov-v-s-quantum.html> [Date accessed April 30, 2018].
- [4] Vladimir Leonov ORCID <https://orcid.org/0000-0001-5270-0824>
- [5] Vladimir Leonov – blogger. <https://www.blogger.com/profile/03427189015718990157>. [Date accessed April, 2011].
- [6] William R. Smythe. Static and Dynamic Electricity. McGraw-Hill Book Company Inc. New York – Toronto – London, 1950, 637 p.
- [7] Leonov V.S. Calculation and analysis of ponderomotive forces in sign-alternating electric fields. Moscow: Collection of scientific works of the MIISP, vol. 16, issue 5, 1979, p. 36-42.
- [8] Janke E., Emde F., Lesh F., Special functions, formulae, diagrams, tables. Moscow, Nauka, 1977, 344 p.
- [9] Leonov V.S. Application of the theory of the function of a complex variable for calculating the field of a bifilar winding. Moscow: Collection of scientific works of the MIISP, vol. 15, issue 5, 1978, p. 25-27.
- [10] Author's Certificate USSR No 680762 /Leonov V.S., Tarushkin V.I. Dielectric separator. - Bulletin of Inventions, 1979, No. 31, priority 1976.
- [11] Vladimir S. Leonov and etc. Non-rocket, non-reactive quantum engine: idea, technology, results, prospects. Published: // Aerospace Sphere Journal (ASJ) 2019, №1, pp. 68-75.  
DOI: 10.30981/2587-7992-2019-98-1-68-75
- [12] Vladimir Leonov. Tensioning of the Electromagnetic Superstring. viXra:1910.0506 submitted on 2019-10-25.
- [13] Vladimir Leonov. Quantized Structure of Nucleons. The Nature of Nuclear Forces. viXra:1910.0290 submitted on 2019-10-17.
- [14] Leonov V.S., Electrical nature of nuclear forces, Agrokonsalt, Moscow, 2001.

## DYNAMIC LEONOV INTERFEROMETER FOR DETECTING THE FIELD OF DARK MATTER PARTICLES

**Leonov Vladimir Semenovich**

Ph.D., Professor

International Academy of System Studies – IASS, Moscow

**Abstract.** We present the design of a Leonov dynamic interferometer for detecting the field of dark matter particles and obtained positive results from its testing. Unlike the Michelson interferometer, in which the arms of the interferometer are located at an angle of  $90^\circ$  and rotate in a horizontal plane, in the Leonov interferometer, the shoulders are turned in opposite directions at an angle of  $180^\circ$  and the light rays from the laser in the shoulders also move in opposite directions and converge on the screen, forming interference fringes. In this case, the slightest deviation of the arms of the interferometer from the horizontal leads to a sharp shift of the interference fringes on the screen. We have given a theoretical justification for the fact that the shift of interference fringes is caused by the deformation (Einstein curvature) of the field of dark matter in the field by terrestrial gravity. We have shown that the spherical field of terrestrial gravity is formed as a result of spherical deformation of the field of dark matter, which is a four-dimensional quantized space-time. We found that the carrier of the field of dark matter is a four-dimensional particle - a quantum of space-time (quanton), which has no mass but accumulates electromagnetic energy. Quanton is the only four-dimensional particle that combines time and space, and is the carrier of electromagnetism and gravity. The concentration of quantons in a unit volume characterizes the quantum density of the medium, which in accordance with the theory of Superunification sets the speed of light in vacuum. In the Earth's gravitational field, a field of dark matter is deformed, which leads to a change in the quantum density of the medium in the vertical direction (along the radius). This leads to a change in the speed of light in the radial direction relative to the earth's horizontal. We see this fact as a shift of interference fringes when the shoulders of the dynamic interferometer are turned relative to the horizontal (Leonov effect), thereby registering a change in the concentration of dark matter particles. This experiment confirms the validity of the theory of Superunification [1-5].

**Keywords:** dark matter, quanton, quantized space-time, quantum density of the medium, speed of light, interferometer, gravity, theory of Superunification.

**1. The problem of finding particles of dark matter.** The search for dark matter particles is one of the most important tasks of fundamental physics. Physicists have made numerous attempts over the past two decades (and even earlier) to detect experimentally dark matter particles have proved to be untenable and failure. There you can specify about 50 such unsuccessful projects. In [6], a list of projects for the search for dark matter particles was carried out. So, in 2013 there were 36 such projects, and in three years by 2016 their number increased to 48. Moreover, new projects appeared there, and some of the old projects were liquidated due to their inefficiency. In addition, there are other projects that are not listed in these lists. In total, physicists currently have more than 50 projects for the search for dark matter particles [6].

Paradoxically, physicists do not have a unified theory explaining the nature of dark matter with so many active projects to search for dark matter particles (table 1, [6]). At the same time, physicists have a large number of diverse and conflicting hypotheses, which is about 20 (Table 2, [6]) and causes us to be perplexed. With such a large number of universities (table 3, [6]) and scientists involved in projects to search for dark matter particles, we can talk about the crisis of global fundamental science. We see the helplessness of scientists who cannot explain the nature of the new observed astrophysical effects (curvature of a ray of light in the absence of gravitational masses, accelerated motion of galaxies and others).

The reason for these failures lies in the complete misunderstanding by modern physicists of the nature of dark matter and its quantized discrete structure [7]. This, despite the fact that the basis of dark matter is the quantum of space-time (quanton), which I introduced into theoretical physics back in 1996, and dark matter is nothing but quantized space-time [1, 7-10]. I apologize to readers that I have to give references mainly only to my published works due to the absence of other convincing works about the nature of dark matter and the structure of cosmic vacuum.

**2. Quanton is the only four-dimensional particle carrier of dark matter.** The fact that dark matter is the basis of the cosmic (physical) vacuum is now beyond doubt. In this case, from the standpoint of Einstein's general theory of relativity (GR), dark matter should possess the properties of four-dimensional space-time, that is, it should be a carrier of time and space at the same time. In addition, dark matter must possess electromag-

netic and gravitational properties in order to be simultaneously a carrier of electromagnetic and gravitational fields. In the experiments of Michelson and Morley it was found that the cosmic vacuum does not consist of particles having mass, like a gas-like mechanistic ether that does not exist in nature. Thus, dark matter is weightless matter. Therefore, all attempts to find a dark matter particle with mass (like an axion) were unsuccessful [11].

So, a particle of dark matter should have the following properties:

- ✓ this particle must be four-dimensional;
- ✓ this particle must be a carrier of time and a carrier of space at the same time;
- ✓ this particle should not have mass;
- ✓ this particle must be a carrier of electromagnetic and gravitational fields, simultaneously;
- ✓ this particle should be the carrier of a new previously unknown field of dark matter and the fifth fundamental force [1].

Quanton is the only four-dimensional particle satisfying the properties listed above. Fig. 1 show the structure of a quanton consisting of four quarks in a projection. Quanton is formed as a result of electromagnetic compression of an electromagnetic quadrupole (Fig. 2), previously unknown in physics [1, 9, 12].

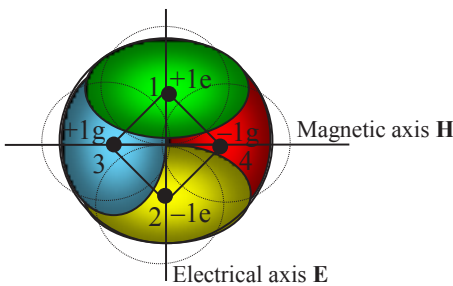


**Fig. 1. The quanton in projection (rotated in space).**

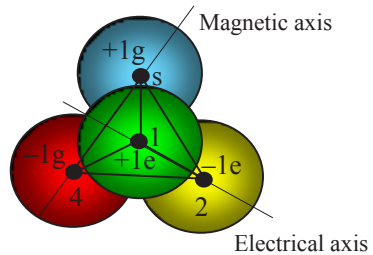


**Fig. 2. The electromagnetic quadrupole (top view).**

Quanton includes four integer quarks (charging): two electrical ( $+1e$  and  $-1e$ ), and two magnetic ( $+1g$  and  $-1g$ ), installed at the vertices of the tetrahedron. Magnetic quarks were previously unknown in physics. Magnetic and electric integer quarks have no mass, but are carriers of electromagnetic energy. For the first time in 1996, I found the correct relationship between a integer magnetic quark ( $\pm 1g$ ) and a integer electric quark ( $\pm 1e$ ) [1, 9, 12]:

$$g = C_0 e = 4.8 \cdot 10^{-11} \text{ Am} \quad (\text{Leon}) \tag{1}$$

where  $C_0 \sim 3 \cdot 10^8 \text{ m/s}$  is the speed of light in vacuum.

The calculated diameter of the quanton is  $L_{q0} \sim 10^{-25} \text{ m}$  and it represents the fundamental length (Leonov's length) [1, 13]:

$$L_{q0} = 0.74 \cdot 10^{-25} \text{ m} \tag{2}$$

The process of physical quantization is the process of filling space with quantons. Figure 3 show a grid model of quantized space-time in projection onto a plane in the form of lines of force of an electromagnetic field. Figure 4 show a solid-state model of quantized space-time is presented. These models clearly characterize the structure of dark matter as a discrete structure.

Quantized space-time (dark matter) is characterized by the quantum density of the medium  $\rho_0, \rho_1, \rho_2$  (there is a concentration of quantons per unit volume [ $\text{q/m}^3$ ]) taking into account  $L_{q0}$  (2) [1, 14]:

$$\rho_0 = \frac{k_3}{L_{q0}^3} = \frac{1.44}{L_{q0}^3} = 3.55 \cdot 10^{75} \frac{\text{q}}{\text{m}^3} \tag{3}$$

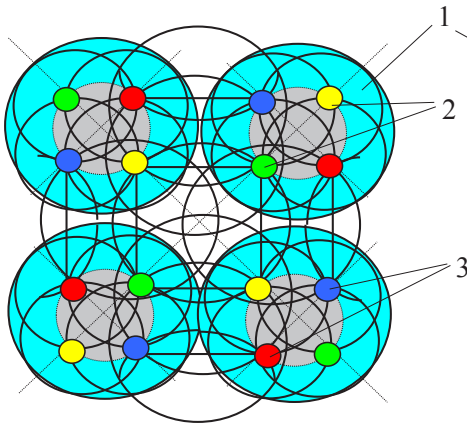


**Fig. 3. Grid model of the quantized space-time in projection in the form of lines of force. 1) quantons; 2) electrical quarks; 3) magnetic quarks.**

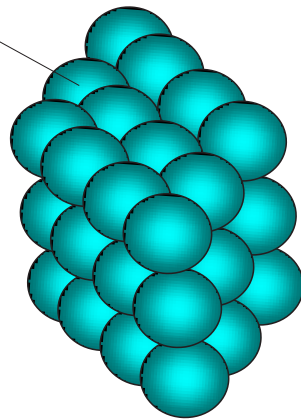


**Fig. 4. Solid-state model of quantized space-time.**

In order to experimentally fix the traces of dark matter particles, we need to control the quantum density of the medium  $\rho_1$  and record its change. It should be noted that it is not possible to detect single quantons. First, the diameter of the quanton is very small and amounts to about  $10^{-25}$  m (2). The sensitivity of electromagnetic methods is insufficient to penetrate so deep into the depths of dark matter. Secondly, single quantons in nature do not exist; they are connected into the global electromagnetic field of dark matter in the form of a power electromagnetic grid of the Universe (Fig. 3) [1, 14].

**3. Justification of the design of the interferometer for recording the field of dark matter particles.** One of the most sensitive instruments for recording the field of dark matter is considered to be a Michelson interferometer. The interferometer arms in the projects have a length of: LIGO - 4 km, VIRGO - 3 km, KAGRA - 3 km and are located horizontally in a static state. The results of these experiments are negative [15]. An analysis of negative experiments on the search for dark matter particles indicates that experimenters do not fully understand the quantized structure of dark matter as a luminiferous medium.

An interferometer reacts to a change in the speed of light by a phase shift of an electromagnetic light wave in the form of a shift of interference fringes when two light beams are superimposed. The change in the speed of light under terrestrial conditions can be observed as a result of the deformation of the field of dark matter by the gravitational field of the Earth. In the theory of Superunification, it is established that the speed of light  $C$  is a variable that is determined by the square root of the quantum density of the medium  $\rho_1$  (dark matter) around the Earth [1, 16]:

$$C = C_0 \sqrt{\frac{\rho_1}{\rho_0}} \quad (4)$$

The distribution of the quantum density of the medium  $\rho_1$  for the Earth's spherical gravitational field is described by solving the two-component Poisson equation with distance  $r$  from the center of the earth [1, 17]:

$$\rho_1 = \rho_0 \left( 1 - \frac{R_g}{r} \right) \quad (5)$$

where  $R_g$  is the gravitational radius of the Earth (without a factor of 2):

$$R_g = \frac{Gm}{C_0^2} \quad (6)$$

where  $G$  is gravitational constant;  $m$  is mass, kg;  $C_0^2$  is maximum gravitational potential of quantized space-time (dark matter), J/kg.

We substitute (5) in (4) and obtain the formula for the speed of light  $C$  in the central gravitational field:

$$C = C_0 \left( 1 - \frac{R_g}{r} \right)^{\frac{1}{2}} \quad (7)$$

We expand (7) in a series and for  $r \gg R_g$  and discard terms of higher orders, we get:

$$C = C_0 \left( 1 - \frac{R_g}{r} \right)^{\frac{1}{2}} \approx C_0 \left( 1 - \frac{1}{2} \frac{R_g}{r} \right) = C_0 - \frac{C_0 R_g}{2r} \quad (8)$$

Formula (8) allows you to calculate the deceleration of the speed of light  $\Delta C$  on the Earth's surface in comparison with remote space. For this, we substitute the values in (8): the speed of light  $C_0 \sim 3 \cdot 10^8$  m / s; Earth's gravitational radius  $R_g = 4.44 \cdot 10^{-3}$  m (6); the average radius of the Earth  $r = 6.67 \cdot 10^6$  m and we get the value  $\Delta C$  (8) on the surface of the Earth:

$$\Delta C = -\frac{C_0 R_g}{2r} = -\frac{3 \cdot 10^8 \cdot 4.44 \cdot 10^{-3}}{2 \cdot 6.67 \cdot 10^6} = -0.1 \text{ m/s} \quad (9)$$

The deceleration of the speed of light  $\Delta C$  (9) on the Earth's surface is 0.1 m/s. This is consistent with GR. But we are interested in the change in the speed of light  $C$  in the Earth's radial gravitational field as a gradient  $\text{grad}C$  in the direction along the radius  $r$ :

$$\text{grad}C = \frac{dC}{dr} = \frac{d}{dr} C_0 \left( 1 - \frac{1}{2} \frac{R_g}{r} \right) = \frac{C_0 R_g}{2r^2} \quad (10)$$

Formula (10) allows us to estimate the sensitivity of the interference method of changing the speed of light of the radial gravitational field of the Earth on its surface under spherical deformation of quantized space-time (dark matter). To do this, we substitute the corresponding parameters in (10) and we obtain the value  $\text{grad}C$  (10) on the surface of the Earth:

$$\text{grad}C = \frac{C_0 R_g}{2r^2} = \frac{3 \cdot 10^8 \cdot 4.44 \cdot 10^{-3}}{2 \cdot (6.67 \cdot 10^6)^2} = 15 \cdot 10^{-9} \frac{\text{m/s}}{\text{m}} = 15 \frac{\text{nm/s}}{\text{m}} \quad (11)$$

So, the change in the speed of light inside dark matter deformed by spherical Earth's gravity on the Earth's surface in the radial direction is 15 nm/s/m (11). A sensitivity of 15 nm/s / m of the interference method are sufficient to observe a shift in the interference fringes at the arm of the interferometer less than 1 m at a red laser wavelength of 635 nm.

A change in the speed of light will not be observed in the horizontal direction at  $r = \text{const}$  and  $C = \text{const}$  in accordance with (11):  $\text{grad}C = 0$ :

$$\text{grad}C = \frac{d(C = \text{const})}{dr} = 0 \quad (12)$$

Therefore, in LIGO, VIRGO, KAGRA projects, even with a horizontal interferometer arm length of 3–4 km, experimenters cannot detect the horizontal change in the speed of light from the change in the quantum density of the medium (dark matter):  $\text{grad}C = 0$  (12), obtaining negative results in experiments on the search for dark matter particles [15].

**4. The design of a dynamic interferometer and the results of its tests.** Fig. 5 shows a scheme of a dynamic interferometer: a) a top view, b) a side view that includes: laser 1, splitter 2, mirrors 3-6, lens 7, screen 8, base 9, axis 10.

The interferometer works as follows. The light beam 11 from laser 1 enters the splitter 2. The splitter is a 4 mm thick transparent glass plate mounted at an angle of  $45^\circ$  to the laser beam. Next, the laser beam is divided into two beams, which are directed in opposite directions to the mirrors 3 and 4, and being reflected from them, converge on the screen 8, forming interference fringes. For this, mirrors 4 and 5 are additionally installed. Lens 7 serves to enlarge the image on the screen 8. The base 9 is a massive slab of black marble with an axis 10, excluding its thermal and mechanical deformation. The length of the interferometer arms  $L_1$  and  $L_2$  is 250 mm, but it works well with shoulders of 100 mm or less.

As we see, in contrast to the Michelson interferometer in which the arms of the interferometer are located at an angle of  $90^\circ$ , the Leonov interferometer arms are turned in opposite directions at an angle of  $180^\circ$ . In this case, the light rays 11 from the laser 1 in the arms  $L_1$  and  $L_2$  also move in opposite directions, and further the rays converge on the screen 8, forming interference fringes (Fig. 5a). In this case, the slightest deviation of the interferometer arms on the axis 10 from the horizontal by an angle  $\varphi$  leads to a sharp shift of the interference fringes on the screen 8 (Fig. 5b). We observe this effect as a result of a change in the speed of light in the deformed gravitational field of the Earth in accordance with formulas (10) and (5).

I want to note that the principle of operation of the Leonov interferometer based on the new physics (the theory of Superunification [1]), which established the quantized structure of dark matter and gave the rationale of the new design of the interferometer for detecting of field of the dark matter particles. Many dynamic laser interferometers of various applications are produced in the world, but they cannot detect the field of dark matter particles unlike the Leonov dynamic interferometer.

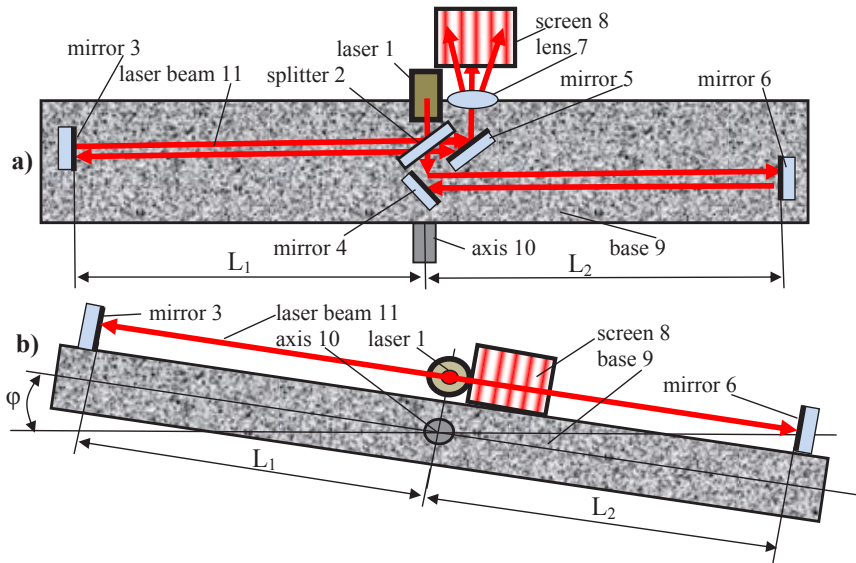


**Fig. 5. The dynamic Leonov interferometer scheme for detecting the field of dark matter particles in the Earth’s gravitational field (Fig. 5b not shown: splitter 2, mirrors 4-5 and lens 7).**

**5. Conclusion:** We were the first in the world to successfully detect the field of dark matter particles, confirming experimentally the validity of the theory of Superunification. This new theory completed the unification of fundamental interactions begun by Einstein in GR [1-18, 19]. I introduced a new parameter in quantum theory is the quantum density of the medium. This allowed us to significantly simplify the computational mathematical apparatus of the quantum theory of gravity and make it clear to the engineer. This allows us to study the properties of dark matter in terrestrial conditions using a dynamic Leonov interferometer.

Currently, we are developing a whole series of small-sized various devices of the type Leonov interferometer for controlling cosmic quantized space-time and controlling the concentration of dark matter which makes up 100% of the Universe and not 85% as is commonly believed.

**References:**

[1] V. S. Leonov. Quantum Energetics. Volume 1. Theory of Superunification. Cambridge International Science Publishing, 2010, 745 pgs.

[2] V.S. Leonov. Quantum Energetics: Theory of Superunification. Viva Books, India, 2011, 732 pages.

[3] Download free. Leonov V. S. Quantum Energetics. Volume 1. Theory of Superunification, 2010. <http://leonov-leonovstheories.blogspot.com/2018/04/download-free-leonov-v-s-quantum.html> [Date accessed April 30, 2018].

[4] Vladimir Leonov ORCID <https://orcid.org/0000-0001-5270-0824>

[5] Vladimir Leonov – blogger. <https://www.blogger.com/profile/03427189015718990157>. [Date accessed April, 2011].

[6] Vladimir Leonov. Registration of the field of dark matter particles on a Leonov's dynamic interferometer. <https://vladimir-leonov.livejournal.com/34765.html> [Date accessed May 10, 2020].

[7] Vladimir Leonov. Understanding the nature and structure of dark matter. <https://vladimir-leonov.livejournal.com/35283.html> [Date accessed May 10, 2020].

[8] Vladimir Leonov. Fundamental Discoveries of the Space-Time Quantum (Quanton) and Superstrong Electromagnetic Interaction (SEI). viXra:1910.0267 submitted on 2019-10-16.

[9] Vladimir Leonov. Electromagnetic Nature and Structure of Cosmic Vacuum. viXra:1910.0287 submitted on 2019-10-16.

[10] Vladimir Leonov. Einstein vs Higgs: or what is the mass? <https://docs.google.com/file/d/0B1gwB1O4JZNwbjFPM0hmdU5KcW8/edit> [Date accessed February 12, 2013].

[11] Borsanyi, S. et al. Axion alert! Exotic-particle detector may miss out on dark matter. Nature <http://dx.doi.org/10.1038/nature20115> (2016).

[12] Vladimir Leonov. Unit of Measurement of Magnetic Charge is Leon. viXra:1910.0436 submitted on 2019-10-22.

[13] Vladimir Leonov. Fundamental Length - Leonov's Length. viXra:1910.0478 submitted on 2019-10-23.

[14] Vladimir Leonov. Quantum Density of the Universe. viXra:1910.0468 submitted on 2019-10-23.

[15] H. Grote and Y. V. Stadnik. Novel signatures of dark matter in laser-interferometric gravitational-wave detectors. Phys. Rev. Research 1, 033187 – Published 19 December 2019  
DOI: 10.1103/PhysRevResearch.1.033187.

[16] Vladimir Leonov. The Formula of the Speed of Light in a Quantized Space-Time.

viXra:1911.0063 submitted on 2019-11-04.

[17] Vladimir Leonov. Two-Component Solution of the Poisson Gravitational Equation.

viXra:1910.0533 submitted on 2019-10-26.

[18] Vladimir Leonov. The Einstein Posthumous Phrase.

viXra:1910.0170 submitted on 2019-10-11.

[19] Vladimir S. Leonov and etc. Non-rocket, non-reactive quantum engine: idea, technology, results, prospects. Published: // Aerospace Sphere Journal (ASJ) 2019, №1, pp. 68-75.

DOI: 10.30981/2587-7992-2019-98-1-68-75

ON HOMOMORPHISMS OF SOME PARTIAL GROUPOIDS

**Arapina-Arapova Elena Sergeevna**

Candidate of Physical and mathematical Sciences, Associate Professor

Taganrog Institute named after A. P. Chekhov (branch)

Rostov state University of Economics (RINH)

**Abstract.** It is proved that the direct product of partial semilattices is a partial semilattice, i.e. the class of partial semilattices is multiplicatively closed. This class is hereditary in the sense that every subgroup of a partial semilattice is again a partial semilattice. However, it is shown that it is not homomorphically closed.

**Keywords:** Partial groupoids, semigroup, , algebraic operation, congruence, homomorphism.

A partial action [1] on a set  $S$  is a ternary relation  $\theta$  on  $S$  that satisfies the condition:  $(\forall a, b, c, c' \in S)[(a, b, c), (a, b, c') \in \theta] \rightarrow c = c'$ .

Instead of  $(a, b, c') \in \theta$ , usually write  $a \circ b = c$  ( $\theta$ ). If it is clear about what partial action we are talking about, then we will not write. If for elements  $a, b \in S$  under no circumstances does  $s \in S$  take place  $(a, b, s) \in \theta$ , then we will write  $a \circ b = \emptyset$  (of course, assuming that this symbol  $\emptyset$  is not an element of the set  $S$ ).

A partial action ( $\circ$ ) on a set  $S$  is called complete if for any  $a, b \in S$  we have  $a \circ b \neq \emptyset$ . A partial groupoid  $(S; \cdot)$  is called idempotent (commutative, weakly associative, associative, catenary) if  $a^2 = a$  ( $ab = ba$ ; from  $(ab)c \neq \emptyset \neq a(bc)$  what follows  $ab)c = a(bc)$ ;  $ab)c = a(bc)$ ; from  $ab \neq \emptyset \neq bc$  what follows  $(ab)c \neq \emptyset \neq a(bc)$ ) for any  $a, b, c \in S$ .

A groupoid  $S$  is called *weakly idempotent* if  $a^2 \neq \emptyset$  always implies  $a^2 = a$  for any  $a \in S$ . A groupoid  $S$  is called *connected* if for any  $a, b \in S$  there exists an element  $x \in S$  such that  $ax \neq \emptyset$ ,  $xb \neq \emptyset$ . Podgruppam  $B$  of a groupoid  $(A; \cdot)$  is called *closed* [1] if for any  $b_1, b_2 \in B$  such that  $b_1 \cdot b_2 \neq \emptyset$ , should  $b_1 \cdot b_2 \in B$ .

A *partial semilattice* is called [4] an idempotent commutative weakly associative partial groupoid. Every semilattice is a partial semilattice, but not Vice versa. Since an idempotent associative complete groupoid is called

a bundle, it is natural to call an idempotent weakly associative groupoid a *partial bundle*. Obviously, a commutative partial bundle is a *partial semilattice*.

The groupoid  $S^\circ = S \cup \{0\}$  is called the *null extension of the groupoid S*. It is easy to see that a groupoid is associative if and only if its null extension is a semigroup. Therefore, the study of associative groupoids is equivalent to the study of semigroups with zero.

Let  $S, S'$  be arbitrary groupoids. Displaying  $\varphi: S \rightarrow S'$  it is called a [1] *homomorphism* if  $(\forall a, b \in S)(ab \neq \emptyset) \rightarrow (a\varphi) \cdot (b\varphi) = (ab)\varphi$ . A homomorphism  $*$  is called *strong* if  $(a\varphi) \cdot (b\varphi) \neq \emptyset$  follows  $ab \neq \emptyset$  for any  $a, b \in S$ . V. T. Kulik [2] noted that the study of strong homomorphisms of groupoids is equivalent to the study of those homomorphisms of zero extensions of these groupoids, for which only zero is displayed in zero.

An equivalence  $*$  on a groupoid  $(S; \cdot)$  is called a *congruence* if for any  $a, b \in S$  there exists a  $c \in S$ , such that

$$\tau_a \cdot \tau_b \subset \tau_c.$$

Congruence  $\tau$  is called *strong* if for any  $x, x', y, y' \in S$  such that  $x \tau x', y \tau y', xy \neq \emptyset$  always

$$x' y' \neq \emptyset.$$

On a groupoid  $S$ , every congruence is strong if and only if either  $S$  is a complete groupoid or  $S$  is a groupoid with empty multiplication.

Let  $\tau$  be a congruence on the groupoid  $(S; \cdot)$ . A factorset  $S/\tau$  with respect to a partial action

$$\tau_a \circ \tau_b = \begin{cases} \tau_c, & \text{если } \emptyset \neq \tau_a \cdot \tau_b \subset \tau_c, \\ \emptyset, & \text{если } \tau_a \cdot \tau_b = \emptyset \end{cases}$$

it is called a *factorgroupoid* of a groupoid  $S$  by congruence  $\tau$ .

These definitions directly imply the following properties of an arbitrary congruence  $\tau$  of a groupoid  $S$ .

1°. A factorgroupoid  $S/\tau$  is idempotent if and only if every  $\tau$ -class is a closed subgroup in  $S$ .

2°. A factorgroupoid  $S/\tau$  is commutative if and only if the condition

$$\emptyset \neq \tau_a \cdot \tau_b \subset \tau_c \text{ entails } \emptyset \neq \tau_b \cdot \tau_a \subset \tau_c$$

3°. If the groupoid  $S$  is associative, then the groupoid  $S/\tau$  is weakly associative, and every  $*$ -class is an associative subgroup in  $S$ .

4°. If the factorgroupoid  $S/\tau$  is weakly associative and every  $\tau$ -class is a weakly associative subgroup, then the groupoid  $s$  is also weakly associative  $S$ .

5°. If  $S$  is an associative groupoid, and  $\tau$  is a strong congruence on  $S$ , then the factorgroupoid  $S/\tau$  is associative.

Property 5° has no place for arbitrary congruence  $\tau$ . for Example, let the groupoid  $S$  be defined by a table:

$\cdot$	$a$	$b$	$c$	$d$	$e$	$f$
$a$	$a$	–	$c$	–	$e$	–
$b$	–	$b$	–	$d$	–	$f$
$c$	–	$c$	–	$e$	–	$c$
$d$	$d$	–	$f$	–	$d$	–
$e$	$e$	–	$c$	–	$e$	–
$f$	–	$f$	–	$d$	–	$f$

Using, for example, the Light associativity test, we conclude that  $S^\circ$  is a semigroup. Hence,  $S$  is an associative groupoid. Let  $\tau$  be an equivalence on  $S$  corresponding to the partition  $\alpha=\{a\}$ ,  $\beta=\{e\}$ ,  $\gamma=\{c, d, e, f\}$ . It is easy to see that  $\tau$  is a congruence. This congruence is not strong, for  $e\tau e$ ,  $c\tau f$ ,  $ec \neq \emptyset$ , but  $ef = \emptyset$ . The factorgroupoid  $S/\tau$  has a table

$\mathbf{O}$	$a$	$\beta$	$\gamma$
$a$	$a$	–	$\gamma$
$\beta$	–	$\beta$	$\gamma$
$\gamma$	$\gamma$	$\gamma$	$\gamma$

The factorgroupoid  $S/\tau$  is not associative, since  $(\gamma \circ \alpha) \circ \beta = \gamma \circ \beta = \gamma \neq \emptyset$ , but  $\gamma \circ (\alpha \circ \beta) = \emptyset$ , since  $\alpha \circ \beta = \emptyset$ . Although, as can be seen from the table,  $S/\tau$  – it is an idempotent commutative weakly associative catenary connected groupoid, that is, it is a catenary connected partial semilattice.

6°. The factorgroupoid  $S/\tau$  of a catenary groupoid is catenary if every  $\tau^*$ -class is a weakly associative connected closed subgroup of the groupoid  $S$ . Note that the catenarity of the groupoid  $S$  and the factorgroupoid  $S/\tau$  does not yet imply the connectivity of the  $\tau^*$ -class. For example, let  $s$  be a groupoid  $S$ :

$\cdot$	$a$	$b$	$c$	$d$
$a$	$a$	$b$	$-$	$-$
$b$	$b$	$b$	$-$	$-$
$c$	$-$	$-$	$c$	$d$
$d$	$-$	$-$	$d$	$d$

and  $\tau$  is the equivalence to  $S$  corresponding to the partition  $\alpha = \{a\}$ ,  $\beta = \{c\}$ ,  $\gamma = \{b, d\}$ . It is clear that  $\tau$  - congruence on  $S$ . the factorgroupoid  $S/\tau$  is given by the table

$\circ$	$a$	$\beta$	$\gamma$
$a$	$a$	$-$	$\gamma$
$\beta$	$-$	$\beta$	$\gamma$
$\gamma$	$\gamma$	$\gamma$	$\gamma$

These tables show that  $(S; \cdot)$ ,  $(S/\tau; \circ)$  are catenary groupoids, but the groupoid  $\tau_\gamma$  is not connected.

7°. A factorgroupoid  $S/\tau$  of an associative groupoid is a partial copula if and only if every  $\ast$  - class is a closed subgroup of  $S$ .

8°. If in an associative groupoid  $S$  every  $\ast\tau$  - class is a closed subgroup and the condition  $\emptyset \neq \tau_a \cdot \tau_b \subset \tau_c$  always implies  $\emptyset \neq \tau_b \cdot \tau_a \subset \tau_c$ , then  $S/\tau$  it is a partial semilattice. If the groupoid  $S$  is catenary, and every  $\tau$  - class is a connected subgroup in  $S$ , then the partial semilattice  $S/\tau$  is catenary.

Proposition 1. Strong homomorphic image of a partial semilattice (catenary groupoid) it is also a partial semilattice (catenary groupoid).

Thus, the class of partial semilattices is closed with respect to strong homomorphisms. However, the class of partial semilattices is not homomorphically closed. For example, an identical transformation on the basis set of an anti-chain  $Y = \{a, b\}$  (an anti-chain is a partially ordered set in which any different elements are incomparable) is an epimorphism of this anti-chain to a groupoid  $(Y; \cdot)$ , where  $(\cdot)$  is defined by the table

$\circ$	$a$	$b$
$a$	$a$	$a$
$b$	$-$	$b$

But the groupoid  $(Y; \mathbf{O})$ , being noncommutative, is not a partial semilattice.

Note that an arbitrary homomorphic image of a catenary groupoid is not necessarily catenary. In fact, the identical transformation of the set  $S = \{e, f, g\}$  is an epimorphism of the anti-chain  $(S; \mathbf{O})$  defined by the table

<b>O</b>	<i>e</i>	<i>f</i>	<i>g</i>
<i>e</i>	<i>e</i>	<i>e</i>	–
<i>f</i>	<i>e</i>	<i>f</i>	<i>g</i>
<i>g</i>	–	<i>g</i>	<i>g</i>

**Lemma.** The homomorphic image of a connected groupoid (associative commutative connected catenary groupoid) is connected (catenary).

Evidence. Let  $S$  be a connected groupoid  $\varphi: S \rightarrow T$  is an epimorphism  $t_1, t_2 \in T$ , then there are  $s_1, s_2 \in S$ , such that  $s_1\varphi = t_1, s_2\varphi = t_2$ . Since the groupoid  $S$  is connected, there exists  $s \in S$ , that  $s_1s \neq \emptyset, ss_2 \neq \emptyset$ , whence  $(s_1s)\varphi = (s_1\varphi)(s\varphi) = t_1t \neq \emptyset, (ss_2)\varphi = (s\varphi)(s_2\varphi) = tt_2 \neq \emptyset$ , where  $t = s\varphi$ .

Let  $S$  be a commutative associative connected catenary groupoid,  $\varphi: S \rightarrow T$  is an epimorphism,  $t_1t_2 \neq \emptyset, t_2t_3 \neq \emptyset$  ( $t_1, t_2, t_3 \in T$ ). There are  $s_1s_2s_3 \in S$  such that  $s_i\varphi = t_i$  ( $i \in \{1, 2, 3\}$ ). Since  $S$  is a connected groupoid, there are  $s', s'' \in S$ , that

$$s_1s' \neq \emptyset, s's_2 \neq \emptyset \text{ и } s_2s'' \neq \emptyset, s''s_3 \neq \emptyset,$$

and, in view of the catenarity of the groupoid  $S$ ,

$$(s_1s')s_2 \neq \emptyset, s_1(s's_2) \neq \emptyset \text{ и } (s_2s'')s_3 \neq \emptyset, s_2(s''s_3) \neq \emptyset$$

where we get  $((s_1s')s_2)(s''s_3) \neq \emptyset$ . Due to the associativity and commutativity of the groupoid  $S$ , we have  $((s_1s')s_2)(s''s_3) = ((s'_1s_1)s_2)(s_3s'') = s'_1s_1s_2s_3s'' \neq \emptyset$ , i.e.  $(s_1s_2)s_3 \neq \emptyset, s_1(s_2s_3) \neq \emptyset$  and since  $\varphi$  is a homomorphism, then  $(t_1t_2)t_3 \neq \emptyset, t_1(t_2t_3) \neq \emptyset$ .

Definition. Let  $A, B$  -groupoids. A groupoid whose base set is the Cartesian product  $A \times B$ , and the action is defined by the rule:

$$(a, b) \cdot (c, d) = \begin{cases} (ac, bd) \\ 0, \text{ if } a_1a_2 = 0_A, b_1b_2 = 0_B, \text{ otherwise} \end{cases}, \text{ if } ac \neq \emptyset \neq bd$$

it is called the direct product of the groupoids  $A$  and  $B$ . Let  $A$  and  $B$  be groupoids with zeros  $0_A, 0_B$ . Set  $((A \setminus \{0_A\}) \times (B \setminus \{0_B\})) \cup \{0\}$ , along with the binary operation

$$(a_1, b_1) \cdot (a_2, b_2) = \begin{cases} (a_1a_2, b_1b_2) \\ 0, \text{ if } a_1a_2 = 0_A, b_1b_2 = 0_B \end{cases}, \text{ if } a_1a_2 \neq 0_A, b_1b_2 \neq 0_B,$$

is a complete groupoid and is called [3] the direct product of groupoids  $A$ ,  $B$  with a combined zero.

Note that the direct product of the groupoids  $A$ ,  $B$  is exactly the zero restriction of the direct product with the combined zero of their zero extensions. It is easy to prove the following

Offer 2. The direct product of two idempotent (commutative, associative, weakly associative, connected, catenary) groupoids is an idempotent (commutative, associative, weakly associative, connected, catenary) groupoid.

It is not difficult to introduce the concept of a direct product of any set of groupoids and prove proposition 2 for this General case as well.

According to proposition 2, the direct product of partial semilattices is a partial semilattice, that is, the class of partial semilattices is multiplicatively closed. This class is hereditary in the sense that every subgroup of a partial semilattice is again a partial semilattice. However, as we saw above, it is not homomorphically closed.

### References

1. Lyapin E. S., Evseev A. E. Partial algebraic actions// St. Petersburg, 1991.
2. Kulik V. T. Simple  $f$ -semigroups// Research in algebra. Saratov: ed. Saratov. UN-TA. 23-31
3. Kozhevnikov O. B. Categorical semigroups// Dissertation for the degree of candidate of physical and mathematical Sciences. Taganrog. 1975.
4. Arapina-Arapova E. S. on partial semilattices of inverse semigroups// Collection of scientific works of TSPI teachers and postgraduates. Taganrog, 2000, Pp. 216-222.

## GENERALIZATION OF ONE THEOREM OF NEWMAN<sup>1</sup>

**Bezverkhniy Vladimir Nikolaevich**

Doctor of Physico-mathematical Sciences, Full Professor  
Civil Defence Academy EMERCOM of Russia

**Bezverkhniaia Natalia Borisovna**

Candidate of Physico-mathematical Sciences, Associate Professor  
Civil Defence Academy EMERCOM of Russia

**Abstract.** The article summarizes Newman's result on the antinormal of magnus subgroups in groups with one defining relation with torsion and Bagerzade's theorem for groups with one defining relation without torsion.

**Keywords:** magnus subgroups, antinormal, groups.

The main goal of this article is to generalize the well-known B. Newman theorem on the small normality of magnus subgroups in groups with one defining relation with torsion [1], and Bagerserzade's theorem [2] for groups with one defining relation without torsion. Consider a group with one defining relation

$$G = \langle a_1, a_2, \dots, a_n; r(a_1, a_2, \dots, a_n) \rangle \quad (1)$$

We assume that the defining relation  $r(a_1, a_2, \dots, a_n)$  in a free group  $F_n = \langle a_1, a_2, \dots, a_n \rangle$  is a cyclically irreducible word. For definiteness, we assume that each generator of the group  $G$  is included in  $r(a_1, a_2, \dots, a_n)$ .

**Definition 1.** The subgroup  $M$  of  $G$  groups generated by the set of generators

$X \subset \{a_1, a_2, \dots, a_n\}$  is called a magnus subgroup.

A group with one defining relation of the form

$$G = \langle a_1, a_2, \dots, a_n; r^m(a_1, a_2, \dots, a_n), m > 1 \rangle \quad (2)$$

called a group with one defining relation with torsion.

---

<sup>1</sup>This work was supported by a grant from the RFBR №19-41-71002p\_a

**Theorem 1.** [1] (B. Newman). Assume  $G$  - a group with one defining relation and with torsion, and  $M$  – magnus subgroup of the group  $G$ , and assume  $g \in G \setminus M$ , then

$gMg^{-1} \cap M = E$ , where  $E$  - singular subgroup.

**Definition 2.** Assume a group  $G$  with one defining relation

$$G = \langle a_1, a_2, \dots, a_n; r^m(a_1, a_2, \dots, a_n), m > 1 \rangle$$

and  $G = G_1 * F$ , where  $F = \langle a_{n+1}, a_{n+2}, \dots, a_{n+s}, \dots \rangle$  free group,  $X = \{a_1, \dots, a_n, a_{n+1}, \dots, a_{n+s}, \dots\}$  and assume  $X_1 \subset X$  and  $X_1 \cap \{a_1, \dots, a_n\} \subset \{a_1, \dots, a_n\}$

Then subgroup  $M = \langle X_1 \rangle$  – magnus subgroup of the group  $G$ .

**Lemma 1.** Suppose  $G = G_1 * F$ , where  $G_1$  – a group with one defining relation with torsion,  $F$  - free group, and  $M$  – magnus subgroup of the group  $G$  and  $g \in G$ . Then, if  $g \in G \setminus M$ , then  $gMg^{-1} \cap M = E$ . The proof is obvious.

**Lemma 1.** Suppose  $G = G_1 * F$ , where  $G_1$  group with one defining relation with torsion and assume for any magnus subgroups  $M_1, M_2$  groups  $G_1$ , and any  $g \in G_1$  by condition  $M_1gM_2 \neq M_1M_2$  then  $gM_1g^{-1} \cap M_2 = E$ , then the group  $G$  inherits this property. The proof is obvious.

The following theorem generalizes B. Newman's theorem.

**Theorem 2.** Suppose  $G = \langle a_1, \dots, a_n; r^m(a_1, \dots, a_n), m > 1 \rangle$  group with one defining relation with torsion and assume  $M_1$  and  $M_2$  magnus subgroups of the group  $G$  and  $g \in G$  are such, that  $M_1gM_2 \neq M_1M_2$  then  $g^{-1}M_1g \cap M_2 = E$ .

The proof is carried out by mathematical induction along the length of the base  $r(a_1, \dots, a_n)$  defining relation  $r^m(a_1, \dots, a_n)$  of group  $G$  and the number of generators. If  $G = \langle a_1, \dots, a_{n-1}, c; c^m, m > 1 \rangle$ , the statement is obvious. Suppose that the statement of the lemma is valid for all groups with one defining relation with torsion and with the basis of a defining relation satisfying the condition  $|r(a_1, \dots, a_n)| < n_0$  (symbol  $|r|$  denotes the word length of  $r$  in a free group).

Consider the group  $G = \langle t, a, b, \dots, d, c; r^m(t, a, b, \dots, d, c), m > 1 \rangle$ . The base  $r = (t, a, b, \dots, d, c)$  contains all generators of  $G$ , cyclically irreducible, begins with  $c^\varepsilon, \varepsilon = \pm 1$  and satisfies the condition  $|r(t, \dots, c)| = n_0$ . Assume  $\sigma_t(r) = 0, M_1 = \langle a, b, \dots, d \rangle, M_2 = \langle b, \dots, d, c \rangle, \bar{\sigma}_1(z) = 0$  and in  $G$  there is the relation  $z^{-1}uz = v$ ,

where  $u \in M_1, v \in M_2, M_1 z M_2 \neq M_1 M_2$  ( $\sigma_t(r)$  - sum of indicators for  $t$  in  $r$ ). We represent  $G$  in the form of  $HNN$  - extensions of the group  $H = \langle a_i, \dots, b_i, \dots, d_i, \dots, c_\mu, c_{\mu+1}, \dots, c_M, (i \in \mathbb{Z}); s^m \rangle$  using associated subgroups  $U_1 = \langle a_i, \dots, b_i, \dots, d_i, \dots, c_\mu, c_{\mu+1}, \dots, c_{M-1} \rangle, U_{-1} = \langle a_i, \dots, b_i, \dots, d_i, \dots, c_{\mu+1}, \dots, c_M \rangle$  and fixed isomorphism  $\theta: U_1 \rightarrow U_{-1}$  defined as follows:  $\forall i, i \in \mathbb{Z}, \theta(a_i) = a_{i+1}, \dots, \forall j, \mu \leq j < M, \theta(c_j) = c_{j+1}$ , that is  $G = \langle t, H, relH, t^{-1}at = \theta(a), \forall a \in U_1 \rangle$ .

Assume  $\tau$  - is the process rewriting the words of the group  $G$  in the generators  $\{t^{\pm 1}, a^{\pm 1}, \dots, c^{\pm 1}\}$  into the words of the group  $G$  in the generators  $\{t^{\pm 1}, a_i^{\pm 1}, \dots, c_j^{\pm 1}, i \in \mathbb{Z}, \mu \leq j < M\}$ . Denote by  $\tau(M_i)$  the subgroup  $M_i, i = \overline{1, 2}$ , given on generators  $\{t^{\pm 1}, a_i^{\pm 1}, \dots, c_j^{\pm 1}, i \in \mathbb{Z}, \mu \leq j < M\}$ . Then  $\tau(M_1) = \langle a_0, \dots, b_0, \dots, d_0 \rangle, \tau(M_2) = \langle b_0, \dots, d_0, c_0 \rangle, \tau(M_2) < U_\gamma$ , where  $\gamma = \pm 1$ . Element  $\tau(z)$ , satisfying the relation  $\tau(z)^{-1} \tau(u) \tau(z) = \tau(v)$  choose minimal in the double adjacency class  $\tau(M_1) \tau(z) \tau(M_2)$ . Suppose  $\tau(z) = B_0 t^{\varepsilon_1} B_1 t^{\varepsilon_2} \dots t^{\varepsilon_\vartheta} B_\vartheta, \varepsilon_i = \pm 1, i \in \overline{1, \vartheta}, B_j, j \in \overline{0, \vartheta - 1}$  - representatives of left adjacency classes  $H$  on  $mod U_{\varepsilon_{i+1}}$ . Then, the ratio  $\tau(z)^{-1} \tau(u) \tau(z) = \tau(v)$  will have the form:

$$B_\vartheta^{-1} t^{-\varepsilon_\vartheta} \dots t^{-\varepsilon_2} B_0^{-1} \tau(u) B_0 t^{\varepsilon_1} B_1 t^{\varepsilon_2} \dots t^{\varepsilon_\vartheta} B_\vartheta = \tau(v). \quad (3)$$

Assume, that  $B_0 \notin U_{\varepsilon_1}$ , then in order for the ratio (3) occurred, the condition  $B_0^{-1} \tau(u) B_0 \in U_{\varepsilon_1}$ , is necessary. But since  $U_{\varepsilon_1} B_0 U_{\varepsilon_1} \neq U_{\varepsilon_1} U_{\varepsilon_1}$  and  $\tau(M_1) \subset U_{\varepsilon_1}$ , then by Lemma I and the inductive hypothesis we have that  $B_0^{-1} U_{\varepsilon_1} B_0 \cap U_{\varepsilon_1} = E$ , hence,  $\tau(u) = 1$ . If  $\tau(z) = t^{\varepsilon_s} B_s t^{\varepsilon_2} \dots t^{\varepsilon_\vartheta} B_\vartheta$  where  $B_s \neq 1, s \in \overline{0, \vartheta - 1}$ , then we get the case considered above. Assume  $\tau(z) = t^{\varepsilon_\vartheta} B_\vartheta$ . Then the following cases are possible:

1)  $\tau(M_1)_\vartheta B_\vartheta \tau(M_2) \neq \tau(M_1)_\vartheta \tau(M_2)$  and

2)  $\tau(M_1)_\vartheta B_\vartheta \tau(M_2) \neq \tau(M_1)_\vartheta \tau(M_2)$

where  $\tau(M_1)_\vartheta = \langle a_\vartheta, b_\vartheta, \dots, d_\vartheta \rangle, a_\vartheta = t^{-\vartheta} a_0 t^\vartheta, \dots, d_\vartheta = t^{-\vartheta} d_0 t^\vartheta$ . In any of them, as is easy to see,  $\tau(u) = \tau(v) = 1$ . Assume that each of the subgroups  $M_1, M_2$  contains generatrix  $t$ . Suppose  $M_1 = \langle t, a, b, \dots, d \rangle, M_2 = \langle t, b, \dots, d, c \rangle$ . We represent  $G$  in the form of a semidirect product of groups  $\langle t \rangle$  and  $N$ , i.e.  $G = \langle t \rangle \lambda N$ , where  $N = \dots * N_{-j_{H-j}} * N_{-j+1_{H-j+1}} * \dots * N_{0_{H_0}} * N_1 \dots$  Each factor  $N_j$  has a

representation  $N_i = \langle a_i, \dots, b_i, \dots, d_i, \dots, c_{\mu+j}, \dots, c_{M+j}, (i \in \mathbb{Z}), s_j^M \rangle$ ;  
 factors  $N_i, N_{i+1}$  are united by the subgroup  $H_i = \langle a_i, \dots, b_i, \dots, d_i, \dots, c_{\mu+i+1}, \dots, c_{M+j}, (i \in \mathbb{Z}) \rangle$  and each  $x_j = t^{-j}xt^j$ . Subgroups  $M_1, M_2$  in new generators will have representation  $\tau(M_1) = \langle t, \bar{M}_1 \rangle$ ,  $\tau(M_2) = \langle t, \bar{M}_2 \rangle$ , where  $\bar{M}_1 = \langle a_i, \dots, \bar{M}_i = \langle a_i, \dots, b_i, \dots, d_i, \dots (i \in \mathbb{Z}) \rangle$ ,  $\bar{M}_2 = \langle b_i, \dots, d_i, c_i, \dots (i \in \mathbb{Z}) \rangle$ ,  $\bar{M}_i \triangleleft \tau(M_i), i = 1, 2, \bar{M}_1 < \bigcap_{-\infty}^{\infty} H_j$

Suppose that  $G$  has a relation  $z^{-1}uz = v$ , where  $u \in M_1, v \in M_2, M_1z M_2 \neq M_1M_2$ . It follows from it that  $\sigma_t(u) = \sigma_t(v)$ . Suppose  $\sigma_t(u) = \sigma_t(v) = 0$ . Rewrite  $z^{-1}uz = v$  in the new generators of the group  $G$ :  $\tau(z)^{-1}\tau(u)\tau(z) = \tau(v)$ . Here  $\tau(u) \in \bar{M}_1, \tau(v) \in \bar{M}_2$  and  $\tau(z)$  can be considered belonging to  $N$ . Assume that  $\tau(z)$  has the smallest syllable length in a double adjacency class  $\bar{M}_1\tau(z)\bar{M}_2$ . Assume that  $\tau(z) \in N_j, \tau(v) \in N_i$ . Since  $\tau(v) \in \bar{M}_2 \cap N_j$ , where  $\bar{M}_2 \cap N_j$  - magnus subgroup in  $N_j, \tau(u) \in \bar{M}_1 < N_j$ , then on the basis of the inductive hypothesis and Lemma I we have  $\tau(u) = \tau(v) = 1$ . Assume that for any  $j, \tau(z) \notin N_j$ . Symbol  $\|\tau(z)\|$  denotes the syllable length of an element in a group, which is a free product of groups with a union. If  $\|\tau(z)\| > 1$  and  $\|\tau(v)\| \leq 1$ , it follows from the inductive hypothesis that  $\tau(u) = 1$ . Consider the case when  $\|\tau(z)\| = k + 1, \|\tau(v)\| = l + 1$ . Suppose  $\tau(z) = A_0A_1 \dots A_k, \tau(v) = B_1 \dots B_l$  - normal forms  $\tau(z), \tau(v)$  in  $N$ . Then ratio  $\tau(z)^{-1}\tau(u)\tau(z) = \tau(v)$  will take the form

$$A_k^{-1}A_{k-1}^{-1} \dots A_0^{-1}\tau(u)A_0A_1 \dots A_k = B_1B_2 \dots B_l. \tag{4}$$

If  $l < 2k + 1$ , then from the inductive hypothesis we get  $\tau(u) = 1$ . Assume  $l = 2k + 1$ . The word  $B_1B_2 \dots B_l$  is a transform; otherwise, raising both sides of relation (4) to some extent, we find that the syllable length of the left side of (4) is less than the length of the right. In this way,  $\tau(v) = \bar{B}_k^{-1} \dots \bar{B}_1^{-1}B_0\bar{B}_1 \dots \bar{B}_k$ , where each  $\bar{B}_i \in \bar{M}_2$ . However, this contradicts minimality  $\tau(z)$  in the class  $\bar{M}_1\tau(z)\bar{M}_2$ . It follows that  $\|\tau(u)\| = \|\tau(v)\| = 1$ , that is, the previously considered case.

Consider the case when in the relation  $z^{-1}uz = v, \sigma_t(z^{-1}uz) = \sigma_t(v) = \eta \neq 0$ , and we can assume that  $\sigma_t(z) = 0$ , that is  $\tau(z) \in N$ . Suppose  $\tau(u) = \bar{u}t^\eta, \tau(v) = \bar{v}t^\eta$ , where  $\bar{u} \in \bar{M}_1, \bar{v} \in \bar{M}_2$ . We assume that  $\eta$  is such that the condition (a)  $\forall j, N_j \cap N_{j+\eta} = \bigcap_{-\infty}^{\infty} H_j$

Otherwise, raising both sides of the relation  $\tau(z)^{-1}\tau(u)\tau(z) = \tau(v)$  to the appropriate degree, we will achieve the fulfillment of condition (a) By

the choice of  $\tau(z)$  we have  $\|\tau(z)\| \leq 1$ . Suppose  $\tau(z) = A, \|A\| = 1, \bar{v} \notin \bar{M}_1$ . Then

$$A^{-1}\tau(u)t^\eta A = \bar{v}t^\eta \tag{5}$$

Since  $\|A^{-1}\tau(u)A_{-\eta}\| = 2, A_{-\eta} = t^\eta A t^{-\eta}$ , then  $\bar{v} = B_1 B_2, \|v\| = 2$ . But then from the relation  $A^{-1}\tau(u)A_{-\eta} = B_1 B_2$ , it follows that  $A^{-1}h = B_1, h \in \bigcap_{-\infty}^{\infty} H_i$ , that is, the syllable length  $\tau(z)$  can be reduced by multiplying on the right by elements from  $\bar{M}_2$ . Suppose  $\|A\| < 1, \|\bar{v}\| \leq 1$ . In this case, relation (5) does not hold in  $G$ , since, raising both its parts to the power  $n > 2$ , we get that  $\|A^{-1}\tau(u)A_{-n\eta}\| \neq \|A^{-1}\tau(u)A_{-n\eta}\| \neq$ , where  $\tau(u) \in \bar{M}_1, \bar{v} \notin \bar{M}_1, \tau(u) = 1 \text{ if } \bar{v} \in \bar{M}_1$ , then in this case  $u, v$  belong to the subgroup  $\langle t, a, \dots, d \rangle$  which is the magnus subgroup of  $G$ , and by Theorem 1 the statement of the theorem is true.

Consider the case when the base  $r(t, a, \dots, c)$  defining relations of the group  $G$  satisfies the conditions:  $\sigma_\alpha(r) \neq 0, \alpha \in \{t, a, \dots, d, c\}$ . Suppose  $M_1 = \langle t, a, \dots, d \rangle, M_2 = \langle t, b, \dots, d, c \rangle, \sigma_t(r) = \vartheta_1, \sigma_c(r) = \vartheta_2$ . It is known [2] that in this case the group  $G$  can be embedded isomorphically into the group  $G^* = \langle x, a, \dots, d, y; r^m(x^{\vartheta_2}, a, \dots, d, yx^{-\vartheta_1}), m > 1 \rangle$  using isomorphism  $f: t \rightarrow x^{\vartheta_2}, a \rightarrow a, \dots, d \rightarrow d, c \rightarrow yx^{-\vartheta_1}$ . In this case, subgroups  $M_1, M_2$  in  $G^*$  correspond to subgroups:  $f(M_1) = \langle x^{\vartheta_2}, a, \dots, d \rangle, f(M_2) = \langle x^{\vartheta_2}, b, \dots, d, vx^{-\vartheta_1} \rangle$ . Consider in  $G^*$  the subgroups  $\tilde{M}_1 = \langle x^{\vartheta_2}, a, \dots, d \rangle, \tilde{M}_2 = \langle x^{\vartheta_2}, b, \dots, d, y \rangle, f(M_i) < \tilde{M}_i, i = 1, 2$ . Since the basis of the determining relation  $r^m(x^{\vartheta_2}, a, \dots, d, vx^{-\vartheta_1})$  of the group  $G^*$  satisfies the condition  $\sigma_x(r^m(x^{\vartheta_2}, a, \dots, d, vx^{-\vartheta_1})) = 0$ , then in  $G^*$  for any  $z \in G^*$ , satisfying condition  $\tilde{M}_1 z \tilde{M}_2 \neq \tilde{M}_1 \tilde{M}_2$ , can be shown in the same way as above, that  $z^{-1} \tilde{M}_1 z \cap \tilde{M}_2 = E$ . Since the ratio  $z^{-1} u z = v$  of  $G$  in a group  $G^*$  corresponds to  $f(z)^{-1} f(u) f(z) = f(v)$  and  $f(z)$  satisfies the conditions  $\sigma_x(f(z)) = 0, f(M_1) f(z) f(M_2) \neq f(M_1) f(M_2)$ , it can be shown that  $\tilde{M}_1 f(z) \tilde{M}_2 \neq \tilde{M}_1 \tilde{M}_2$ . It follows that  $z^{-1} M_1 z \cap M_2 = E$ . The theorem is proved.

2 In this section of the article, we consider a generalization of Bagerzade's theorem:

**Theorem 3.** Suppose  $G = \langle X, r \rangle$  – a group with one defining torsion-free relation,  $r$  is cyclically given. If  $M$  – magnus subgroup  $G$  and  $g \in G \setminus M$ , then  $g^{-1} M g \cap M$  - cyclic subgroup.

**Theorem 4.** Suppose  $G = \langle X, r \rangle$  – a group with one defining relation without torsion,  $r$  is cyclically given.  $M_1, M_2$ , - magnus subgroups and  $g \in G$ , are such that  $M_1 g M_2 \neq M_1 M_2$ . Then  $g^{-1} M_1 g \cap M_2$  - cyclic subgroup.

We carry out the *proof* by the method of mathematical induction along the length of the defining relation. Suppose  $G = \langle t, a, b, \dots, d, c; r(t, a, b, \dots, d, c) \rangle$ . Assuming that  $r(t, a, b, \dots, d, c) \equiv c^m$  ( $\equiv$  - graphic equality), then the theorem follows from Theorem 2. Suppose the theorem holds for all groups with one defining relation for which  $|r(t, a, b, \dots, d, c)| < n$ , (the symbol  $||$  denotes the length of a word in a free group). Let us prove this theorem for groups for which the length of the defining relation  $|r(t, a, b, \dots, d, c)| = n$ . We assume that  $r(t, a, b, \dots, d, c)$  starts with  $c$  and all generators of the group are contained in  $r$ ;  $r$  is cyclically irreducible.

1. Suppose  $\sigma_t(r(t, a, b, \dots, d, c)) = 0$

a) Consider the case when  $M_1, M_2$  do not contain  $t$ .  
 $M_1 = \langle a, b, \dots, d \rangle, M_2 = \langle b, \dots, d, c \rangle$ .

Represent in the form of HNN – expansion:  $G = \langle t, H: rel H, t^{-1} U_+ t = U_- \rangle$  where  $H = \langle a_i, \dots, b_i, \dots, d_i, (i \in \mathbb{Z}), c_\mu, \dots, c_M; S_0 \rangle, S_0 = S_0(a_\nu, \dots, c_\nu, \dots, c_M, \dots, d_\mu) . |S_0| < n, U_+ = \langle a_i, \dots, b_i, \dots, d_i, c_\mu, \dots, c_{M-1} \rangle, U_- = \langle a_i, \dots, b_i, \dots, d_i, c_{\mu+1}, \dots, c_M \rangle$  and  $t^{-1} a_i t = a_{i+1}, t^{-1} b_i t = b_{i+1}, \dots, t^{-1} d_i t = d_{i+1}, t^{-1} c_j t = c_{j+1},$  where  $\mu \leq j < M$ .

Suppose  $z \in G$  is such that  $M_1 z M_2 \neq M_1 M_2$  and  $\text{rang}(z^{-1} M_1 z \cap M_2) > 1$  and suppose  $\exists u_1, u_2 \in M_1$ , respectively,  $\exists v_1, v_2 \in M_2$ , are such that  $\text{rang} \langle u_1, u_2 \rangle = 2, \text{rang} \langle v_1, v_2 \rangle = 2$  and

$$z^{-1} u_1 z = v_1, z^{-1} u_2 z = v_2 \tag{6}$$

Subgroups  $M_1, M_2$  are set in new generators. Denote by  $\tau(M_i)$  – subgroups  $M_i, i = \overline{1, 2}$  in new generators:  $\tau(M_1) = \langle a_0, b_0, \dots, d_0 \rangle, \tau(M_2) = \langle c_0, b_0, \dots, d_0 \rangle$ . By choice  $r(t, a, b, \dots, d, c)$ . ( $r(t, a, b, \dots, d, c)$  starts at  $c$ ) generator  $c_0 \in \{c_\mu, c_{\mu+1}, \dots, c_M\}$ . Therefore  $\tau(M_1) \subset H, \tau(M_2) \subset H$ , moreover,  $\tau(M_1) \subset U_\varepsilon, \varepsilon = \pm 1; \tau(M_2) \subset U_1$  or  $\tau(M_2) \subset U_{-1}$  it is possible that  $\tau(M_2)$  is contained both in  $U_1$  and in  $U_{-1}$ . Assume that  $\tau(z) \notin H$ , then  $\tau(z) = B_0 t^{\varepsilon_1} B_1 \dots t^{\varepsilon_s} B_s$ , where  $B_0 \notin U_{\varepsilon_1}, B_s \notin U_{-\varepsilon_1}$ . Besides,  $B_0 \notin \tau(M_1), B_s \notin \tau(M_2)$ , since  $\tau(z)$  we choose minimal in a double

adjoining class  $\tau(M_1)\tau(z)\tau(M_2)$ . Consider the relationship:

$$\tau(z)^{-1}\tau(u_1)\tau(z) = \tau(v_1), \quad \tau(z)^{-1}\tau(u_2)\tau(z) = \tau(v_2) \quad (7)$$

Suppose  $\tau(u_i) = \bar{u}_i, \tau(v_i) = \bar{v}_i, \tau(z) = \bar{z}$ . Then:

$$B_s^{-1}t^{-\varepsilon_s}B_{s-1}^{-1} \dots t^{-\varepsilon_1}B_0^{-1}\bar{u}_iB_0t^{\varepsilon_1}B_1 \dots B_s = \bar{v}_i, \quad i = \overline{1,2}. \quad (8)$$

If  $s > 1, B_0 \neq 1$ , and since  $B_0 \notin U_{\varepsilon_1}$ , and  $\|\bar{z}^{-1}\bar{u}_i\bar{z}\| \leq \|\bar{v}_i\|$ , where  $\|\bar{v}_i\| < 1$ , then  $B_0^{-1}\bar{u}_iB_0 \in U_{\varepsilon_1}$ , where  $\bar{u}_i \in U_{\varepsilon_1}$  which follows from the relation:  $\tau(M_1) \subset U_1 \cap U_{-1}$ ; since  $U_{\varepsilon_1}B_0U_{\varepsilon_1} \neq U_{\varepsilon_1}U_{\varepsilon_1}$  and  $B_0^{-1}\bar{u}_iB_0 \in U_{\varepsilon_1}$ , then based on an inductive hypothesis  $\text{rang}(\langle \bar{u}_1, \bar{u}_2 \rangle) \leq 1$ .

Suppose  $B_0 = B_1 = \dots = B_j = 1, j \leq s$ ; suppose  $j = s$ ;  $\bar{z} = t^{ss}h, h \in U_{-s}$  and  $s \geq 1$ ; then relations (6) take the form:  $h^{-1}t^{-ss}\bar{u}_i t^{ss}h = v_i$ . We introduce the notation  $t^{-ss}\bar{u}_i t^{ss} = \bar{u}_{i,s}$ . The words  $\bar{u}_{i,s} \in M_{i,s} = t^{-ss}M_i t^{ss} = \langle a_{\varepsilon_s}, b_{\varepsilon_s}, \dots, d_{\varepsilon_s} \rangle$  where  $a_{\varepsilon_s} = t^{-\varepsilon_s}a_\varepsilon t^{\varepsilon_s}, b_{\varepsilon_s} = t^{-\varepsilon_s}b_0 t^{\varepsilon_s} \dots, d_{\varepsilon_s} = t^{-\varepsilon_s}d_\varepsilon t^{\varepsilon_s}$ . By assumption  $h \in U_{-s}$  and subgroups  $\tau(M_{i,s}), \tau(M_2) \in U_{-1}$ . Assume that  $h \in U_{-1}$ . Then ratios  $h^{-1}\bar{u}_{i,s}h = \bar{v}_i, i = \overline{1,2}$  must be performed in a free group  $U_{-1}$ , what is impossible since words  $\bar{u}_{i,s}$  and  $\bar{v}_i$  contain different generators. Suppose  $h \notin U_{-1}$ , then  $h \in U_1$ . Hence,  $h = h(\dots, c_\mu, \dots, c_{M-1})$ , that is  $c_\mu$  is contained in the word  $h$  and therefore, since  $\tau(M_{i,s}), \tau(M_2) \in U_{-1}$ , then  $\tau(M_{i,s})h\tau(M_2) \neq \tau(M_{i,s})\tau(M_2)$ . Therefore, by the inductive hypothesis, the relation  $h^{-1}\bar{u}_{i,s}h = \bar{v}_i, i = \overline{1,2}$  takes place then and only then, when  $\text{rang}(\langle \bar{u}_1, \bar{u}_2 \rangle) < 1$ . Suppose  $j < s, \tau(z) = t^{-\varepsilon_j}B_{j+1}t^{\varepsilon_{j+2}}B_{j+2} \dots B_s$ , where  $B_{i+1} \notin U_{\varepsilon_1}$ . Then ratios (6) will be equivalent to the relations  $B_{i+1}^{-1}\bar{u}_{i,s}B_{i+1} \notin U_{\varepsilon_1}$ . Since  $\bar{u}_{i,\varepsilon_j} \in U_{\varepsilon_{j+2}}$ , on  $i = \overline{1,2}$  and  $U_{\varepsilon_{j+2}}B_{j+1}U_{\varepsilon_{i+2}} \neq U_{\varepsilon_{j+2}}U_{\varepsilon_{i+2}}$ , then by the inductive hypothesis we have  $\text{rang}(\langle \bar{u}_1, \bar{u}_2 \rangle) \leq 1$ . If  $z \in H$ , then  $\tau(M_1), \tau(M_2)$  – magnus subgroups in  $H$  and the theorem holds.

b) suppose each subgroup  $M_1, M_2$  contains generator  $t$ , that is  $M_1 = \langle t, a, b, \dots, d \rangle, M_2 = \langle t, b, \dots, d, c \rangle$ . We represent the group  $G$  as follows:  $G = \langle t \rangle \lambda N$ , where  $N \triangleleft G$  and

$$N = \dots * N_{-j} *_{H_{-j}} N_{-j+1} *_{H_{-j+1}} N_{-j+2} * \dots * N_0 *_{H_0} N_1 * \dots *_{H_{k-1}} N_k * \dots$$

where factor  $N_j = \langle a_i, \dots, b_i, \dots, d_i, \dots, c_{u+i}, \dots, c_{M+i}; S_i, i \in \mathbb{Z} \rangle$  and associative groups  $H_i = \langle a_i, \dots, b_i, \dots, d_i, \dots, c_{\mu+j+1}, \dots, c_{M+j}, i \in \mathbb{Z} \rangle$  where each  $x_j = t^{-j}xt^j$ . Then in the new generators of the subgroup  $M_1, M_2$  will have the form:  $M_1 = \langle t, \bar{M}_1 \rangle, M_2 = \langle t, \bar{M}_2 \rangle$ , where  $\bar{M}_1 = \langle a_i, \dots, b_i, \dots, d_i, i \in \mathbb{Z} \rangle, \bar{M}_2 = \langle b_i, \dots, d_i, \dots, c_i, i \in \mathbb{Z} \rangle = \dots$

... $M_{2,-i} *_{B_i} M_{2,-i+1} *_{B_{i+1}} \dots *_{B_{2,0}} M_{2,1} *_{B_1} \dots *_{B_{j-1}} M_j * \dots$ ,  
 where  $M_{2,-i} = \langle b_i, \dots, d_i, \dots, c_{\mu+j}, \dots, c_{M+j} \rangle$   
 $B_j = \langle b_j, \dots, d_j, \dots, c_{\mu+j+1}, \dots, c_{M+j} \rangle$ , where  $B_j \subset H_j$  and  
 $M_{2,j} \subset N_j$

From equality (6) it follows that  $\sigma_t(z^{-1}u_i z) = \sigma_t(v_i)$  and  $\sigma_t(u_i) = \sigma_t(v_i)$ ,  $i = \overline{1, 2}$ .

In addition, we can assume that  $\sigma_t(z) = 0$ .

c) Consider the case, when  $\sigma_t(u_i) = \sigma_t(v_i) = 0$ . b1) Consider the case when  $\|\bar{u}_i\| = \|\bar{v}_i\| \leq 1$ . Suppose  $\bar{z} = A_0 A_1 \dots A_k$ , where  $\bar{z} \in N$  and  $A_0 A_1 \dots A_k$  is a normal form  $\bar{z}$  in  $N$ . Assume that  $\|\bar{z}\| > 1$ , then relation (6) will have the form:

$$A_k^{-1} A_{k-1}^{-1} \dots A_1^{-1} A_0^{-1} \bar{u}_i A_0 A_1 \dots A_k = \bar{v}_i \quad (9)$$

In what follows, we assume that the word  $\bar{z}$  is chosen in the double coset  $\bar{M}_1 \bar{z} \bar{M}_2$  to be the smallest. Since in the ratio (9)  $\|\bar{v}_i\| \leq 1$ , and  $k > 1$ , we get the previously considered cases.

c2) Suppose for certain  $i$ ,  $i = \overline{1, 2}$ ,  $\|\bar{v}_i\| > 1$ . Then we can assume that  $\|\bar{v}_1\| > 1$  and  $\|\bar{v}_2\| > 1$ . Really, if  $\|\bar{v}_1\| = 1$  and  $\|\bar{v}_2\| > 1$ , then consider instead of  $\bar{v}_1$  the element  $\bar{v}_1 \bar{v}_2$ , and if  $\|\bar{v}_1 \bar{v}_2\| > 1$ , that equality  $\bar{z}^{-1} u_1 \bar{z} = \bar{v}_1$  is replaced by equality  $\bar{z}^{-1} \bar{u}_1 \bar{u}_2 \bar{z} = \bar{v}_1 \bar{v}_2$ , if  $\|\bar{v}_1 \bar{v}_2\| \leq 1$ , then in this case the equality  $\bar{z}^{-1} u_2 \bar{z} = \bar{v}_2$  is replaced by  $\bar{z}^{-1} \bar{u}_1 \bar{u}_2 \bar{z} = \bar{v}_1 \bar{v}_2$ .

Therefore, we will assume that  $\|\bar{v}_i\| > 1$ ,  $i = \overline{1, 2}$ , and suppose that equalities (6) have the form:

$$\begin{cases} A_k^{-1} A_{k-1}^{-1} \dots A_1^{-1} A_0^{-1} \bar{u}_1 A_0 A_1 \dots A_k = B_1 B_2 \dots B_{m_1} \\ A_k^{-1} A_{k-1}^{-1} \dots A_1^{-1} A_0^{-1} \bar{u}_2 A_0 A_1 \dots A_k = B'_1 B'_2 \dots B'_{m_2} \end{cases} \quad (10)$$

where  $\bar{v}_1 = B_1 B_2 \dots B_{m_1}$ ,  $m_1 > 1$ ,  $\bar{v}_2 = B'_1 B'_2 \dots B'_{m_2}$ ,  $m_2 > 1$ , and  $B_1 B_2 \dots B_{m_1}, B'_1 B'_2 \dots B'_{m_2}$  - normal form of words  $\bar{v}_1, \bar{v}_2 \in \bar{M}_2$ , respectively. Note that in normal form  $\bar{v}_1, \bar{v}_2$  each of the syllables  $B_i \in \bar{M}_2$  (written in generators  $\bar{M}_2$ ). We will assume that  $m_1 = m_2 = 2k + 1$ , that is  $A_0^{-1} u_i A_0 \notin H_j$ , then from equalities (10) we obtain that the syllable length  $\bar{z}$  can be reduced by multiplying by  $\bar{M}_2$ , that is the word  $\bar{z}$  is not minimal. If  $m_1 < 2k + 1$  and  $m_2 < 2k + 1$ , then by virtue of equalities (10) we have that  $A_0^{-1} \bar{u}_i A_0 \in H_j$ ,  $i = \overline{1, 2}, \forall j: \bar{M}_1 \subset H_j$ , and since in class  $\bar{M}_1 \bar{z} \bar{M}_2$  the word  $\bar{z}$  has a minimum syllable length and a minimum length, then  $A_0 \notin \bar{M}_1$ . Suppose  $A_0 \in \bar{N}_{i_1}, A_1 \in \bar{N}_{i_2}, i_1 \neq i_2$ , and

suppose  $\bar{N}_{i_1} *_H \bar{N}_{i_2}$ , where  $\bar{M}_1 \subset H$ , and assume that  $i_1 < i_2$ , then  $H \subset H_{i_1} \cap H_{i_2}$ . Under the assumptions, in order for the relation (6) to be made, it is necessary that  $A_0^{-1}\bar{u}_i A_0 \in H$ , but since  $A_0 \notin H_{i_1}$ , then  $HA_0H \neq HH$ , therefore, by the inductive assumption, it follows that  $\text{rang}(\langle \bar{u}_1, \bar{u}_2 \rangle) \leq 1$ . Assume that  $\bar{z} = A_0$ ; then relations (6) take the form:

$$A_0^{-1}\bar{u}_1 A_0 = \bar{v}_1, A_0^{-1}\bar{u}_2 A_0 = \bar{v}_2 \tag{11}$$

It's obvious that  $\|\bar{v}_1\| = \|\bar{v}_2\| = 1$ , since  $\|A_0^{-1}\bar{u}_i A_0\| = 1$ . By condition  $\bar{M}_1 A_0 \bar{M}_2 \neq \bar{M}_1 \bar{M}_2$ , and there exist such  $i_1, i_2, i_3$ , that  $A_0 \in \bar{N}_{i_1}, \bar{v}_1 \in \bar{N}_{i_2}, \bar{v}_2 \in \bar{N}_{i_3}$ . It's obvious that  $\bar{v}_1, \bar{v}_2$  must be contained in one factor. Really, if  $i_3 \neq i_2$  and  $\bar{v}_1, \bar{v}_2$  are not contained in one factor, then the ratio  $A_0^{-1}\bar{u}_1 A_0 = \bar{v}_1$  we replace by the relation  $A_0^{-1}\bar{u}_1 \bar{u}_2 A_0 = \bar{v}_1 \bar{v}_2$ , for which  $|A_0^{-1}\bar{u}_1 \bar{u}_2 A_0| = 1$  and  $|\bar{v}_1 \bar{v}_2| > 1$ , which is impossible. In this way,  $\bar{v}_1, \bar{v}_2 \in \bar{N}_{i_2}$ . Consider the subgroup  $\bar{N}_{i_1} *_H \bar{N}_{i_2}, i_1 < i_2$ . In order for relations (11) to take place, it is necessary that  $A_0^{-1}\bar{u}_1 A_0 \in H, \bar{M}_1 \subset H, A_0 \notin H$ . Therefore, by the inductive assumption, we obtain that  $\text{rang}(\langle \bar{u}_1, \bar{u}_2 \rangle) \leq 1$ .

(d) Now, consider the case when  $\sigma_t(u_1) = \sigma_t(v_1) \neq 0 \vee \sigma_t(u_2) = \sigma_t(v_2) \neq 0$

Assume that  $\sigma_t(u_1) = \sigma_t(v_1) \neq 0$ , then we can assume that  $\sigma_t(u_2) = \sigma_t(v_2) \neq 0$ . Really, if  $\sigma_t(u_2) = \sigma_t(v_2) = 0$ , then the equation  $z^{-1}u_2 z = v_2$  replace by the equation  $z^{-1}u_1 u_2 z = v_1 v_2$ . Therefore, we will consider the case when  $\sigma_t(u_1) = \sigma_t(v_1) \neq 0, \sigma_t(u_2) = \sigma_t(v_2) \neq 0$ . Assume that  $\sigma_t(u_1) = p_1, \sigma_t(u_2) = p_2$ . Then  $u_1 = \bar{u}_1 t^{p_1}, u_2 = \bar{u}_2 t^{p_2}, v_1 = \bar{v}_1 t^{p_1}, v_2 = \bar{v}_2 t^{p_2}$ , where  $\bar{u}_1, \bar{u}_2 \in \bar{M}_1, \bar{v}_1, \bar{v}_2 \in \bar{M}_2$ . Obviously there is such  $p > 0$ , that  $\forall j : N_j \cap N_{j+p} = \bigcap_{-\infty}^{\infty} H_i$ , moreover  $\bar{M}_1 \subseteq \bigcap_{-\infty}^{\infty} H_i$ . We will assume that  $p_1 > p, p_2 > p$ , otherwise replace  $u_1, u_2, v_1, v_2$  their respective degrees. As and in case (c), we consider the group  $G$  as an extension of  $N$  with the help of the subgroup  $\langle t \rangle$ . We will assume that  $\sigma_t(z) = 0$  and  $\tau(z) = \bar{z} = A_0 A_1 \dots A_s$ , where  $\|\bar{z}\| \geq 0$ . Suppose in  $G$ , at least one of the equalities (6) holds, i.e.

$$A_k^{-1} A_{k-1}^{-1} \dots A_1^{-1} A_0^{-1} \bar{u}_i t^{p_i} A_0 A_1 \dots A_k = \bar{v}_i t^{p_i}, i = \overline{1, 2} \tag{12}$$

Since  $\bar{z}$  is minimum in double class  $\bar{M}_1 \bar{z} \bar{M}_2$ , then  $A_0 \notin \bar{M}_1$  and  $A_k \notin \bar{M}_2$  in addition, it is obvious that  $A_0 \notin (\bigcap_{-\infty}^{\infty} H_i)$ , since otherwise the syllable

length of  $\bar{z}$  would be less; so  $A_0$  and  $A_{0p} = t^{pi}A_0t^{-pi}$  are not contained in one factor  $N_j$  of the group  $N$ . Further, if  $\bar{v}_i \notin \bar{M}_1$ , then  $\bar{v}_i$  contains in its irreducible record  $c_j$ , therefore, if  $\|\bar{v}_i\| \leq 1$ , then  $\bar{v}_i$  and  $t^{pi}\bar{v}_it^{-pi} = \bar{v}_{i,pi}$  is also contained in different factors. Therefore, raising both sides of relation (12) to a power  $m > 2k + 3$  we get that the syllable word length  $(v_i t^{pi})^m t^{-pi m}$  will be greater than the syllable length of the left side of equality (12), which is impossible. Therefore, we assume that  $\|\bar{v}_i\| > 1$ ,  $\bar{v}_i = B_1 B_2 \dots B_s$ ,  $s > 1$ ,  $B_i \in \bar{M}_2$ , but then it follows from equality (12) that the syllable length  $\bar{z}$  can be shortened by multiplying by elements from  $\bar{M}_2$ , which is also impossible by inductive hypothesis. Which proves the case in question. The case when one of the subgroups  $M_i$  contains the generator  $t$ , while the other does not contain it, it is similar to the one considered above.

Consider the case when the defining relation  $r(t, a, \dots, d, c)$  of the group  $G$  satisfies the conditions:  $\sigma_\alpha(r) \neq 0, \alpha \in \{t, a, \dots, d, c\}$ .

It is known that in this case the group  $G$  can be embedded isomorphically into the group  $G^* = \langle x, t, a, \dots, d, y; r(x^{\theta_2}, t, a, \dots, d, yx^{-\theta_2}) \rangle$  using isomorphism  $f: t \rightarrow x^{\theta_2}, a \rightarrow a, \dots, d \rightarrow d, c \rightarrow yx^{-\theta_2}$ . Under this isomorphism, subgroups  $M_1, M_2$  in  $G^*$  will correspond to the subgroups:  $f(M_1): \langle x^{\theta_2}, a, \dots, d \rangle, f(M_2): \langle x^{\theta_2}, b, \dots, d, yx^{-\theta_2} \rangle$ . Consider in  $G^*$  the subgroups  $\tilde{M}_1 = \langle x, a, \dots, d \rangle, \tilde{M}_2 = \langle x, b, \dots, d, y \rangle, f(M_1) \subseteq \tilde{M}_1, f(M_2) \subseteq \tilde{M}_2$ .

Since defining relation  $r(x^{\theta_2}, t, a, \dots, d, yx^{-\theta_2})$  of the group  $G^*$  satisfies the condition  $\sigma_x(r(x^{\theta_2}, t, a, \dots, d, yx^{-\theta_2})) = 0$ , then in  $G^*$  for any  $z \in G^*$  satisfying the condition  $\tilde{M}_1 z \tilde{M}_2 \neq \tilde{M}_1 \tilde{M}_2$ , can also be shown in the way that it is done above, that  $\text{rang}(\tilde{M}_1 z \tilde{M}_2 \cap \tilde{M}_1 \tilde{M}_2) \leq 1$ . Correlation  $M_1 z M_2 \neq M_1 M_2$  in the group  $G$  corresponds to the ratio  $f(M_1) f(z) f(M_2) \neq f(M_1) f(M_2)$  in the group  $G^*$ . We show that from the relation  $f(M_1) f(z) f(M_2) \neq f(M_1) f(M_2)$  follows the ratio  $\tilde{M}_1 f(z) \tilde{M}_2 \neq \tilde{M}_1 \tilde{M}_2$  in  $G^*$ . Suppose the contrary, that is  $\exists A \in \tilde{M}_1, \exists B \in \tilde{M}_2$ , such that  $f(z) = AB$ .

Note that the word  $B$  does not contain generators  $a, a^{-1}$ ,  $A$  does not contain  $y$ . Since  $f$  is an isomorphic embedding,  $z = f^{-1}(AB)$ , that is  $f^{-1}$  maps the subgroup isomorphically  $f(G) < G^*$  on  $G$ , then there is such  $m \in \mathbb{Z}$ , that  $f^{-1}(x^m B) \in G$ . Then  $x^m B \in f(G)$ . Consider the product  $f^{-1}(AB) f^{-1}(B^{-1} x^{-m}) \in G$ ; hence  $f^{-1}(ABB^{-1} x^{-m}) = f^{-1}(A x^{-m}) \in G$ . It's obvious that

$f^{-1}(Ax^{-m}) \in M_1$  and  $f^{-1}(x^m B) \in M_2$ . Hence,  $Ax^{-m} \in f(M_1)$ ,  $x^m B \in f(M_2)$  and  $f(M_1)f(z)f(M_2) = f(M_1)f(M_2)$ ; we obtain a contradiction. It follows that  $\text{rang}(f(z^{-1})\tilde{M}_1f(z) \cap \tilde{M}_2) \leq 1$ . Hence,  $\text{rang}(f(z^{-1})f(\tilde{M}_1)f(z) \cap f(\tilde{M}_2)) \leq 1$ , which proves our theorem.

## References

- 1 Newman B.B. Some results of one-relator group// Bull. Amer. Math. Soc. 1968, V. 74, P. 568-571.
- 2 Lyndon R. Schupp P. Combinatorial group theory. M. Science, 1980.





*Scientific publication*

**International Conference  
“Process Management and Scientific Developments”**

Birmingham, United Kingdom  
(Novotel Birmingham Centre, June 9, 2020)

Signed in print 09.06.2020 г. 60x84/16.  
Ed. No. 1. Circulation of 500 copies.  
Scientific publishing house Infinity, 2020.